CIVIL ENGINEERING STUDIES

STRUCTURAL RESEARCH SERIES NO. 283

PRIVATE COMMUNICATION
NOT FOR PUBLICATION

BOND CHARACTERISTICS OF PRESTRESSING STRAND

By
G. F. ANDERSON
J. H. RIDER
M. A. SOZEN

Issued as a Part of Progress Report No. 13 of
The Investigation of Prestressed Reinforced
Concrete for Highway Bridges
Project IHR-10
Illinois Cooperative Highway Research Program

Conducted by

THE STRUCTURAL RESEARCH LABORATORY
DEPARTMENT OF CIVIL ENGINEERING
ENGINEERING EXPERIMENT STATION
UNIVERSITY OF ILLINOIS

in cooperation with

THE STATE OF ILLINOIS
DIVISION OF HIGHWAYS

and

THE U.S. DEPARTMENT OF COMMERCE
BUREAU OF PUBLIC ROADS

UNIVERSITY OF ILLINOIS
URBANA, ILLINOIS
JUNE 1964

PRIVATE COMMUNICATION
NOT FOR PUBLICATION

BOND CHARACTERISTICS OF PRESTRESSING STRAND

By
G. F. Anderson
J. H. Rider
M. A. Sozen

Issued as a Part of Progress Report No. 13 of
The Investigation of Prestressed Reinforced
Concrete for Highway Bridges
Project IHR-10
Illinois Cooperative Highway Research Program

Conducted by

THE STRUCTURAL RESEARCH LABORATORY
DEPARTMENT OF CIVIL ENGINEERING
ENGINEERING EXPERIMENT STATION
UNIVERSITY OF ILLINOIS

in cooperation with

THE STATE OF ILLINOIS
DIVISION OF HIGHWAYS

and

THE U.S. DEPARTMENT OF COMMERCE
BUREAU OF PUBLIC ROADS

UNIVERSITY OF ILLINOIS
URBANA, ILLINOIS
June 1964

TABLE OF CONTENTS

1. INTRODUCTION

1.1 Introductory Remarks

In reinforced concrete members, forces can be transmitted directly between the reinforcing element and the concrete. The means by which such a transfer of stress is accomplished is commonly referred to as bond. Bond is usually expressed as a stress measured in terms of force per unit area. When considering prestressing strand, the concept of stress or force per unit area loses its significance because of the irregular nature of the strand surface. Throughout this report the quantity "unit bond" rather than bond stress will be used. Unit bond represents the average rate of shear flow and is given in units of load per unit length.

In the fabrication of a pretensioned prestressed concrete member the prestressing strand is first tensioned to the desired level and the concrete then cast around the strand. When the concrete is strong enough, the strand tension is released and is transferred to the concrete by means of bond. The length of beam required for the complete transfer of prestress from the strand to the concrete is called the anchorage length and the bond by which this transfer is accomplished will be referred to as anchorage bond.

When a beam is loaded in flexure the steel reinforcement helps the concrete resist the externally applied moment. To accomplish this in a pretensioned flexural member, tensile forces are transferred from the concrete to the prestressing strand by bond. That is, bond between the concrete and strand is developed as a result of flexure. This type of bond will be referred to as flexural bond.

The amount of bond which can be developed between concrete and prestressing strand depends, among other things, upon the existing stress conditions in the strand and the surrounding concrete. Thus a distinction must be made between anchorage and flexural bond because, as will be explained in Section 1.2, the stress conditions in the concrete and in the prestressing strand are different in the two cases.

1.2 Object and Scope

The main object of this study was to investigate the anchorage and flexural bond characteristics of certain types of prestressing strand.

Three types of clean strand were investigated; 7/16-in. nominal diameter 7-wire round-wire strand, 7/16-in. nominal diameter 7-wire rectangular-wire strand, and 1/4-in. nominal diameter 3-wire rectangular-wire strand. A similar investigation (Series 1) was made on 1/4-in. nominal diameter 7-wire round-wire strand by R. W. Keuning (1)*. Some of the results from that investigation are also included in this report.

The first part of the investigation was concerned primarily with anchorage bond. The primary objective was to provide basic information for use in the determination of the anchorage length in pretensioned beams. In connection with this, a unit bond-slip relation was developed for each type of strand.

The ideal specimen to be used in the study of anchorage bond would be the end block of a pretensioned beam. By measuring the strain in the reinforcement or even in the concrete, if a reliable method of converting strain to stress is available, the rate of transfer of stress from the strand to the concrete could be determined which would indicate the bond characteristics of the strand under actual conditions. However, because of the elaborate instrumentation required and the size of test specimen involved, this type of specimen becomes impractical. The specimens actually used were comparatively small and consisted of a block of concrete of square cross section with the strand passing lengthwise through the center of the block. Various specimen lengths were used. Most of the tests conducted were standard pull-out tests with slip measurements taken at both ends of the specimen as the load was applied. The conditions existing in a pull-out specimen are different

---

* Numbers in parentheses refer to entries in the list of references

from those in the end block of a pretensioned beam. Although the concrete is in longitudinal compression and some radial stresses are present in both cases, the points of maximum strand stress and maximum slip between the concrete and steel coincide in the pull-out tests while the maximum stress exists at the point of zero slip in the end block. In addition, the strand in a pull-out specimen undergoes a radial contraction as it is pulled out of the concrete, thus reducing the radial pressure between the strand and the concrete, while the strand in an end block undergoes an expansion when the pretension force is released causing an increase in the radial pressure between the strand and the concrete. To investigate the effect on bond of these differences in stress conditions, some tests were conducted on a special prestressed pull-out specimen in which the conditions are analogous to those in an end block. In this type of specimen, the strand was first pretensioned in the test frame and the concrete cast around the strand. The strand was then "released into the concrete" rather than pulled out of it.

The second part of the investigation was concerned primarily with flexural bond. The main objective was to provide basic information for use in the determination of length of embedment required to develop the strength of the strand in flexure. Since the standard pull-out test is a quick and inexpensive test to perform, it would be desirable to use such a specimen to investigate flexural bond. But again, the conditions existing in a standard pull-out specimen are different from those in the tension region of a beam. In the latter, the concrete is in longitudinal tension and no radial stresses exist. To investigate the effect of these differences in stress conditions on flexural bond, a special twin pull-out specimen was devised (Sketch 1.1c). The stress conditions in this type of specimen are analogous to those existing in the region between two tension cracks in a beam as can be seen by comparing the free body sections from the beam and the twin pull-out specimen given in (b) and (d) of Sketch 1.1.

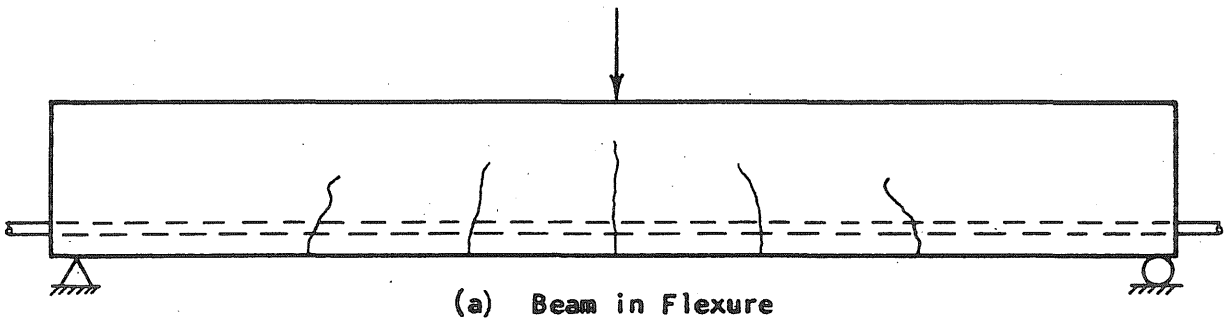

(a) Beam in Flexure

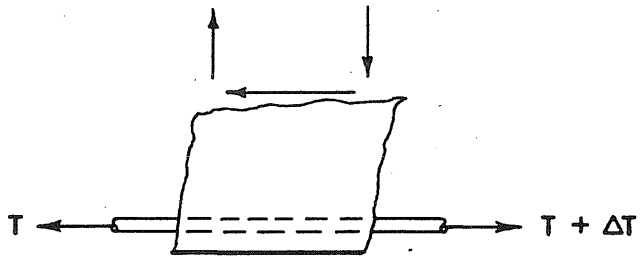

(b) Free Body, Region Between Two Tension Cracks

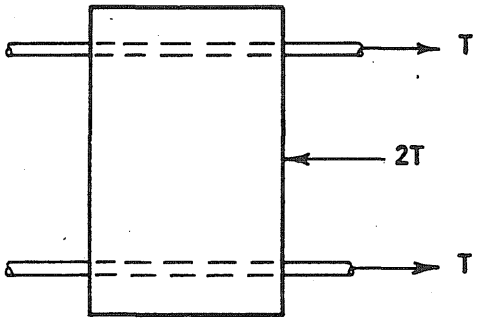

(c) Twin Pull-Out Specimen

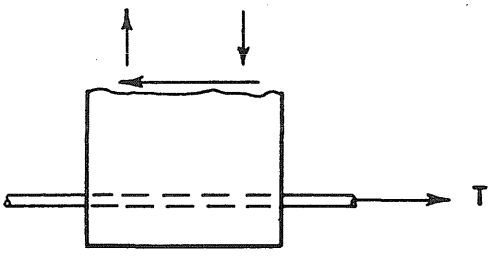

(d) Free Body, Bottom Half Twin Pull-Out Specimen

SKETCH 1.1

Also included in this part of the investigation were 7 beam tests containing non-prestressed 7/16-in. round strand. Three of the beams were 72 in. long while the remaining four were 104 in. long.

1.3 Outline of Tests

A total of 74 specimens were tested in six series as indicated below:

Series	No. of Specimens	Type of Test	Strand
7	13	Standard Pull-out	1/4-in. 3-wire rectangular-wire strand
7	4	Prestressed Pull-out	1/4-in. 3-wire rectangular-wire strand
8	30	Standard Pull-out	7/16-in. 7-wire round-wire strand
9	16	Standard Pull-out	7/16-in. 7-wire rectangular-wire strand
10	4	Twin Pull-out	7/16-in. 7-wire round-wire strand
72-in. Beam	3	Flexure	7/16-in. 7-wire round-wire strand
104-in. Beam	4	Flexure	7/16-in. 7-wire round-wire strand

All of the tests were made on clean strand. The specimens of Series 7 had a cross section measuring 4 by 4 in. Embedment lengths of 1 1/2, 3,6, and 9 in. were used. Companion prestressed specimens of 3-in. length were cast with the 3-in. pull-out specimens. The cross sections of all of the specimens used in Series 8 and 9 measured 6 by 6 in. It was necessary to use a larger cross section here than in Series 7 in order to prevent splitting of the specimens under the higher loads attained in these tests. Embedment lengths of 6, 12, 18, 24, 30, and 36 in. were used in Series 8 and lengths of 3, 6, 12, 18 and 24 in. were used in Series 9. These embedment lengths were chosen such that the test loads would vary from some small value up to the strength of the strand. In all of the specimens of Series 7, 8, and 9 the strand passed lengthwise through the center of the block.

The twin pull-out specimens of Series 10 each contained two strands embedded at mid-height 9 in. on center in a block of concrete having a 6 by 15-in.

cross section. Three of the specimens were 6 in. long while the fourth was 7 in. long.

The specimens of Series 7, 8, 9, and 10 were designated by two letters and two or three numbers, e.g. N712a. The first letter refers to the state of stress of the reinforcement. The letter N indicates the reinforcement was non-prestressed, whereas the letter P refers to a specimen in which the reinforcement was prestressed. The first numeral refers to the series number except for the specimens of Series 10 where the first two numbers refer to the series. The second numeral indicates the length of the specimen in inches, except for the 1 1/2-in. specimens which are designated as 1. The lower case letter differentiates between tests which were otherwise identical.

All of the beams tested contained only one non-prestressed strand located in the center of the beam at a depth of 6 1/2 in. Each beam was 8-in. wide and had 1 1/2-in. cover below the strand. The beams were loaded at mid-span and had roller supports 1 in. from each end. Each beam was designated by three or four numbers and one letter, e.g. 104-2N. The numbers to the left of the hyphen give the over-all length of the beam while the number to the right differentiates between beams of the same length. The letter, when used, refers to the end of the beam in question, N for north and S for south.

For detailed descriptions of the strands, casting procedures, instrumentation, and so forth, see the Appendices.

1.4 Acknowledgments

This study was carried out as a part of the research under the Illinois Cooperative Highway Research Program Project IHR-10, "Investigation of Prestressed Reinforced Concrete for Highway Bridges." The work on the project was conducted by the Department of Civil Engineering of the University of Illinois in cooperation with the Division of Highways, State of Illinois, and the U. S. Department of Commerce, Bureau of Public Roads.

On the part of the University, the work covered by this report was carried out under the general administrative supervision of W. L. Everitt, Dean of the College of Engineering, Ross J. Martin, Director of the Engineering Experiment Station, N. M. Newmark, Head of the Department of Civil Engineering, and Ellis Danner, Director of the Illinois Cooperative Highway Research Program and Professor of Highway Engineering.

On the part of the Division of Highways of the State of Illinois, the work was under the administrative direction of Virden E. Staff, Chief Highway Engineer, Theodore F. Morf, Assistant Chief Highway Engineer, and J. E. Burke, Engineer of Research and Development.

The program of investigation has been guided by a Project Advisory Committee consisting of the following:

Representing the Illinois Division of Highways

J. E. Burke, Engineer of Research and Development, Illinois Division of Highways

W. J. Mackay, Bridge Section, Bureau of Design, Illinois Division of Highways

C. E. Thunman, Jr., Bridge Section, Bureau of Design, Illinois Division of Highways

Representing the Bureau of Public Roads

Harold Allen, Chief, Division of Physical Research, Bureau of Public Roads

E. L. Erickson, Chief, Bridge Division, Bureau of Public Roads

Representing the University of Illinois

C. E. Kesler, Professor of Theoretical and Applied Mechanics

Narbey Khachaturian, Professor of Civil Engineering

Fred Kellam, Bridge Engineer, Bureau of Public Roads and George S. Vincent, Chief, Bridge Research Branch, Bureau of Public Roads, also participated in the meetings of the Advisory Committee and contributed materially to the guidance of the program.

A special note of acknowledgment is due the late Mr. W. E. Chastain, Sr. for his personal interest in and guidance of the project.

The investigation was directed by Dr. C. P. Siess, Professor of Civil Engineering, as Project Supervisor and as ex-officio chairman of the Project Advisory Committee. Immediate supervision of the investigation was provided by Dr. M. A. Sozen, Professor of Civil Engineering, as Project Investigator.

2. PULL-OUT TEST RESULTS

2.1 Introductory Remarks

The method of fabrication and the materials used in the pull-out specimens are given in Appendix A. Appendix B provides descriptions of the instrumentation and test procedure used in each series of tests.

Table 1 presents the data on the concrete mixes used for the various specimens and the compressive and tensile strengths attained. The compressive strengths of the pull-out specimens at time of test ranged from 3440 to 5120 psi. The tensile strengths, based on splitting tests of 6 by 6-in. cylinders, ranged from 290 to 440 psi.

The basic results from the pull-out tests are reported in the form of measured load-slip curves for the attack and trail ends of the specimen. The attack end is defined as the end first to experience a relative movement between the concrete and reinforcement. The trail end is the end opposite the attack end. These curves are presented in Figs. 2.1 through 2.38. Each point on a given curve indicates the relative movement between the strand and the concrete at the face of the specimen when the corresponding force was being carried by the specimen.

Each figure presenting load-slip curves contains a table giving the compressive strength (f'_c), the tensile strength (f_t), and the average loading rate (ALR) of each of the specimens whose load-slip curve appears in that figure. The values of average loading rates were obtained by dividing the total load applied to the specimen by the total time it took to apply this load in increments. It was necessary to load the specimens containing the 7/16-in. diameter strand at a much faster rate than the specimens containing the 1/4-in. diameter strand because of the difference in total loads required to produce the desired amount of trail end slip or the strength of the strand.

During the tests of Series 7 through 10, it was observed that the strand rotated as it was pulled into the concrete. The rotation was not measured. At a trail end slip of 0.3 in., the rotation was on the order of 15^{o}.

In some of the specimens the load applied to the strand was large enough to cause one or more wires of the strand to break. Such a break in the strand always occurred inside the grip.

In Figs. 2.39 through 2.42 are presented the average load-slip curves for the specimens of Series 7 through 10. The average curves were obtained by averaging the loads of the individual curves at a given slip. The concrete strengths and average loading rates shown in these figures are also average values.

2.2 Series 7, 1/4-in. Rectangular-Wire Strand

The measured load-slip curves for Series 7 are presented in Figs. 2.1 through 2.10. The 17 tests in this series were conducted on 1/4-in. nominal diameter 3-wire rectangular-wire strand embedded in blocks of concrete having a 4 x 4-in. cross section. Concrete compressive strengths ranged from 4320 to 5120 psi and tensile strengths from 375 to 395 psi. All of the strand used was cut from the same roll (S4A3-1). All slips were measured by use of metal strips and traveling microscopes as explained in Appendix B.

Figures 2.1 and 2.2 contain the attack and trail-end measured load-slip curves for the 1 1/2-in. specimens. The curve corresponding to specimen N71c is considerably below the other three curves. Possible reasons for this were the slower rate of loading, improper alignment of the specimen in the test frame, or insufficient vibration of the specimen at the time of casting. This specimen was split after completion of the test and a large number of air pockets were observed around the strand. This can be ascribed to insufficient vibration.

Curves for the attack and trail ends of the 3-in. specimens are shown in Figs. 2.3 and 2.4. Specimen N73c had a slightly higher rate of loading than the

other specimens which may account for its higher values.

The curves for the prestressed specimens of 3-in. embedment length are shown in Figs. 2.5 and 2.6. The load-slip curves for P73a, P73b, and P73c have a broken line section which indicates the point at which the entire prestress force had been released. The portion of the curve to the right of this section was obtained by applying load to the trail end after the complete release of the prestress. The test on specimen P73d was discontinued at a low load because of damage to the metal strips used to measure slip.

Figures 2.7 and 2.8 contain the results of the 6-in. specimens. In the test curve for specimen N76a, the broken line segment represents slip that occurred when the load was removed and then reapplied to allow changing of the dynamometer. This specimen split at the maximum load attained. The test on specimen N76d was discontinued because the metal strips used to measure slip became dislocated early in the tests.

Only one specimen of 9-in. embedment length was tested and its load-slip curves are given in Figs. 2.9 and 2.10. The test was discontinued at the load indicated because excessive yielding of the strand made further loading difficult.

Average load-slip curves for each embedment length used in this series are shown in Fig. 2.39. These curves represent slips measured at the trail ends. Out of the four tests conducted for each of the 1 1/2, 3, and 6-in. embedment lengths, only three were used in computing the average since in each case, the fourth test did not give results consistent with the other three. The specimens omitted were N71c, N73d, P73d, and N76d. No average curve is presented for the 9-in. length as only one specimen was tested. The average value of concrete strength and loading rate for each length is also presented.

These average curves show that for all embedment lengths the load increased as slip progressed, the initial rate of increase being the greatest and then decreasing

to a smaller almost constant value at larger slip. A maximum load was never attained in the tests of any of the specimens.

2.3 Series 8, 7/16-in. Round-Wire Strand

This series of tests consisted of 30 pull-out specimens having 7/16-in. nominal diameter 7-wire round-wire strand embedded in concrete blocks of 6 x 6-in. cross section. The concrete compressive strengths ranged from 3440 to 4960 psi and the tensile strengths from 290 to 440 psi. All of the strand used was made by the same manufacturer and was cut from the same roll (R7W7-1) except that used in specimensN824a, N824b,N824c, and N824d which was cut from roll R7A7-1. The strand used in these four specimens was manufactured by a different company. All 30 specimens were tested at an age of 7 days. The attack-end slip of each specimen was measured with a traveling microscope as explained in Appendix B. The load applied to the strand was increased in increments until the trail end had slipped 0.30 in. or the strength of the strand was developed.

The attack and trail-end load-slip curves for the four 6-in. specimens are presented in Figs. 2.11 and 2.12. All of these specimens show a slightly increasing load as the slip increases.

The load-slip curves for the 12-in. specimens are presented in Figs. 2.13 and 2.14. Only three specimens of this length were tested since the results were relatively consistent. The curves for N812b and N812c exhibit a nearly elasto-plastic condition by leveling off after a trail-end slip of about 0.03 in.

Figs. 2.15 and 2.16 contain the curves for the 18-in. specimens. Slip readings for the attack end of N818a were not taken and hence there is no load-slip curve for the attack end of the specimen. The higher values of N818c cannot be attributed to either a high rate of loading or concrete strength.

Figs. 2.17 through 2.20 contain the attack and trail-end load-slip curves for the 24-in. specimens. There were a total of 11 specimens of this embedment length. The results of specimens N824a, N824b, N824c, and N824d were quite inconsistent as shown in Figs. 2.17 and 2.18. No insight as to the reason for this inconsistency can be gained from comparing the concrete strengths or the average loading rate values. This inconsistency may have resulted from some peculiarity of the strand, since the strand used in these four specimens was made by a different manufacturer than that used in the other specimens of this series.

The results from the tests on the remaining seven 24-in. specimens whose load-slip curves appear in Figs. 2.19 and 2.20, are relatively consistent with the exception of N824k. It was necessary to discontinue the test on N824j before reaching a trail-end slip of 0.30 in. since the strand grip broke at a load of 19 kips.

The results from the 30-in. specimens are presented in Figs. 2.21 and 2.22. As these results are relatively consistent only three specimens were tested.

Figs. 2.23 and 2.24 contain the load-slip curves for the four 36-in. specimens. The test on N836a was discontinued at a trail-end slip of 0.04 in. because the strand grip broke at this point. The attack-end load-slip curve for N836b does not go beyond 0.20 in. because the slip measurement instrumentation on this end did not function properly beyond this point. However the test was continued until the trail end had slipped over 0.30 in. The test on N836c was discontinued after a load of 27 kips had been attained due to excessive yielding of the strand.

The average trail-end load-slip curves for specimens of this series are presented in Fig. 2.40. All of the tests on the 6, 12, 30, and 36-in. specimens were included in the averaging procedure. However the average curve for the 18-in. specimens does not include N818c since the results for this specimen were inconsistant. Specimens N824a, N824b, N824c, and N824d were excluded from the 24-in. specimen average for the same reason. In addition, the average curve for the 36-in. specimens between a slip of 0.04 and 0.12 in. is obtained by averaging the results of only three specimens and beyond a slip of 0.12 in. it is obtained by averaging the results

of only two specimens. The slope of each of these curves is greatest at the point of initial trail-end slip and gradually decreases as the slip progresses. However a maximum load was never attained in any of the specimens.

2.4 Series 9, 7/16-in. Rectangular-Wire Strand

The load-slip curves shown in Figs. 2.25 through 2.34 are for the tests conducted on the 16 specimens with 7/16-in. nominal diameter 7-wire rectangular-wire strand embedded in concrete blocks of 6 x 6-in. cross section. The concrete compressive strengths for these specimens ranged from 4320 to 4730 psi. All of the strand used in this series was cut from the same roll (S7A7-2). A traveling microscope and metal strips were used to measure trail-end slips while the attack-end slips were measured with a dial gage as explained in Appendix B.

Figs. 2.25 and 2.26 contain the load-slip curves for the attack and trail ends of the 3-in. specimens. These tests were discontinued after a trail-end slip of about 0.3 in. had been reached.

The results of the tests on the three 6-in. specimens are presented in Figs. 2.27 and 2.28. In all three tests the specimen split at the maximum load shown.

Load-slip curves for the 12-in. and 18-in. specimens are shown in Figs. 2.29 through 2.32. In all cases the tests were discontinued at the loads shown because of excessive yielding or actual breaking of the strand.

The results of the 24-in. specimens are given in Figs. 2.33 and 2.34. The test on N924a was discontinued when the strand broke while that on N924b and N924d was discontinued due to excessive yielding of the strand. The attack-end load-slip curve of N924c does not go beyond 0.04 in. because the slip measurement instrumentation did not function properly beyond this point. However the test was continued and trail-end slip readings taken until the strand grip broke at a load of about 21 kips.

Figure 2.41 presents the average trail-end load-slip curves for specimens of Series 9. All the specimens of each embedment length were included in the averaging procedure. The average concrete strengths and loading rates for each embedment length are also given. For all embedment lengths, the load increased as slip progressed, the initial rate of increase being the greatest and then decreasing to a smaller almost constant value at larger slips. A maximum load was never attained in any of the specimens.

2.5 Series 10, Twin Pull-out Tests

The twin pull-out test is a modified pull-out test in which the loading conditions are such as to make the concrete stresses in the specimens analogous to the concrete stresses which exist in the region between two tension cracks in a beam. (For a more detailed explanation of this type of specimen see Section 1.2 and Appendix B.)

In the twin pull-out tests conducted in this series, two 7/16-in. nominal diameter 7-wire round-wire strands were embedded in concrete blocks of 6 x 15-in. cross section as described in Section A.2. All of the strand used was cut from the same roll (R7W7-1) as that used in the specimens of Series 8. All four twin pull-out specimens were 7 days old when tested. The attack-end slips were measured with dial gages and the trail-end slips with a traveling microscope and metal strips as described in Appendix B. The load was applied in constant load increments until a trail-end slip of about 0.25 in. was measured.

Figures 2.35 and 2.36 present the attack and trail-end load-slip curves for the three 6-in. specimens of this series. Since each specimen contains two strands there are a total of six load-slip curves. The results are relatively consistent.

Figures 2.37 and 2.38 contain the load-slip curves for the single 7-in. specimen tested.

The average load-slip curve for the 6-in. specimens of this series is given in Fig. 2.42. The result of all three specimens were included in this average curve. The average concrete strength and loading rate are also given in this figure.

3. DISCUSSION OF PULL-OUT TEST RESULTS

3.1 Unit Bond-Slip Curves

One of the goals of this study was to determine a unit bond-slip relationship for an infinitesimal length of each type and size of strand studied. If the amount of strain occurring at several points along the strand in a pull-out specimen is known it is possible to obtain the unit bond-slip curve directly from this information. About the only way such strain values can be obtained directly is from strain gages. But because of the irregularity in the strand surface, the installation of strain gages is quite difficult and at best, any results obtained from such gages would be questionable. Because of this, it was decided to approach the problem differently.

Each series of tests contains specimens of various lengths such as shown in Sketch 3.1. Consider these specimens to be identical in every way except for the lengths of embedment. If the trail-end slip of each specimen is the same, it is plausible to assume that the 12-in. specimen is identical to the first 12 in. of the 24-in. specimen, measured from the trail end, and that the 3-in. specimen is identical to the end 3-in. section of the 24-in. specimen. Thus the forces P_3 and P_{12} should be the force in the strand 3 in. and 12 in. respectively from the trail end of the 24-in. specimen. Since the values of P_3, P_{12}, and P_{24}, for the same trail-end slip, can be obtained from the load-slip curves, we can obtain the strand force distribution in the 24-in specimen as shown in 3.1a. If the stress-strain relationship and the cross-sectional area of the strand are known, the value of strain corresponding to each value of strand force can be calculated yielding the strain distribution curve as shown in 3.1b. The difference in the strand force between two points on the strand is the amount of force which has been transferred to the the concrete by means of bond.

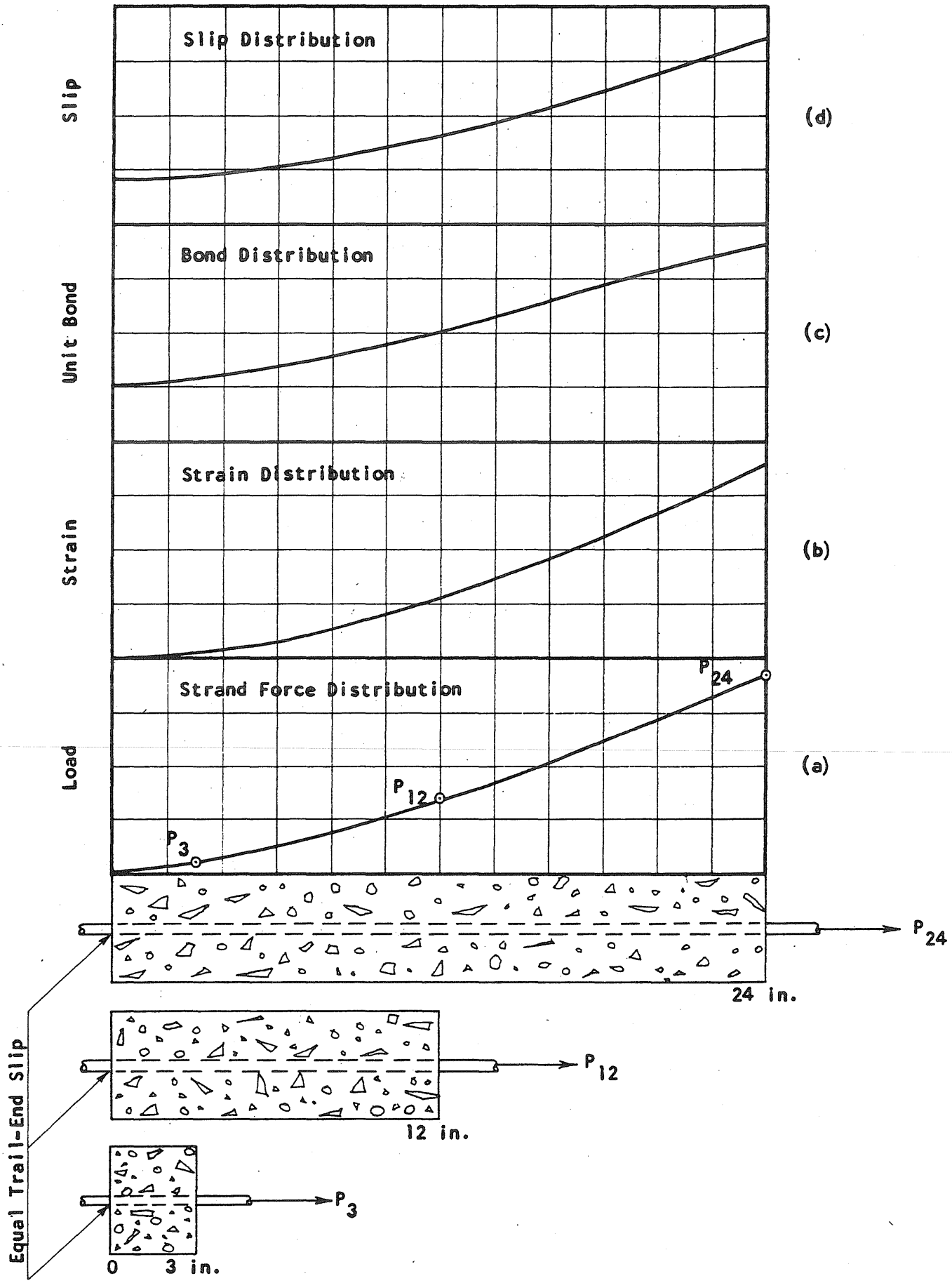
Slip Distribution
Slip
(d)
Bond Distribution
Unit Bond
(c)
Strain Distribution
Strain
(b)
Strand Force Distribution
Load
(a)
P_{24}
P_{12}
P_3
P_{24}
24 in.
P_{12}
12 in.
P_3
0
3 in.
Equal Trail-End Slip

SKETCH 3.1

If the two points are a distance ΔL apart and the difference in strand force is ΔP, the average bond per unit length of strand which must act over ΔL is $\Delta P/\Delta L$. Taking the limit of this quantity as ΔL approaches zero shows that the bond acting at a point is equal to the corresponding slope of the strand force distribution curve. Thus the bond distribution along the length of the strand can be determined as in 3.1c. If the concrete strain is neglected, the relative movement between the concrete and strand, which will be referred to as slip, results from the strain in the strand. Thus, in general, the amount of slip between the concrete and the strand at any point can be determined by measuring the area under the strain distribution curve between the point of zero strain and the point in question. However, if slip has occurred at the trail end of the specimen, the above value of slip must be increased by the amount of trail-end slip which the specimen has experienced. Thus, by summing the areas under the strain distribution curve, the slip distribution along the length of the specimen as shown in 3.1d can also be determined. Knowing the slip distribution and the bond distribution along the length of the specimen, it is now possible to plot the corresponding values of slip and unit bond to obtain the unit bond-slip curve.

Figures 3.1 through 3.12 contain the values of strand force (load) obtained from the trail-end load-slip curves of Series 7, 8, and 9. If a curve was drawn through these points it would represent the strand force distribution in that length of specimen at the indicated value of trail-end slip. To clarify this, consider Fig. 3.3. This plot is assumed to represent the strand force at various points in a 9-in. specimen of Series 7 at a trail-end slip of 0.04 in. The values of strand force plotted at 1 1/2, 3, 6, and 9-in. embedment were obtained from the individual trail-end load-slip curves of the 1 1/2, 3, 6, and 9-in. specimens of Series 7, all at a trail-end slip of 0.04 in. Figure 3.4 also represents the strand force distribution in a 9-in. specimen of Series 7, but this time for a trail-end slip of 0.100 in.

There are also two other plots for a 9-in. specimen of this series, one for zero trail-end slip (strand at point of incipient trail-end slip) and the other for 0.010 in. trail-end slip. Similarly, Figs. 3.5 through 3.8 are plots representing the strand force at various points in a 36-in. specimen of Series 8 for four different values of trail-end slip. Again, the plotted values at the various embedment lengths were obtained from the load-slip curves of the individual specimens. Figures 3.9 through 3.12 give the strand force at various points in a 24-in. specimen of Series 9.

The procedure outlined earlier for obtaining the unit bond-slip curve is quite sensitive to differentiation. Thus, since the bond distribution is obtained by differentiating the strand force distribution curve, it is seen that the slope, and thus the shape, of the strand force distribution curve is very important, Referring back to the plots of load versus embedment contained in Figs. 3.1 through 3.12 it is seen that at best any curve drawn through the plotted points would be somewhat arbitrary due to the scatter of test results. Hence this procedure does not yield very good results. However, if the outlined procedure is reversed there is no differentiation involved. Now it is necessary to first assume the unit bond-slip curve after which a numerical procedure can be used to work backwards to obtain the corresponding force distribution curves.

Sketch 3.2 contains an explanation of the numerical procedure used. First the specimen is broken up into a convenient number of equal intervals ΔL. The smaller this interval is taken, the more accurate will be the results. For the moment assume that the slip δ_n at some point n is known. The corresponding value of unit bond g_n, obtained from the assumed unit bond-slip curve, is assumed to act across the interval n. Thus the change in strand force from n to n + 1 is

$$\Delta P_n = g_n \Delta L$$

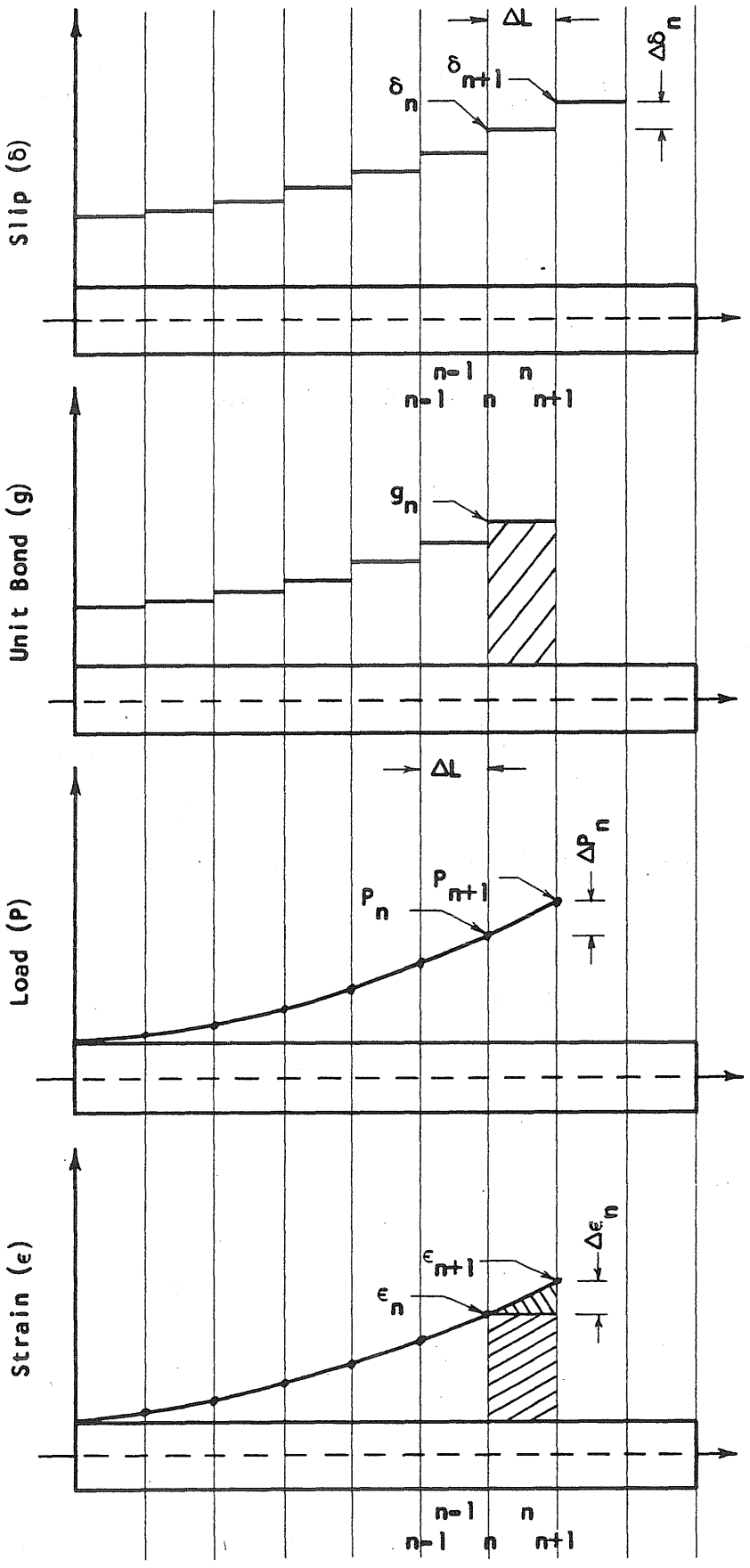

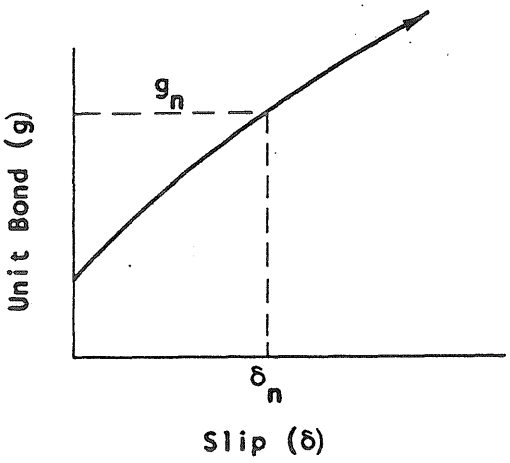

$$\Delta P_n = g_n \Delta L$$

$$P_{n+1} = P_n + g_n \Delta L$$

$$\Delta \epsilon_n = \frac{\Delta P_n}{AE}$$

$$\epsilon_{n+1} = \epsilon_n + \frac{g_n \Delta L}{AE}$$

$$\Delta \delta_n = \epsilon_n \Delta L + \frac{\Delta \epsilon_n}{2} \Delta L$$

$$\delta_{n+1} = \delta_n + \epsilon_n \Delta L + \frac{g_n \overline{\Delta L}^2}{2AE}$$

SKETCH 3.2

and therefore,

$$P_{n+1} = P_n + g_n \Delta L. \tag{3.1}$$

The corresponding change in strain is

$$\Delta\epsilon_n = \frac{\Delta P_n}{AE}$$

where A is the cross-sectional area of the strand and E is the modulus of elasticity. This gives the total strain at n+1 as

$$\epsilon_{n+1} = \epsilon_n + \frac{\Delta P_n}{AE}$$

or

$$\epsilon_{n+1} = \epsilon_n + \frac{g_n \Delta L}{AE} . \tag{3.2}$$

The increase in slip from n to n+1 is the area under the strain curve over the interval n,

$$\Delta\delta_n = \epsilon_n \Delta L + \frac{\Delta\epsilon_n}{2} \Delta L.$$

Thus

$$\delta_{n+1} = \delta_n + \epsilon_n \Delta L + \frac{\Delta\epsilon_n}{2} \Delta L$$

or

$$\delta_{n+1} = \delta_n + \epsilon_n \Delta L + \frac{g_n \overline{\Delta L}^2}{2AE} . \tag{3.3}$$

Knowing δ_{n+1} it is now possible to repeat the procedure to find δ_{n+2} and so forth until the end of the specimen is reached. This procedure must be started at the trail end of the specimen where the desired amount of trail-end slip is assumed to have occurred. If the strand force distribution obtained in this manner is not sufficiently close to that obtained from the test data, it is an indication that the assumed shape of the unit bond-slip curve is wrong and must be adjusted. This process is repeated until the unit bond-slip curve is obtained which yields a strand force distribution close to the distribution indicated by specimens of various lengths.

Using a digital computer to make the necessary calculations in this numerical procedure, the unit bond-slip curves given in Fig. 3.13 were obtained for the 1/4 and 7/16-in. diameter rectangular strand and the curve in Fig. 3.14 was obtained for the 7/16-in. round strand. These curves are valid up to a slip of approximately 0.15 in. An incremental length of ΔL = 1/2 in. and a modulus of elasticity of E = 28 (10^6) psi were used for all three strands. The following cross-sectional areas were used; for the 1/4-in. 3-wire rectangular-wire strand of Series 7, A = 0.0359 $in.^2$; for the 7/16-in. 7-wire round-wire strand of Series 8, A = 0.1089 $in.^2$; for the 7/16-in. 7-wire rectangular-wire strand of Series 9, A = 0.1089 $in.^2$

The unit bond-slip curve for the 1/4-in. rectangular strand (Series 7) in Fig. 3.13 is given by the equation

$$g = 250 + 3000\,\delta + 1500\,\sqrt{\delta} \qquad (3.4)$$

where

g = unit bond in pounds per inch of strand

δ = slip between the concrete and strand in in.

The strand force distributions corresponding to this curve are given by the solid lines in Figs. 3.1 through 3.4. For a trail-end slip of zero, the calculated values are a little high for an embedment greater than 3-in. However, for the remaining values of trail-end slip, the calculated strand force distributions are somewhat low, forming a reasonable lower bound to the test values. In Fig. 3.4, for a trail-end slip of 0.100 in., the calculated strand force distribution curve is given by a broken line above a load of 6.5 kips. This is done because the procedure used to obtain this curve is based on the assumption of a linear stress-strain curve for the strand. Figs. A.3 and A.4 indicate that this is a reasonable assumption only up to about 180 ksi for all three strands under consideration. This corresponds to a force of about 6.5 kips for the 1/4-in. rectangular strand.

The equation

$$g = 250 + 3000\,\delta + 3500\,\sqrt{\delta} \qquad (3.5)$$

defines the unit bond-slip curve given in Fig. 3.13 for the 7/16-in. rectangular strand. The strand force distributions in a 24-in. specimen corresponding to this curve are given by the solid lines in Fig. 3.9 through 3.12. Again, an attempt was made to obtain a unit bond-slip curve which would give a reasonable lower bound to the loads obtained from the test data. The strand force distribution curve is given by a broken line for loads greater than 19 kips because the linear stress-strain assumption is not valid beyond this strand force.

The equation of the unit bond-slip curve given in Fig. 3.14 for the 7/16-in. round strand of Series 8 is

$$g = 300 + 600\,\delta + 600\,\sqrt{\delta} \qquad (3.6)$$

The strand force distributions corresponding to this curve for the various values of trail-end slip are given by the solid lines in Figs. 3.5 through 3.8. As in Series 7, an attempt was made to get a reasonable lower bound to the values of strand force obtained from the test data. The calculated strand force distribution curve for a zero trail-end slip is somewhat high for a lower bound between an embedment of 18 and 24 in. However, for the other values of trail-end slip, the calculated curve does form a reasonable lower bound on the test data. It is to be noted though, that this lower bound is always dictated by the 18 and 24 in. embedment lengths. The lowest value in the scatter band for the 6, 12, 30, and 36 in. embedments is considerably above the calculated strand force distribution curve in every instance. The calculated strand force distribution for a trail-end slip of 0.100 in. is given by a broken line above 19 kips because the linear stress-strain assumption is not valid beyond this strand force.

The unit bond-slip curve for the 1/4-in. 7-wire round-wire strand of Series 1 investigated by Keuning[1] is also presented in Fig. 3.14. Although the load-slip curves for this strand displayed an increase in load after slip had occurred at the trail end, the load-slip curves for these specimens exhibited a nearly elasto-plastic condition by leveling off to a sustained load not greatly below the maximum load. This can be seen in Fig. 3.17, which contains the average load-slip curves for the 6-in. specimen containing the 1/4 and 7/16-in. round strands. A constant unit bond-slip relation given by

$$g = 350 \text{ lb per in.} \tag{3.7}$$

was found to be a reasonable lower bound to the values of sustained unit bond which Keuning reported for this strand.

3.2 Effect of Stress Conditions on Bond

The stress conditions existing in a standard pull-out specimen are different from those in an actual pretensioned beam in both the anchorage zone and in the flexural tension zone as explained in Section 1.2.

To obtain an idea of the effect on bond of the different state of stress which occurs in the anchorage zone, a special prestressed pullout specimen was used. A description of this specimen and how it was set up and tested is given in Sections A.2 and B.4. A comparison of the results obtained from the prestressed and standard pull-out specimens containing the 1/4-in. rectangular strand of Series 7 is shown in Fig. 3.18. The curves presented are the average load-slip curves for the trail ends of the 3-in. specimens. Although both curves are of the same nature, the prestressed specimens attained higher loads at all levels of slip. However, it was felt that this difference was not great enough to warrant using only the more expensive and time consuming prestressed specimens in the investigation of anchorage zone bond. The results of the standard pull-out test are significant and on the safe side. Keuning [1] reached the same conclusion from a similar comparison of prestressed and standard pull-out specimens containing 1/4-in. round strand.

The state of stress in a twin pull-out specimen of Series 10 is analogous to that which exists in the region between two tension cracks in a beam as explained in Section 1.2. In this specimen the concrete is in longitudinal tension and no regions of radial tension and compression exist. In the standard pull-out specimen the concrete is in longitudinal compression and there are regions of radial tension and compression due to the boundary conditions. The effect of these different stress conditions on the bond properties of 7/16-in. round-wire strand is shown in Fig. 3.19 where the average load-slip curves of the 6-in. specimens of Series 9 and 10 are presented. Although both curves are of the same nature, the standard pull-out specimen attained higher loads at all levels of slip. Thus, the stress conditions

present in a pull-out specimen do increase the bond somewhat above that which is developed in a twin pull-out specimen. Hence, while the results of the pull-out test are significant, they are on the unsafe side and therefore should not be used to predict flexural bond. However, it is believed that the effect of the radial compression in a standard pull-out specimen decreases with increasing embedment length. Therefore, the difference in "pull-out bond" and flexural bond may be considerably less for longer embedment lengths.

A comparison of the results from the individual 6-in. standard and twin pull-out specimens can be seen in the plots of load versus embedment length for Series 8 contained in Figs. 3.5 through 3.8. The two scatter bands just touch or overlap slightly at every value of trail-end slip.

3.3 Comparison of Bond Characteristics of Round and Rectangular-Wire Strand

Figure 3.15 contains the unit bond load-slip curves obtained for the two types of 7/16-in. diameter strand. Both of these curves were obtained by the procedure described in Section 3.1. Although the unit bond of each type of strand continues to increase as slip progresses, the rate of increase is much greater for the rectangular strand. The unit bond of the rectangular strand is over twice as great as that of the round strand beyond a slip of about 0.02 in. However, it is to be noted that the unit bond at first slip is about the same for both types of strand.

Figure 3.16 contains the unit bond-slip curves obtained for the two types of 1/4-in. diameter strand. The curve for the rectangular strand was obtained by the procedure described in Section 3.1 while that for the round strand was found to be a reasonable lower bound on the results reported by Keuning. Since one of these strands is a 7-wire strand while the other is only a 3-wire strand, these curves can not be compared directly. However, from the general shape of the curves it is seen that the basic difference between the bond characteristics of the two types of

strand of this diameter is that while the bond increases with increased slip for the rectangular strand, the round strand shows little or no increase in bond with slip.

Thus it is seen that after initial slip, the rectangular-wire strand has better bonding qualities than the corresponding round-wire strand. This can be attributed to the shape and orientation of the wires in the rectangular-wire strand. These wires are not round or flat but are a combination of the two which provides angular grooves and rounded areas as shown in Fig. A.2. These wires are wound to form the strand in such a manner that the rounded and flattened sides of the wires lie in the same plane at all points along the length of the strand. That is, the orientation of the cross section of each wire is the same at any point along the strand. The wires in a round-wire strand have no specific orientation since the wires are round.

When a strand embedded in concrete is subjected to a tensile force, it will not slip until the adhesion between the strand and the concrete is overcome. From the unit bond-slip curves it is seen that the adhesive force is about the same for both types of strand. After it starts to slip, however, the strand has a tendency to rotate or twist out of the concrete in the manner of a screw. For such a twisting or screwing action to occur, there has to be a change in the orientation of the individual wires of the strand. The rectangular strand resists such a change in orientation, causing a special locking action to be set up between the concrete and the strand. The round-wire strand has no such special locking action between the strand and the concrete resisting the change in orientation of the wires since these wires are round and not angular. This locking action causes the resistance to slip of the rectangular strand to be greater than the resistance to slip of the round strand. Thus, the rectangular strand has better bonding qualities than the corresponding round strand after first slip.

4. ANCHORAGE LENGTH

4.1 Introductory Remarks

The anchorage length of a prestressing strand may be defined as the length required to anchor fully the pretensioning load. This length is that over which slip occurs between the strand and concrete as the load is released. It should not be confused with transfer or development length. The transfer length is the distance from the end of the member to the cross section where the distribution of the stress becomes linear and equal to the full effective prestress. The development length is defined as the least length of embedment required to develop the desired strand force regardless of the amount of slip incurred. For prestressing strand, the transfer length is larger than the anchorage length but the development length is equal to or less than the anchorage length.

By definition, the slip at one end of the anchorage length is equal to zero. This condition could be represented by a pull-out test specimen whose strand is loaded to the point of incipient trail-end slip. The load which caused first trail-end slip would be that load which could be anchored in a length equal to the length of the specimen. Therefore a plot of the strand loads attained at zero trail-end slip for the various embedment lengths can be used to estimate the anchorage length required for any pretensioning force.

4.2 1/4-in. Strand

The constant unit bond-slip curve of Fig. 3.14 was found to be a lower bound approximation to results of tests on 1/4-in. round-wire strand reported by Keuning[1]. If the bond is constant for all degrees of slip, the result is the linear relation between strand force and embedment length presented in Fig. 4.1. On the basis of this linear projection of the test results, the required anchorage length for an effective prestress of 150 ksi would be 15 1/2 in.

The results of the pull-out tests on the 1/4-in. rectangular-wire strand are presented in Fig. 3.1. The unit bond-slip curve for this strand as derived in the discussion of the pull-out tests is given in Fig. 3.16. Because the bond capacity of this strand increases with increased slip, a curve with an increasing slope must be used to approximate the strand force-embedment length relation. The curve derived in the pull-out discussion (Fig. 3.1) is presented and extended in Fig. 4.1. The predicted anchorage length for an effective prestress of 150 ksi is 13 1/2 in.

Comparing the round and rectangular strand of 1/4-in. diameter, the anchorage lengths are the same at an effective prestress of 98 ksi (strand force = 3500 lb). As seen in Fig. 4.1, for a higher level of prestress, the anchorage length of the rectangular-wire strand will be smaller than that required for the round strand. The opposite is true for prestress levels below 98 ksi. This is a direct result of the difference in the unit bond-slip curves for the two strands as seen in Fig. 3.16. In an anchorage length of 10 in., the maximum strand slip would be on the order of 0.015 in. and the average slip around 0.005 in. From the unit bond-slip curves, it is seen that the bond capacity of the rectangular strand is less than that of the round strand for slips less than 0.004 in. It is therefore reasonable that the anchorage length of the rectangular strand be the longest for prestress levels and slips less than those above.

If the development length of the strand were being considered, the rectangular strand would have a large advantage over the round strand. The reason for this advantage can be seen in Fig. 3.16. The bond capacity of the rectangular strand is on the order of three times that of the round strand at slips over 0.1 in.

4.3 7/16-in. Strand

Figure 3.5 presents the results of the tests on the 7/16-in. round-wire strand. As for the 1/4-in. rectangular strand, the unit bond-slip curve for this strand seen

in Fig. 3.15 shows increased bond with increased slip and therefore the relation between strand force and embedment length must be represented by a curve. The curve for this strand was derived in the discussion of the pull-out test results (Fig. 3.5) and is extended in Fig. 4.2. Using this curve, the predicted anchorage length for an effective prestress of 150 ksi would be 40 in.

Figure 3.9 presents the results of the comparative tests on 7/16-in. rectangular-wire strand. Again, as a result of the nature of the derived unit bond-slip curve shown in Fig. 3.15, the results are extended by means of the curve derived in the pull-out test discussion (Fig. 3.9) and presented again in Fig. 4.2. The predicted anchorage length for the same level of prestress would be 26 in. for this size of rectangular strand.

The reason for the difference in the required anchorage lengths is found in the comparison of the unit bond-slip curves afforded in Fig. 3.15. In fact, one might expect a larger difference realizing that the bond of the rectangular strand at 0.1-in. slip is approximately twice that developed by the round strand. However, even in an anchorage length of 40 in., the maximum slip would be on the order of 0.1 in. and the average about 0.04 in. At this level of average slip, the difference in unit bond is not as pronounced.

4.4 Concluding Discussion

It must be remembered that these predictions of anchorage lengths are based on an extension of short-time test results by a curve which is not a true lower bound to all test results. It is therefore possible that the predicted anchorage length may be exceeded in some cases. Recalling the improvement in bond capacity caused by prestressing the strand, the predictions should be a safe lower bound for the true anchorage lengths required.

The predicted anchorage lengths for an effective prestress of 150 ksi were:

For 1/4-in. round-wire strand

$$L_a = 15\ 1/2 \text{ in.}$$

for 1/4-in. rectangular-wire strand

$$L_a = 13\ 1/2 \text{ in.}$$

for 7/16-in. round-wire strand

$$L_a = 40 \text{ in.}$$

for 7/16-in. rectangular-wire strand

$$L_a = 26 \text{ in.}$$

It should be noted that the anchorage length for the 1/4-in. round strand is 62 strand diameters while it is 91 diameters for the 7/16-in. round strand. The tests reported do not support the prevailing idea that the anchorage length for strand can be expressed as a constant times the strand diameter. In fact, if the 1/4 and 7/16-in. round strand anchorage lengths are compared, the average anchorage bond for both strands is found to be on the order of 400 lb per in. If the anchorage bond for all sizes of strand were of the same order, the anchorage length of a strand would be a function of the square of the nominal diameter.

5. BEAM TEST RESULTS

5.1 Introductory Remarks

Tests were conducted on seven reinforced concrete beams to provide information on flexural bond of prestressing strand. The beams were of two lengths, 72 and 104-in., and each was reinforced with a single 7/16-in. round-wire prestressing strand. The details of materials, fabrication, instrumentation, and test procedure are presented in Appendix A and C. The beams were tested under mid-span loading applied in increments of 250 lb. Mid-span deflections and strand-slip readings were taken after each load increment. Cracks were marked and recorded as they occurred.

The concrete mix data is included in Table 1. The concrete compressive strengths at the time of test ranged from 4500 to 5150 psi and the splitting tensile strengths from 365 to 410 psi.

The results of the beam tests are presented in the form of load-deflection curves, strand force-slip curves, and beam crack patterns. Figures 5.6 and 5.7 show curves of calculated strand force versus trail-end slip. The strand force was calculated from the mid-span moment using an effective lever arm of 6.25 in. This dimension was based on the observed height of the crack at mid-span. In all beams tested, the crack penetrated to within 0.5 in. of the top of the beam soon after forming. The plotted slip is the measured distance the strand moved relative to the concrete at the end of the beam. The curves are marked with the specimen number followed by the letter N or S to denote the strand in the north or south end of the beam in its test position. Also presented on these figures are the concrete compressive and tensile strengths and the average loading rate (ALR) for the strand. The average loading rate was obtained by dividing the final strand force by the total time required to apply the load.

The beam crack patterns are presented in Figs. 5.3, 5.4, and 5.5. The development of the cracks at various applied loads is indicated. The heavy line portion of the mid-span crack was preformed as explained in Appendix A. Beam 72-1 was the only specimen which did not have this preformed crack.

5.2 Beams of Series 72

The load-deflection curves for the beams of 72-in. length are presented in Fig. 5.1. The individual behavior of the beams varied and will be outlined for each beam.

The load-deflection curve for beam 72-1 shows two sharp breaks, each representing a drop in the applied load related to the formation of a crack. The crack pattern for this beam is shown in Fig. 5.3. It is well to note that this beam did not have a preformed crack at mid-span. Trail-end slip of the strand reinforcement did not occur until the applied load reached 6100 lb. At this load, slip had occurred over the entire anchorage length of the strand, however, the beam was able to carry an increased load without any noticeable change in its response. Slip occurred at the other end of the beam at a load of 6830 lb. The beam failed in compression at a load of 7350 lb after carrying a maximum load of 7600 lb.

The behavior of beam 72-2 was quite different from that of beam 72-1. The apparent stiffness of the beam was less, first strand slip (at the end of the beam) occurred at a lower load, and the ultimate deflection and load capacity were greater. First strand slip occurred at 2860 lb when the only crack was the one preformed at mid-span. The other crack shown in Fig. 5.3 did not occur until after considerable strand slip had occurred. This crack caused the ultimate failure of the beam in compression at a load of 9560 lb. Accurate deflection readings beyond 1 3/4 in. could not be made for this beam because the aluminum angle, which bore against the plunger of the deflection dial, broke loose from the beam. The broken portion of the load-deflection curve represents a linear projection.

Both the stiffness and load at first end slip for beam 72-3 were intermediate to those for beams 72-1 and 72-2. The ultimate deflection of this beam was 2 3/4 in. Failure occurred in the strand reinforcement at a load of 10,350 lb without the presence of cracks on either side of the center line.

Figure 5.6 is a plot of calculated strand force versus end slip for the strand reinforcement of the 72-in. beams. The curves for strands 72-1S and 72-1N indicate a decrease in strand force with increased slip after some initial gain. It must be remembered, however, that this strand force is calculated at mid-span. Strand force-slip curves for the other two beams are much alike in general shape but the magnitude of the force developed at a given slip differs greatly. In all four cases, the strand force did increase with increased end slip. Strand slips over 0.1 in. could not be measured because of limitations of the instruments. The strand force in beam 72-3 was calculated to be 29 kips when failure occurred as a result of fracture of the strand. At this time, considerable slip had occurred at the trail end (at least greater than 0.1 in.). In all cases, the strand was observed to rotate as it slipped into the concrete. The rotation was not measured.

5.3 Beams of Series 104

The load-deflection curves for the beams of 104-in. length are presented in Fig. 5.2. The general response of all four beams was the same. Beam 104-1 was loaded at a higher loading rate because of an error in instrumentation. However, this did not appear to affect the behavior of this beam. The load-deflection curve indicates a short period of plastic behavior. During this period strand slip occurred and cracks formed to the right and left of the centre line. The beam carried additional load after this slip and cracking, the load reaching 5270 lb before failure occurred in compression.

Strand slip and cracking occurred in the north end of beam 104-2 at a load of 3350 lb. After a small increase in load, slip and cracking also occurred at the south end. The beam failed in compression at 4660 lb.

The first crack in the south span of beam 104-3 formed at a load of 3640 lb, slightly above the cracking load of beam 104-2. End strand slip did not accompany this crack as was the case in beam 104-2 and did not occur until a load of 6100 lb had been applied to the beam. At this load, slip occurred at both ends of the beam. The crack in the north span (Fig. 5.5) formed at a load of 6600 lb after considerable slip had occurred. This crack led to an ultimate compression failure at 6840 lb.

End slip occurred at a load of 3850 lb in beam 104-4. At that time the beam was cracked only at the mid-span. The other cracks did not occur until loads of 5730 lb and 6350 lb had been attained. Ultimate failure was in compression at the top of the second crack. During the casting and vibrating of beam 104-4, the sheet metal used to preform the crack at mid-span moved. This caused the inclined crack shown in Fig. 5.5.

Strand force-trail end slip curves for the 104-in. beams are given in Fig. 5.7. The breaks in the curves indicate the drop in the applied beam load related to cracking. All the strands were qualitatively alike, the strand force increasing with increased slip. The magnitudes of the forces developed differed greatly for the individual strands.

Because the slip measurement instruments could not be used for slip over 0.1 in., the slip of strand 104-4N was estimated as shown by the broken line. In all other cases, compression failure occurred in the beam before the trail-end slip had reached this limiting amount.

6. DISCUSSION OF BEAM TEST RESULTS

6.1 Beam Response

Load-deflection curves for prestressed concrete beams show three stages of response. The first stage of linear elastic deflections represents the response before cracking of the concrete. A crack puts the beam in its second stage which may be characterized by the reduced slope of the load-deflection curve. In this stage, reinforcement strains are within the elastic range. If these strains become plastic, the beam is considered to be in a third stage of behavior and the load-deflection curve may become very nearly parallel to the axis. The prominence of the transition points will depend upon the reinforcement properties and percentage, the strength of the concrete, and the method of loading. This response of prestressed concrete beams is discussed more fully by Warwaruk (2).

Of the seven beams tested in this program, beam 72-1 was the only one to exhibit an identifiable first stage of response. This beam did not crack until a load of 2430 lb. had been applied. In all other cases, a crack was preformed at mid-span and this crack opened before the beam load reached 500 lb.

The load-deflection curves for most of the beams show a sudden decrease in load as flexural cracking occurred. This decrease was a result of the method of loading and the transfer of tensile forces from the concrete to the reinforcement. The beams were tested by applying a deflection to the mid-span of the beam and measuring the corresponding load. As the beam cracks, tensile forces originally carried by the concrete must be transferred to the reinforcement. This transferred force caused large steel strains which resulted in additional rotation at the cracked section and an increased deflection. Because the loading apparatus was rigid compared with the beam, this deflection caused a reduction in the measured load. The magnitude of this decrease in load will depend upon the reinforcement percentage. Beams with a high percentage of reinforcement may not show a noticeable decrease in load.

Four of the seven beams tested failed in compression before the third stage of response was reached. The strand reinforcement in beams 72-3, 104-3, and 104-4 did reach plastic strains as indicated by the shape of load-deflection curves.

6.2 Beam Failure

Of the seven beams tested in this program, beam 72-3 was the only one to fail by strand fracture although the reinforcement percentage was very low. This strand fracture was attributed to the single mid-span crack and the confinement of the compression zone provided by the loading block. Strand slip caused the beam to behave much like an unbonded post-tensioned beam. Beam 72-2 failed in compression by gradual crushing of the concrete at the edge of the loading block. Considerable beam deflection had occurred before failure. Failure of the other five beams was violent and a direct result of a flexural crack in the shear span that had propagated horizontally toward the mid-span. This caused the beam to behave as a tied arch which failed by shear-compression near the loading block.

Flexural cracks which occurred in the shear span of the beams were observed to progress rapidly toward the top surface, then turn and travel toward mid-span. This horizontal progression of the crack can be attributed to high tensile stresses acting on a horizontal plane at the head of the crack.

The presence of this tensile stress can be shown by considering the equilibrium of that portion of a beam between two flexural cracks (Sketch 6.1). The beam moment will be greater at the section nearest mid-span and therefore a net steel force will exist directed toward mid-span. This force must be balanced by a shear force τ_2 along the upper surface bc. The couple thus created must be balanced by the compressive force C_2, the tensile force T_2, the friction force T_f along the crack face, and the "dowel force" T_d at d. However until the horizontal crack does form at c, there can be very little relative movement of the faces of the crack cd. If

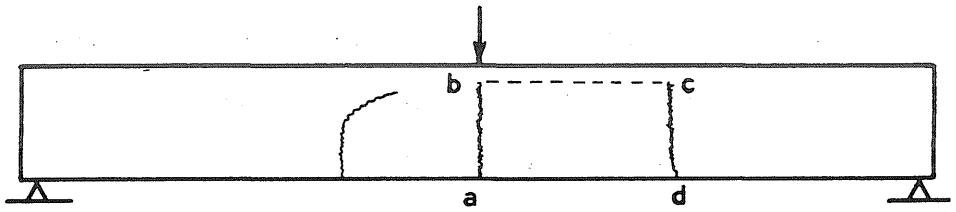
b
c
a
d

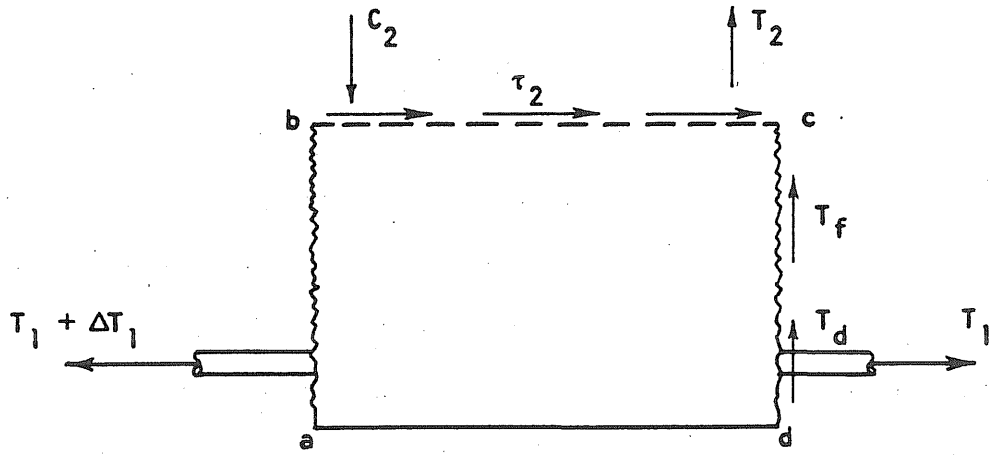
C2
T2
τ2
b
c
Tf
T1 + ΔT1
Td
T1
a
d

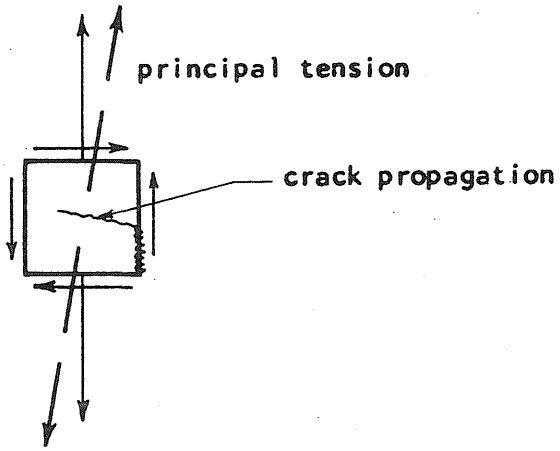
principal tension
crack propagation

SKETCH 6.1

the movement is small, the forces T_f and T_d can only be small and the larger portion of the required force must be provided by the tensile force T_2. This tensile force causes principal tensile stresses in an element near c and therefore the crack propagation. The direction of propagation will depend upon the relative magnitude of the shear and tensile stresses. If the distance between the flexural cracks is large, the tensile stress will be much larger than the shear stress and the crack propagation will be near horizontal. This hypothesis is supported by the crack patterns of the test beams.

6.3 Flexural Bond

Strand force-slip curves for the strand of beam 72-1 (Fig. 5.6) showed a decrease in strand force as slip increased beyond a certain value. This decrease was a result of the beam response and the method used to calculate the strand force. After a deflection of 0.9 in., the beam load decreased with increased deflection. The strand force used in this curve was calculated from the mid-span moment; therefore, it also decreased. If the strand force were calculated at the face of the crack south of mid-span, it would have been shown to remain constant as a result of the horizontal progression of the crack toward mid-span.

Although this argument could not be applied to the strand in the north end of the beam, it was found that the strand force did not continue to decrease at this end of the beam but remained constant. This is shown as a broken line on the strand force-slip diagram because slip measurements were not taken.

In all other cases, strand force increased with slip indicating an increase in bond over the embedment length.

The external bending moment applied to a beam must be resisted by an internal moment. The internal moment is provided by the steel tension force and the concrete compression force. If a tension force is to exist in the strand, the strand must be anchored with the required anchorage being provided by bond over the

embedded length. If the bond over the provided length is not sufficient to anchor the required strand force, slip will occur over the entire length of the strand. For the strand used in this series of beam tests, the bond will increase with slip and thereby provide a larger anchorage force as slip progresses. It has been common practice however to consider bond failure to have occurred if the strand slips at the free end, therefore the same basis will be used in this report.

The results of the beam tests are presented in a plot of strand force versus embedment length (Fig. 6.1). If a curve is drawn to represent the relation between strand force and embedment length, the slope of this curve at any point is equal to the bond that is developed at that point. A straight line on such a plot therefore represents a constant or average bond over an embedment length.

The results have been plotted on two bases, the nominal embedment length and the uncracked embedment length. In the first case (Fig. 6.1) the strand force was that calculated at mid-span at the time of first slip at the free end of the strand. This strand force is plotted against the nominal embedment length equal to one half the beam length. In the second case (Fig. 6.2) the strand force was calculated at the face of the outermost crack and plotted against the uncracked embedment length. Using a straight line to approximate the lower bound of these results, the minimum average bond was found to be approximately 250 lb. per in. in both cases. As the minimum average bond was the same in both cases, it was concluded that the bond capacity of the strand was not reduced or destroyed in the cracked portion of the beam. The upper bound would be an average bond on the order of 750 lb. per in.

7. COMPARISON OF FLEXURAL BOND WITH ANCHORAGE BOND

7.1 Introductory Remarks

It is implied in Chapter 26 of ACI 318-63(5) that the flexural bond capacity of a prestressing strand is less than its bond capacity in anchorage. This trend is confirmed by the interpretations of the tests reported in Reference 3. In the chapter the results of bond tests simulating both flexure and anchorage conditions will be compared. Although the test results do not show directly a clear distinction between anchorage and flexural bond, derived unit bond-slip curves and measured load-slip curves will be used to distinguish between the anchorage and flexural bond capacity of 7/16-in. round-wire strand.

7.2 Bond Tests at the University of Illinois

This test program involved 30 standard pull-out tests, 4 twin pull-out tests, and 7 beam tests on 7/16-in. round-wire strand. These comparative tests were undertaken to enable evaluation and comparison of flexural bond and anchorage bond.

As explained in Section 3.2, the stress conditions existing within a pull-out specimen differ from those in the anchorage zone of a pretensioned beam. It was found, however, that the results of the pull-out tests were significant and that the bond values derived from these tests were a conservative approximation to the actual anchorage bond. The twin pull-out test specimen was designed to simulate the lower portion of a reinforced concrete beam between two flexural cracks. The results of these tests should therefore be directly applicable to the evaluation of flexural bond. Practical considerations limit the twin pull-out test to small embedment lengths. Therefore, seven non-prestressed beams were tested to determine the flexural bond capacity for greater embedment lengths. In all tests conducted, the strand force increased with increased strand slip.

The results of these tests are presented in Fig. 7.1 where the strand force at bond failure is plotted against the strand embedment length. Bond failure was defined as first slip at the trail end of a specimen. On the basis of these test results, no distinction is immediately apparent between flexural and anchorage bond.

7.3 Bond Tests at Other Laboratories

Bond tests have also been conducted at the Portland Cement Association (PCA) Laboratory and at Lehigh University. An extensive beam test program at PCA involved 47 pretensioned beams containing 1/4, 3/8, or 1/2-in. round-wire strand. The results of these tests were published by Hanson and Kaar (3). Four beam tests were conducted at Lehigh University in conjunction with other bond tests. These beams contained 7/16-in. round-wire strand. The results of both test programs are presented in Fig. 7.2 along with those from the University of Illinois tests. As in Fig. 7.1, the strand force at bond failure is plotted against the embedment length. The results designated as flexural failure represent the strand force attained at the time the beam had reached its maximum load. Bond failure had not occurred and the strand force corresponding to the bond capacity of that specimen would be higher than that indicated.

7.4 Discussion

The results of all University of Illinois bond tests on 7/16-in. round strand, the Lehigh beam tests on 7/16-in. round strand, and the PCA beam tests on 3/8 and 1/2-in. round strand are presented in Fig. 7.2. Perhaps a strict comparison of the PCA results should not be made because of the difference in strand size. However as discussed in Section 4.4, the average bond in anchorage was found to be on the order of 400 lb per in. for round strand irrespective of the strand size. This was based upon the average bond over the anchorage lengths of the two strand

sizes tested at The University of Illinois and the corresponding magnitude of strand slip. If this was also found to be true for flexural bond the strand size would have no effect on the results as plotted in Fig. 7.2 and the PCA beam test results could be compared directly. The inclusion of these test results however, does not allow further distinction to be made between flexural and anchorage bond.

In order to make this distinction, the nature of the load-slip curves and the corresponding unit bond-slip curves obtained from the different tests must be considered. The pull-out test results were discussed in Section 3.1. A unit bond-slip curve in which the bond increases with increased slip (Fig. 3.14) was found to yield an approximate lower bound to the test results of the 7/16-in. round strand. The strand force-embedment length curve presented in Fig. 7.3 can be obtained directly from this unit bond-slip curve. As the pull-out test results yield a conservative anchorage bond, this curve can be used to predict anchorage lengths for 7/16-in. round-wire strand.

Now compare the load-slip curve for a twin pull-out test (flexural conditions) with that for an identical standard pull-out test (anchorage conditions) as done in Fig. 3.19. The load is seen to increase with increased slip for both tests. However, the increase is so small in the twin pull-out test that the load, and thus the bond, can be assumed constant for all magnitudes of slip. Based on this assumption, the strand force is a linear function of the embedment length. Such a linear relation corresponding to a flexural bond of 250 lb per in. was found to represent a reasonable lower bound to the beam test results as presented in Fig. 7.2.

In all bond tests conducted at The University of Illinois, the strand force was observed to increase as the strand was pulled from a specimen and no evidence was found to indicate that bond would decrease with increased strand slip. Hanson and Kaar (3) concluded, however, that flexural bond decreased with increased embedment and thus with slip. A basis for this conclusion appears to be a drop in

steel stress indicated by electrical strain gages mounted on the strand within the beam. This stress decrease was indicated although the applied beam load did not decrease. If the beam load does not decrease, however, it is statically inadmissible that the steel stress decrease at any section. It is probable, therefore, that this indicated stress decrease was actually a breakdown of the method used to measure strand strains.

It appears from the available data that the flexural bond capacity of 7/16-in. round-wire strand remains constant for all mangitudes of slip and that the anchorage bond capacity increases with increased slip of the strand. The two curves presented in Fig. 7.3 may therefore be used to calculate the embedment lengths required in anchorage and flexure for any strand force.

As an example, consider a beam with 7/16-in. round-wire strand pretensioned to 150 ksi which is expected to develop the strength of the strand in flexure. The effective pretensioning force of 16.3 kips will require an anchorage length of 40 in. The difference between the strength of the strand, 27.2 kips, and the prestress force is 10.9 kips. Using Fig. 7.3, the required additional embedment length will be 44 in. The total embedment length required for this beam will therefore be 84 in.

As a comparison to the findings of this report, Fig. 7.4 presents the curves suggested by other references to be used in predicting strand embedment lengths. The following are the comparative lengths for the illustrative beam considered above:

ACI 318-63 (5)

L_e = 66 in.

CSA A135-62 (6)

L_e = 94 in.

Reference 3 (3)

L_e = 108 in.

8. SUMMARY

The objective of this study was to develop basic information on the bond characteristics of prestressing strand. This information was then used in the determination of the length required to anchor the pretensioning force and the length required to develop a desired strand force in flexure. The test program involved a total of 74 tests conducted on 1/4 and 7/16-in. round and rectangular-wire strand. Of these tests, 59 were standard pull-out, 4 were prestressed pull-out, 4 were twin pull-out, and 7 were beam tests. In all cases the strand had an uncoated surface free from rust and oil.

Specimens used in the tests of 1/4-in. rectangular strand were 4 by 4 in. in cross section and had embedment lengths of 1 1/2, 3, 6, and 9 in. A 6 by 6-in. specimen was used for the tests on 7/16-in. strand. Embedment lengths were 3, 6, 12, 18 and 24 in. for the rectangular strand and 6, 12, 18, 24, 30, and 36 in. for the round strand. The twin pull-out specimens were 6 by 15 in. in cross section and 6 or 7 in. long. Two strands were embedded at mid-depth spaced at 9-in. centers. All beams were of 8 by 8-in. cross section with a single strand placed at a depth of 6 1/2 in. Tests were made on beams with lengths of 72 and 104 in. The nominal concrete compressive strength was 4500 psi for all tests.

In all tests conducted, strand loads were observed to increase with increased strand slip. The rate of increase varied with the type of strand being considered but always decreased at larger slips. Although the tests were continued to trail-end slips on the order of 0.3 in., the load was never observed to decrease with increased slip.

Special prestressed pull-out specimens, which simulate an anchorage zone more closely than do standard pull-out specimens, were tested to find the effect of the change in stress conditions on bond. Although the prestressed specimens attained higher loads at all levels of slip, the increase was not sufficient to eliminate the significance of the standard pull-out test.

The following unit bond-slip curves were obtained (Section 3.1) for the various types of strand tested:

For 1/4-in. rectangular-wire strand

$$g = 250 + 3000\,\delta + 1500\,\sqrt{\delta}$$

For 7/16-in. round-wire strand

$$g = 300 + 600\,\delta + 600\,\sqrt{\delta}$$

For 7/16-in. rectangular-wire strand

$$g = 250 + 3000\,\delta + 3500\,\sqrt{\delta}$$

where g = unit bond in lb per in.

δ = strand slip in in.

The above expressions represent reasonable lower bounds to the test results. On the basis of tests of 1/4-in. round strand conducted by Keuning, the unit bond for that type of strand remained approximately constant at 350 lb per in. for all values of slip. The unit bond-slip curves for the various strands are presented in Figs. 3.13 through 3.15.

A portion of this investigation was conducted to gain information on the flexural bond characteristics of 7/16-in. round strand. Both twin pull-out and beam tests were conducted. The twin pull-out test was designed to simulate the stress conditions existing in the cracked portion of a beam (Fig. B.5). Load-slip curves for these tests did not exhibit a load increase of the same magnitude as was found for the pull-out tests. It was therefore decided that conservative flexural bond-slip curve would be one of constant bond.

The magnitude of the flexural bond capacity of the 7/16-in. round strand was determined from the beam tests. An average flexural bond of 250 lb per in. represented a lower bound to these results although unit bond as high as 750 lb per in. was developed in one beam. In all beam tests conducted, the capacity of the beam was not lost at strand slip at the end of the beam and the applied load increased considerably after first slip had occurred.

As the pull-out test results yield a conservative unit bond-slip curve for anchorage, the strand force-embedment length curves derived from these bond-slip curves can be used to estimate the short-time anchorage length required for any pretensioning force. These curves were presented in Fig. 4.1 and 4.2. On this basis, the anchorage lengths required for an effective pretensioning force of 150 ksi are:

for 1/4-in. round strand

L_a = 15 1/2 in.

for 1/4-in. rectangular strand

L_a = 13 1/2 in.

for 7/16-in. round strand

L_a = 40 in.

for 7/16-in. rectangular strand

L_a = 26 in.

The anchorage lengths as predicted above are not a linear function of the strand diameter. In fact, the average anchorage bond for round strand appears to be on the order of 400 lb per in. for all strand sizes thus making the anchorage length a function of the square of the strand diameter.

The embedment length required to develop any strand force in a pretensioned beam containing 7/16-in. round-wire strand may be determined with the use of Fig. 7.3. A typical beam pretensioned to 150 ksi will require a total embedment length of 84 in. to develop the strength of the strand in flexure.

REFERENCES

1. R. W. Keuning, M. A. Sozen, and C. P. Siess, "A Study of Anchorage Bond in Prestressed Concrete", Civil Engineering Studies, Structural Research Series No. 251, June 1962.

2. J. Warwaruk, M. A. Sozen, and C. P. Siess, "Strength and Behavior in Flexure of Prestressed Concrete Beams", issued as Part of the Ninth Progress Report of the Investigation of Prestressed Concrete Bridges, Civil Engineering Studies, Structural Research Series No. 207, October 1960.

3. N. W. Hanson and P. H. Kaar, "Flexural Bond Tests of Pretensioned Prestressed Beams", Portland Cement Association, Research and Development Laboratories, Bulletin D28, January 1959.

4. G. A. Dinsmore, P. L. Deutsch, and S. L. Montemayor, "Anchorage and Bond in Pretensioned Prestressed Concrete Members", Lehigh University Institute of Research, Prestressed Concrete Bridge Members, Progress Report No. 19, December 1958.

5. American Concrete Institute, "Building Code Requirements for Reinforced Concrete", (ACI 318-63), Detroit, June 1963.

6. Canadian Standards Association, "Prestressed Concrete", (CSA A135-1962) March 1962.

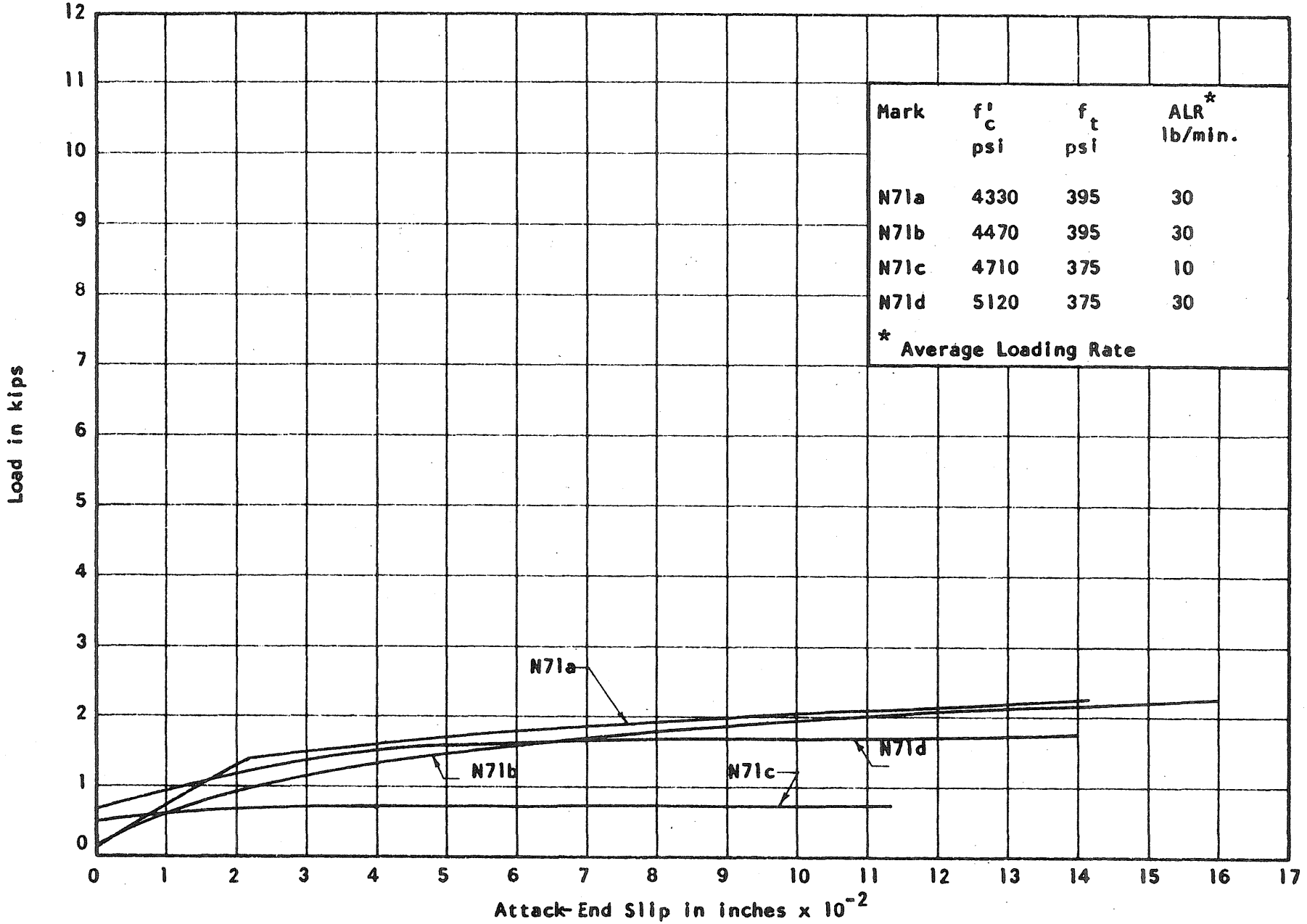

FIG. 2.1 MEASURED LOAD-SLIP CURVES. SERIES 7
Length: 1 1/2 in. Strand: 1/4-in. Rectangular

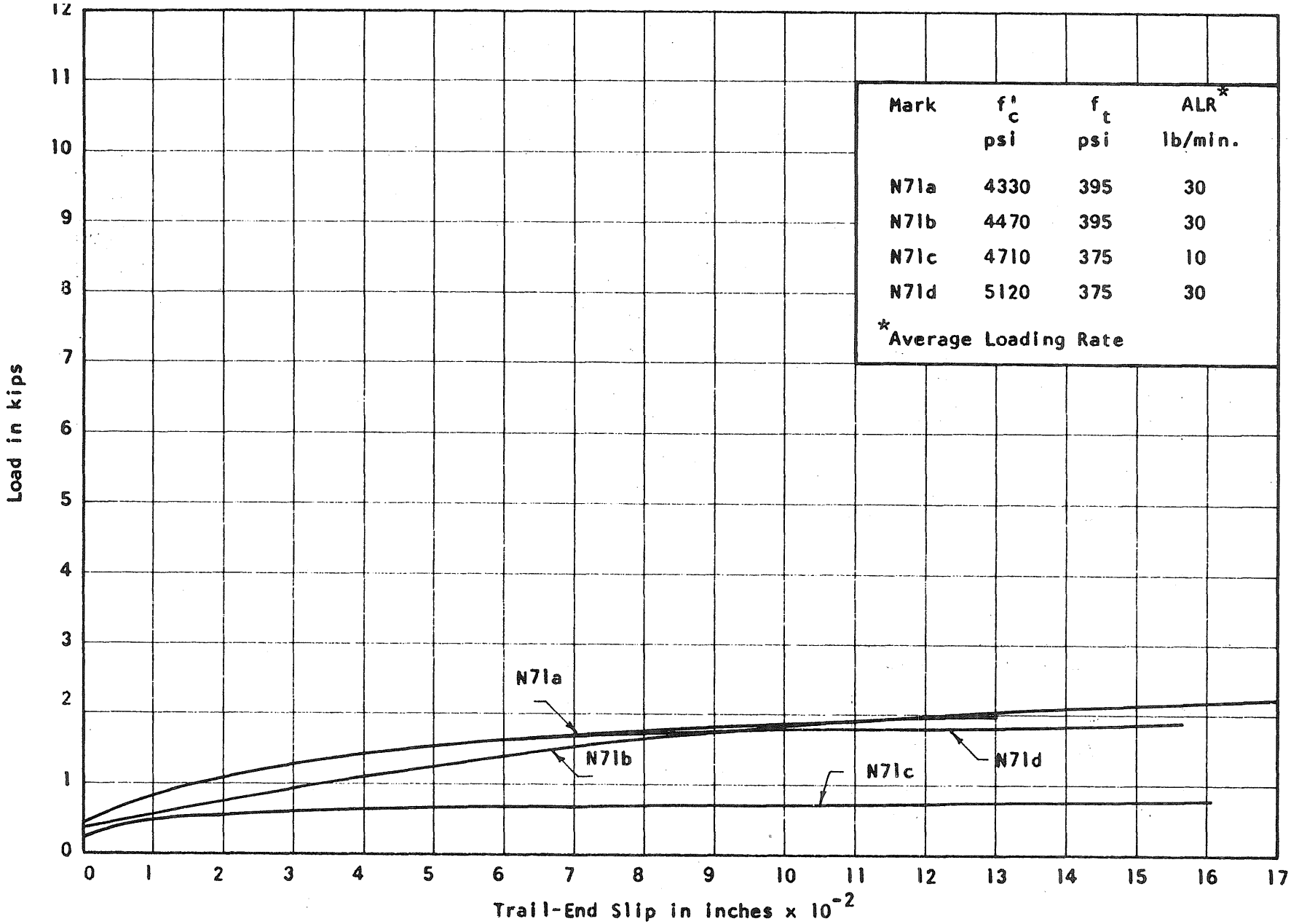

FIG. 2.2 MEASURED LOAD-SLIP CURVES. SERIES 7
Length: 1.5 in. Strand: 1/4-in. Rectangular

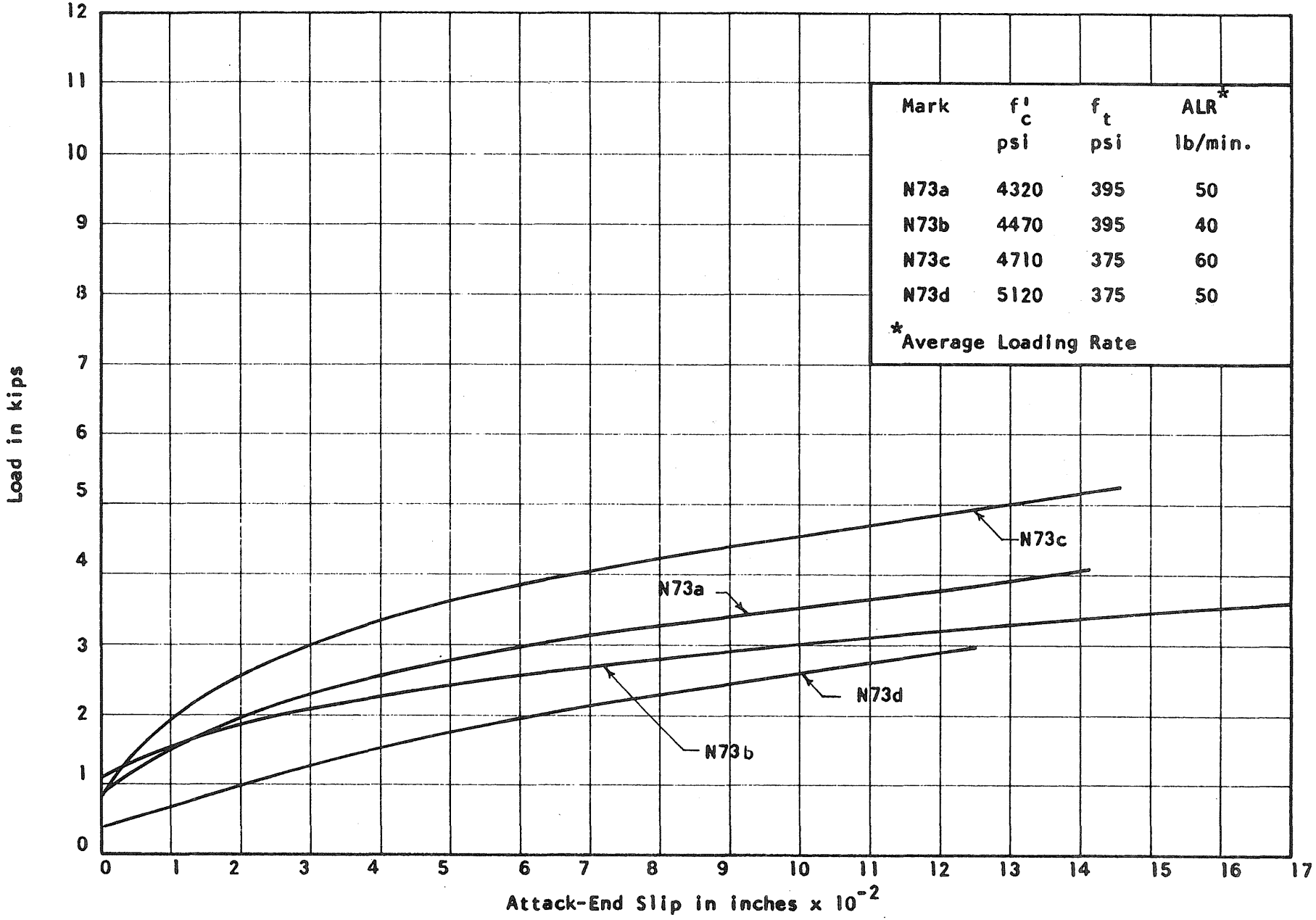

FIG. 2.3 MEASURED LOAD-SLIP CURVES. SERIES 7
Length: 3-in. Strand: 1/4-in. Rectangular

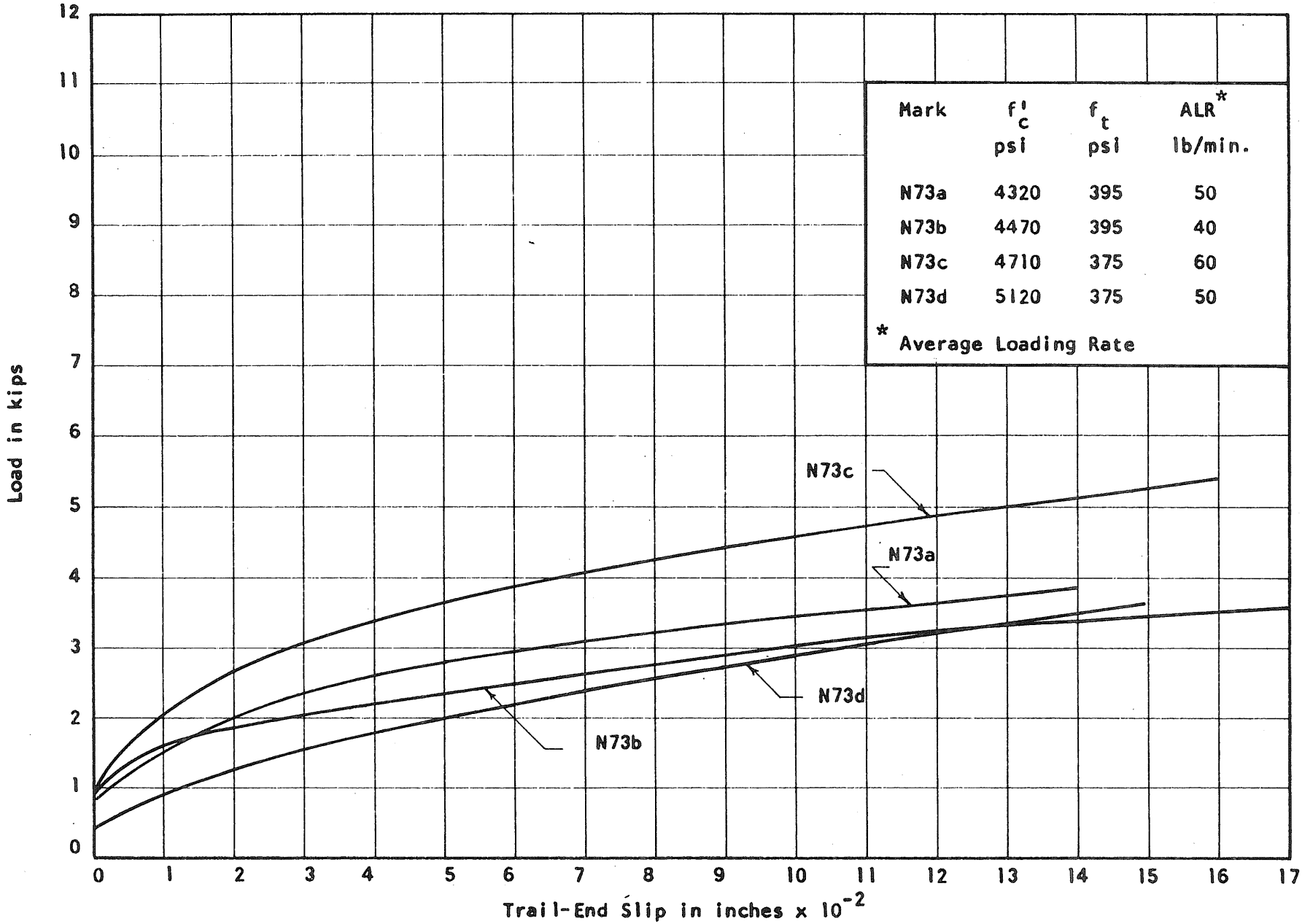

FIG. 2.4 MEASURED LOAD-SLIP CURVES. SERIES 7
Length: 3-in. Strand: 1/4-in. Rectangular

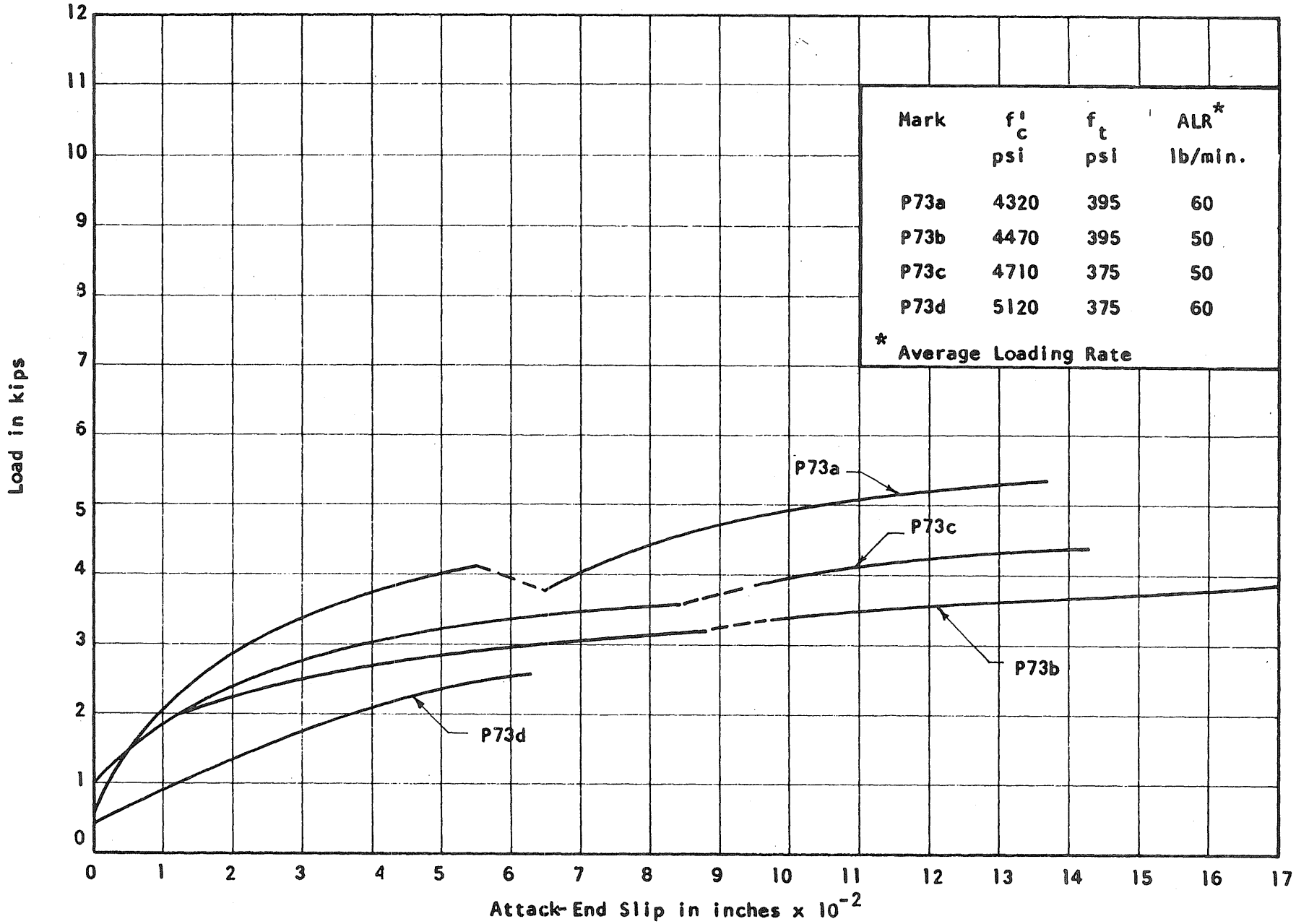

FIG. 2.5 MEASURED LOAD-SLIP CURVES. SERIES 7
Length: 3-in. Strand: 1/4-in. Rectangular

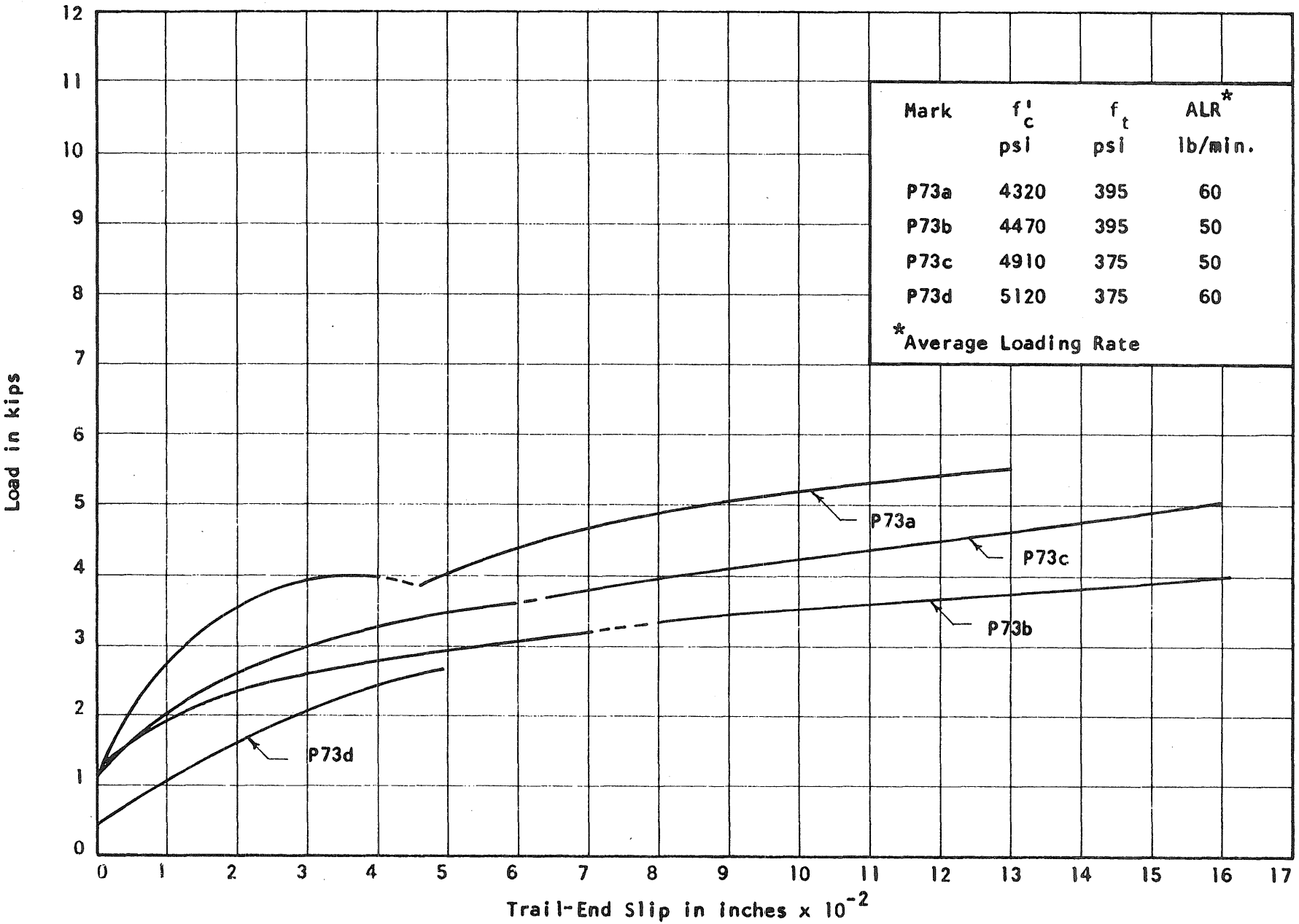

FIG. 2.6 MEASURED LOAD-SLIP CURVES. SERIES 7
Length: 3 in. Strand: 1/4-in. Rectangular

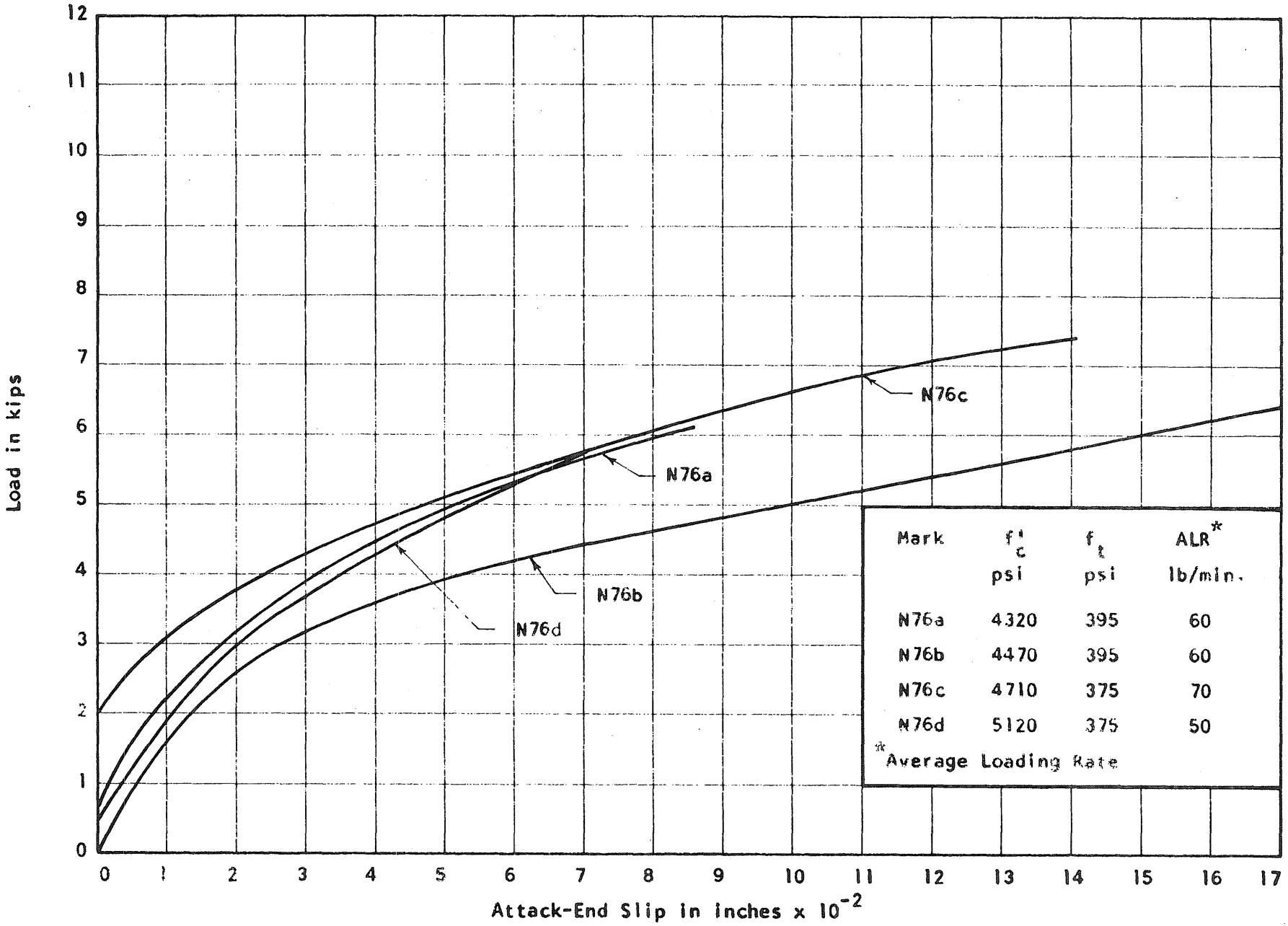

FIG. 2.7 MEASURED LOAD-SLIP CURVES. SERIES 7
Length: 6-in. Strand: 1/4-in. Rectangular

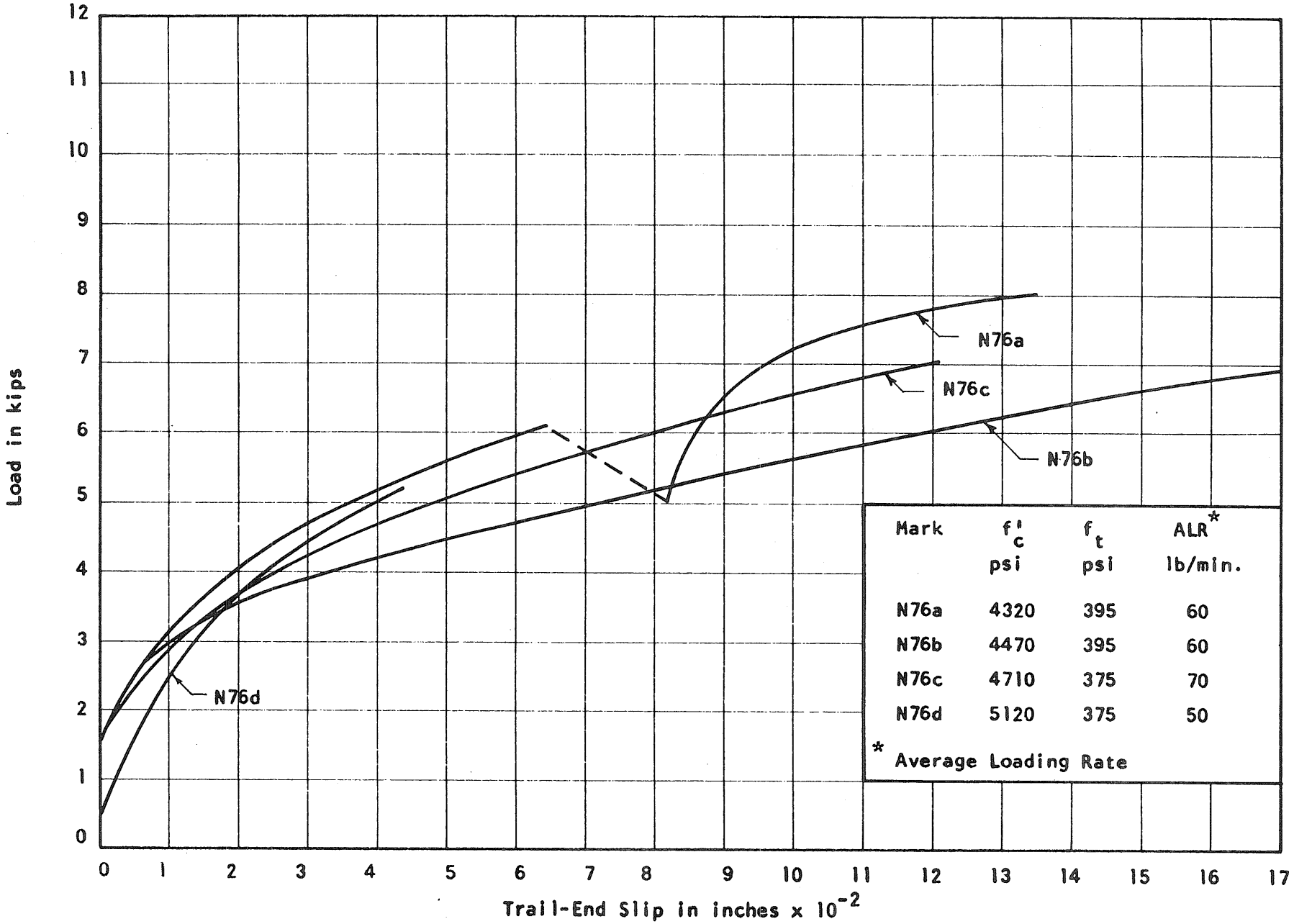

FIG. 2.8 MEASURED LOAD-SLIP CURVES. SERIES 7
Length: 6-in. Strand: 1/4-in. Rectangular

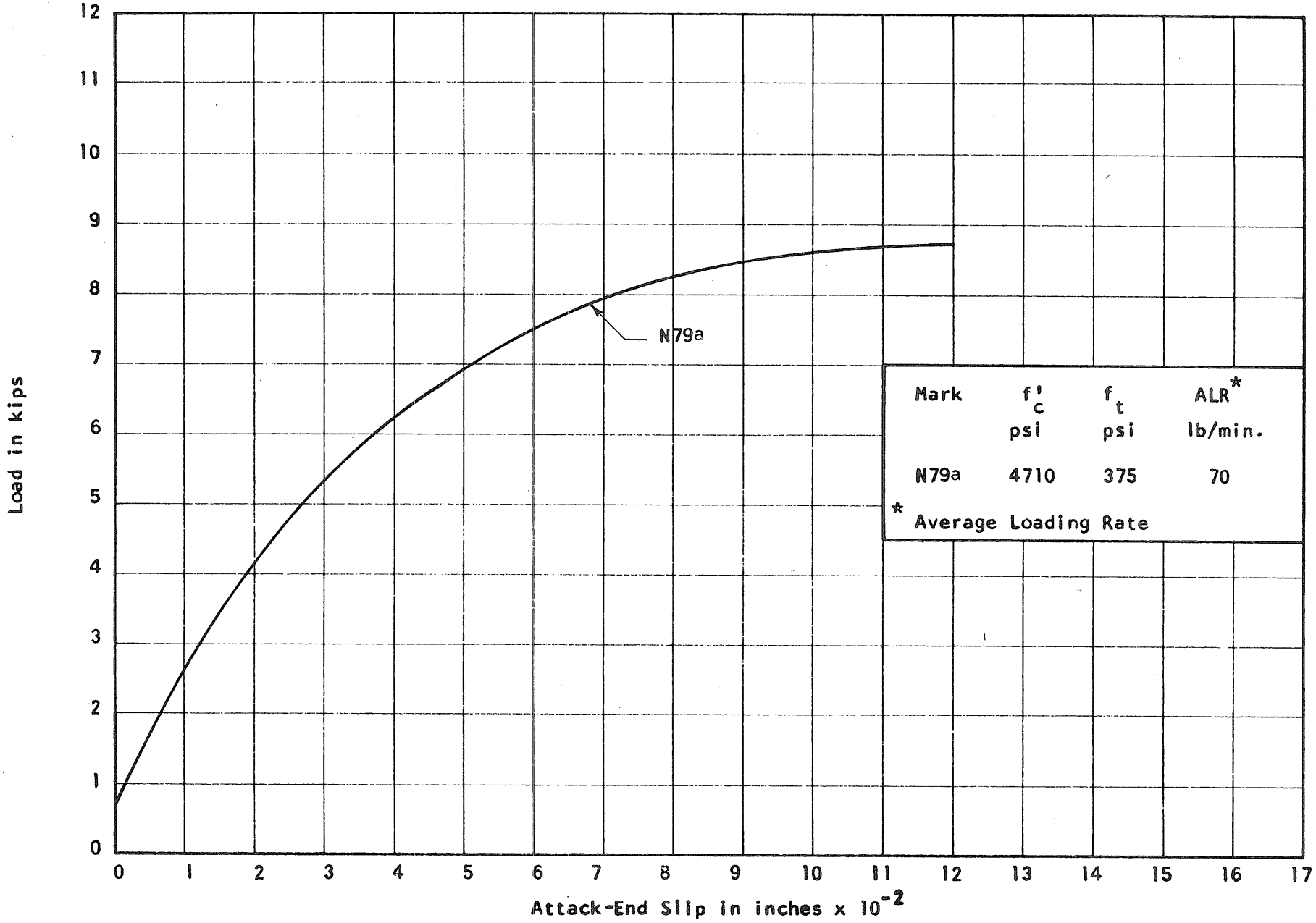

FIG. 2.9 MEASURED LOAD-SLIP CURVE. SERIES 7
Length: 9 in. Strand: 1/4-in. Rectangular

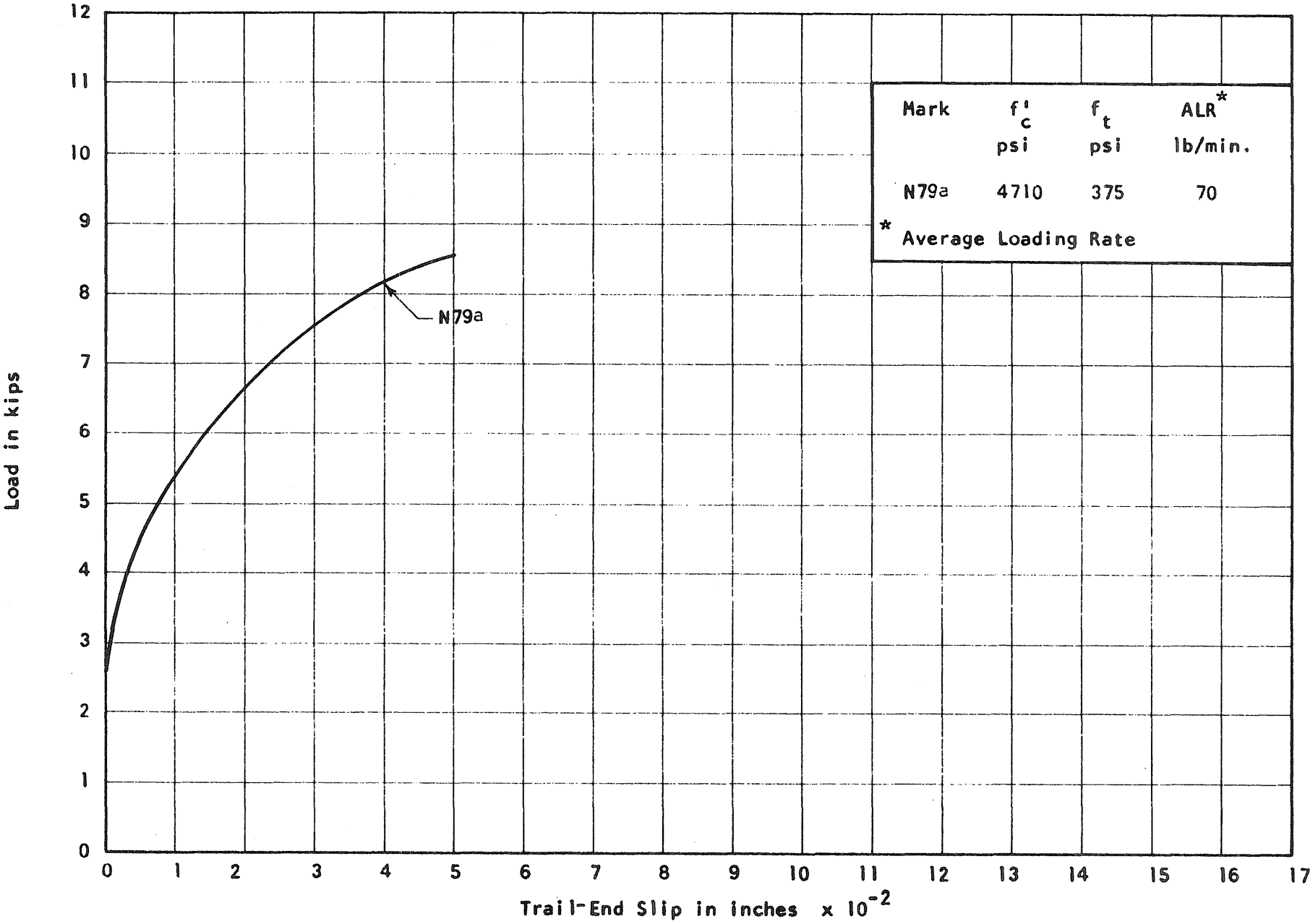

FIG. 2.10 MEASURED LOAD-SLIP CURVE. SERIES 7
Length: 9-in. Strand: 1/4-in. Rectangular

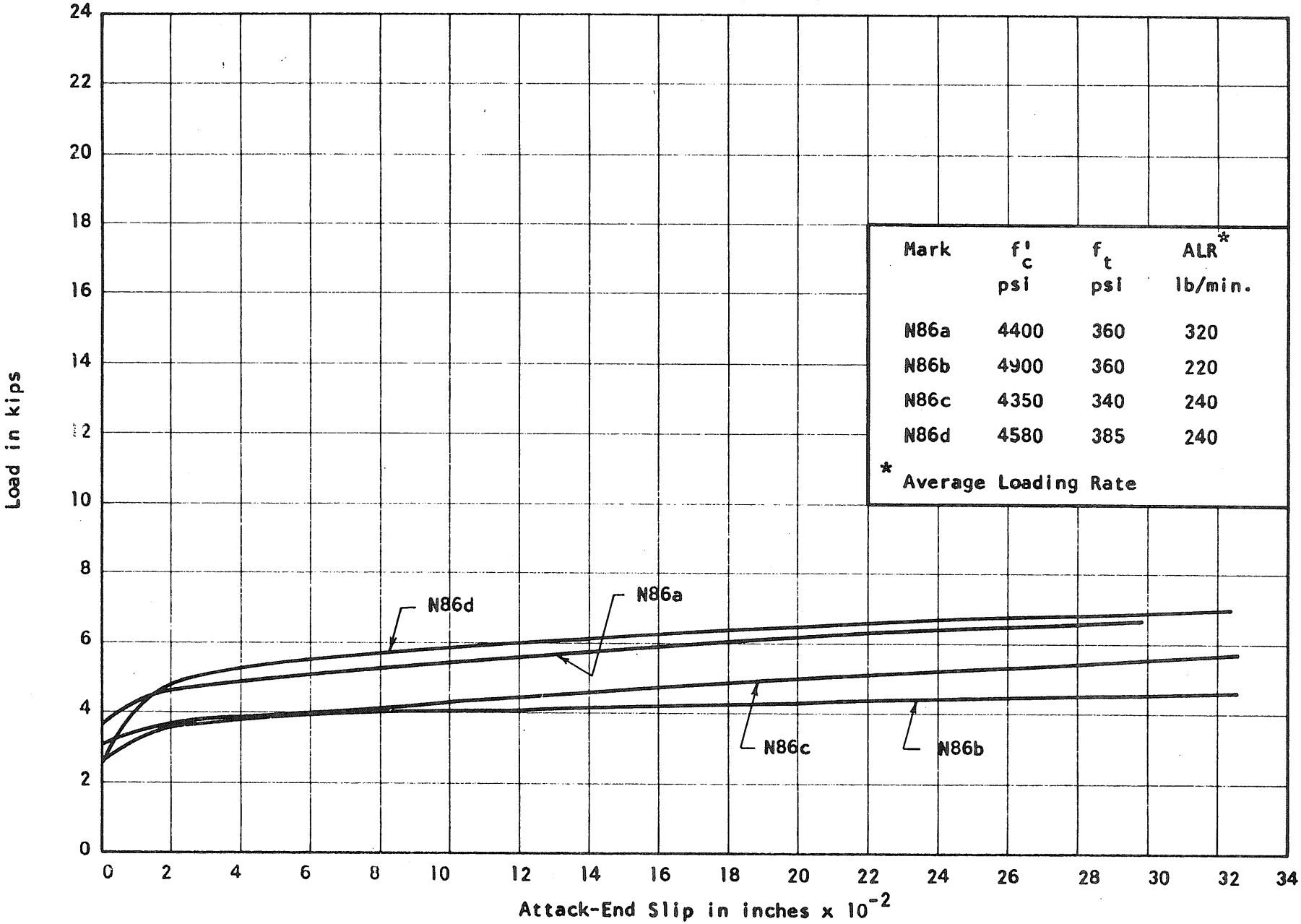

FIG. 2.11 MEASURED LOAD-SLIP CURVES. SERIES 8
Length: 6-in. Strand: 7/16-in. Round

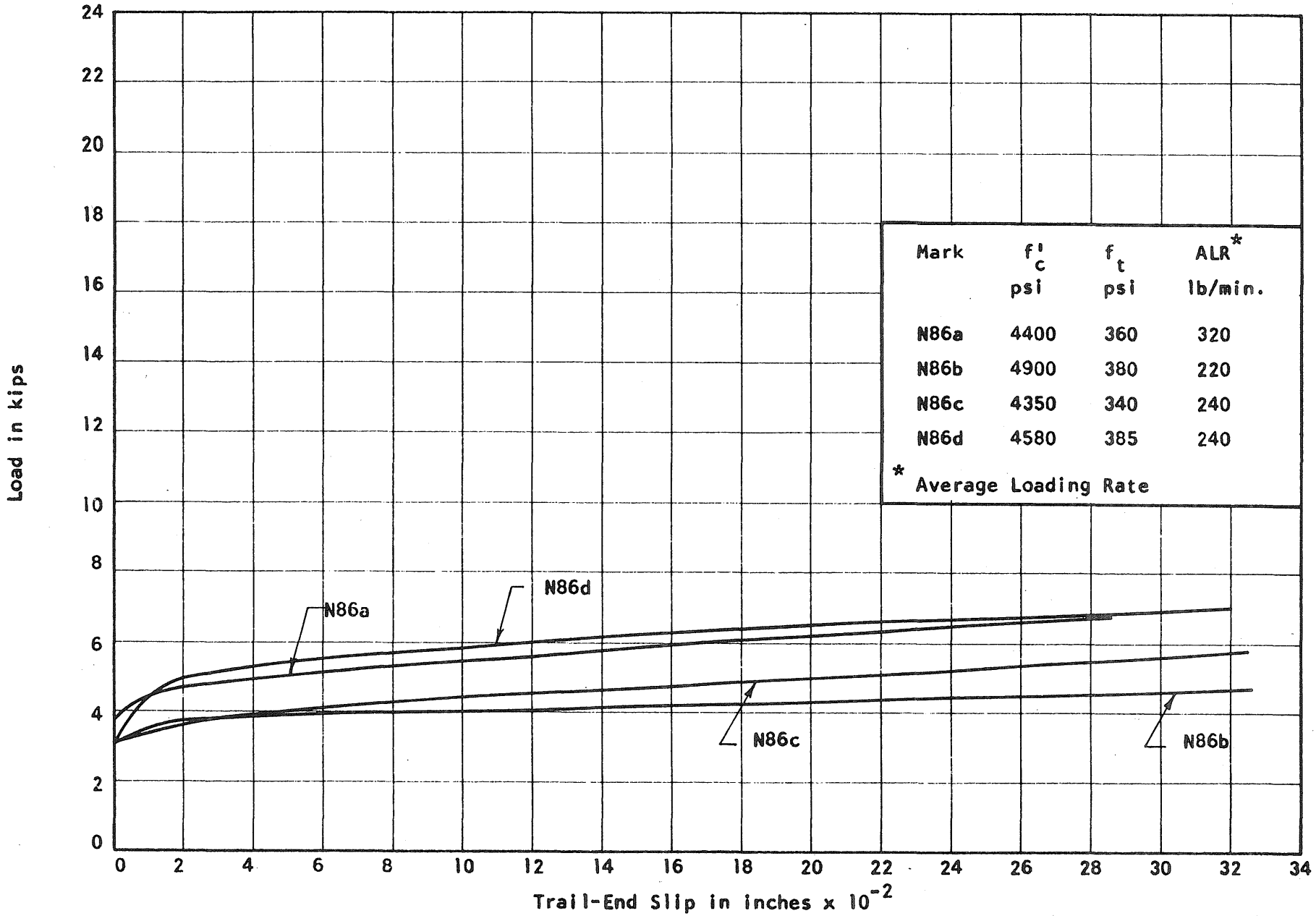

FIG. 2.12 MEASURED LOAD-SLIP CURVES. SERIES 8
Length: 6-in. Strand: 7/16-in. Round

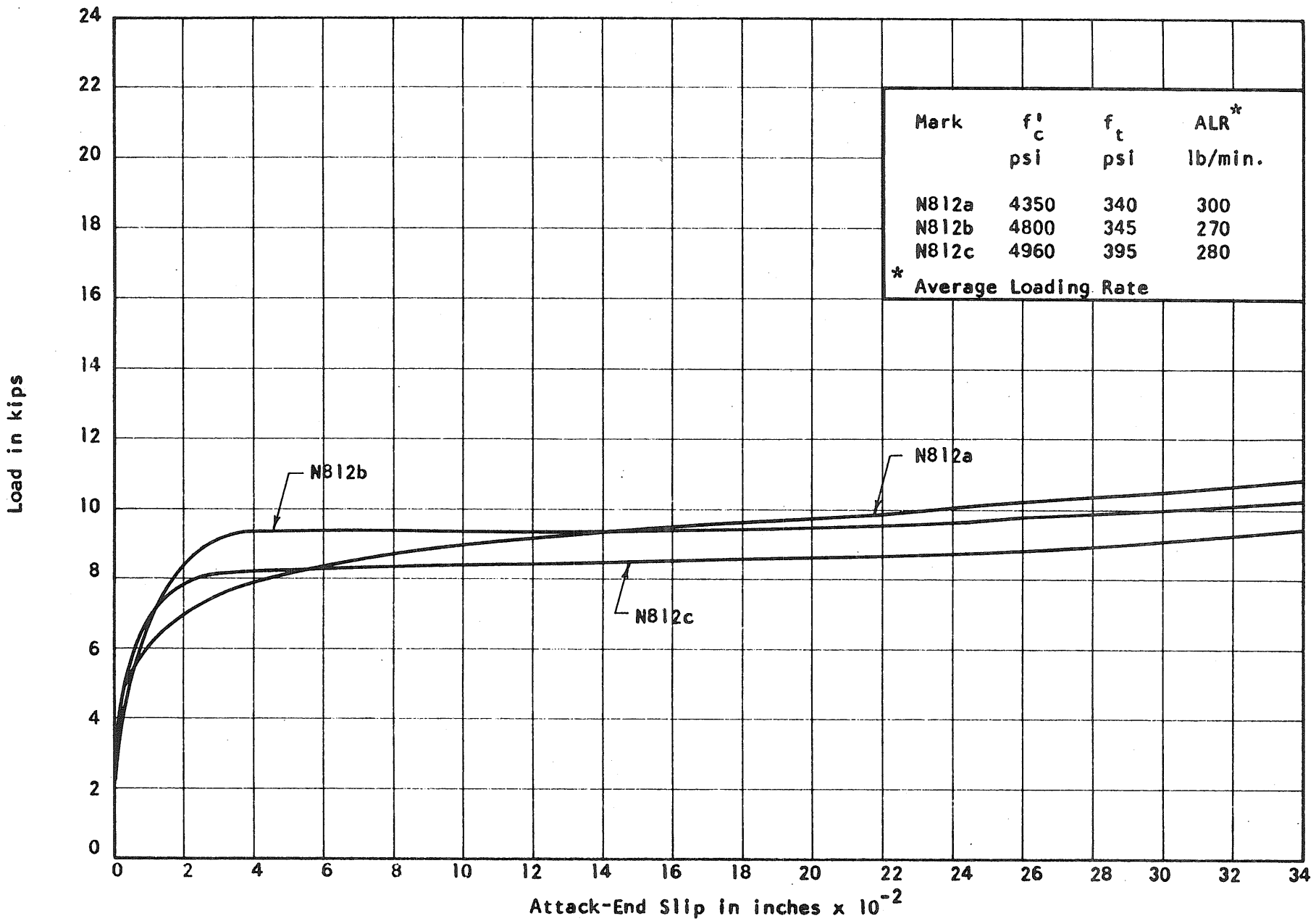

FIG. 2.13 MEASURED LOAD-SLIP CURVES. SERIES 8
Length: 12-in. Strand: 7/16-in. Round

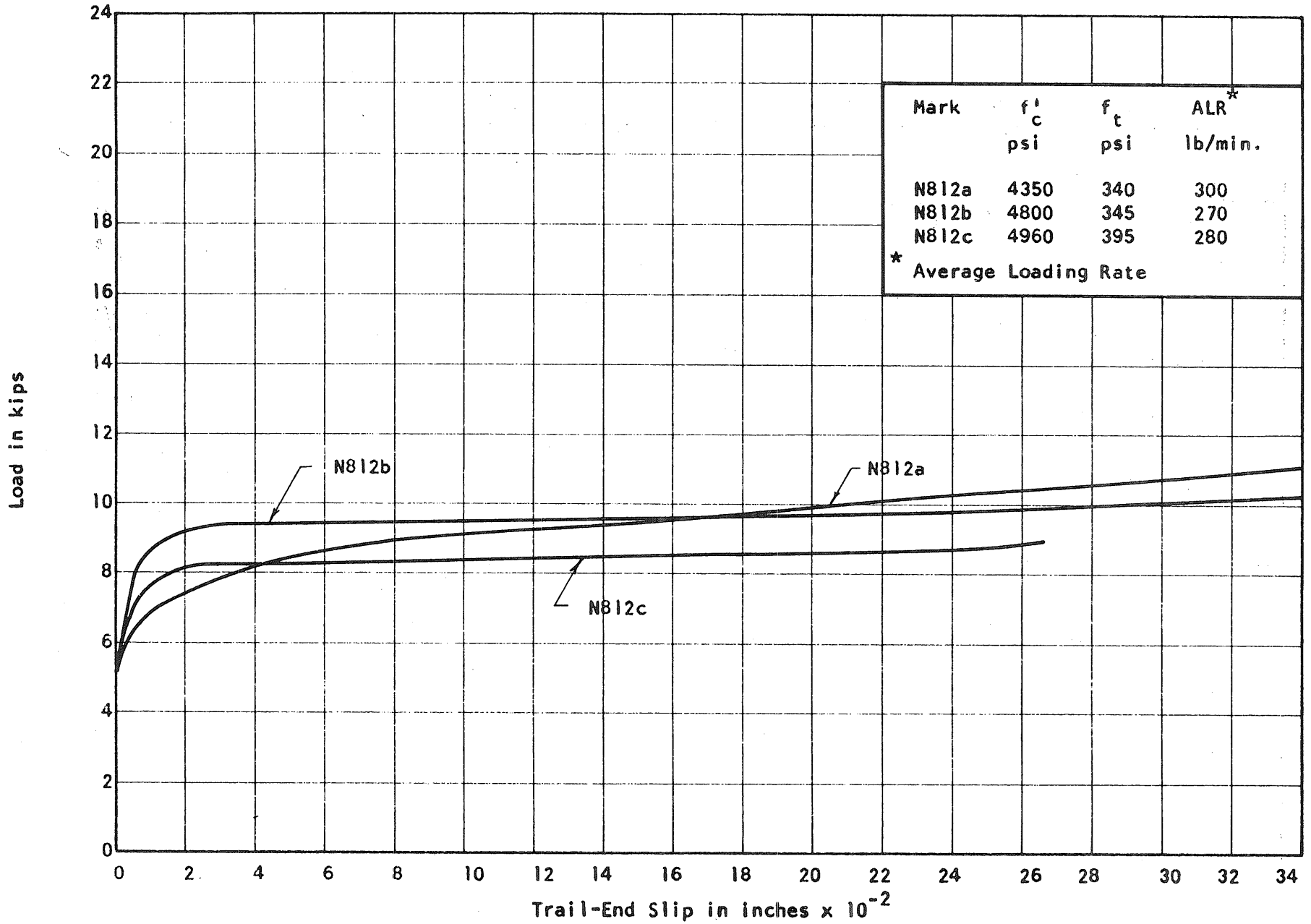

FIG. 2.14 MEASURED LOAD-SLIP CURVES. SERIES 8
Length: 12-in. Strand: 7/16-in. Round

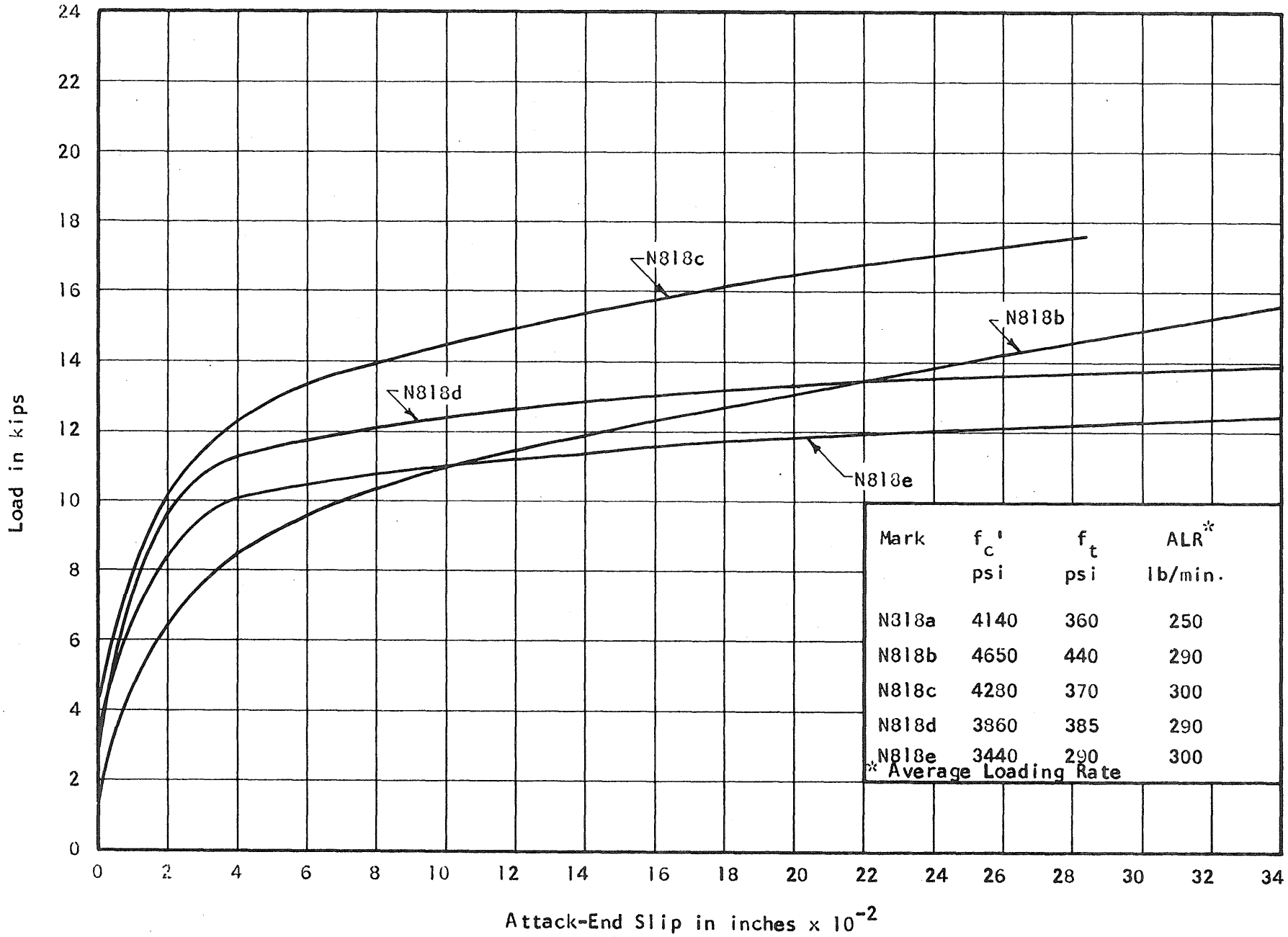

Fig. 2.15 MEASURED LOAD-SLIP CURVES. SERIES 8
Length: 18 in. Strand: 7/16. Round

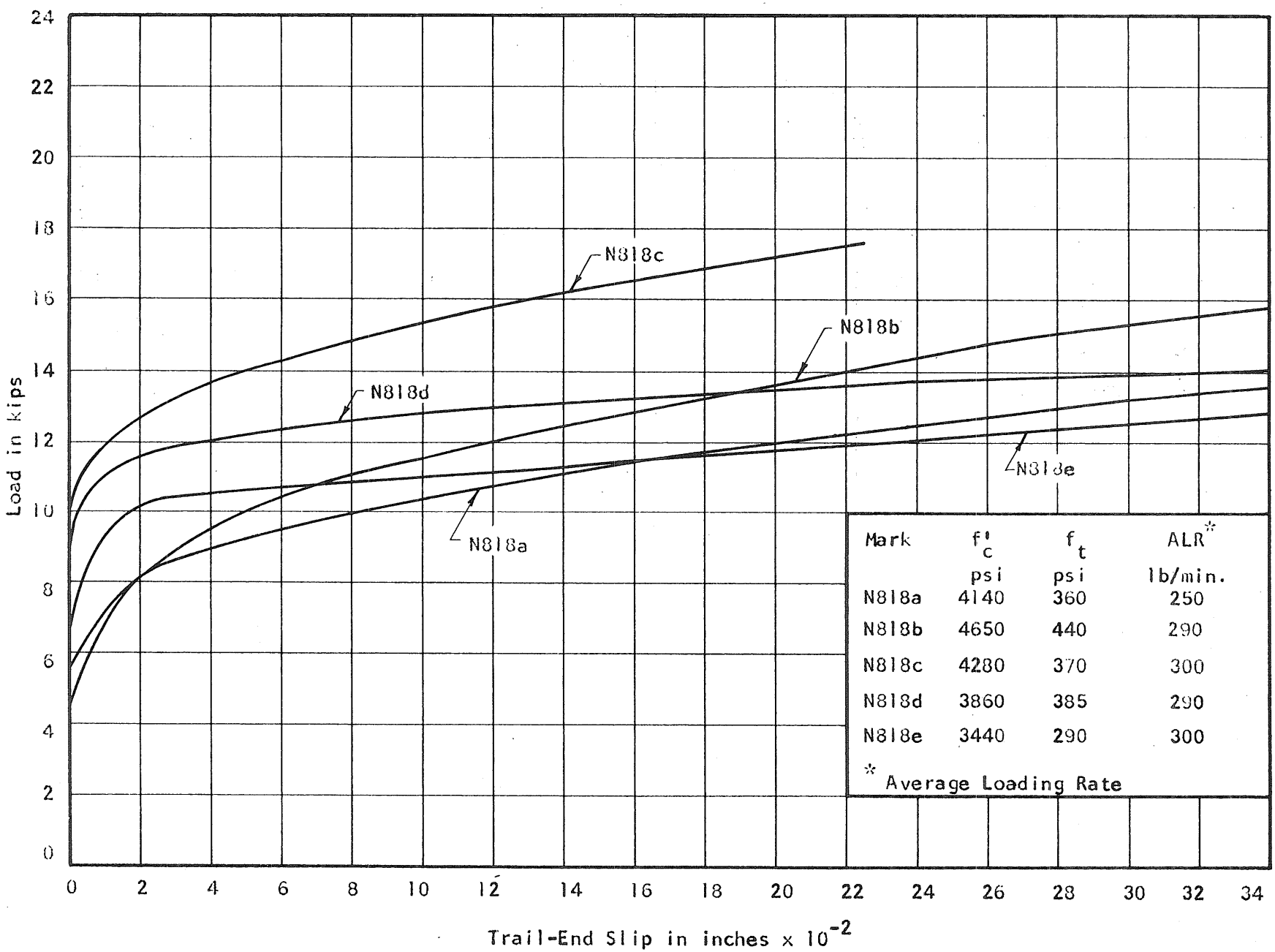

FIG. 2.16 MEASURED LOAD-SLIP CURVES. SERIES 8
Length: 18-in. Strand: 7/16-in. Round

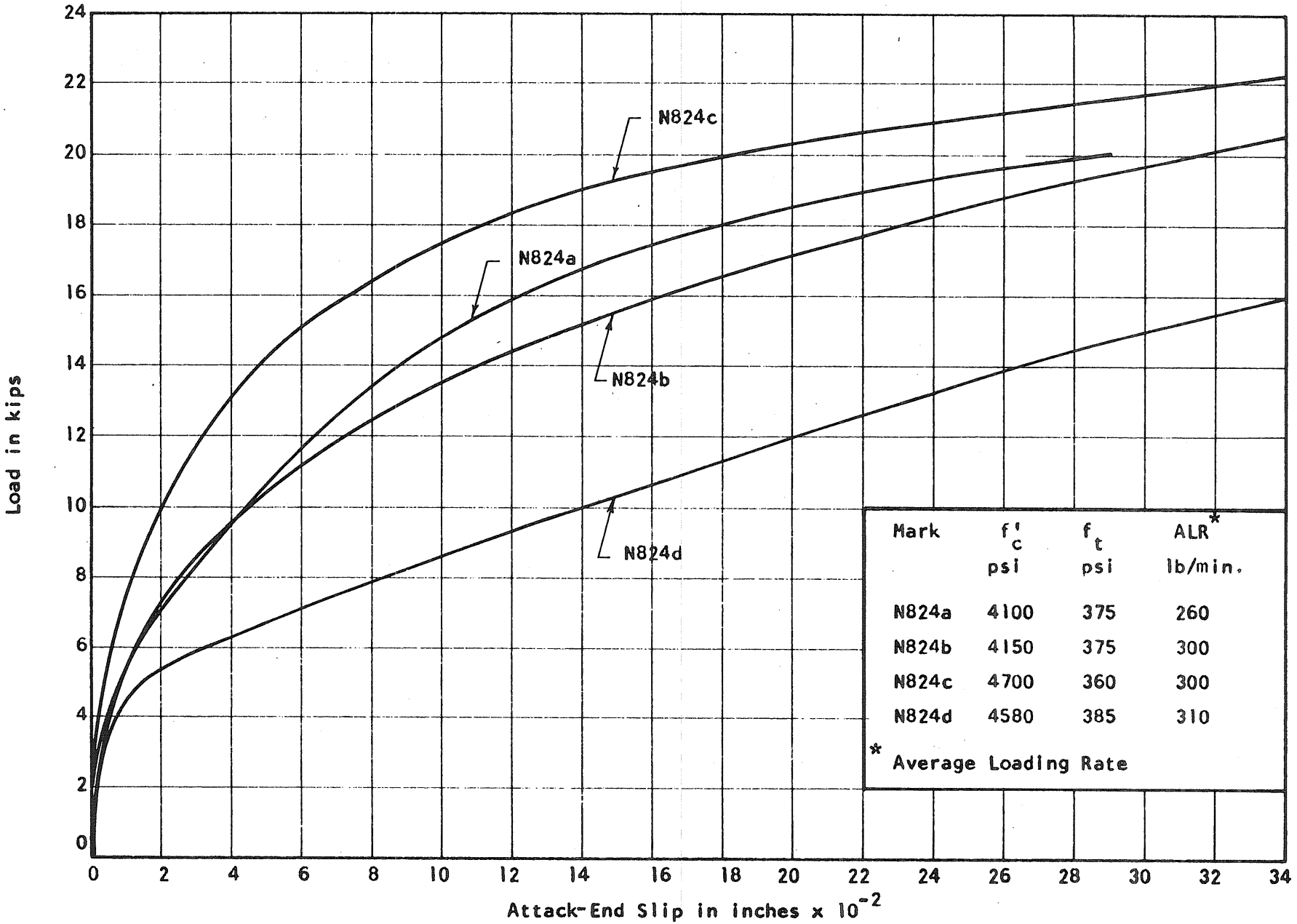

FIG. 2.17 MEASURED LOAD-SLIP CURVES. SERIES 8
Length: 24-in. Strand: 7/16-in. Round

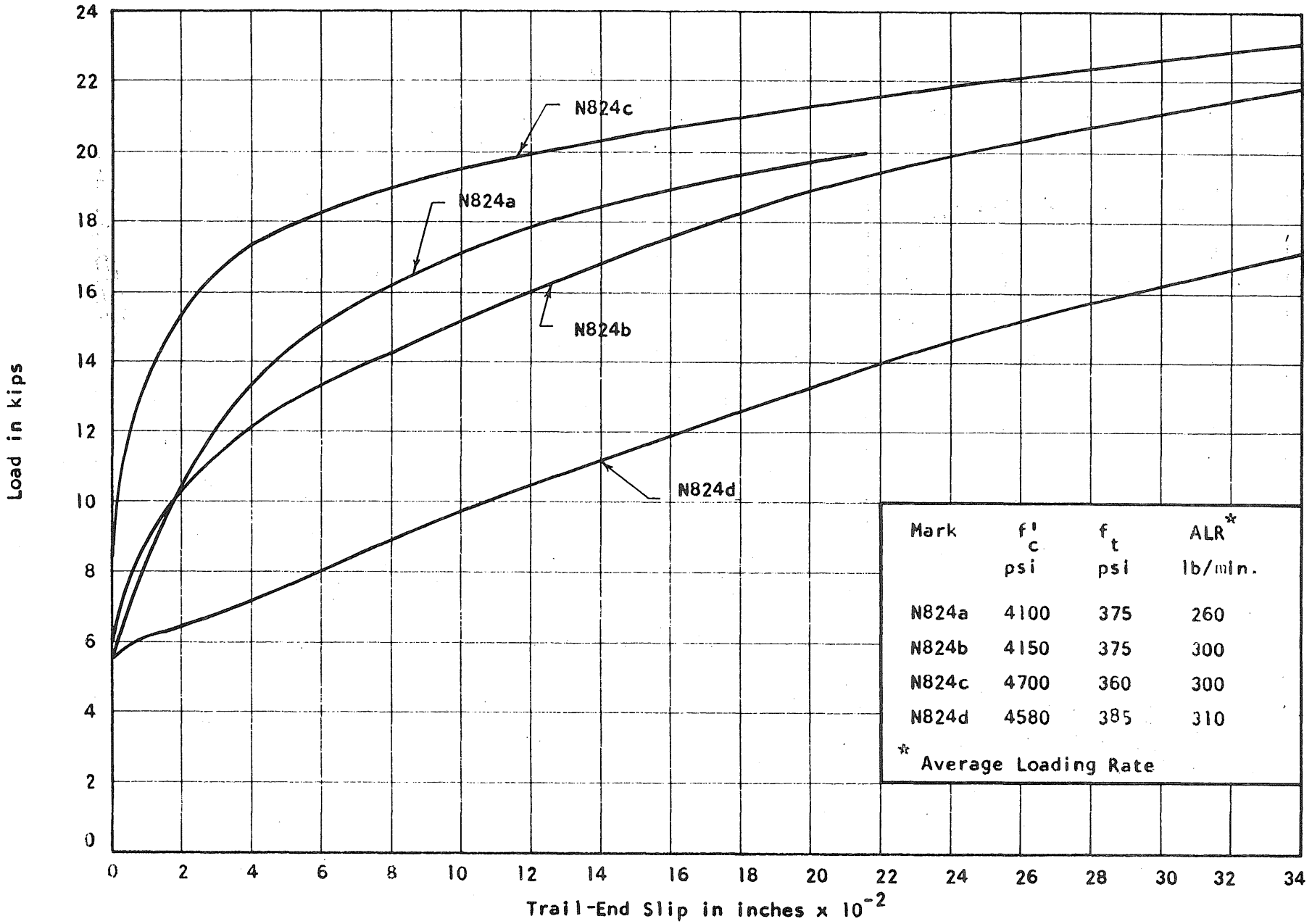

FIG. 2.18 MEASURED LOAD-SLIP CURVES. SERIES 8
Length: 24-in. Strand: 7/16-in. Round

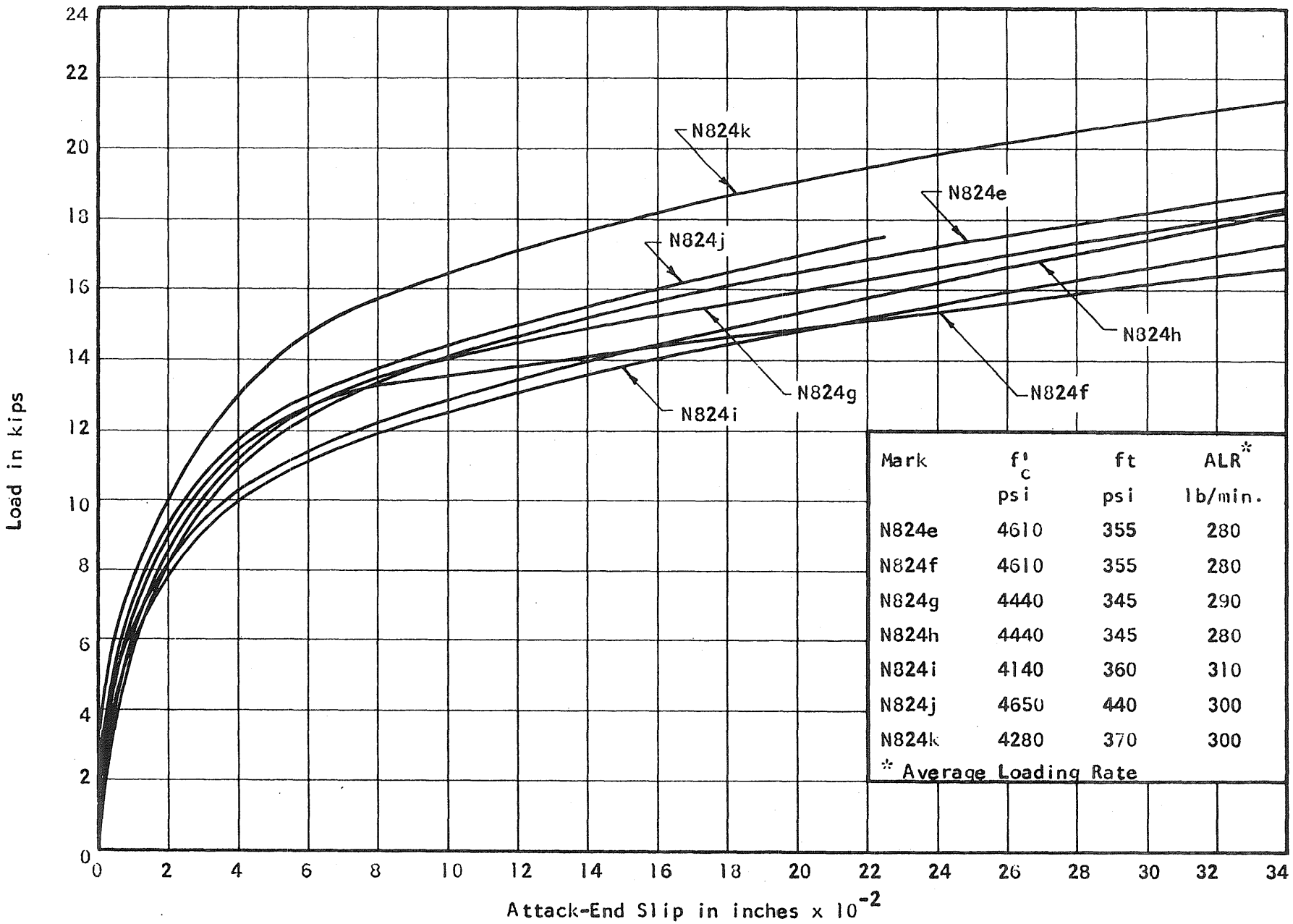

Mark	f'_c psi	ft psi	ALR* lb/min.
N824e	4610	355	280
N824f	4610	355	280
N824g	4440	345	290
N824h	4440	345	280
N824i	4140	360	310
N824j	4650	440	300
N824k	4280	370	300

* Average Loading Rate

FIG. 2.19 MEASURED LOAD-SLIP CURVES. SERIES 8
Length: 24-in. Strand: 7/16-in. Round

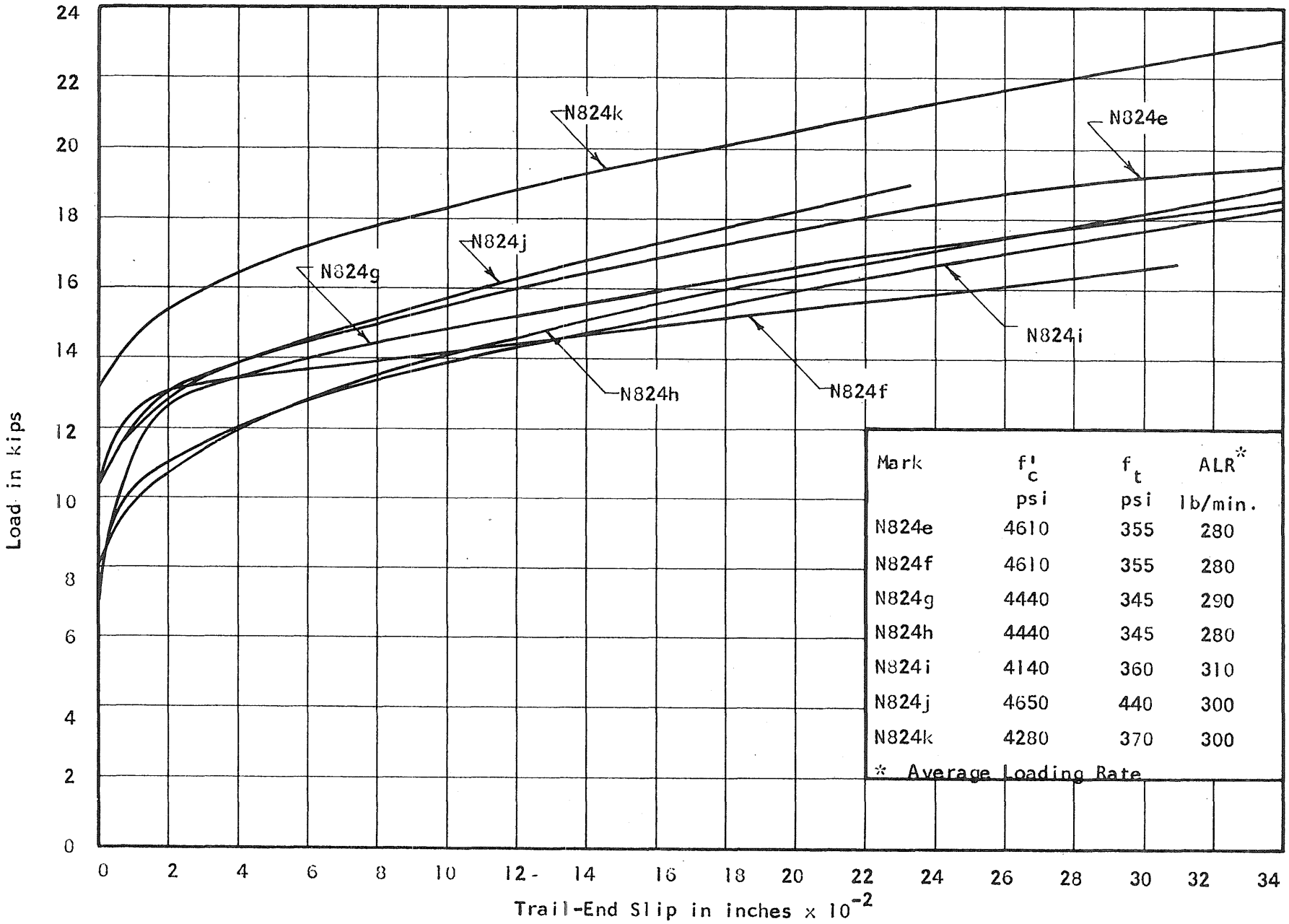

FIG. 2.20 MEASURED LOAD-SLIP CURVES. SERIES 8
Length: 24-in. Strand: 7/16-in. Round

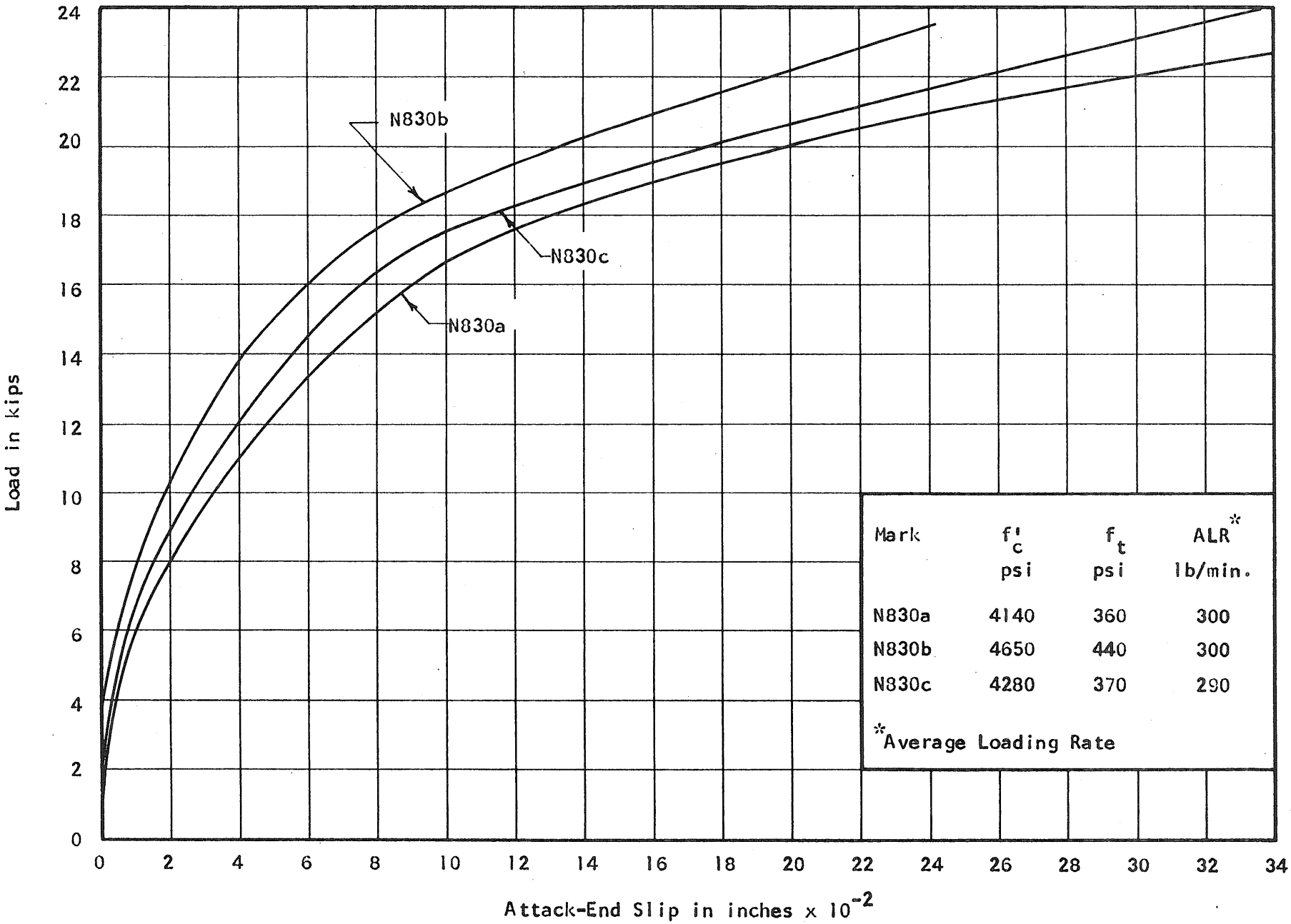

FIG. 2.21 MEASURED LOAD-SLIP CURVES. SERIES 8
Length: 30-in. Strand: 7/16-in. Round

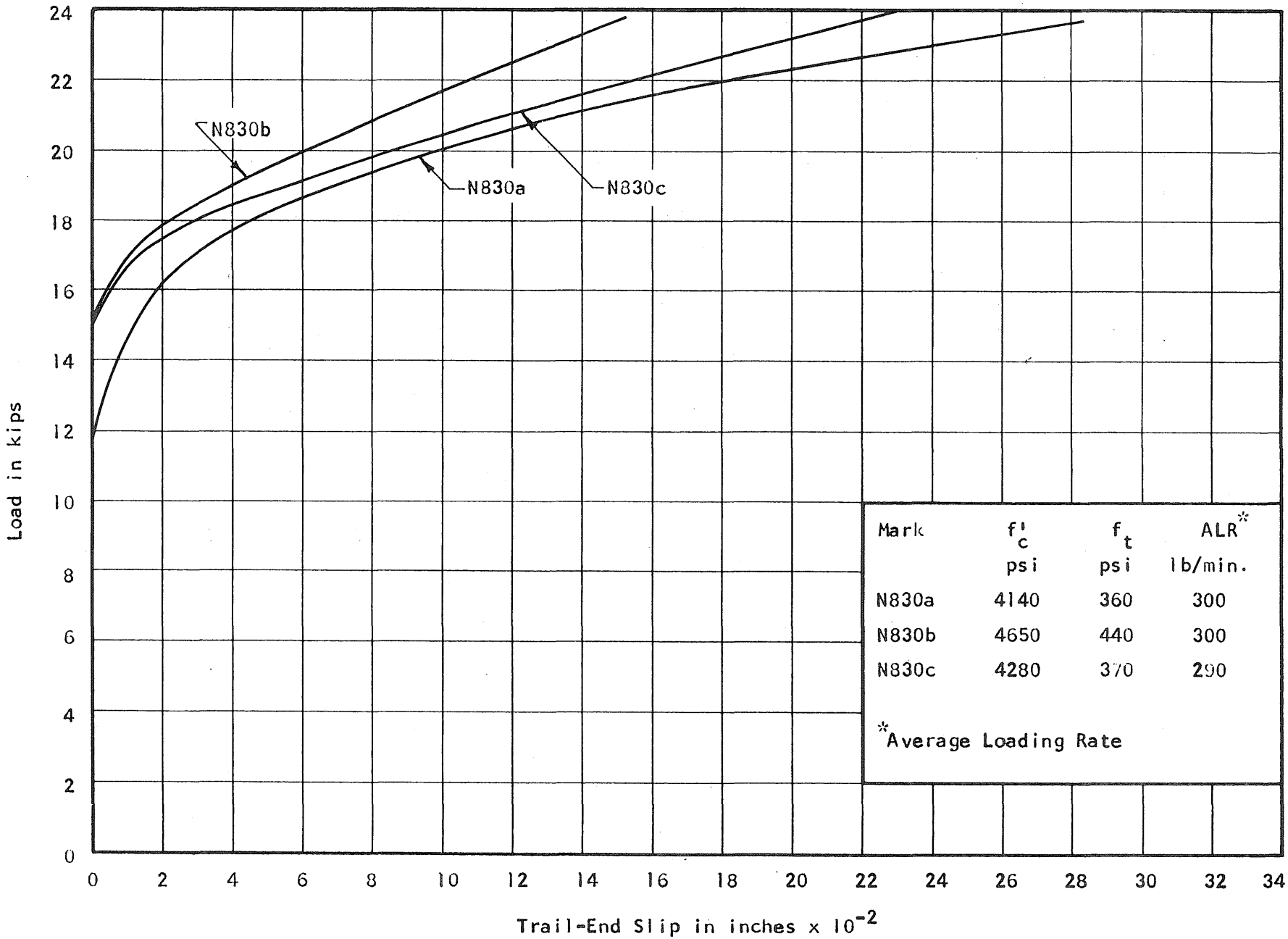

FIG. 2.22 MEASURED LOAD-SLIP CURVES. SERIES 8
Length: 30-in. Strand: 7/16-in. Round

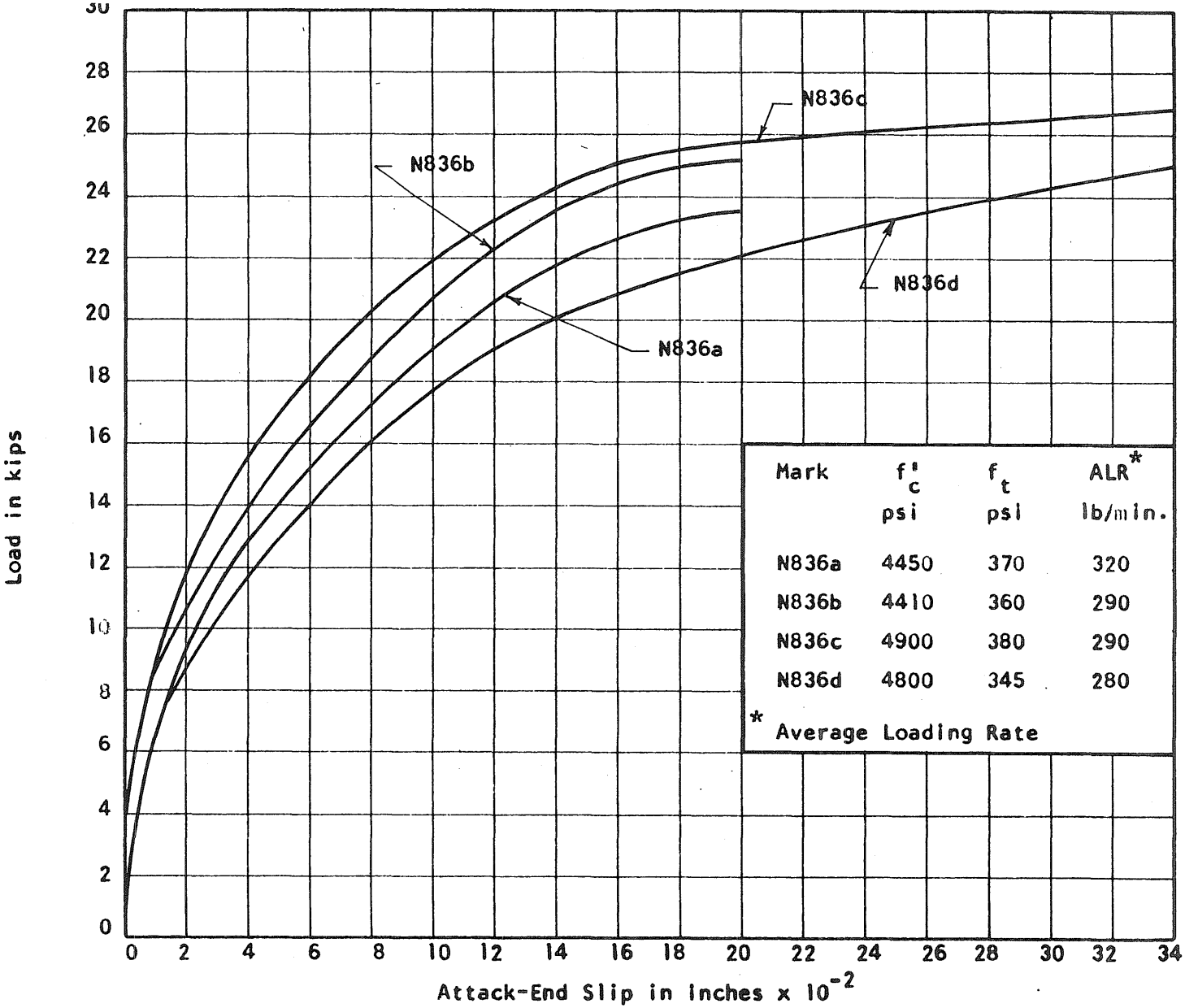

Mark	f'_c psi	f_t psi	ALR* lb/min.
N836a	4450	370	320
N836b	4410	360	290
N836c	4900	380	290
N836d	4800	345	280

* Average Loading Rate

FIG. 2.23 MEASURED LOAD-SLIP CURVES. SERIES 8
Length: 36-in. Strand: 7/16-in. Round

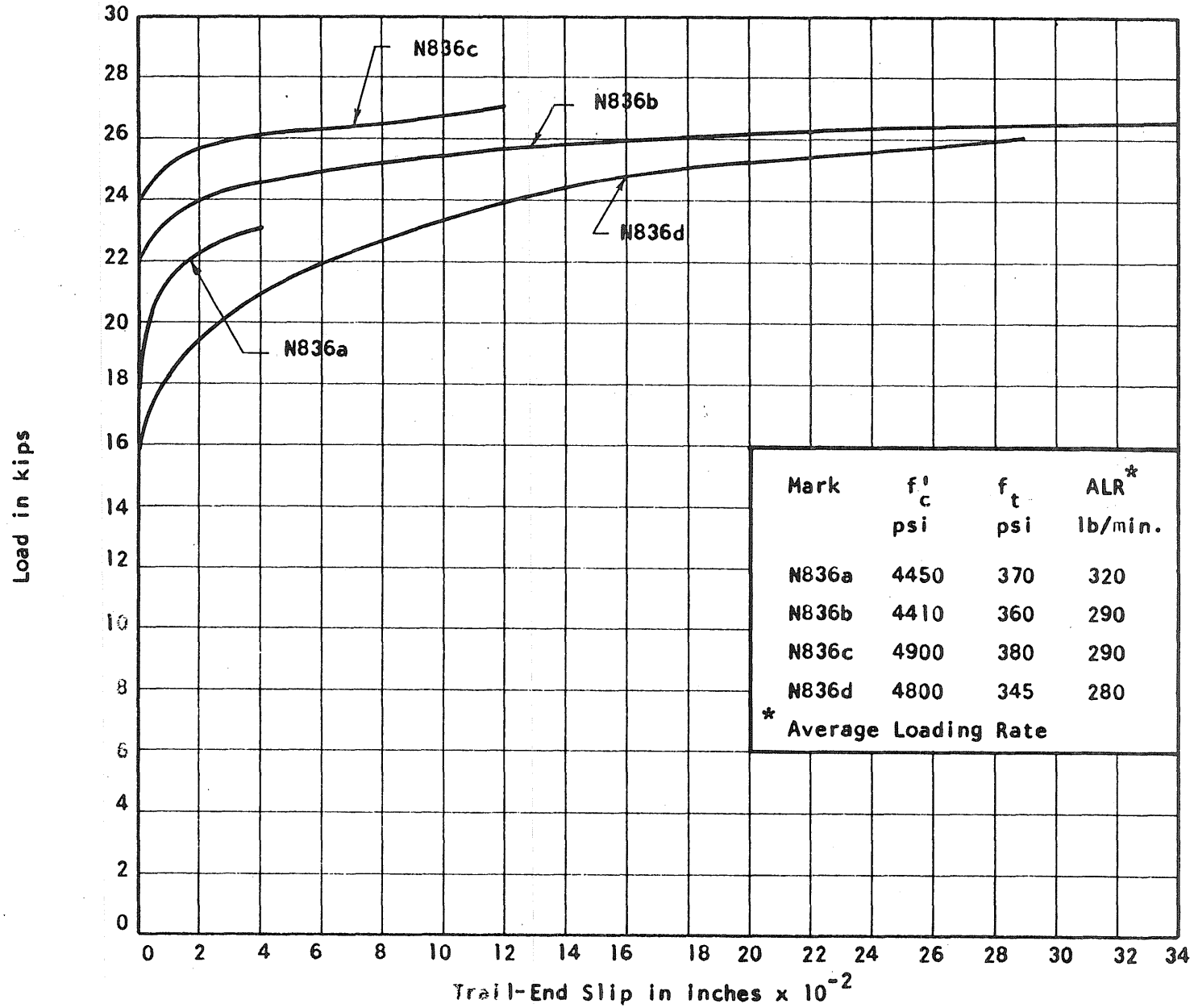

FIG. 2.24 MEASURED LOAD-SLIP CURVES. SERIES 8
Length: 36-in. Strand: 7/16-in. Round

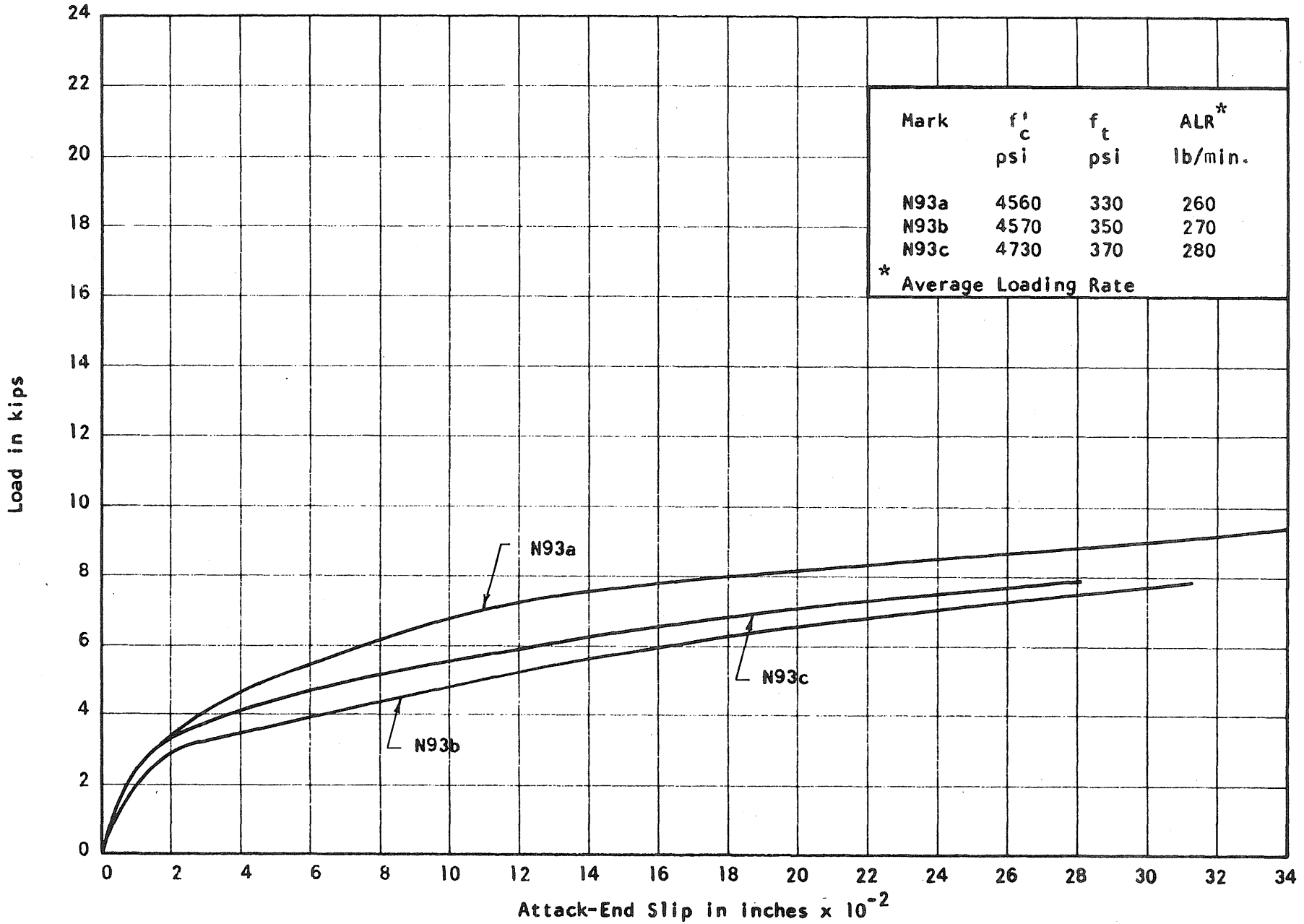

FIG. 2.25 MEASURED LOAD-SLIP CURVES. SERIES 9
Length: 3-in. Strand: 7/16-in. Rectangular

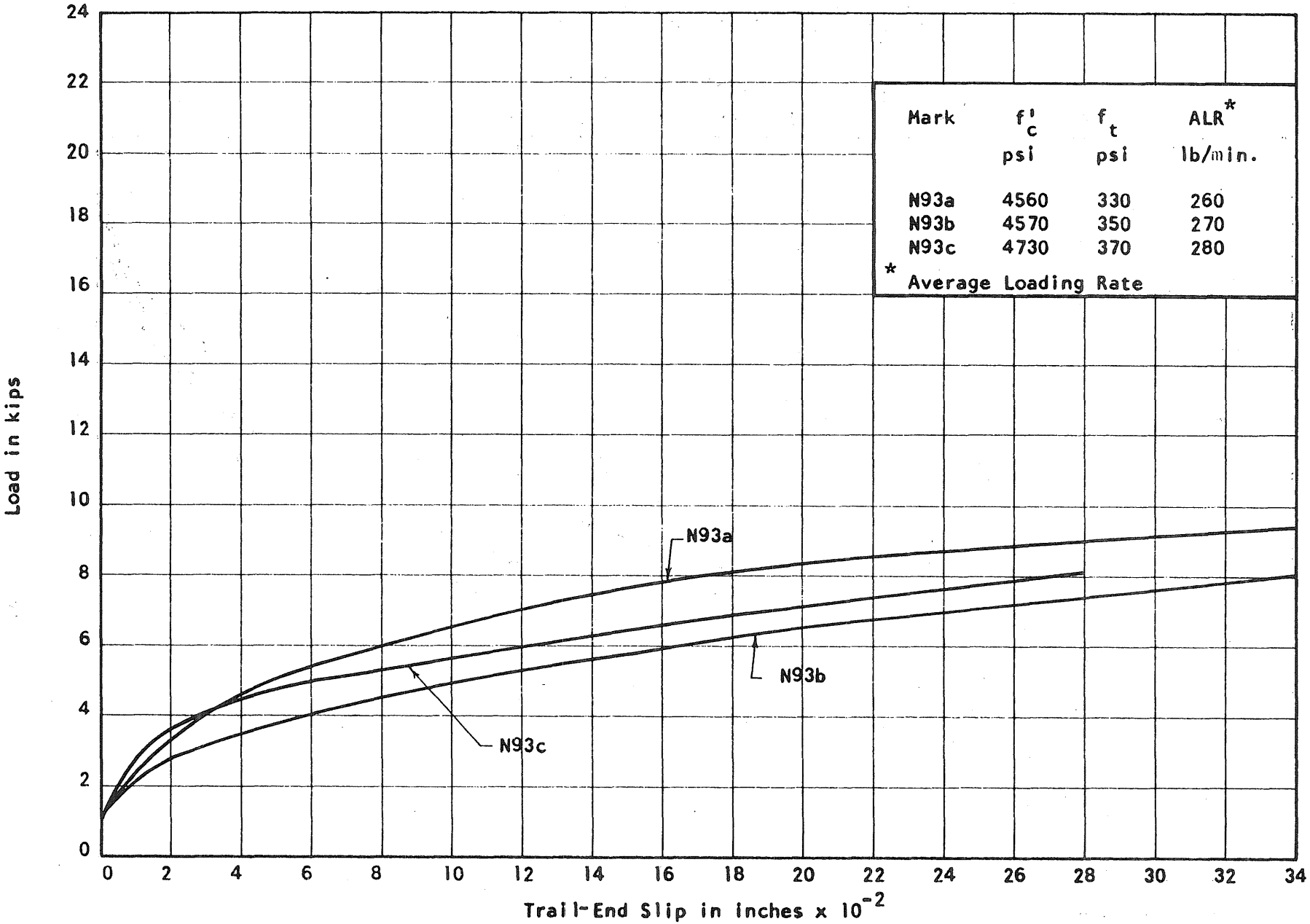

FIG. 2.26 MEASURED LOAD-SLIP CURVES. SERIES 9
Length: 3-in. Strand: 7/16-in. Rectangular

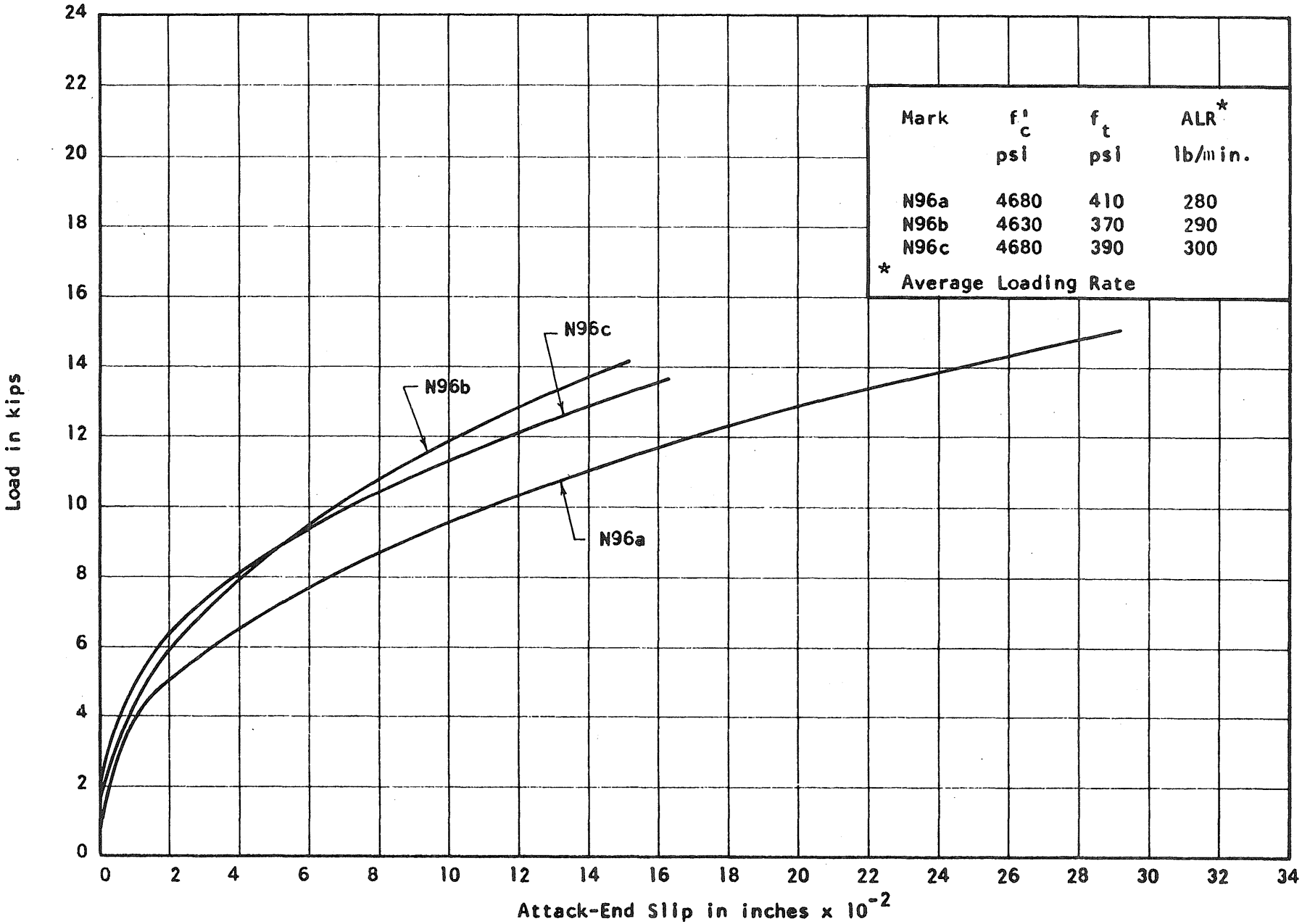

FIG. 2.27 MEASURED LOAD-SLIP CURVES. SERIES 9
Length: 6-in. Strand: 7/16-in. Rectangular

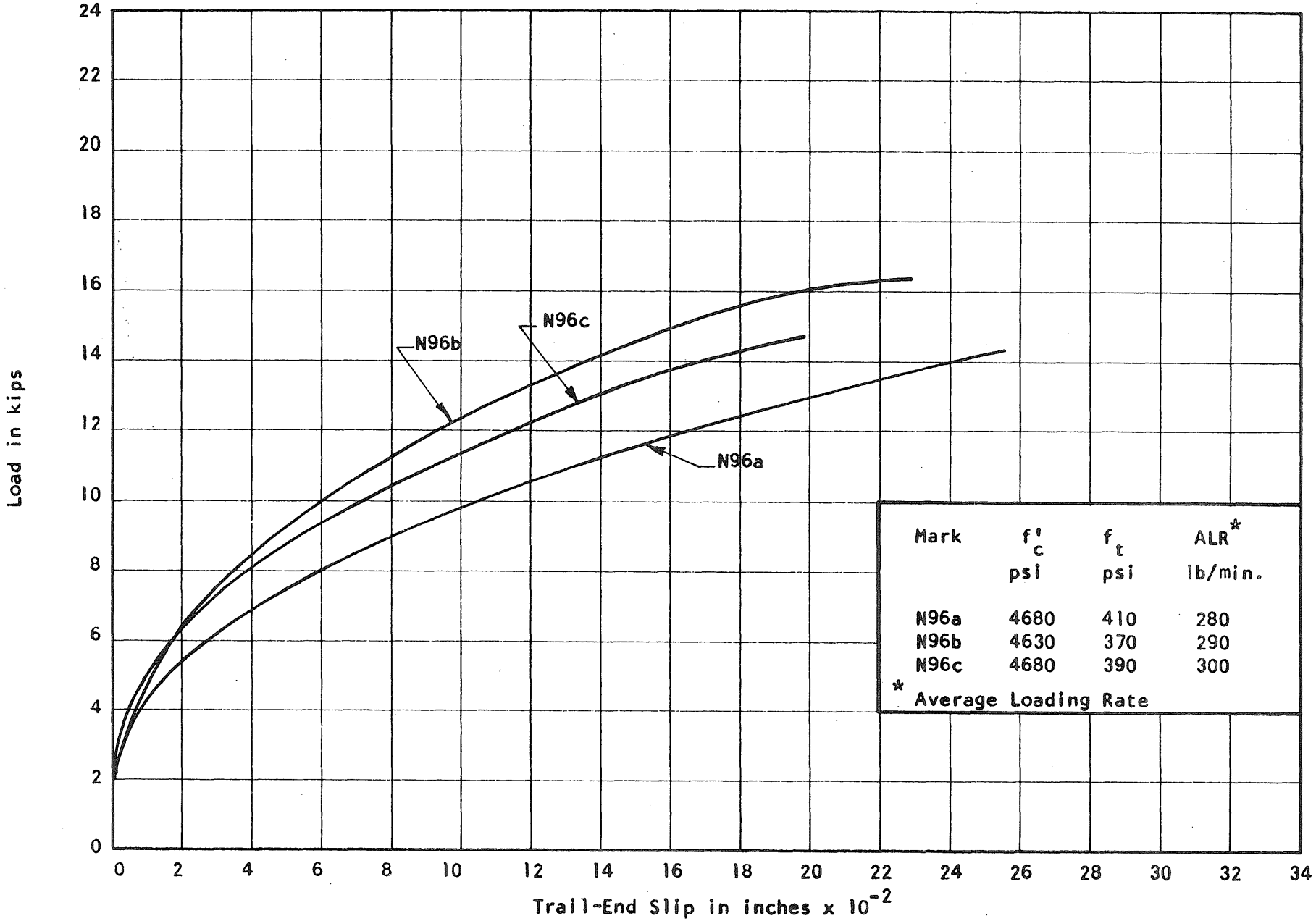

FIG. 2.28 MEASURED LOAD-SLIP CURVES. SERIES 9
Length: 6-in. Strand: 7/16-in. Rectangular

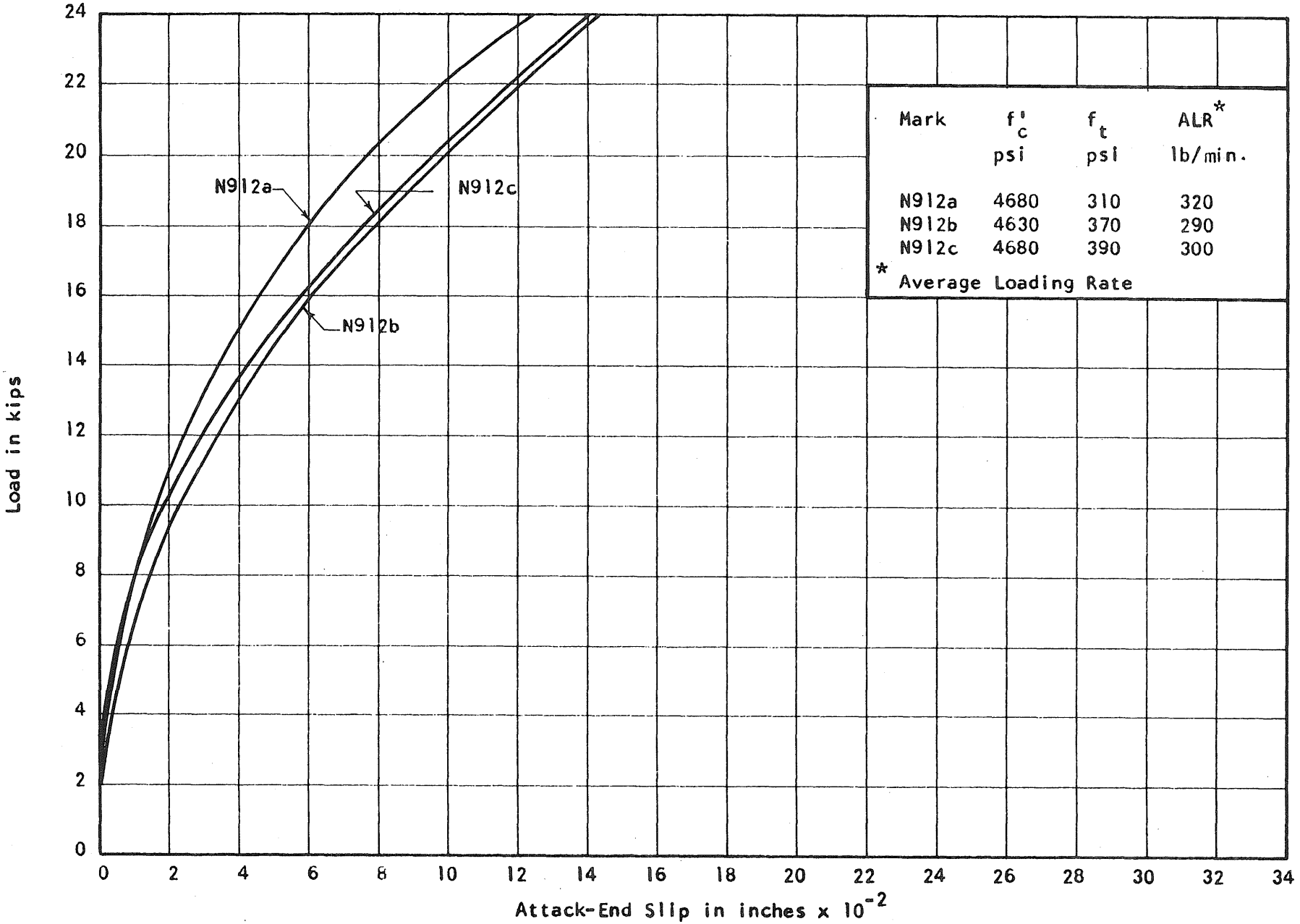

FIG. 2.29 MEASURED LOAD-SLIP CURVES. SERIES 9
Length: 12-in. Strand: 7/16-in. Rectangular

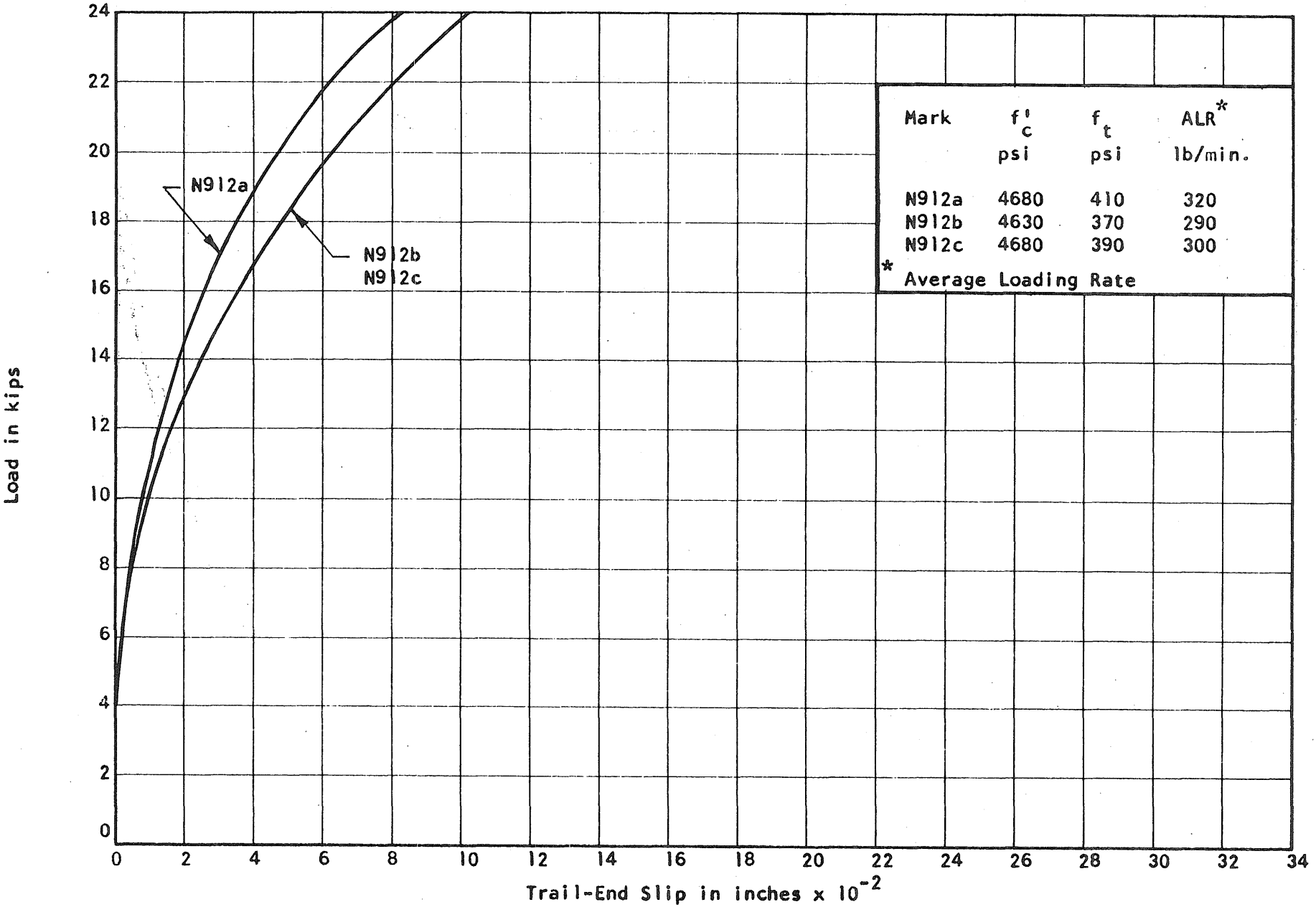

FIG. 2.30 MEASURED LOAD-SLIP CURVES. SERIES 9
Length: 12-in. Strand: 7/16-in. Rectangular

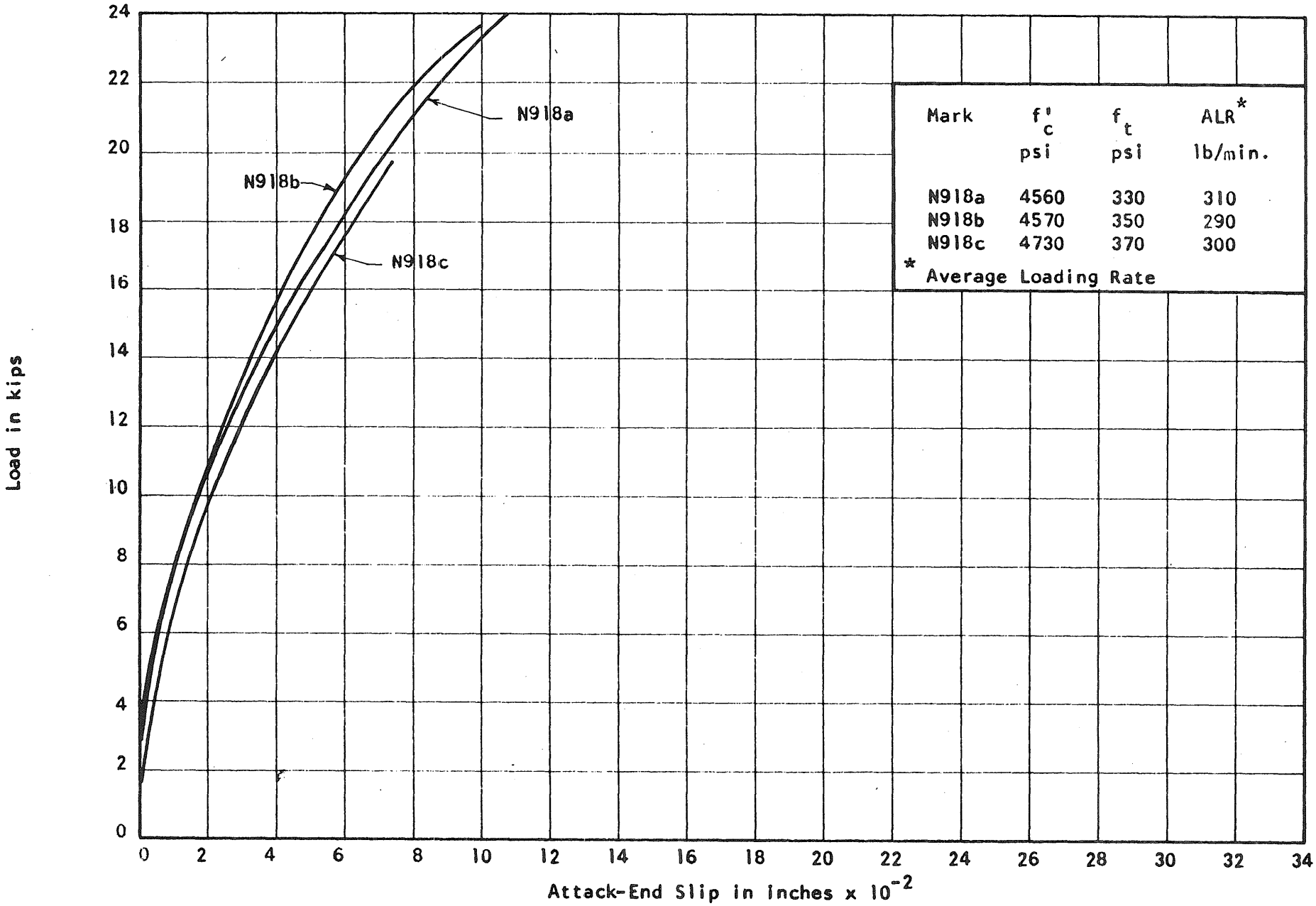

FIG. 2.31 MEASURED LOAD-SLIP CURVES. SERIES 9
Length: 18-in. Strand: 7/16-in. Rectangular

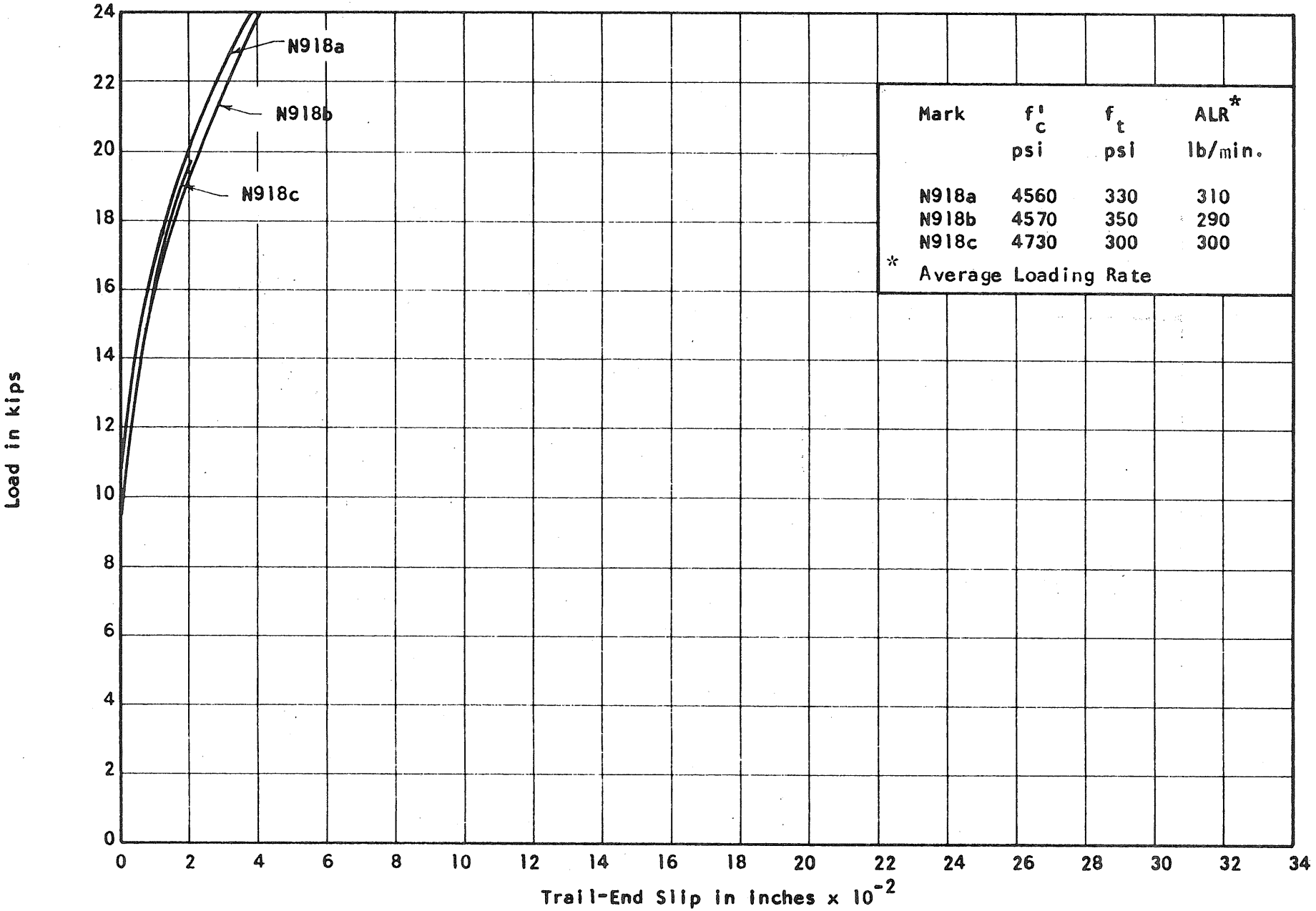

FIG. 2.32 MEASURED LOAD-SLIP CURVES. SERIES 9
Length: 18-in. Strand: 7/16-in. Rectangular

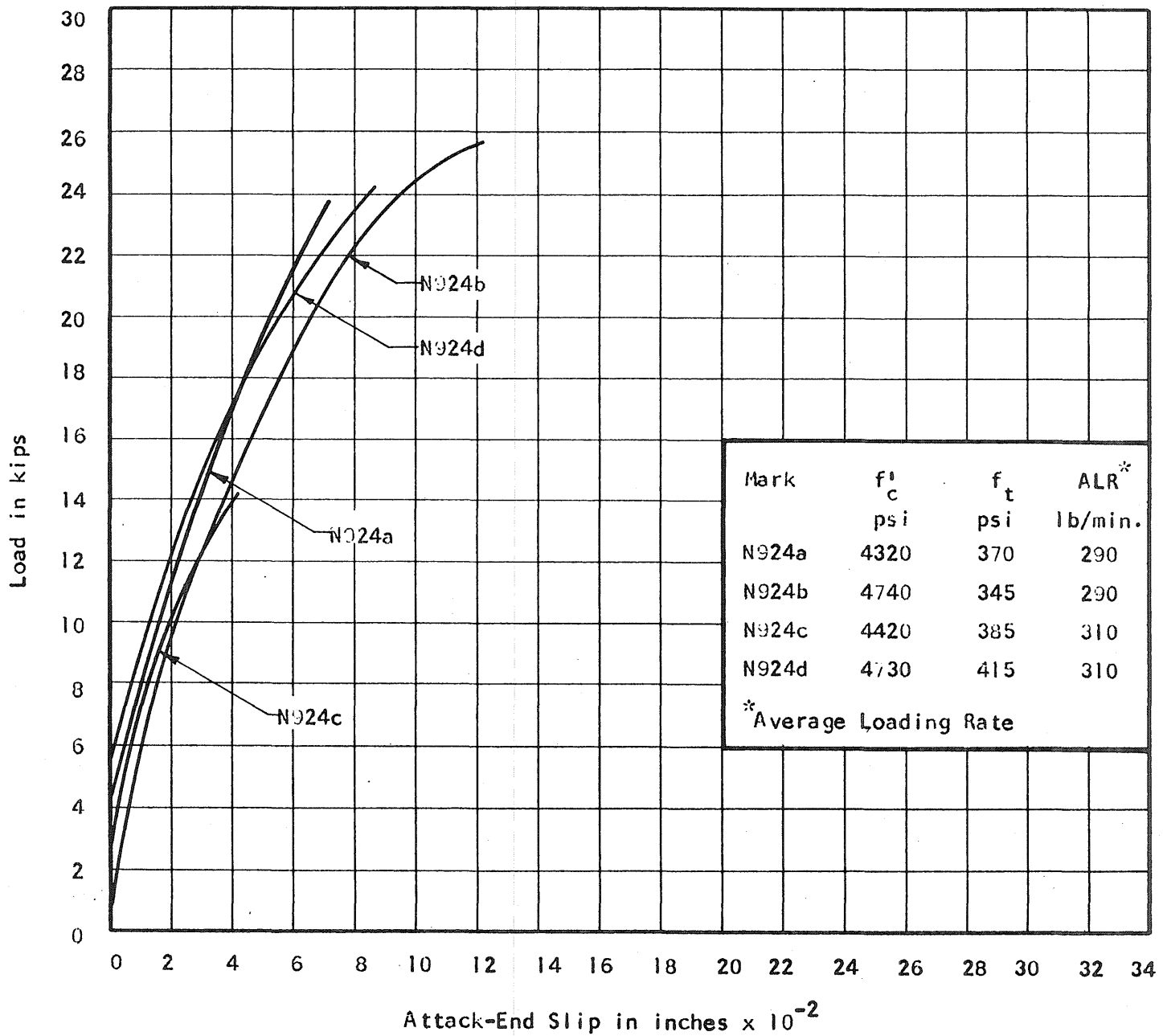

FIG. 2.33 MEASURED LOAD-SLIP CURVES. SERIES 9
Length: 24-in. Strand: 7/16-in. Rectangular

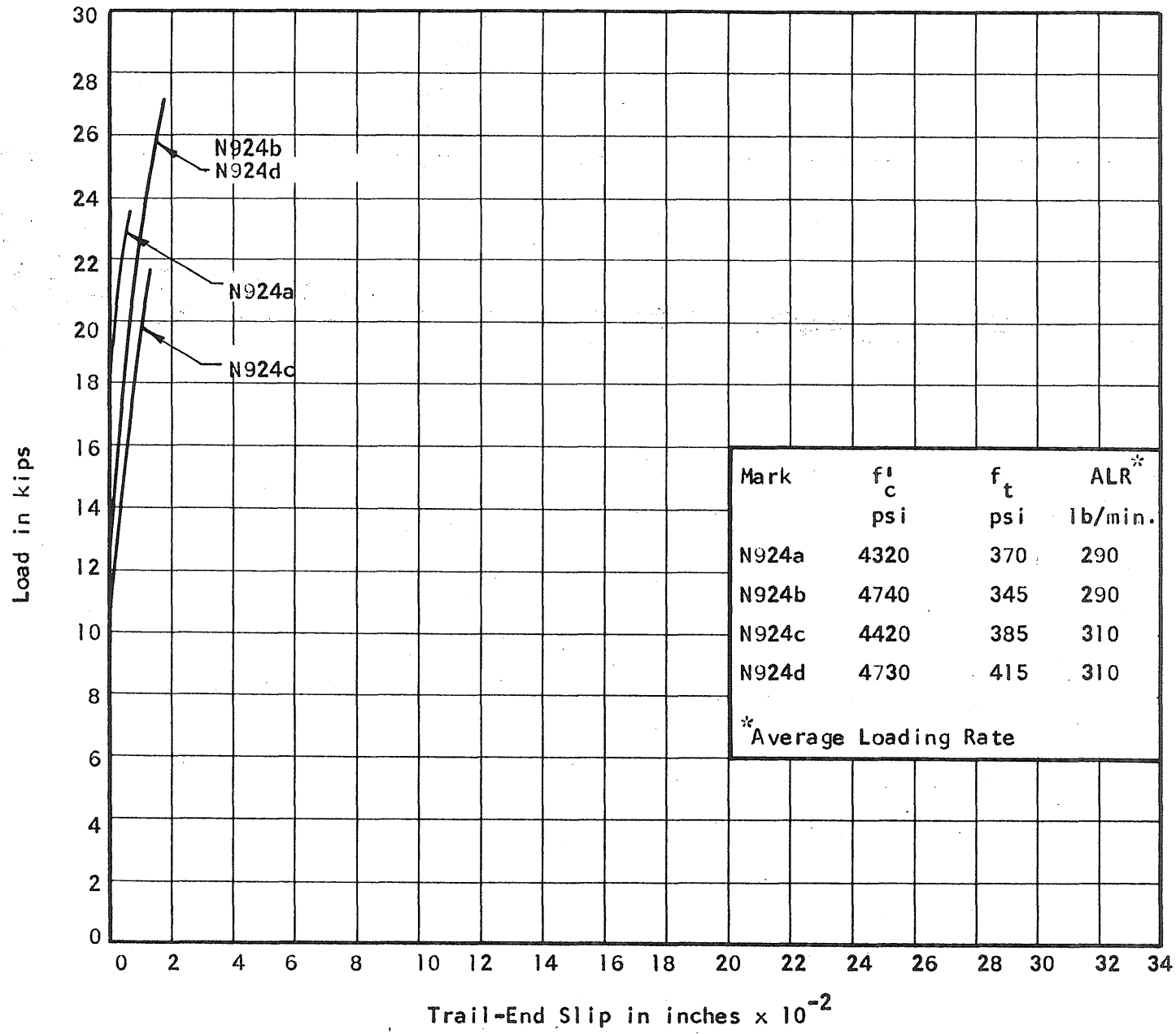

FIG. 2.34 MEASURED LOAD-SLIP CURVES. SERIES 9
Length: 24-in. Strand: 7/16-in. Rectangular

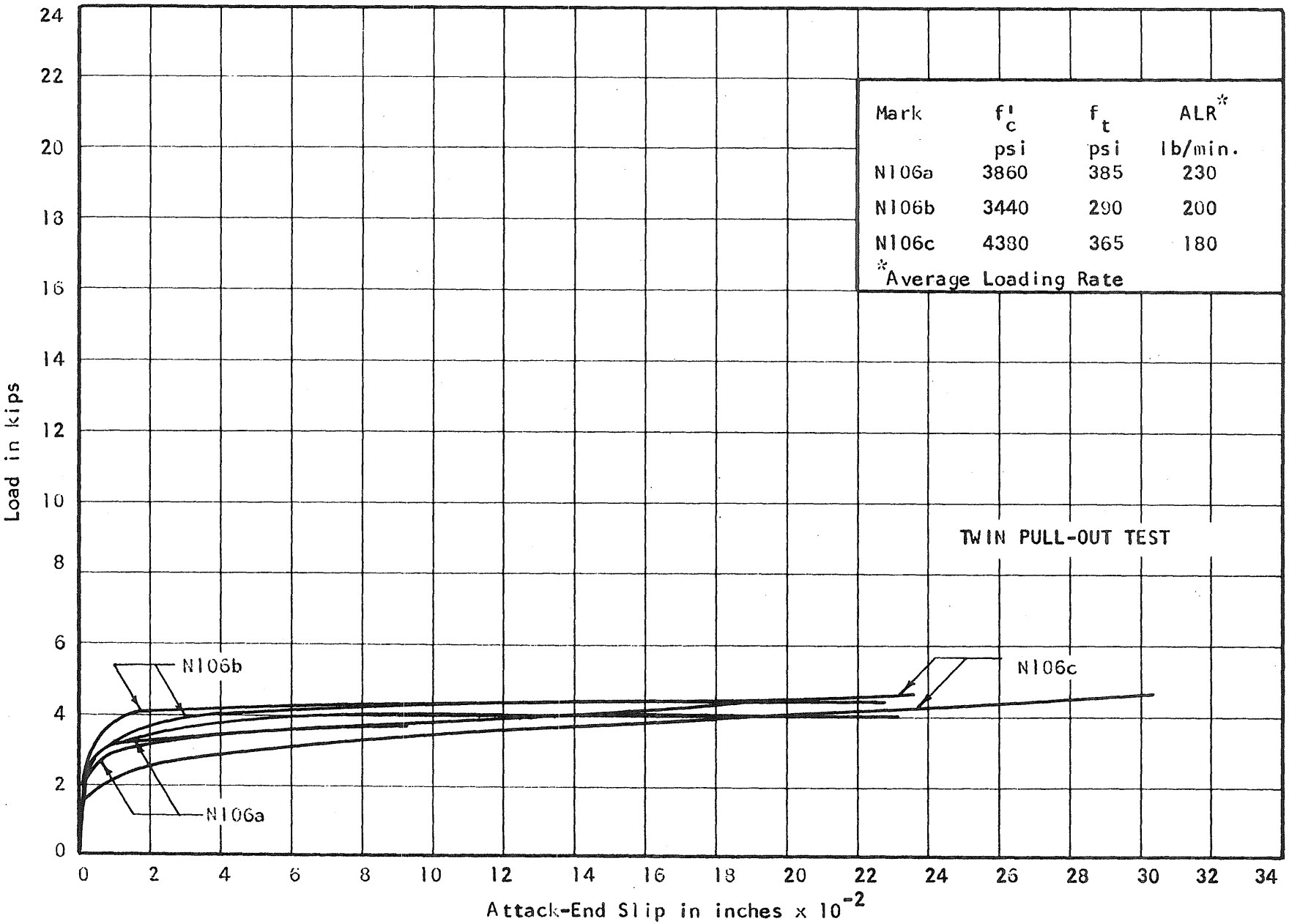

FIG. 2.35 MEASURED LOAD-SLIP CURVES. SERIES 10
Length: 6-in. Strand: 7/16-in. Round

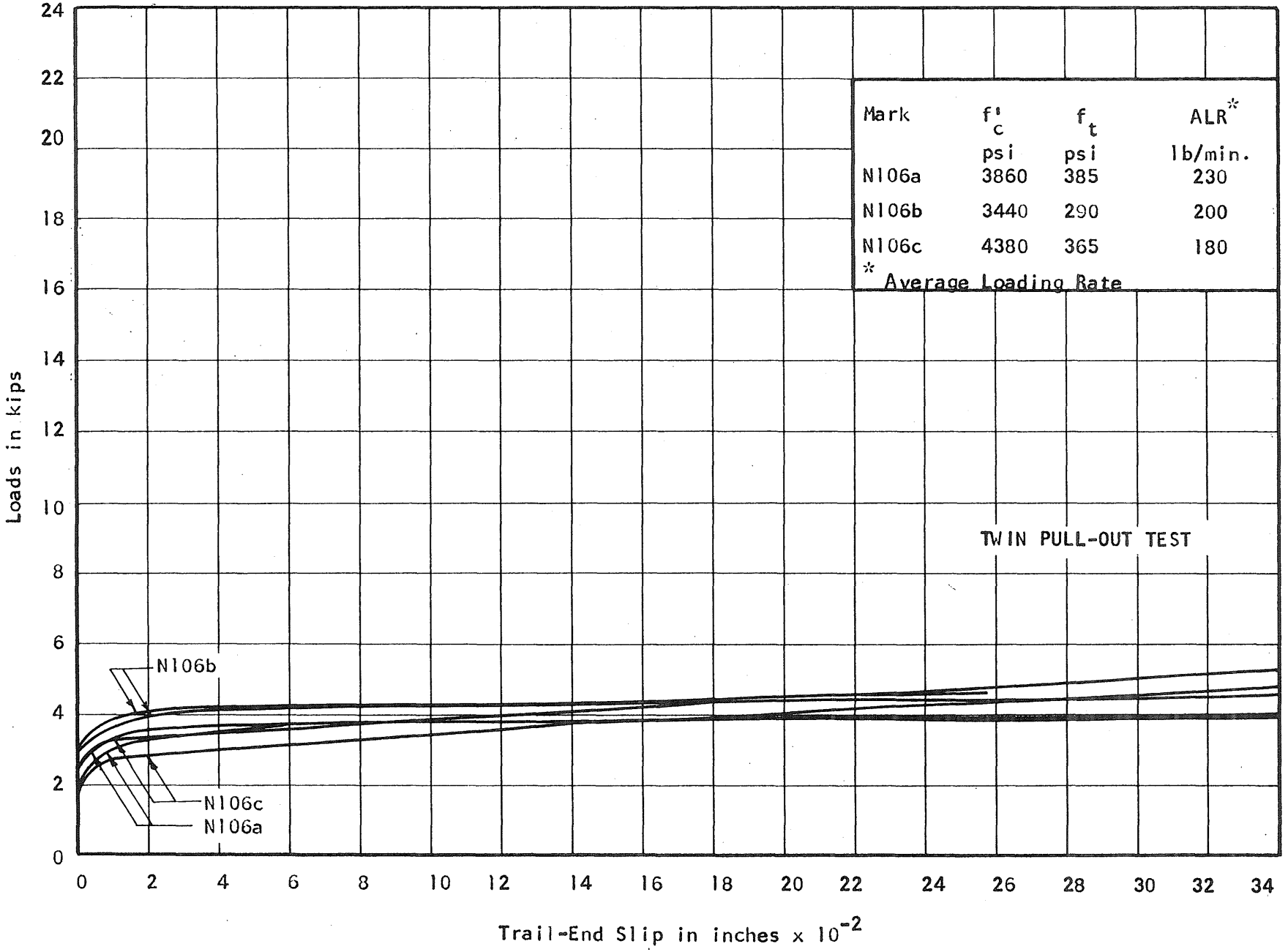

FIG. 2.36 MEASURED LOAD-SLIP CURVES. SERIES 10
Length: 6-in. Strand: 7/16-in. Round

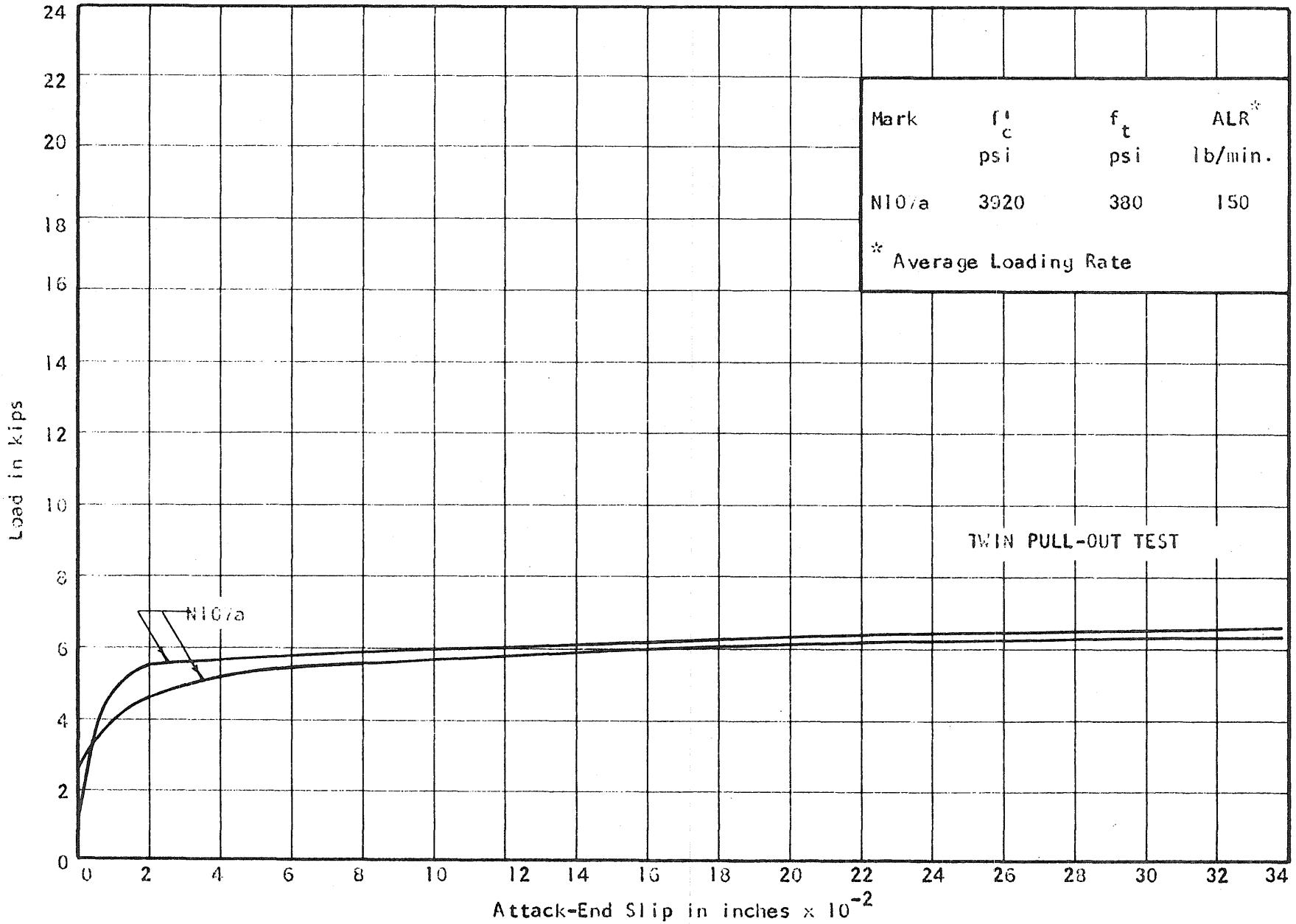

FIG. 2.37 MEASURED LOAD-SLIP CURVES. SERIES 10
Length: /-in. Strand: 7/16-in Round

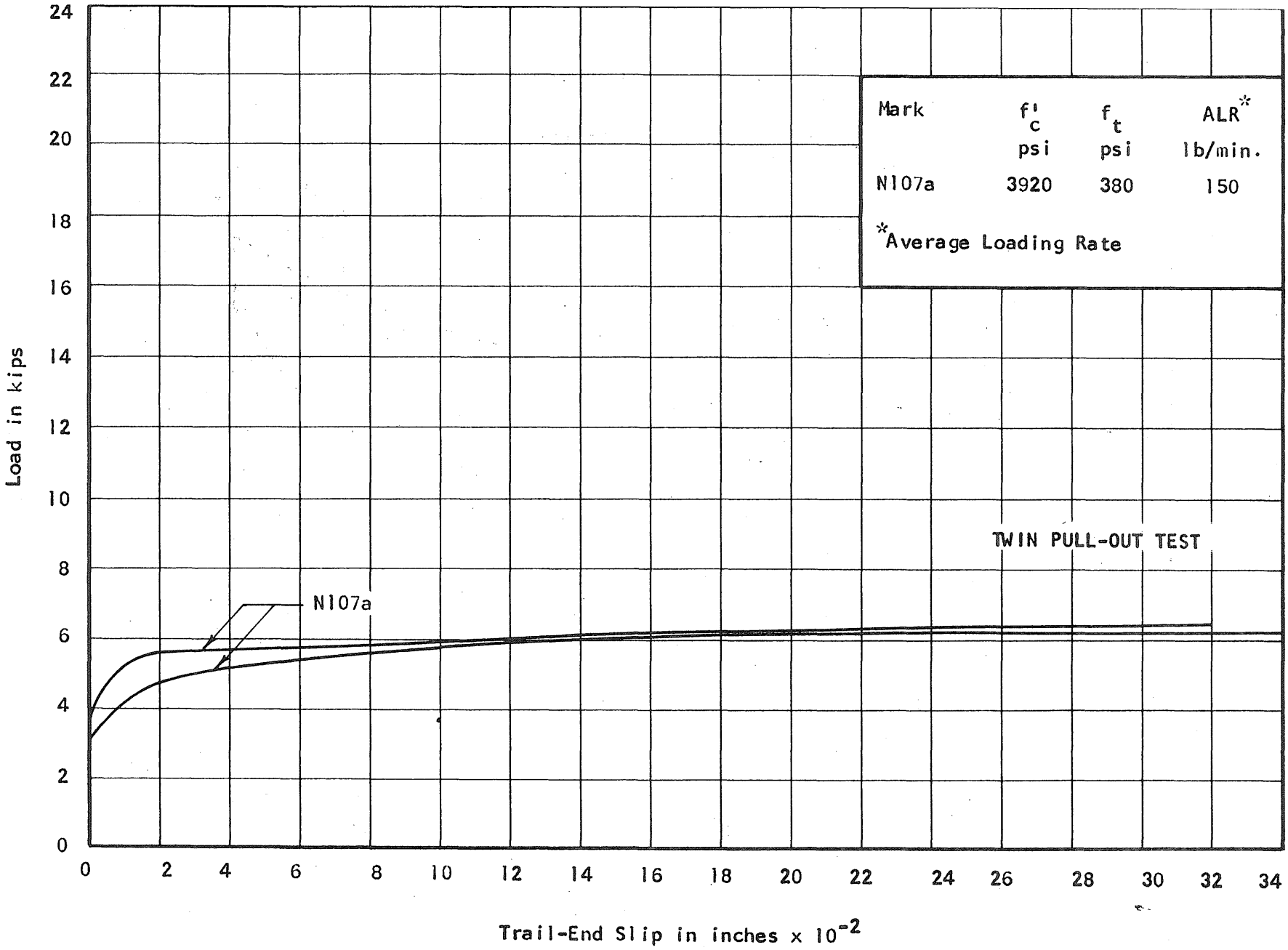

FIG. 2.38 MEASURED LOAD-SLIP CURVES. SERIES 10
Length: 7-in. Strand: 7/16-in. Round

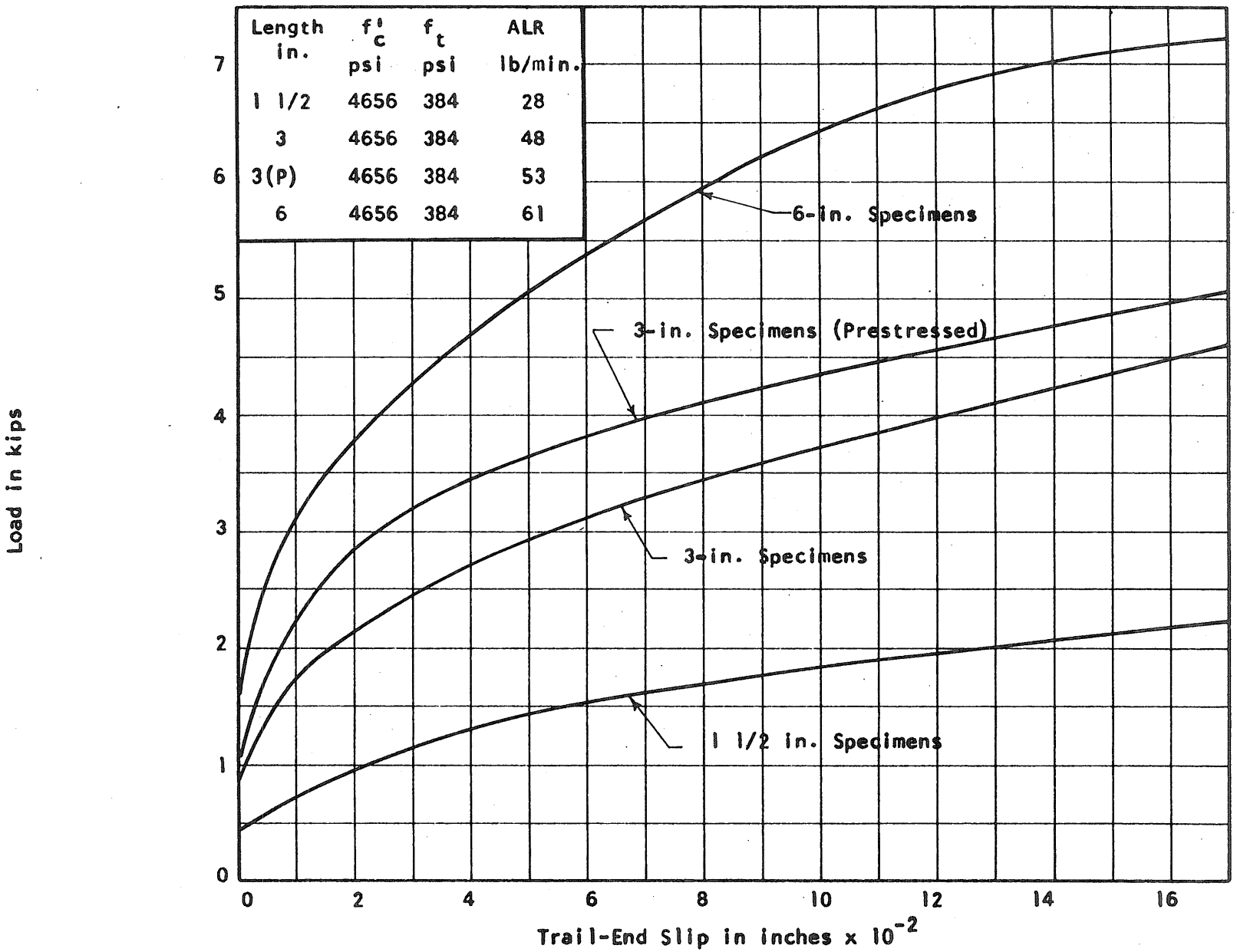

FIG. 2.39 AVERAGE LOAD-SLIP CURVES. SERIES 7
Strand: 1/4-in. Rectangular

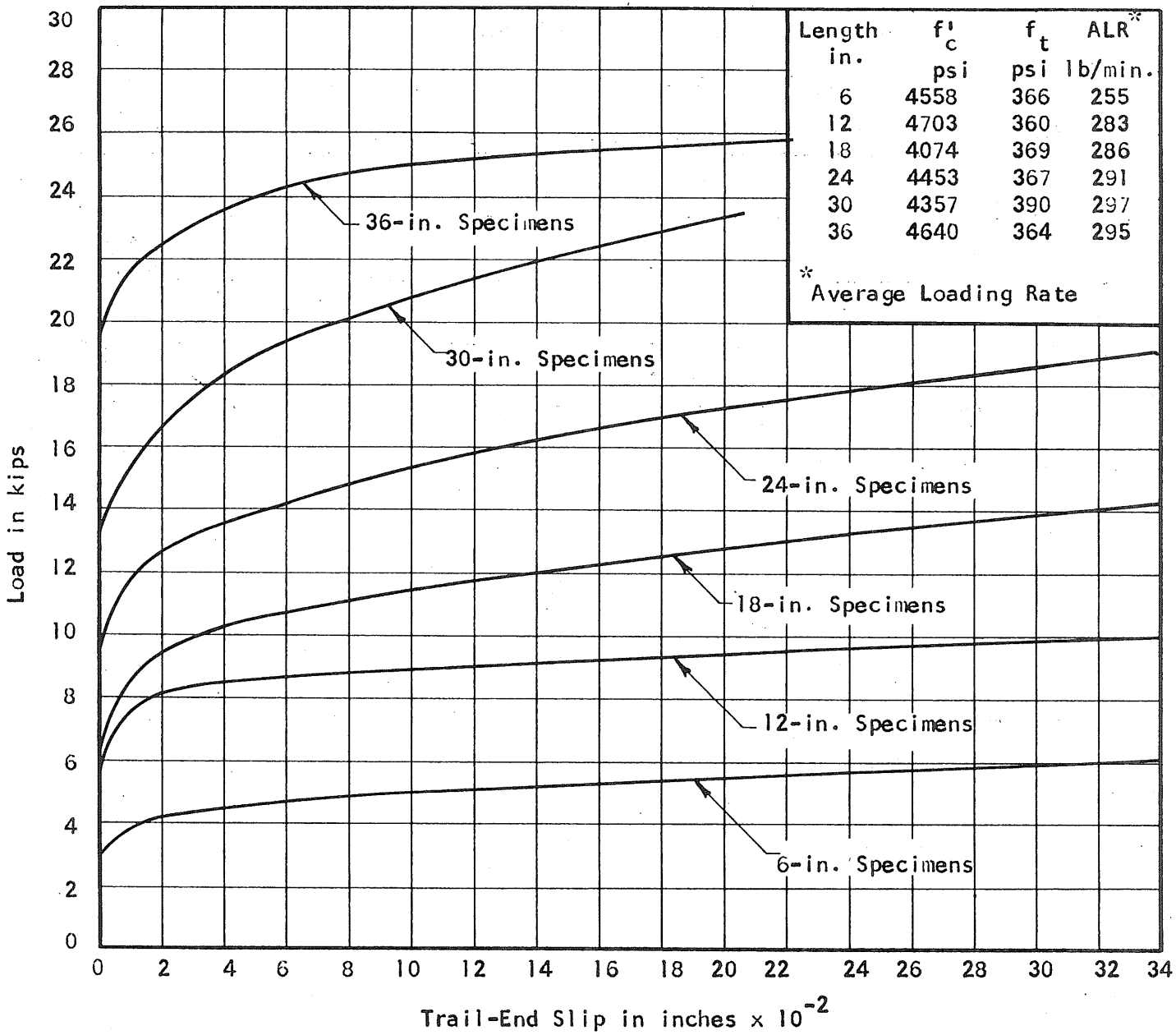

FIG. 2.40 AVERAGE LOAD-SLIP CURVES. SERIES 8
Strand: 7/16-in. Round

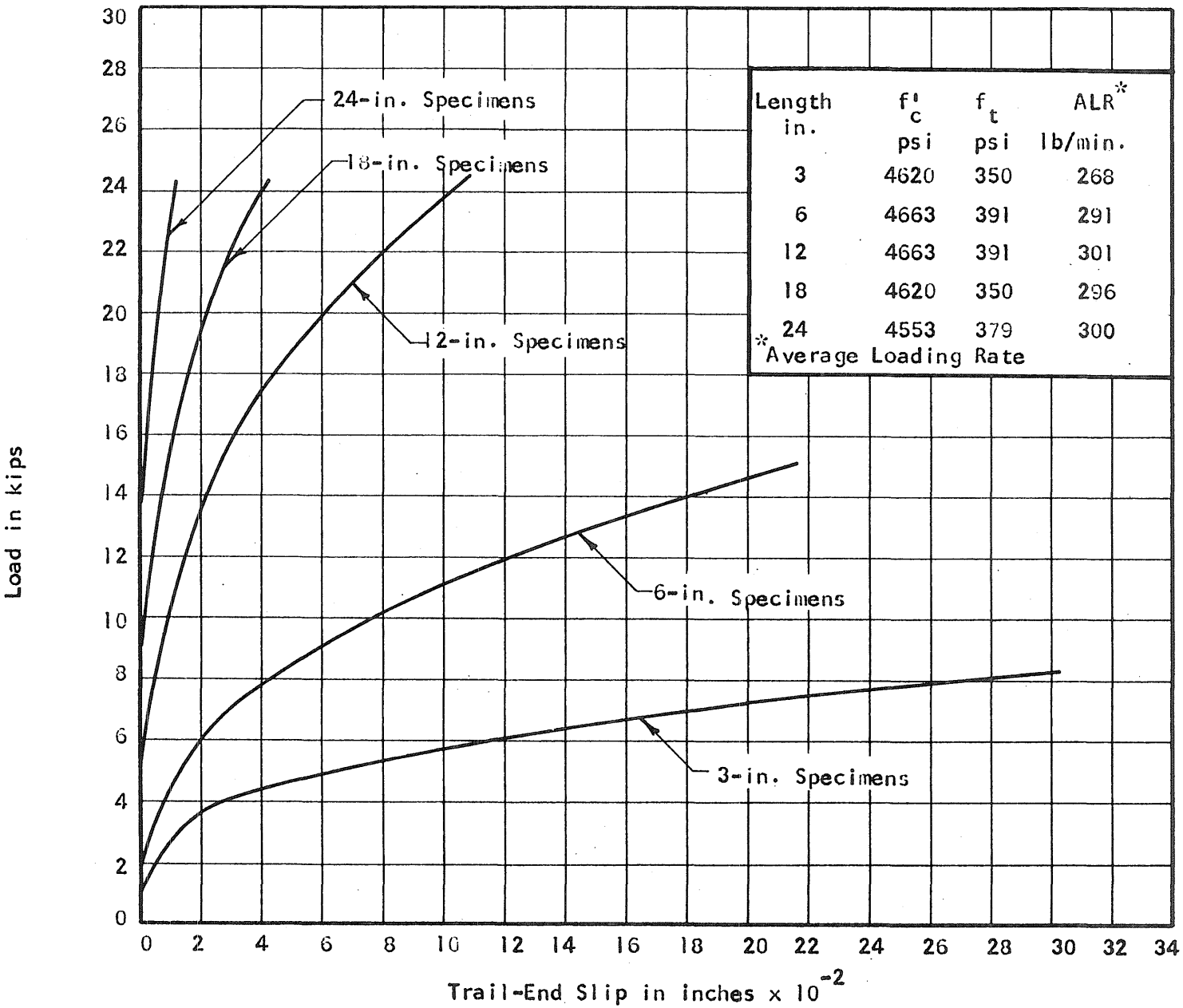

FIG. 2.41 AVERAGE LOAD-SLIP CURVES. SERIES 9
Strand: 7/16-in. Rectangular

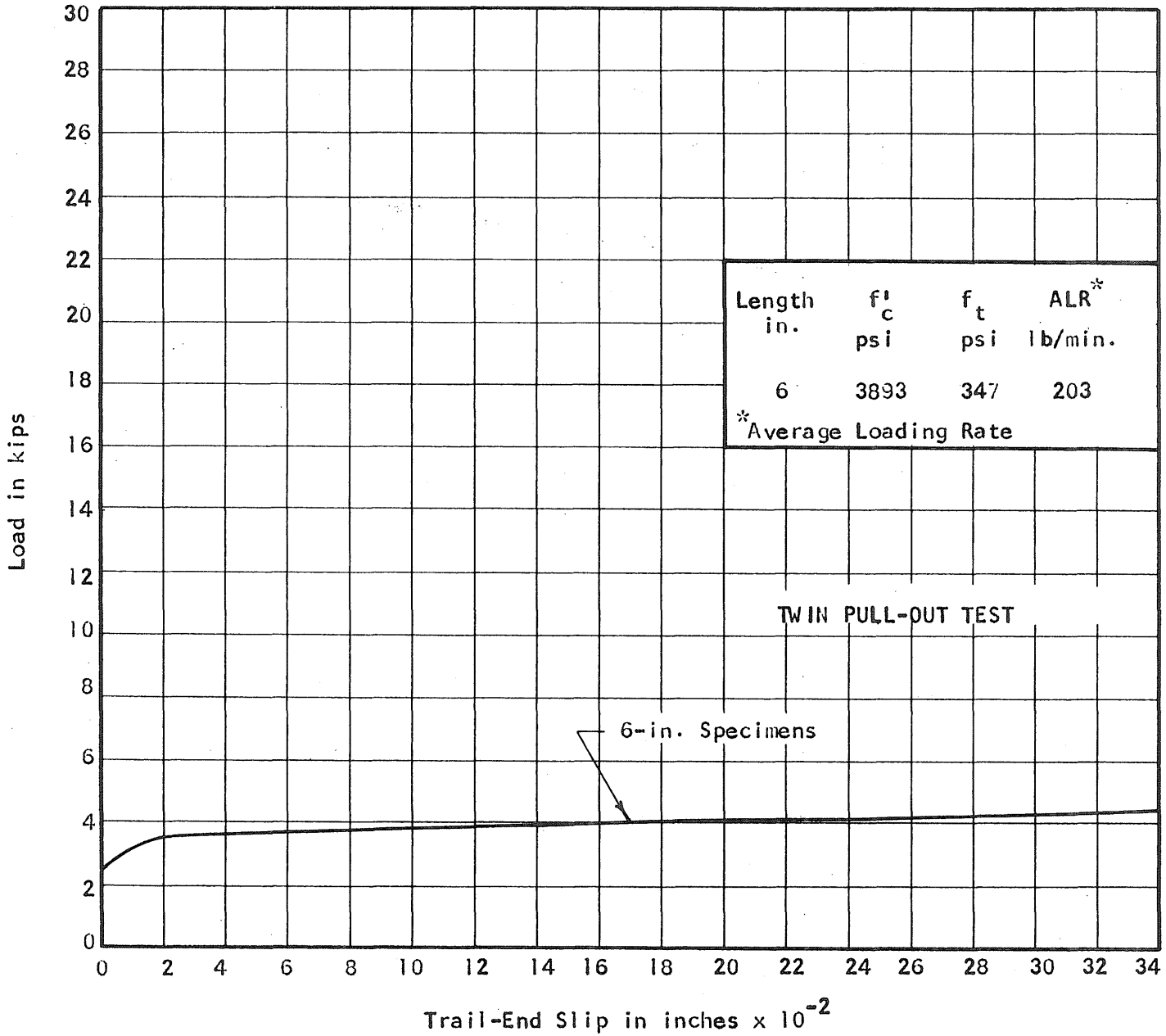

FIG. 2.42 AVERAGE LOAD-SLIP CURVES. SERIES 10
Strand: 7/16-in. Round

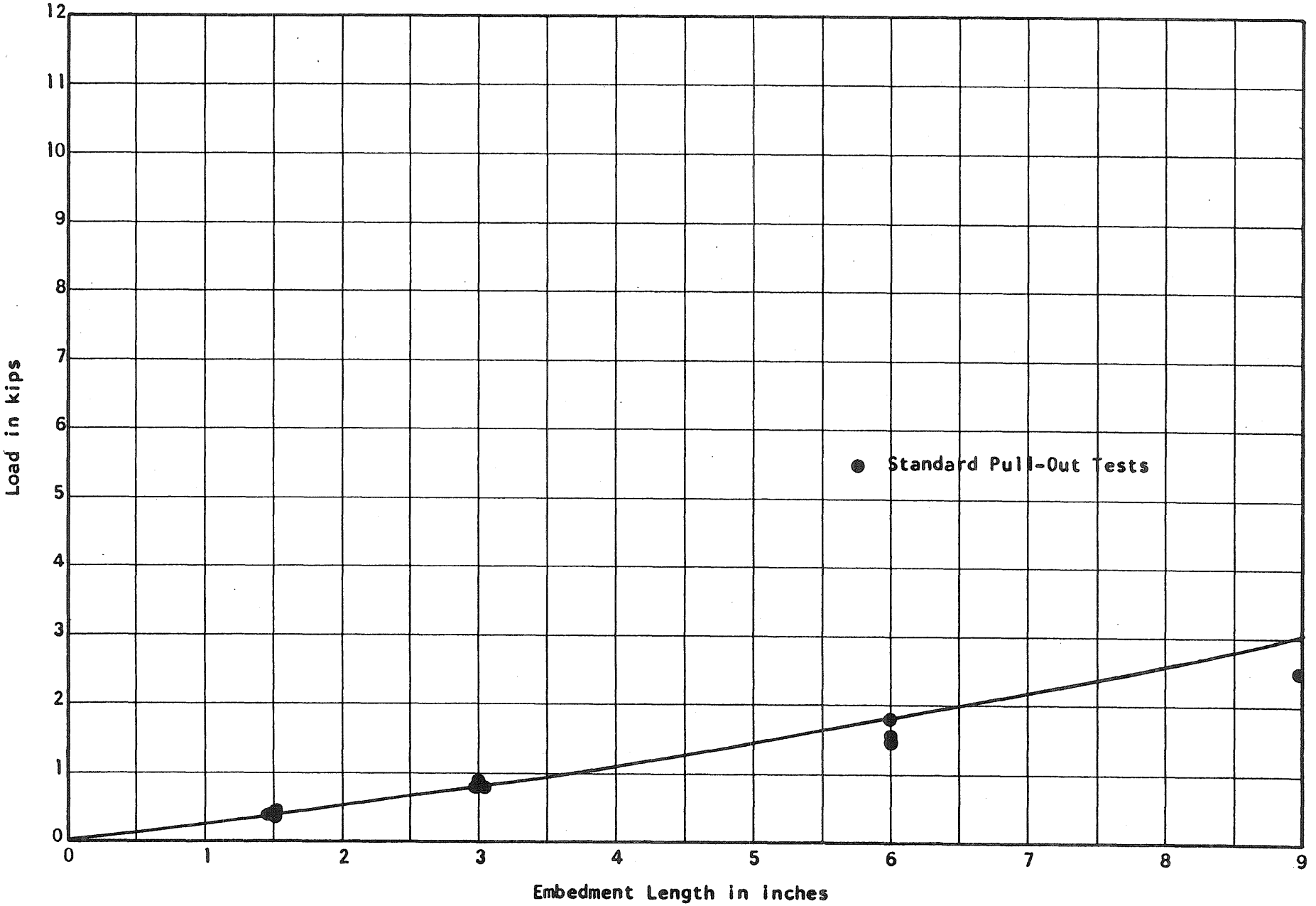

FIG. 3.1 STRAND FORCE DISTRIBUTION. SERIES 7
Trail-End Slip: 0.000 in. Strand: 1/4-in. Rectangular

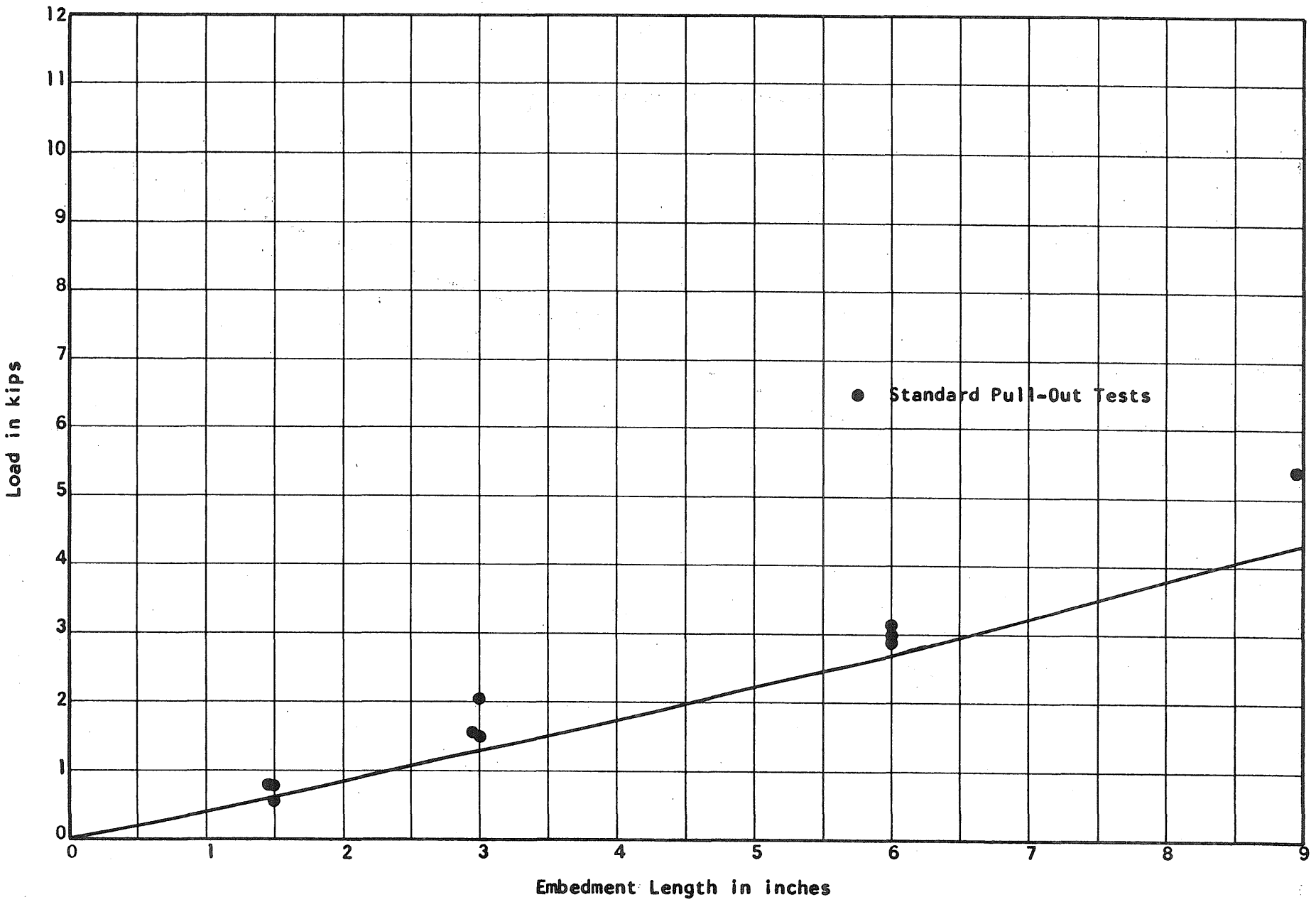

FIG. 3.2 STRAND FORCE DISTRIBUTION. SERIES 7
Trail-End Slip: 0.010 in. Strand: 1/4-in. Rectangular

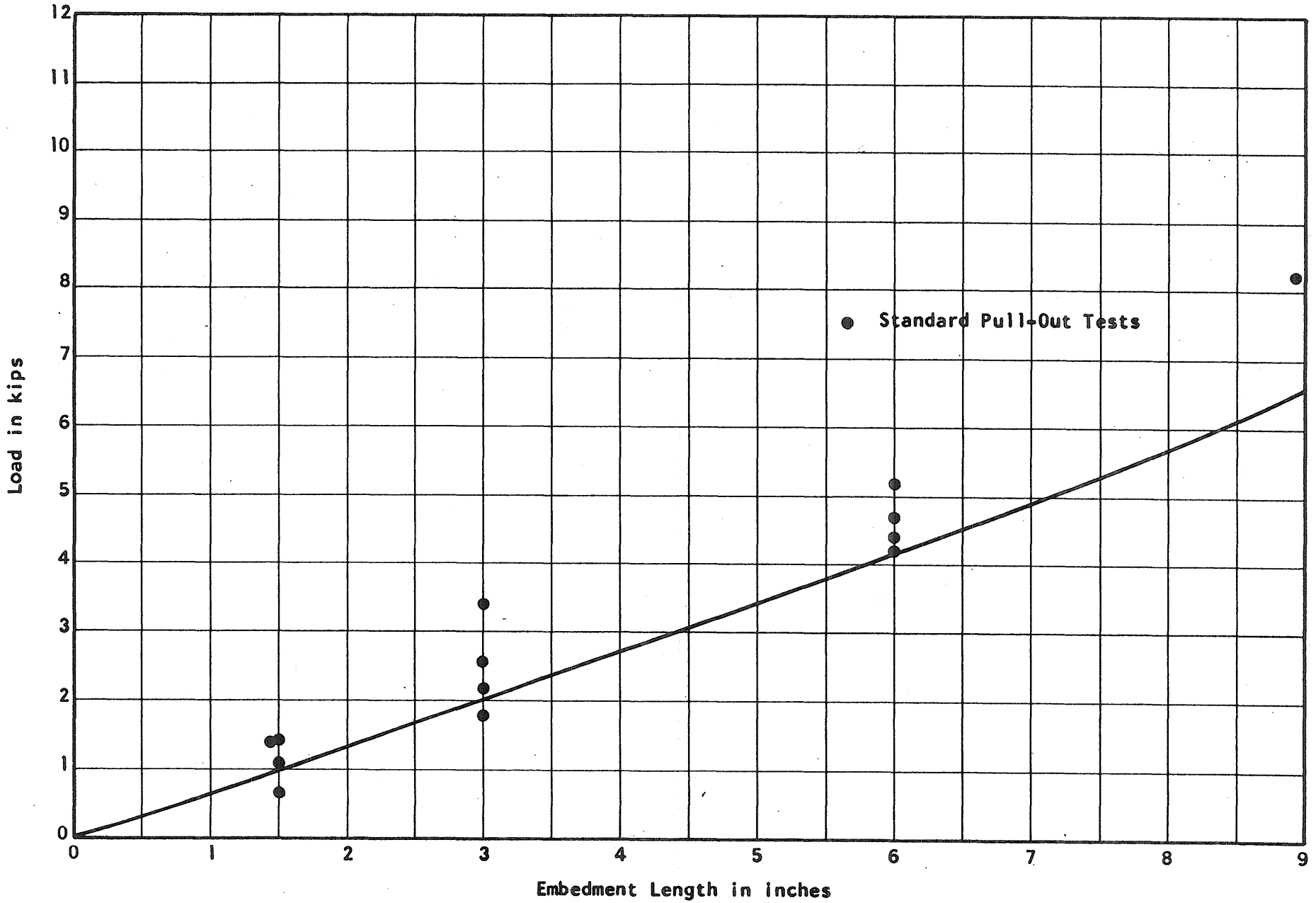

FIG. 3.3 STRAND FORCE DISTRIBUTION. SERIES 7
Trail-End Slip: 0.040 in. Strand: 1/4-in. Rectangular

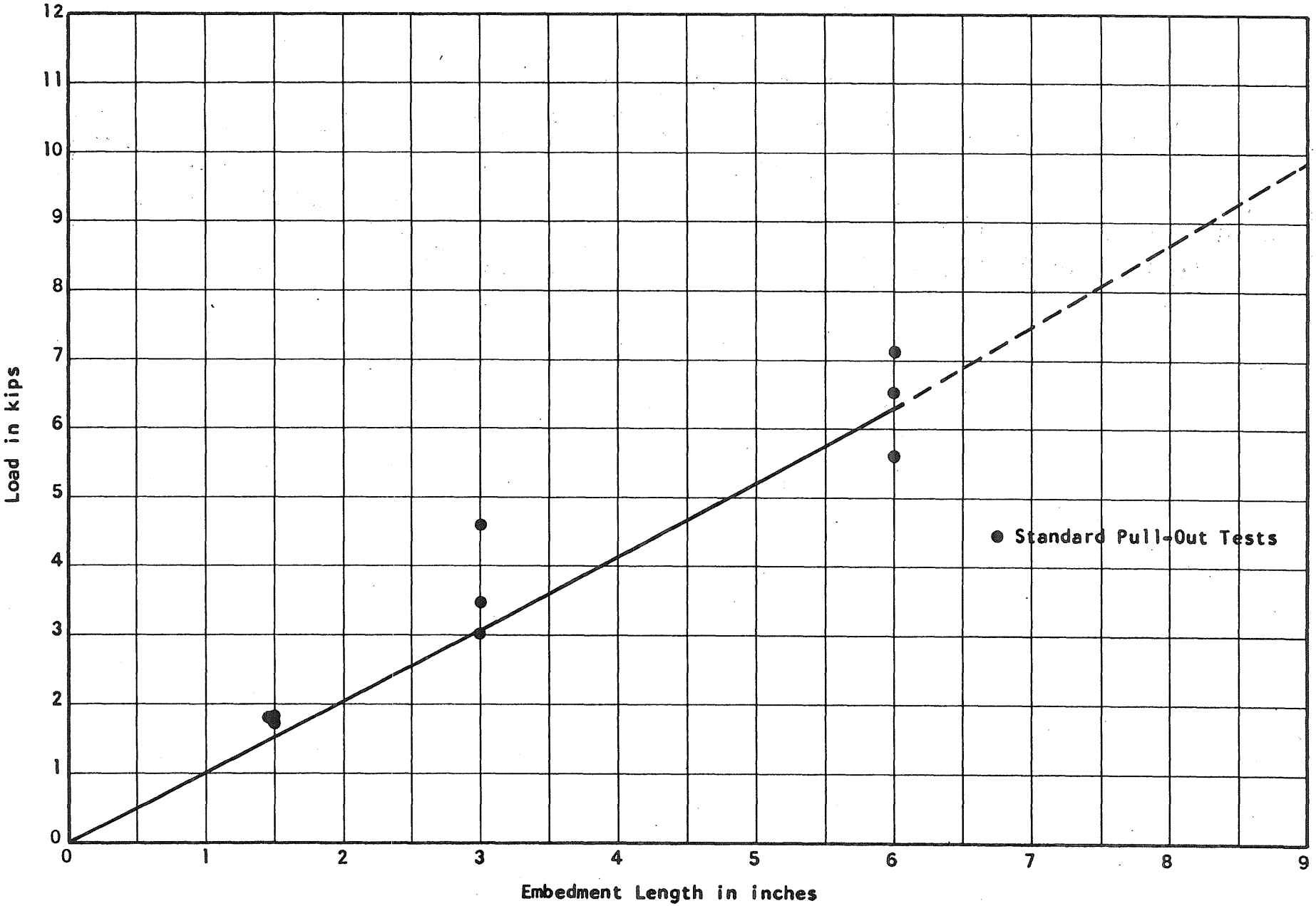

FIG. 3.4 STRAND FORCE DISTRIBUTION. SERIES 7
Trail-End Slip: 0.100 in. Strand: 1/4-in. Rectangular

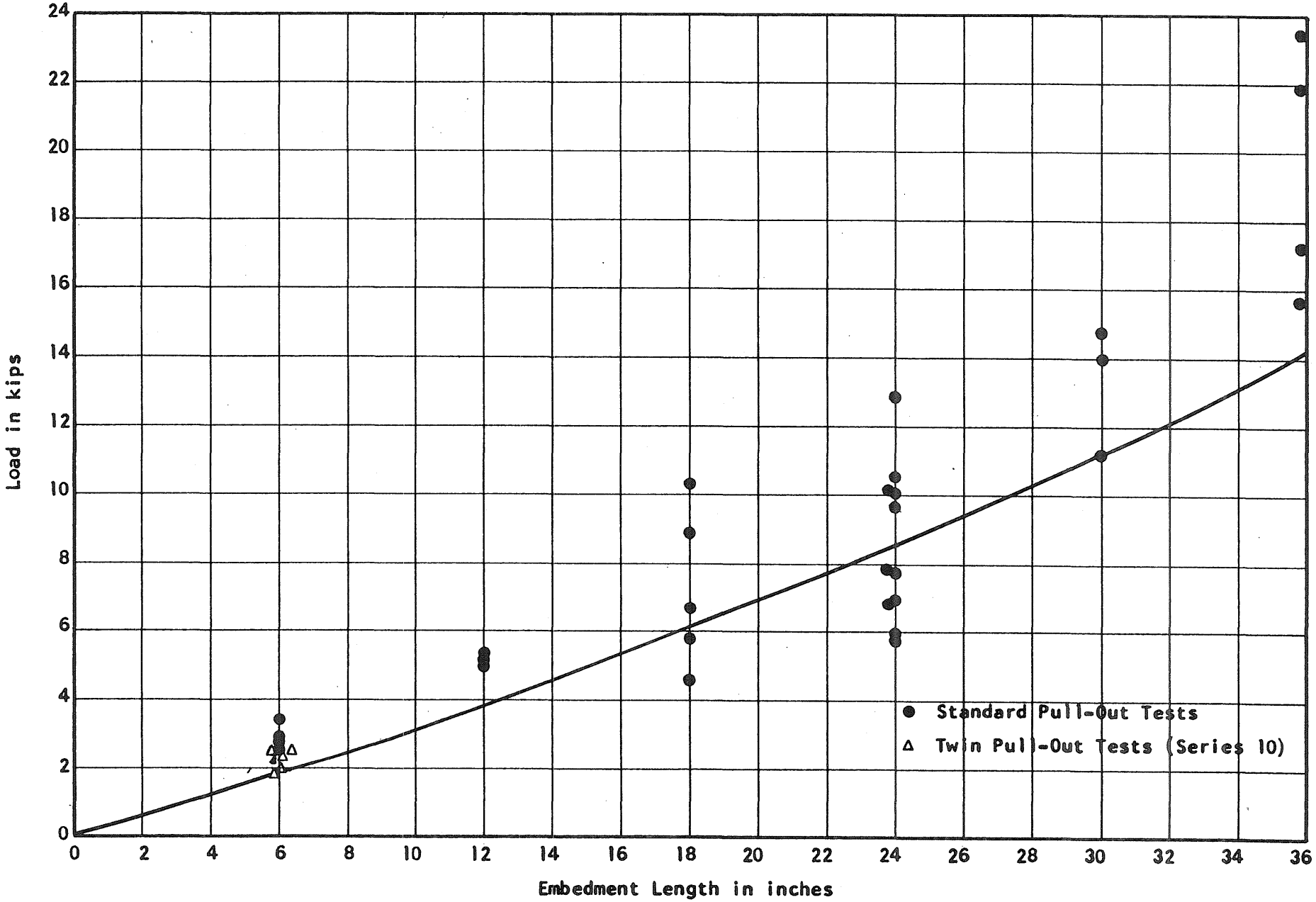

FIG. 3.5 STRAND FORCE DISTRIBUTION. SERIES 8
Trail-End Slip: 0.000 in. Strand: 7/16-in. Round

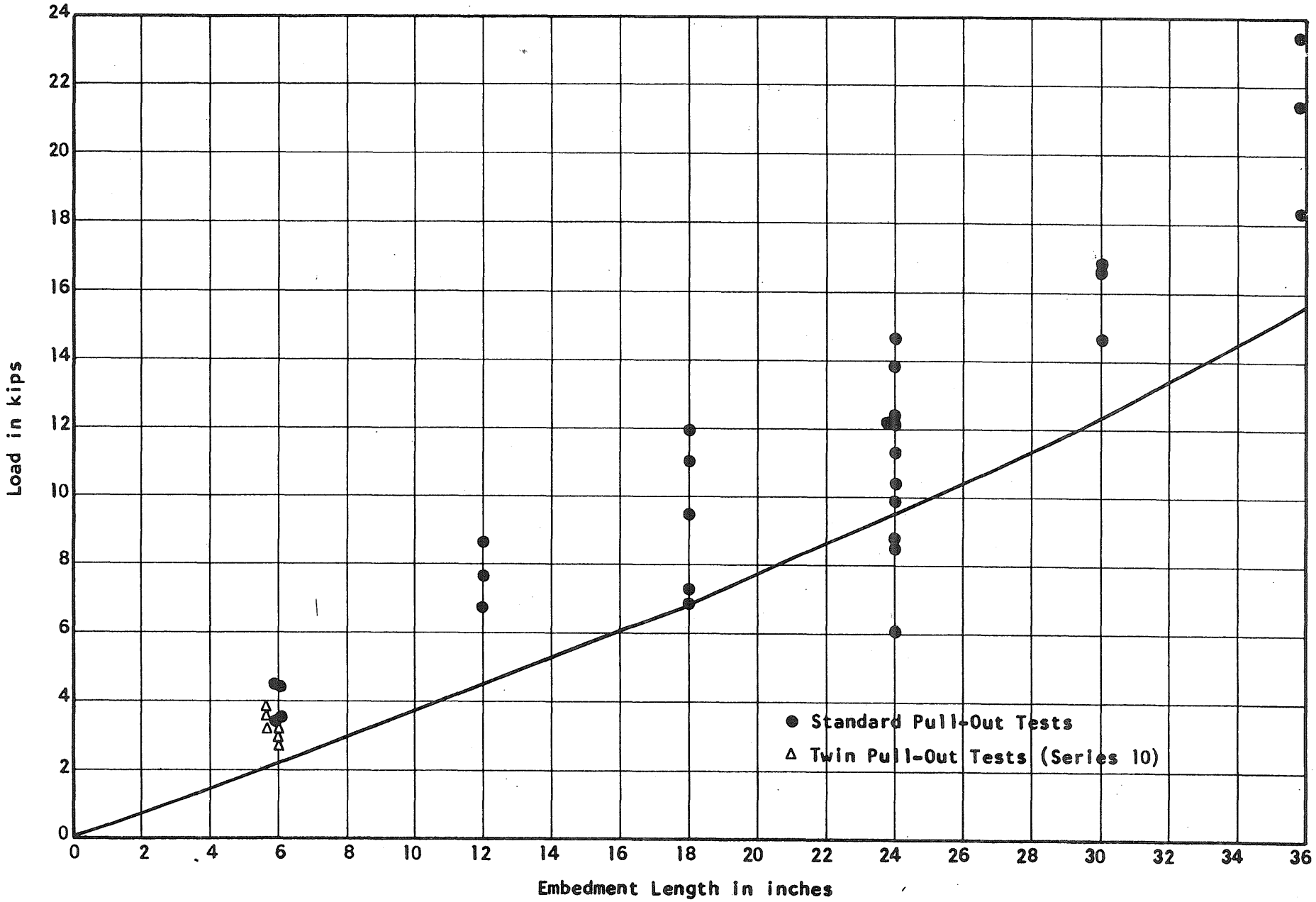

FIG. 3.6 STRAND FORCE DISTRIBUTION. SERIES 8
Trail-End Slip: 0.010 in. Strand: 7/16-in. Round

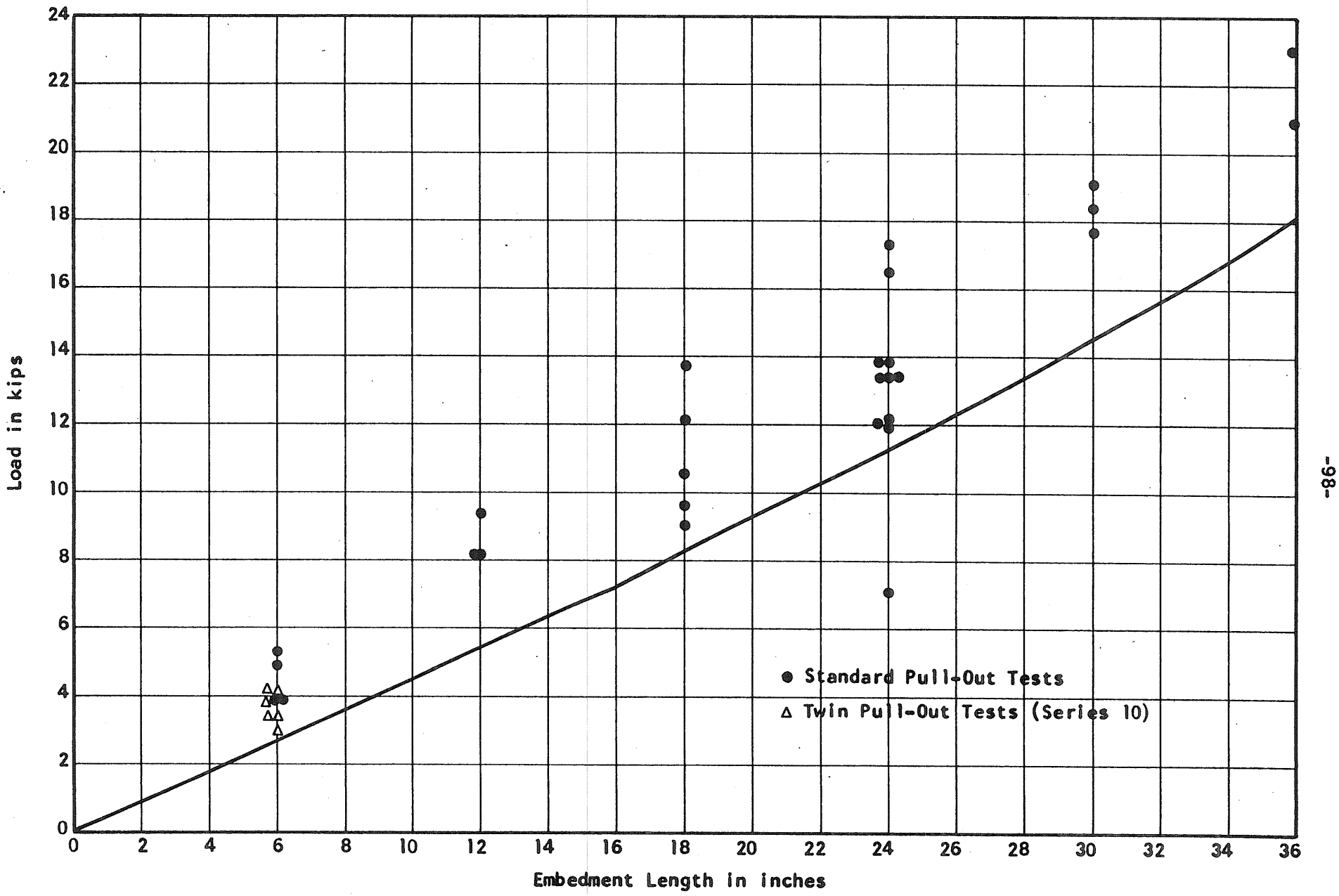

FIG. 3.7 STRAND FORCE DISTRIBUTION. SERIES 8
Trail-End Slip: 0.040 in. Strand: 7/16-in. Round

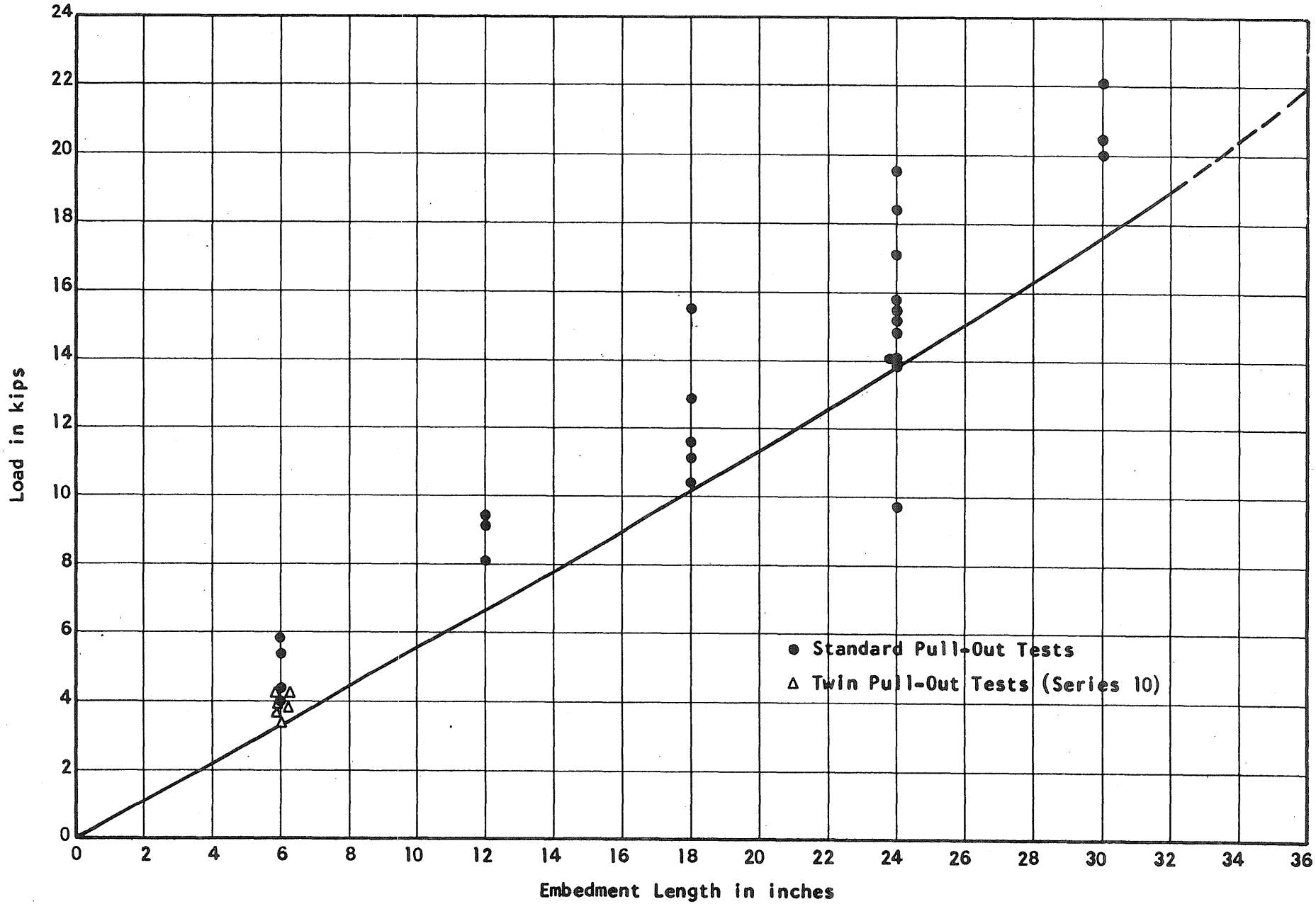

FIG. 3.8 STRAND FORCE DISTRIBUTION. SERIES 8
Trail-End Slip: 0.100 in. Strand: 7/16-in. Round

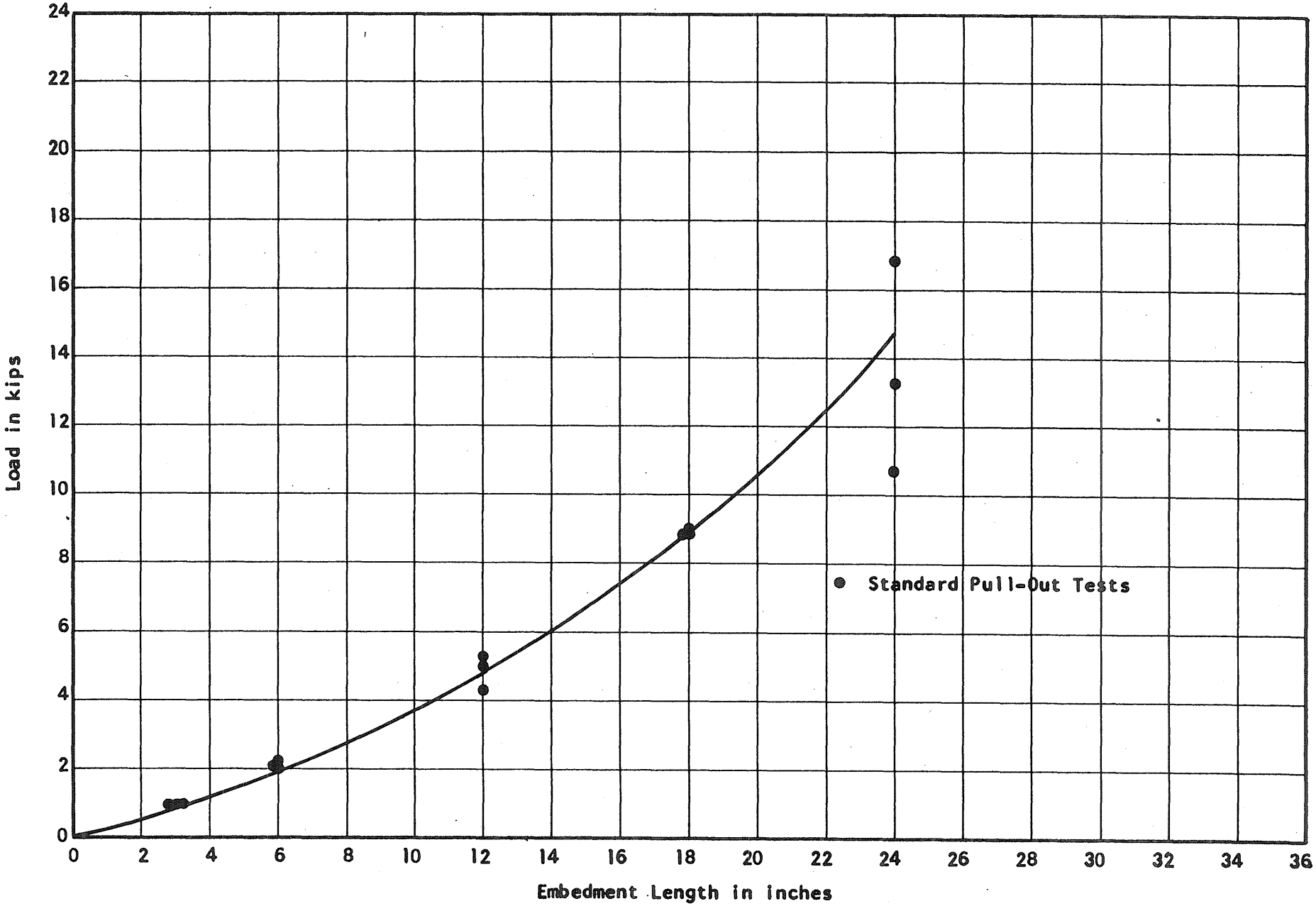

FIG. 3.9 STRAND FORCE DISTRIBUTION. SERIES 9
Trail-End Slip: 0.000 in. Strand: 7/16-in. Rectangular

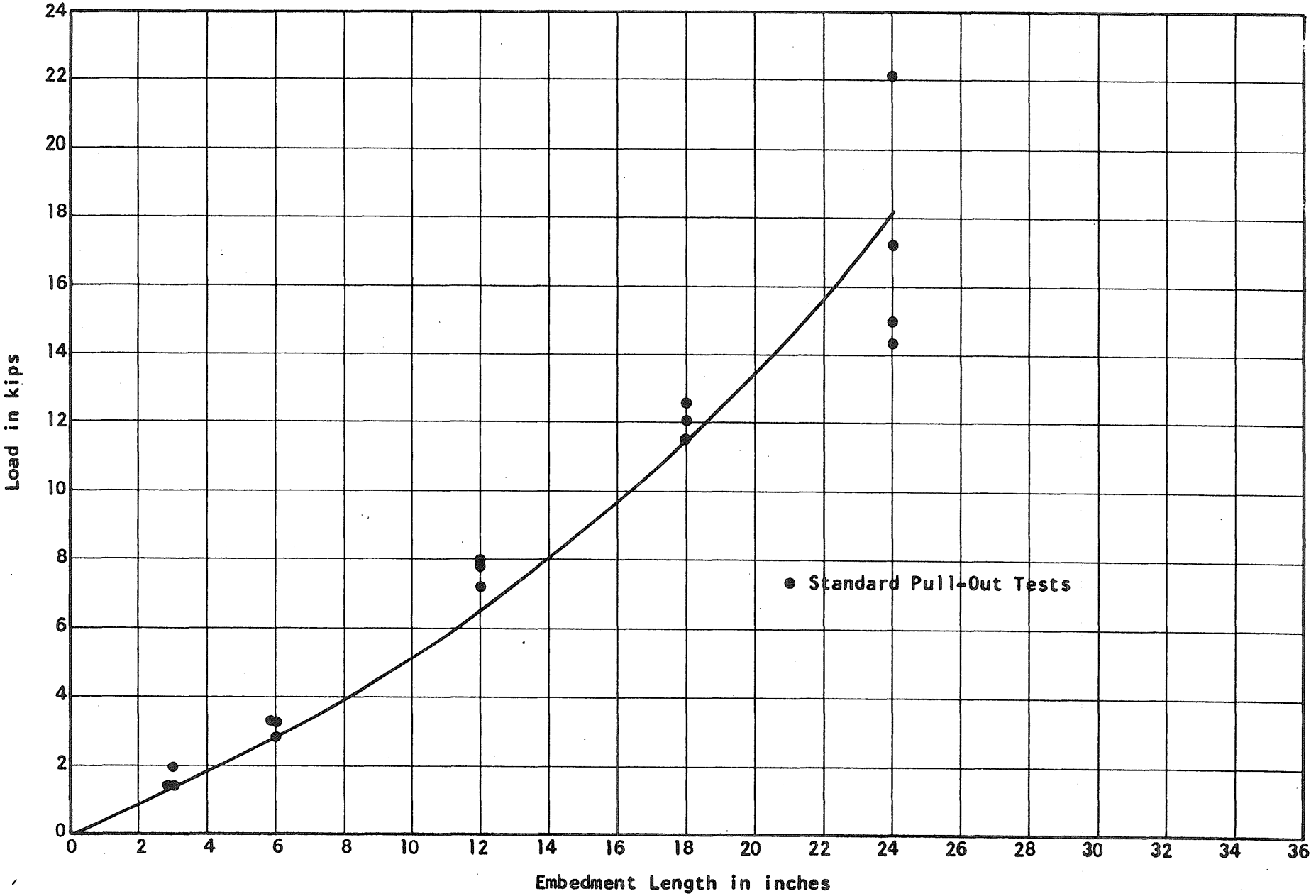

FIG. 3.10 STRAND FORCE DISTRIBUTION. SERIES 9
Trail-End Slip: 0.003 in. Strand: 7/16-in. Rectangular

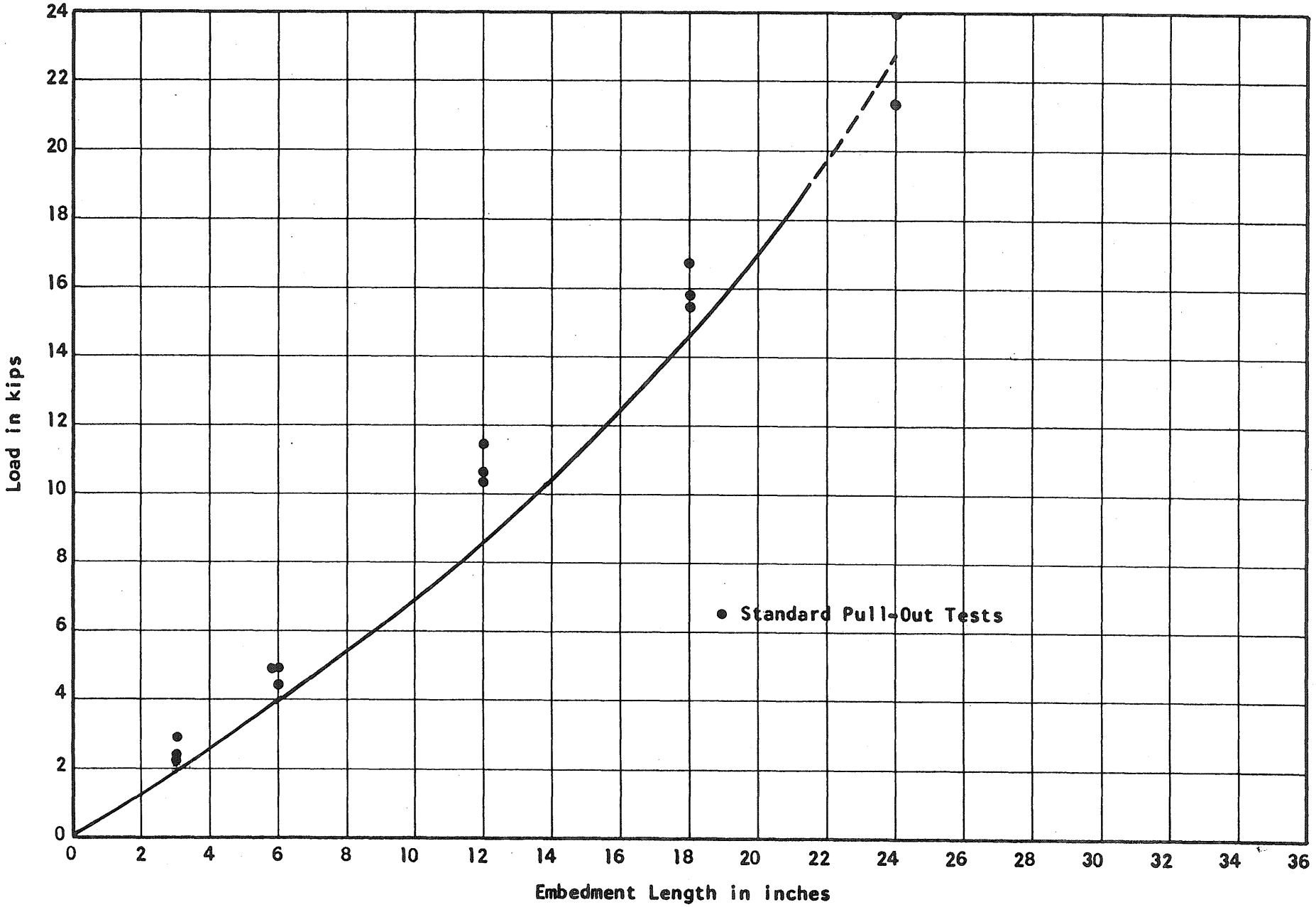

FIG. 3.11 STRAND FORCE DISTRIBUTION. SERIES 9
Trail-End Slip: 0.010 in. Strand: 7/16-in. Rectangular

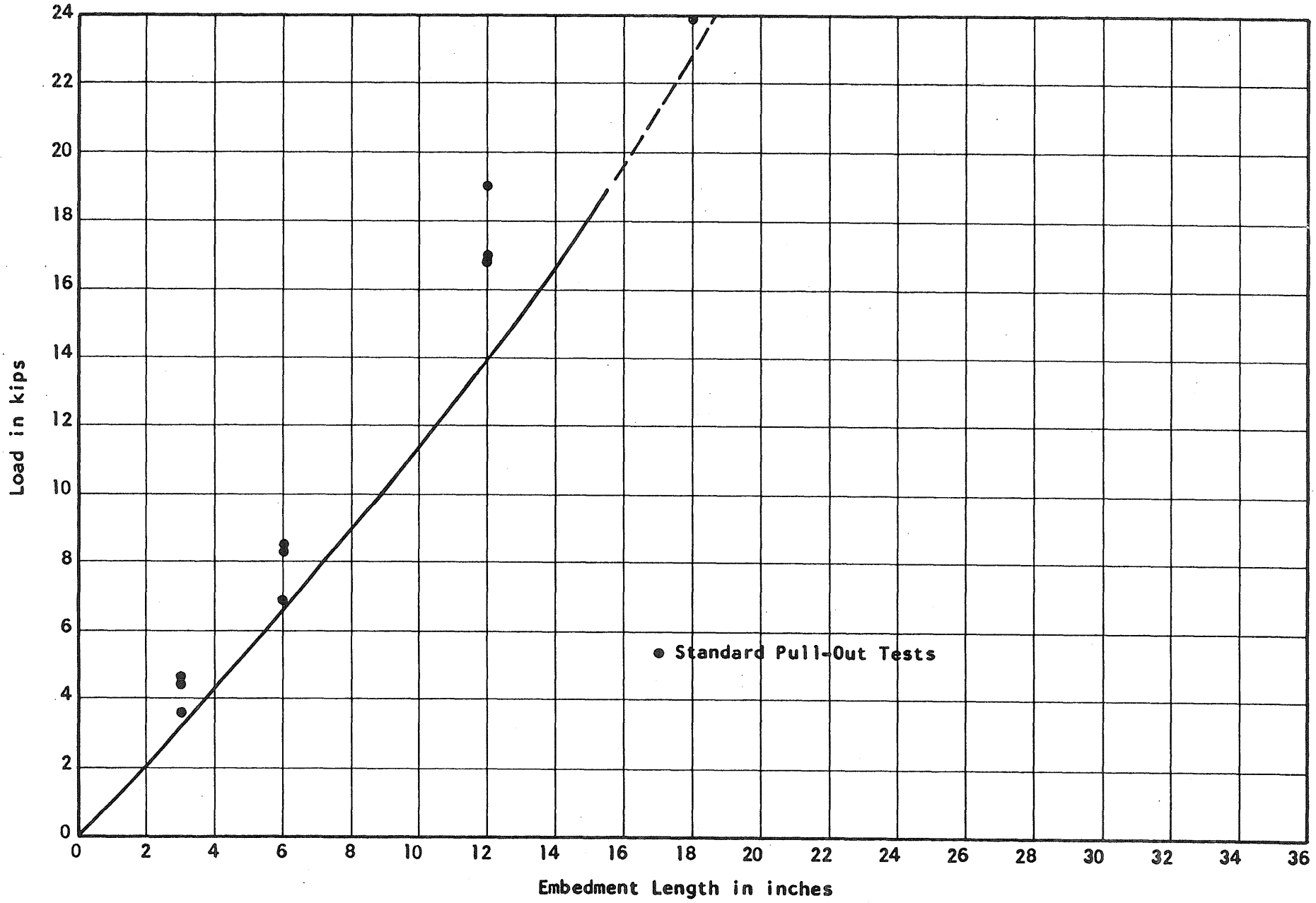

FIG. 3.12 STRAND FORCE DISTRIBUTION. SERIES 9
Trail-End Slip: 0.040 in. Strand: 7/16-in. Rectangular

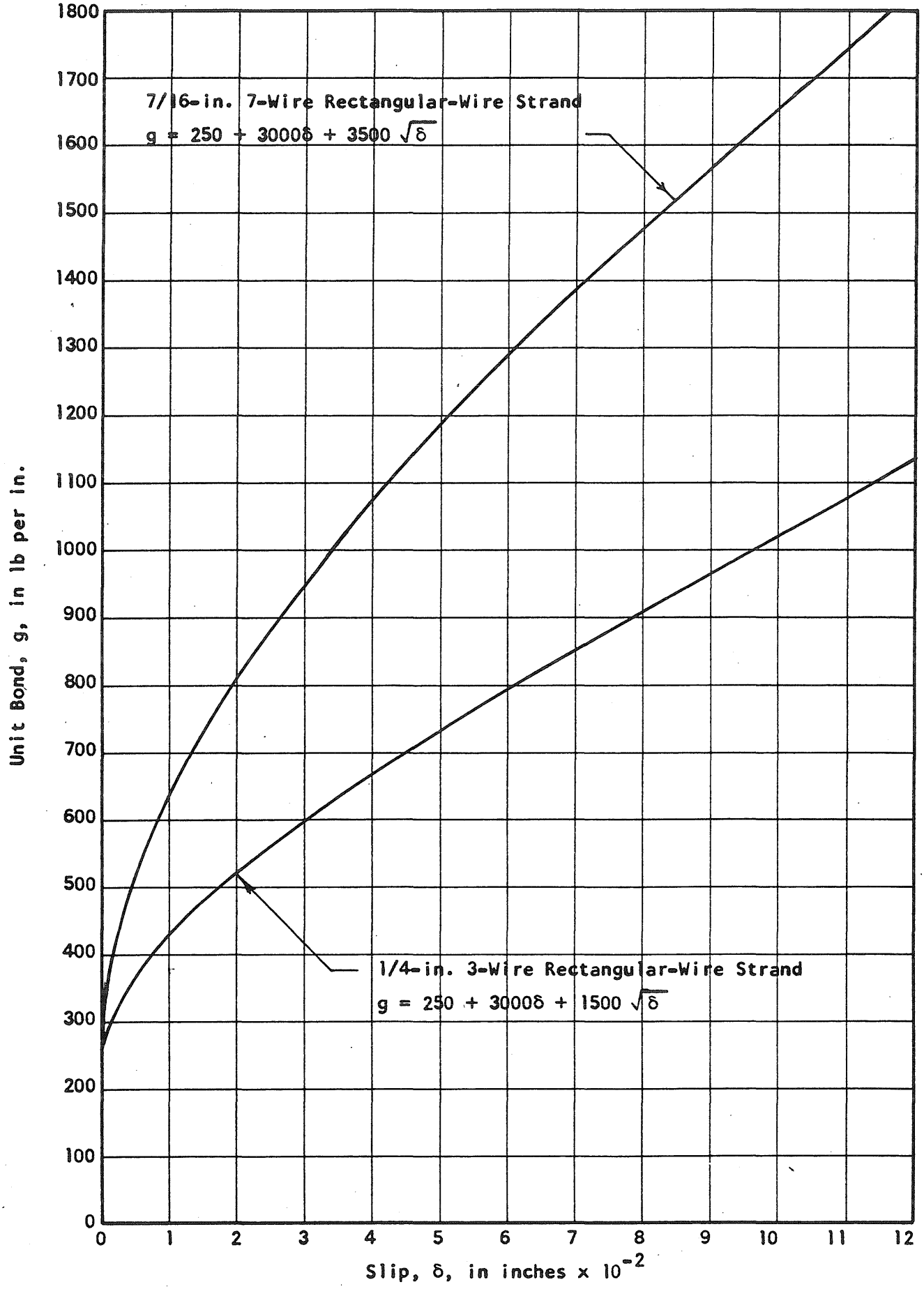

FIG. 3.13 UNIT BOND-SLIP CURVES FOR RECTANGULAR-WIRE STRAND

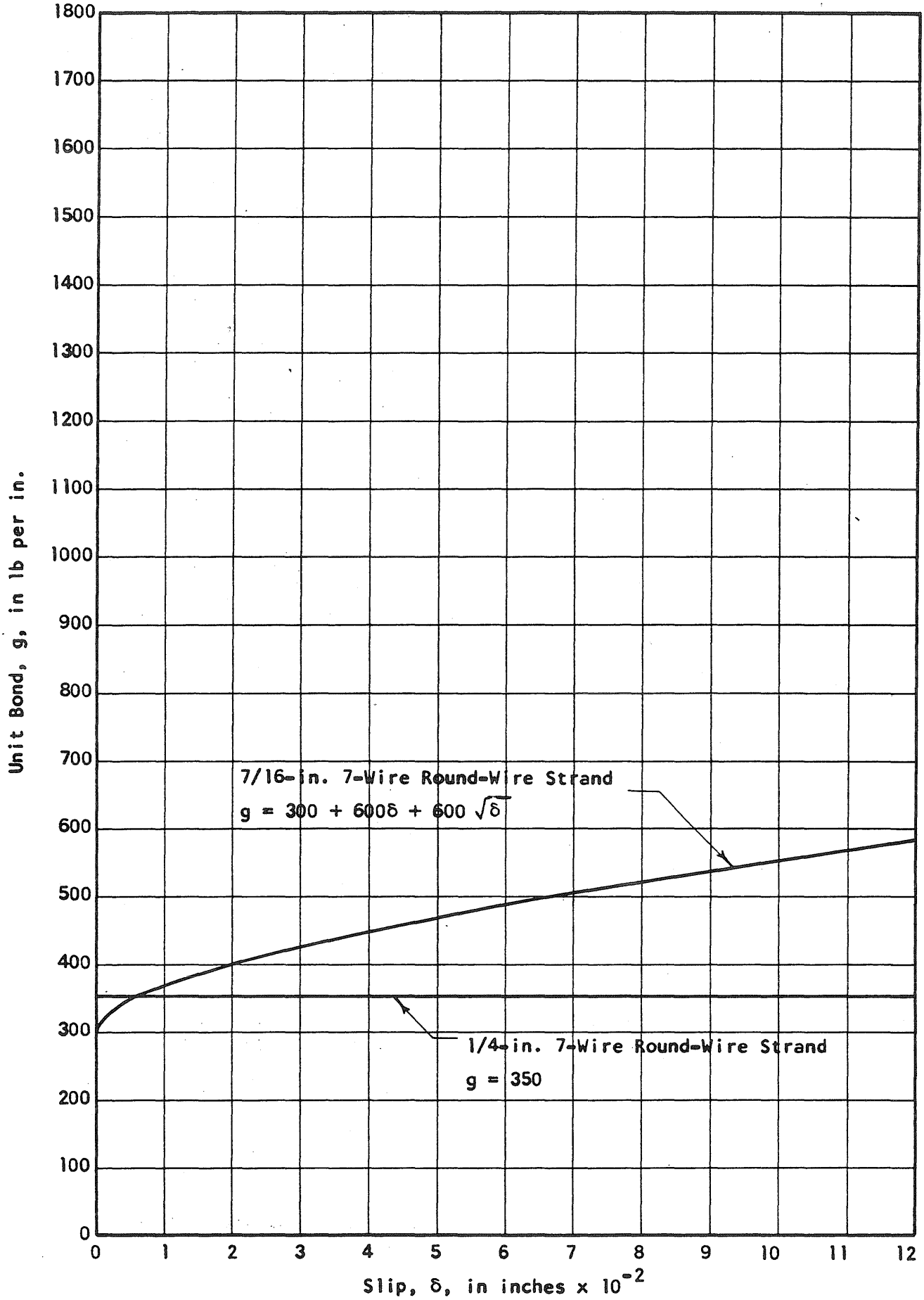

FIG. 3.14 UNIT BOND-SLIP CURVES FOR ROUND-WIRE STRAND

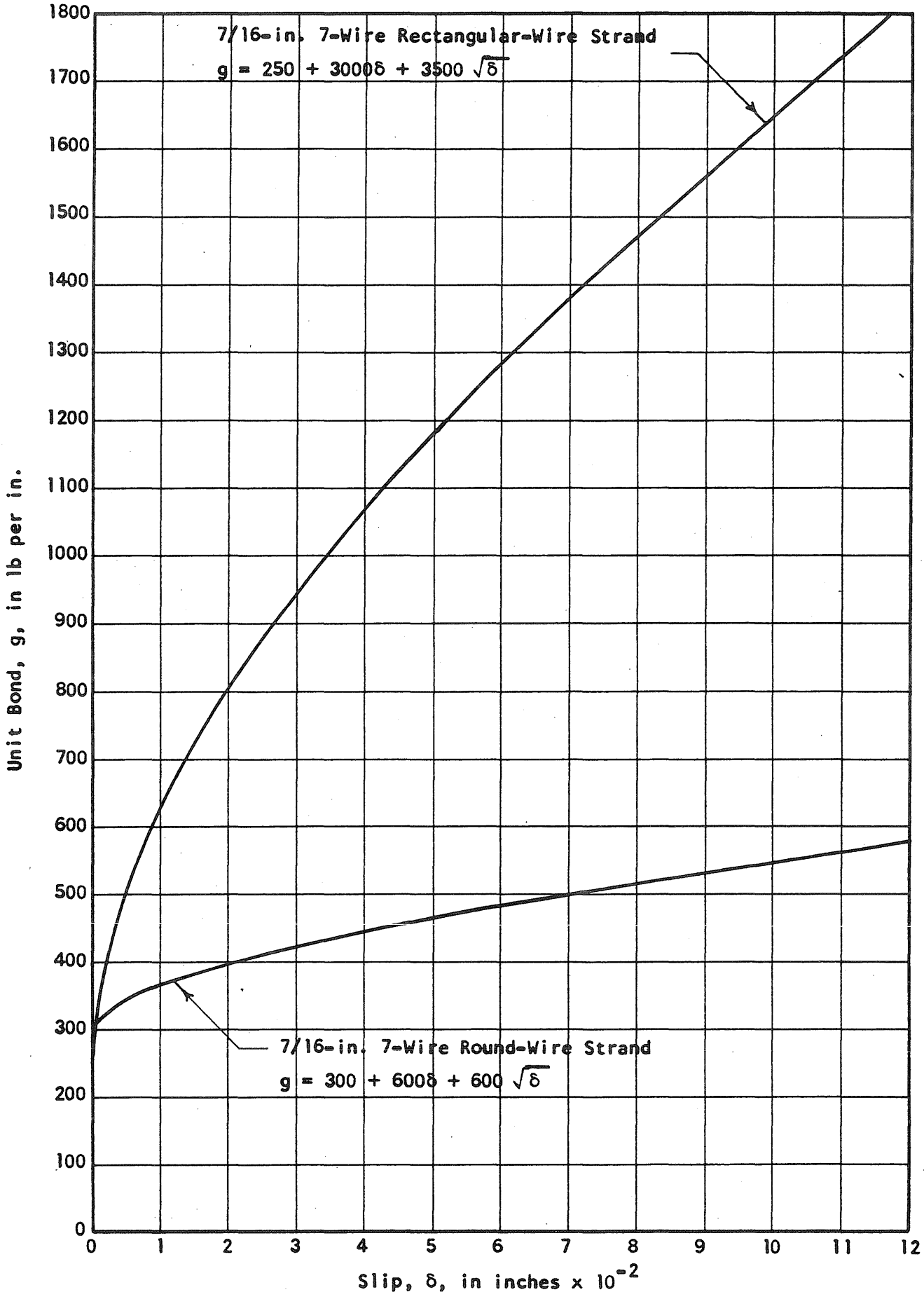

FIG. 3.15 UNIT BOND-SLIP CURVES FOR 7/16-in. DIAMETER STRAND

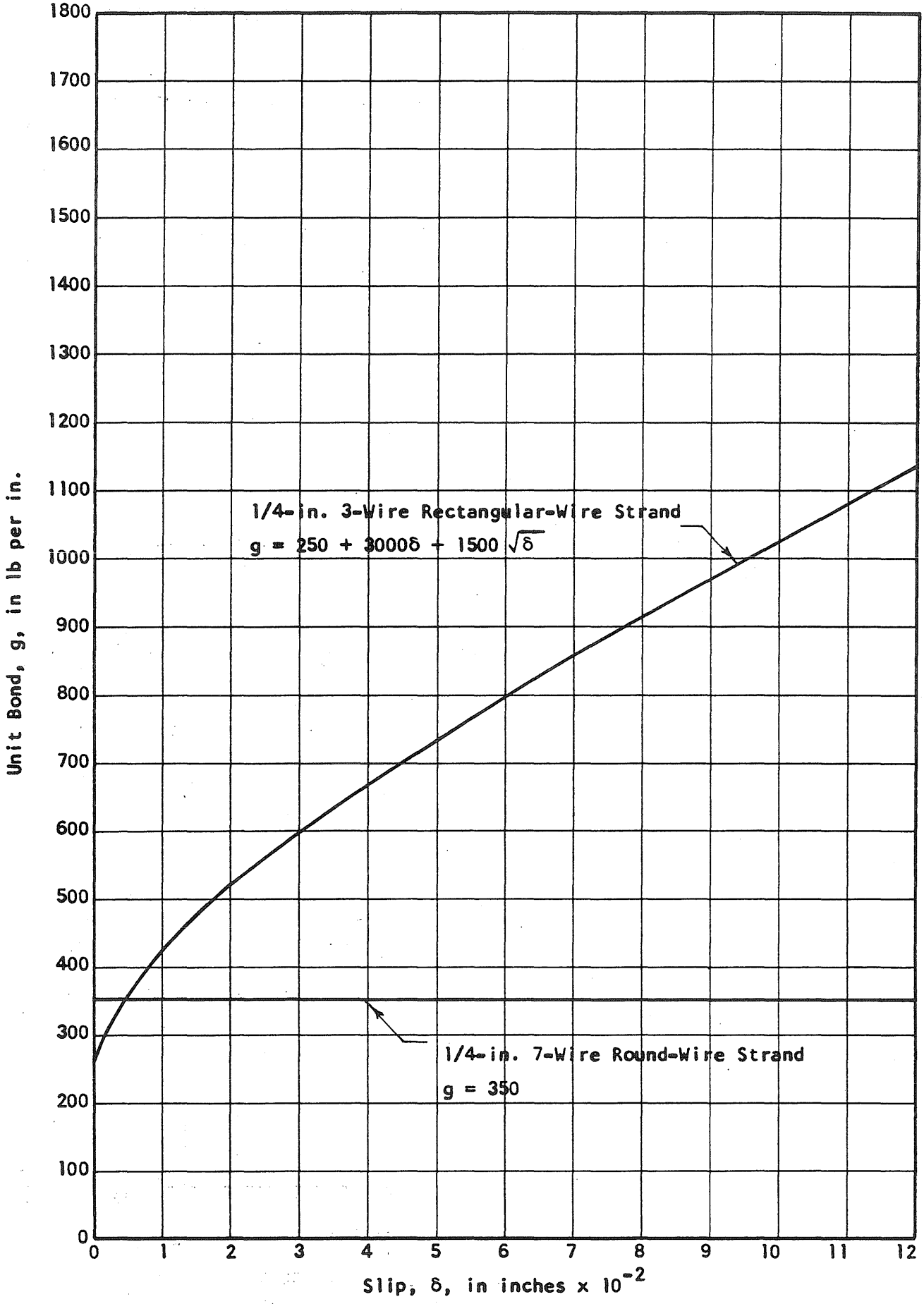

FIG. 3.16 UNIT BOND-SLIP CURVES FOR 1/4-in. DIAMETER STRAND

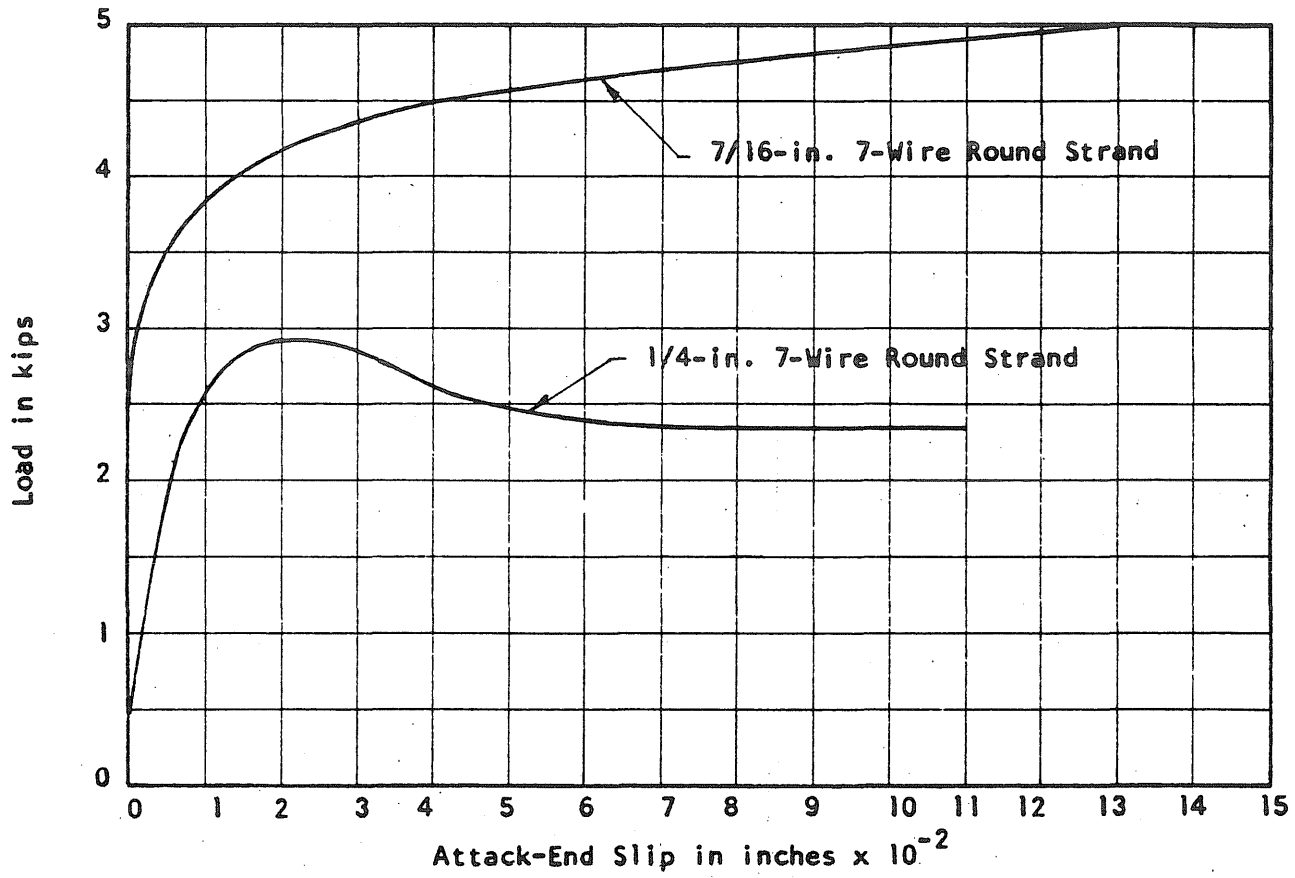

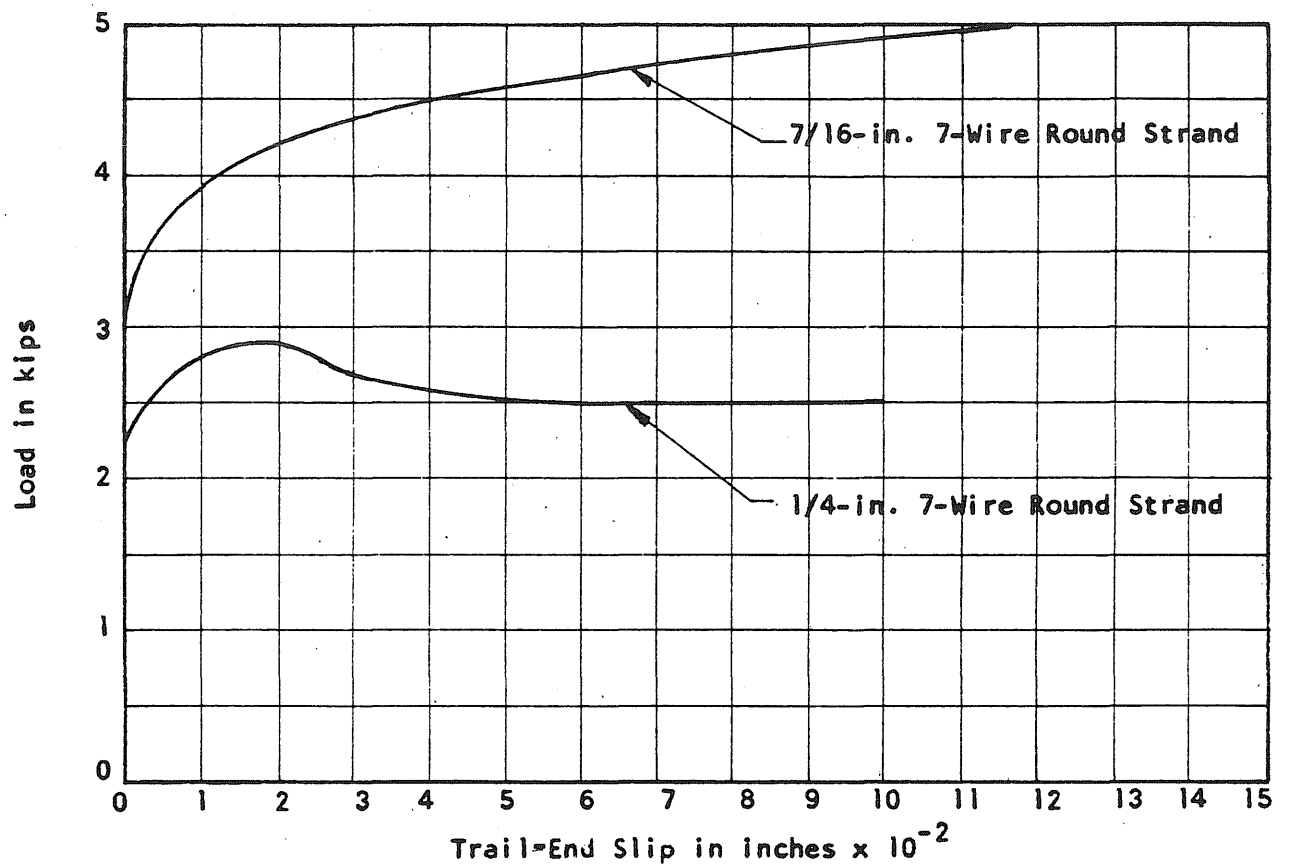

FIG. 3.17 A COMPARISON OF AVERAGE LOAD-SLIP CURVES. SERIES 1 AND 8
Embedment: 6-in. Strand: 1/4 and 7/16-in. Round

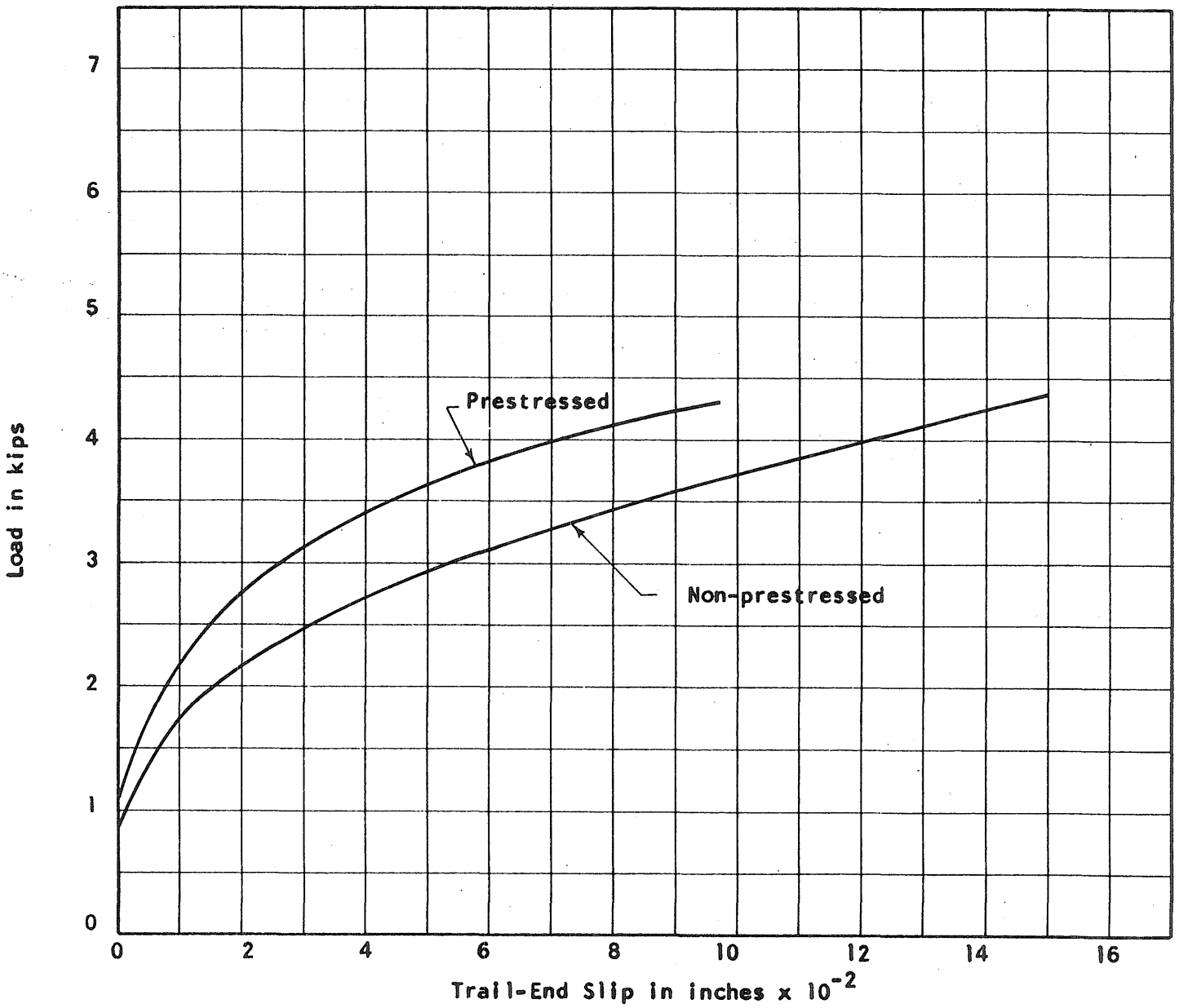

FIG. 3.18 AVERAGE LOAD-SLIP CURVES, PRESTRESSED AND NON-PRESTRESSED SPECIMENS. SERIES 7
Length: 3-in. Strand: 1/4-in. Rectangular

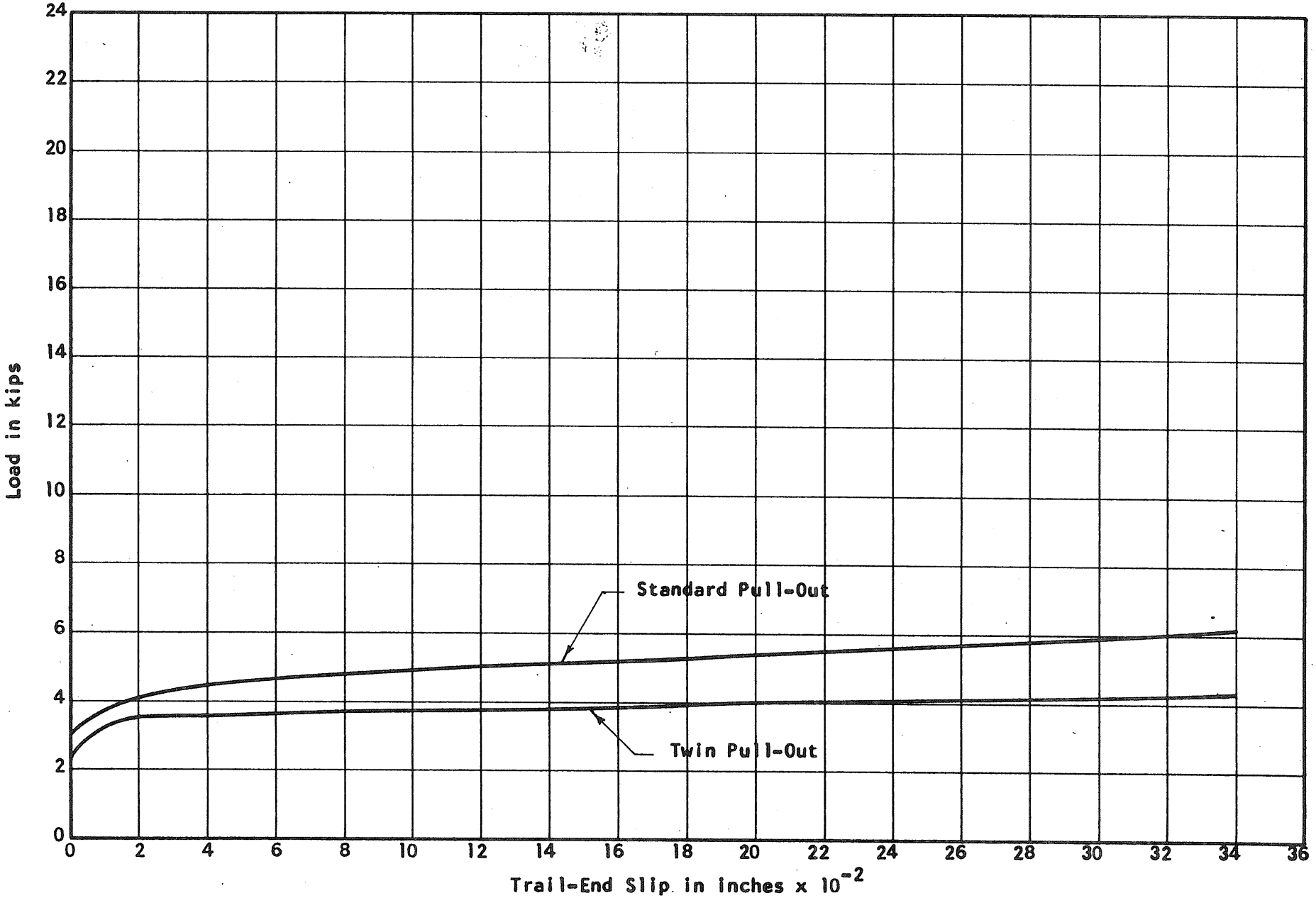

FIG. 3.19 A COMPARISON OF AVERAGE LOAD-SLIP CURVES. SERIES 8 AND 10
Embedment: 6-in. Strand: 7/16-in. Round

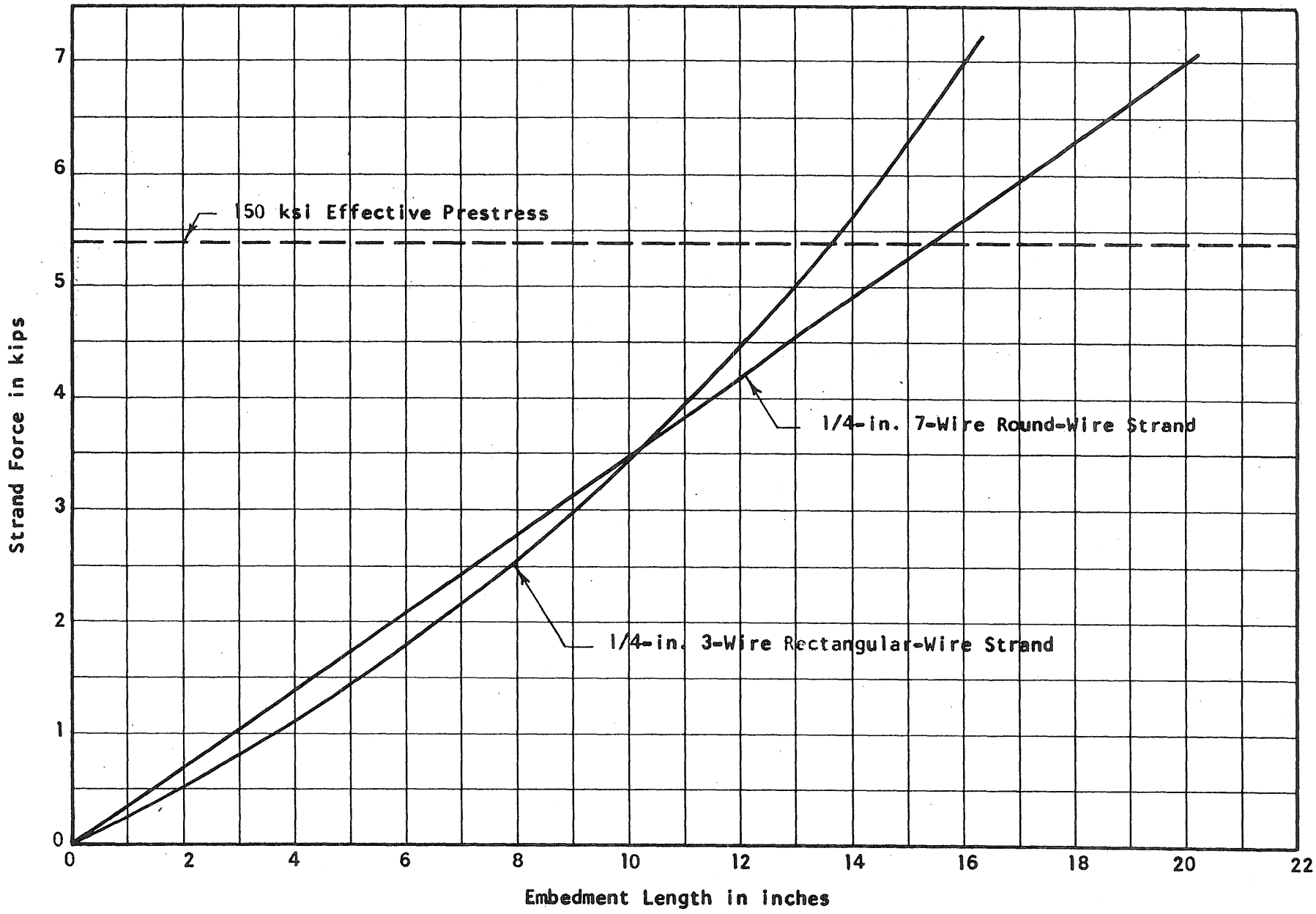

FIG. 4.1 ANCHORAGE LENGTH OF 1/4-in. STRAND

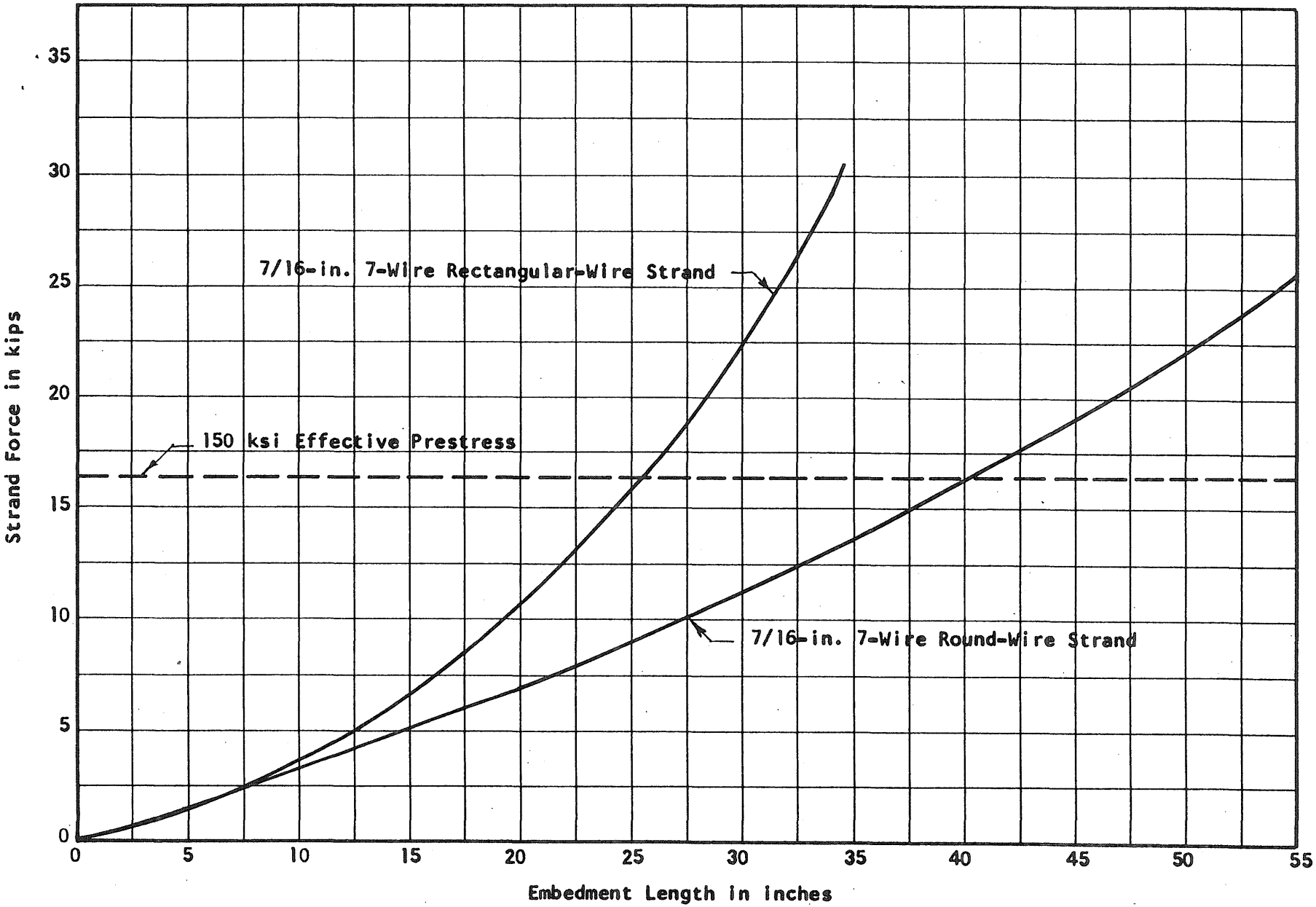

FIG. 4.2 ANCHORAGE LENGTH OF 7/16-in. STRAND

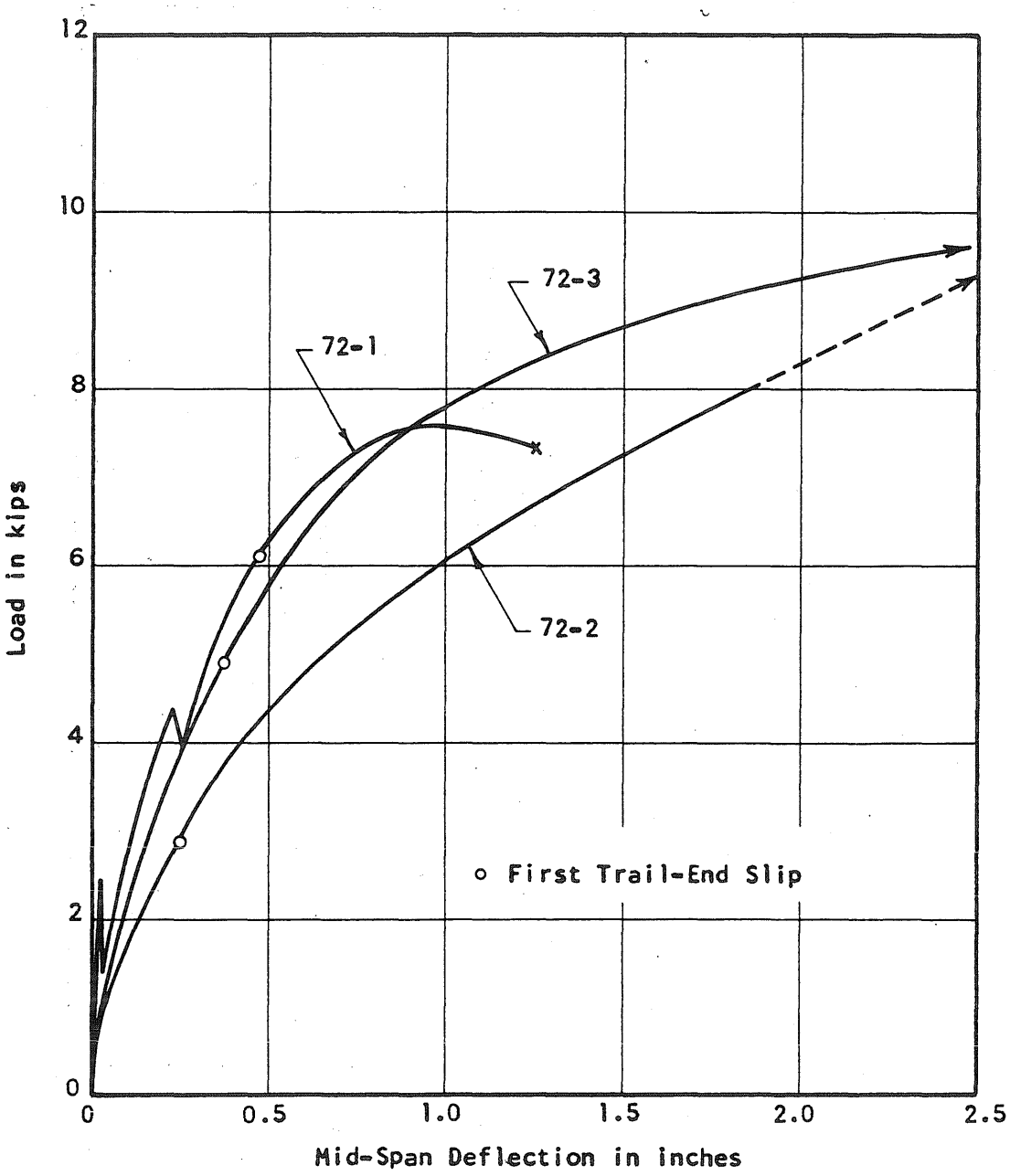

FIG. 5.1 LOAD-DEFLECTION CURVES. BEAM TESTS
Length: 72-in. Strand: 7/16-in. Round

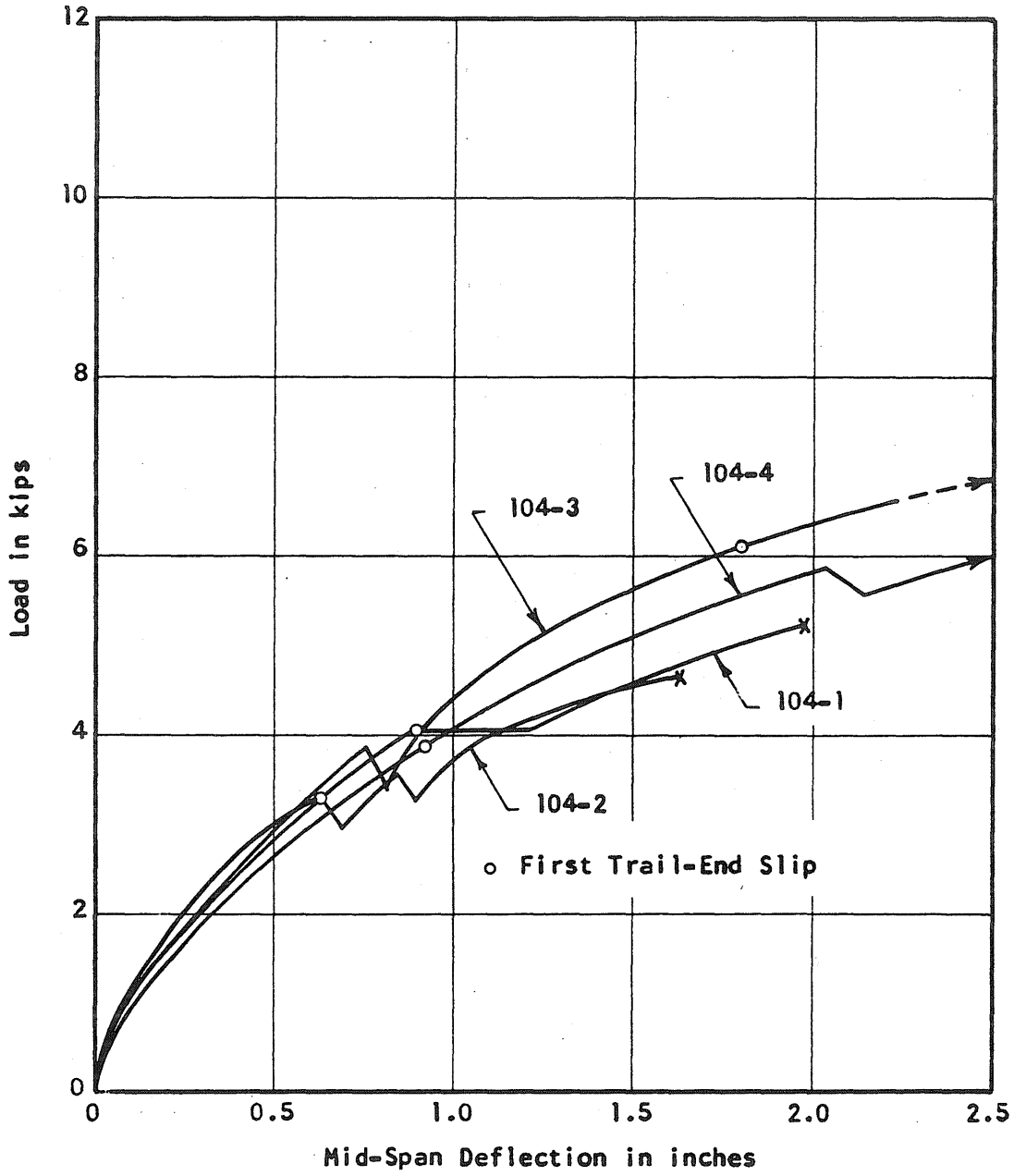

FIG. 5.2 LOAD-DEFLECTION CURVES. BEAM TESTS
Length: 104-in. Strand: 7/16-in. Round

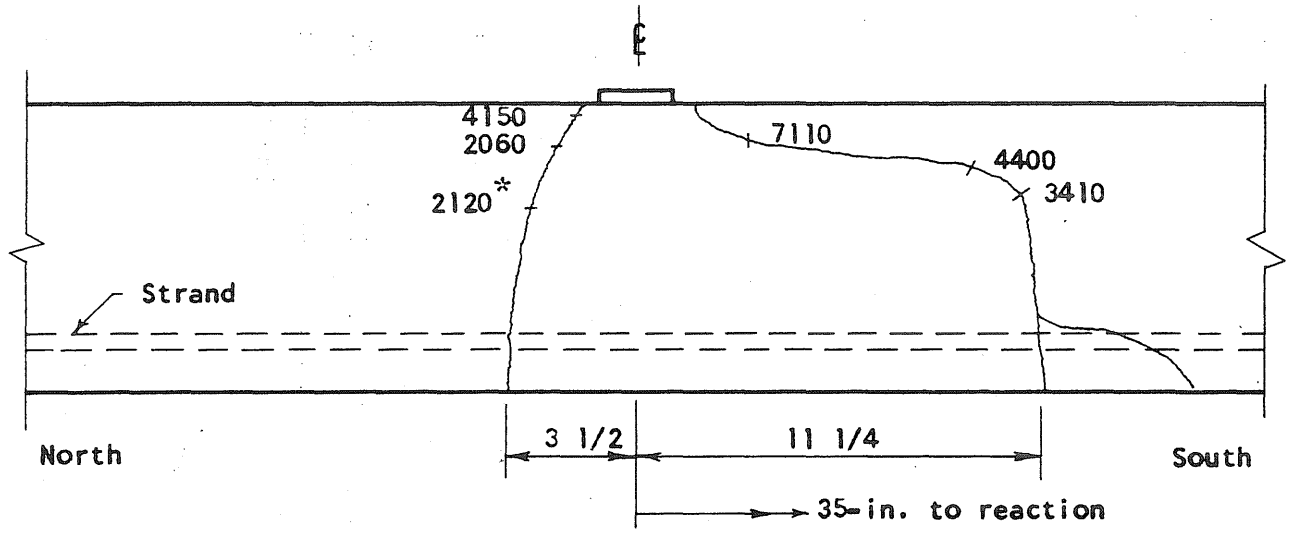

Crack Pattern, Beam 72-1

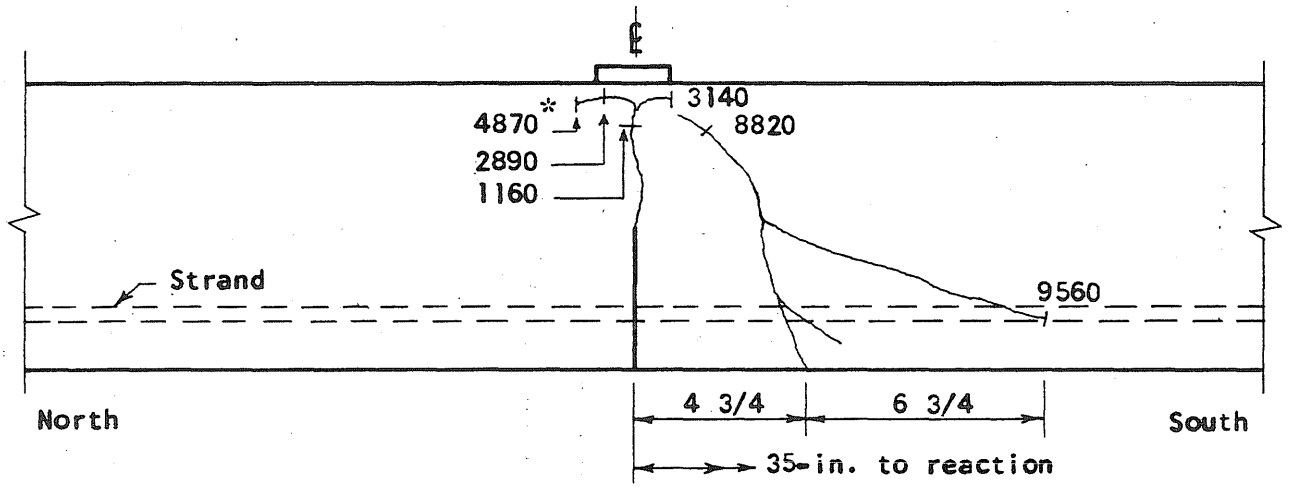

Crack Pattern, Beam 72-2

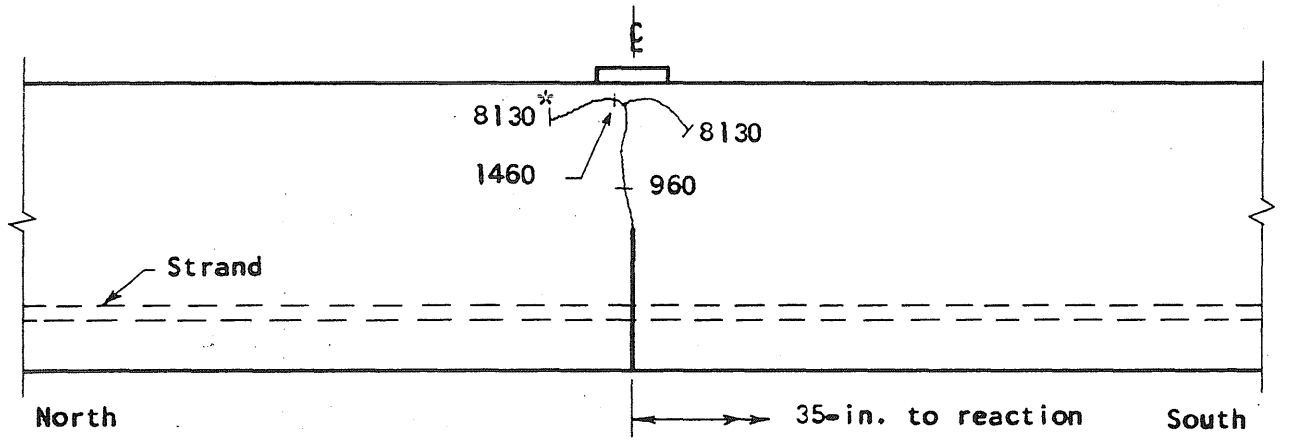

Crack Pattern, Beam 72-3

FIG. 5.3 BEAM CRACK PATTERNS
Length: 72-in. Strand: 7/16-in. Round

*Load in pounds

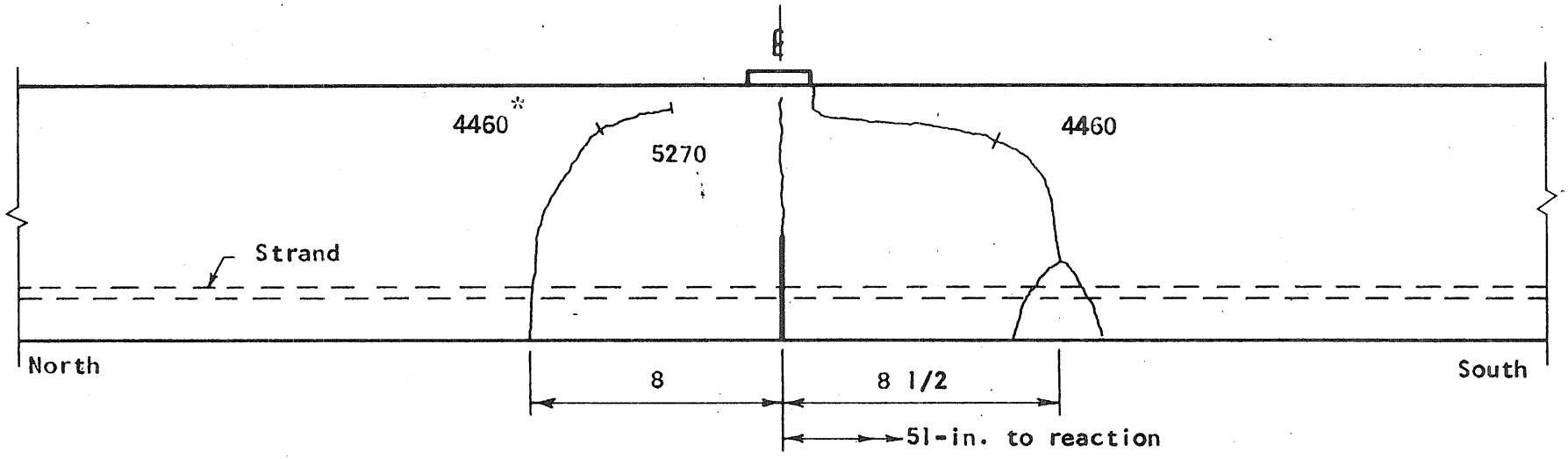

Crack Pattern, Beam 104-1

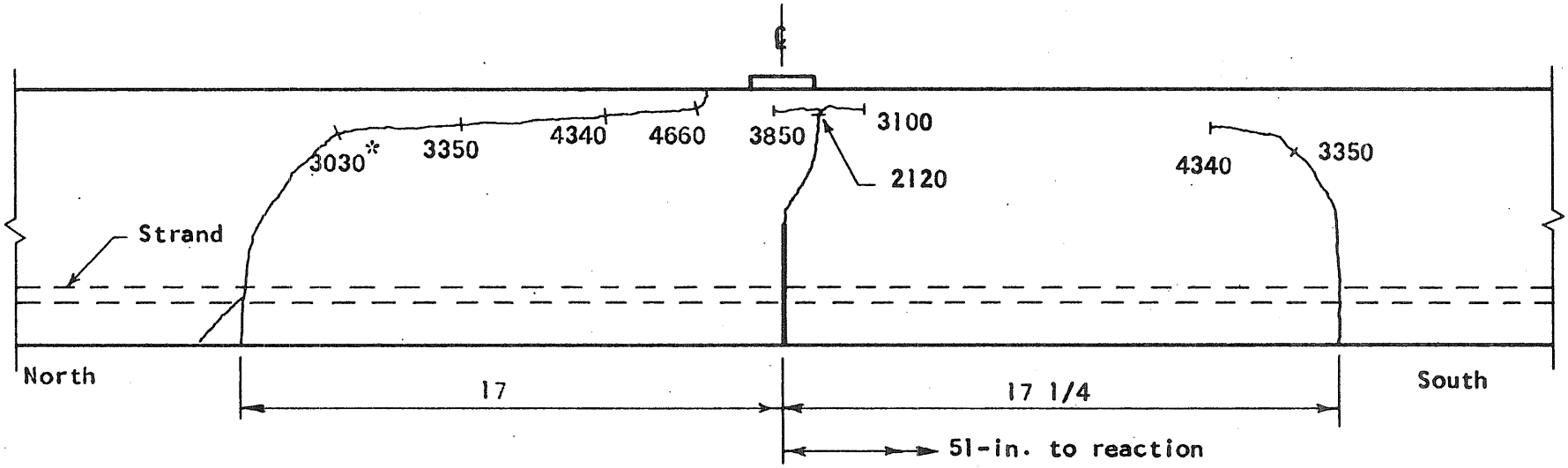

Crack Pattern, Beam 104-2

FIG. 5.4 BEAM CRACK PATTERNS
Length: 104-in. Strand: 7/16-in. Round

*Load in pounds

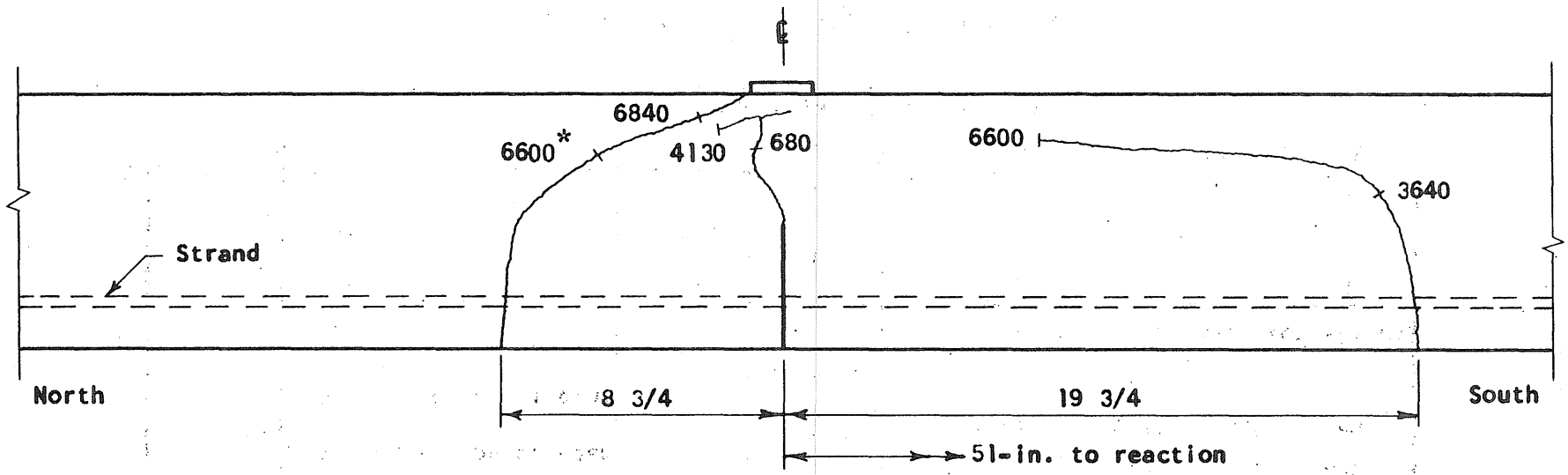

Crack Pattern, Beam 104-3

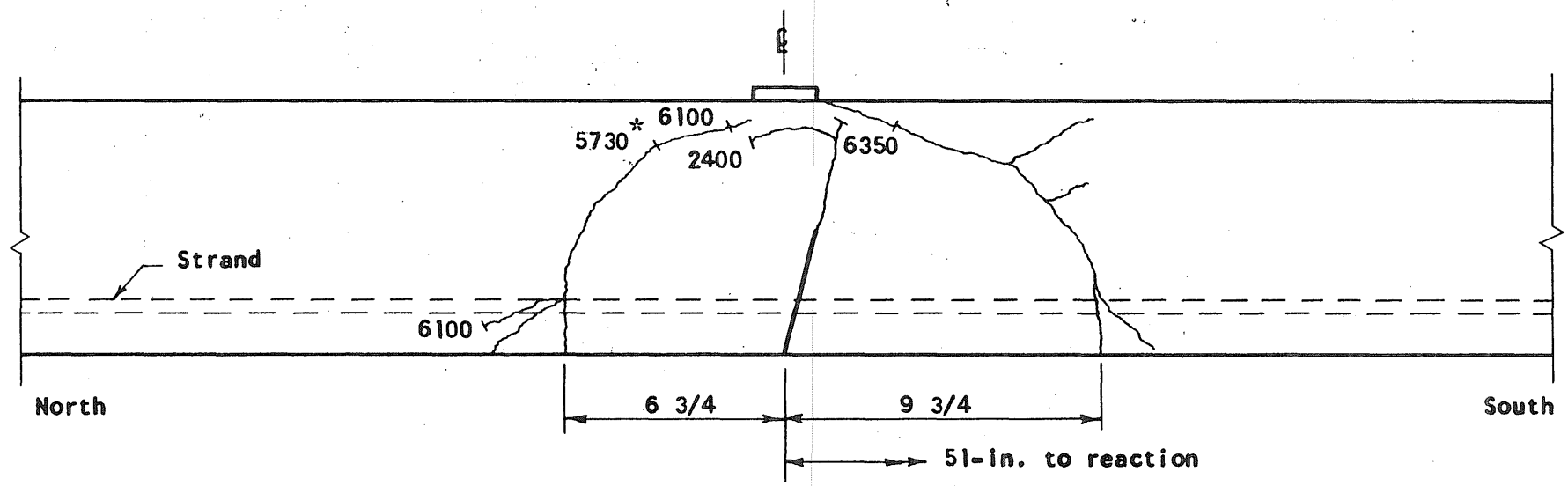

Crack Pattern, Beam 104-4

FIG. 5.5 BEAM CRACK PATTERNS
Length: 104-in. Strand: 7/16-in. Round

*Load in pounds

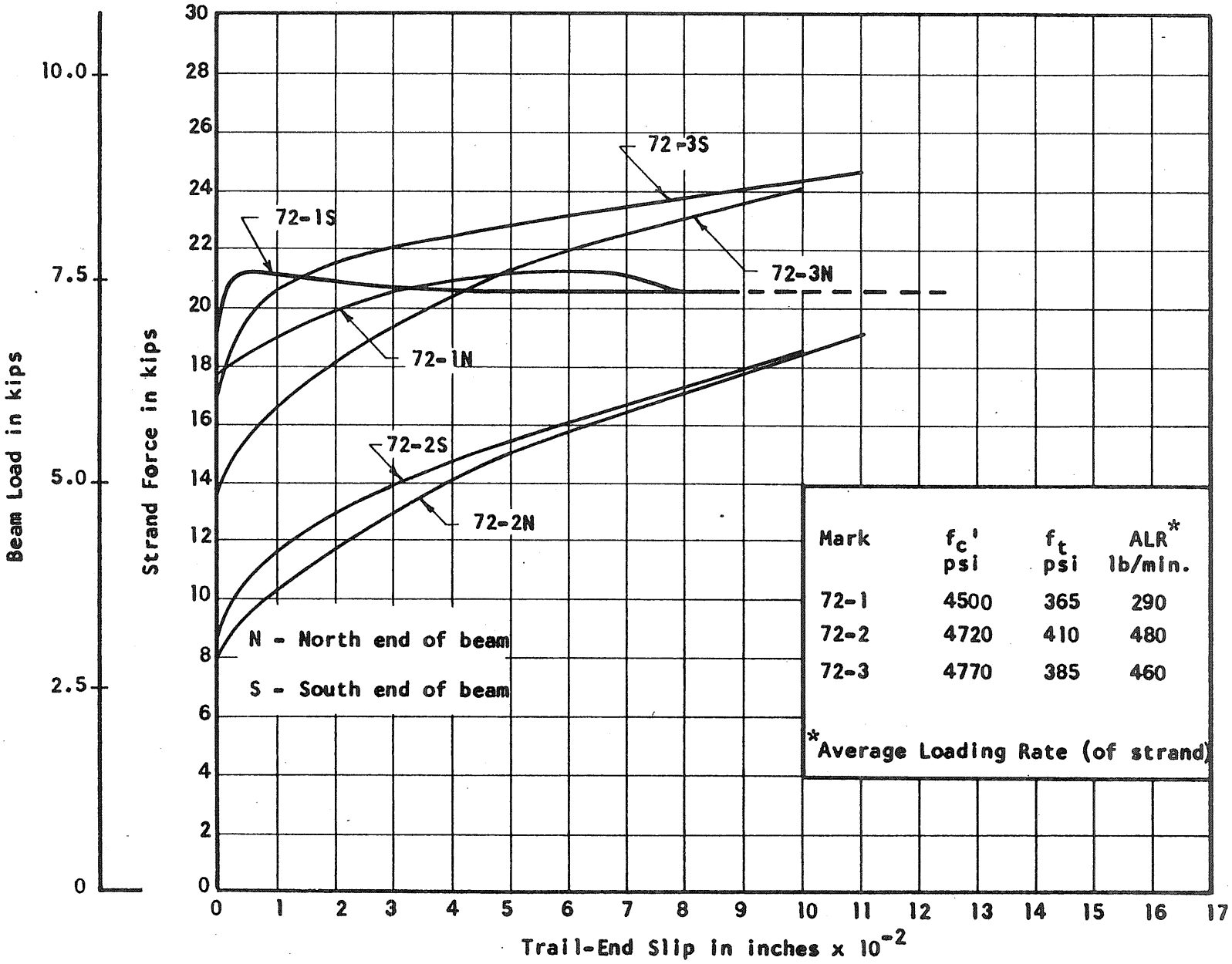

FIG. 5.6 STRAND FORCE-SLIP CURVES. BEAM TESTS
Length: 72-in. Strand: 7/16-in. Round

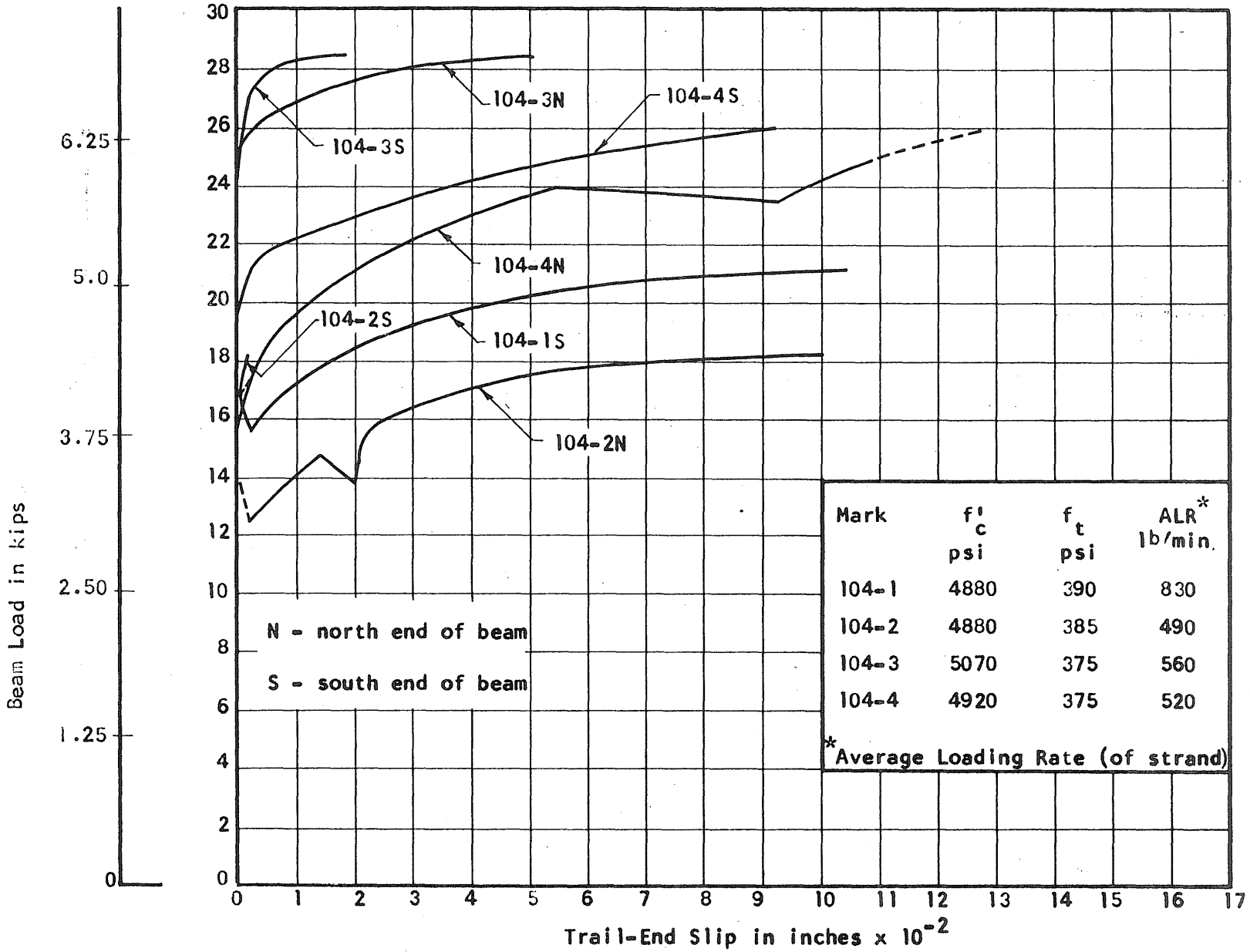

FIG. 5.7 STRAND FORCE-SLIP CURVES. BEAM TESTS
Length: 104-in. Strand: 7/16-in. Round

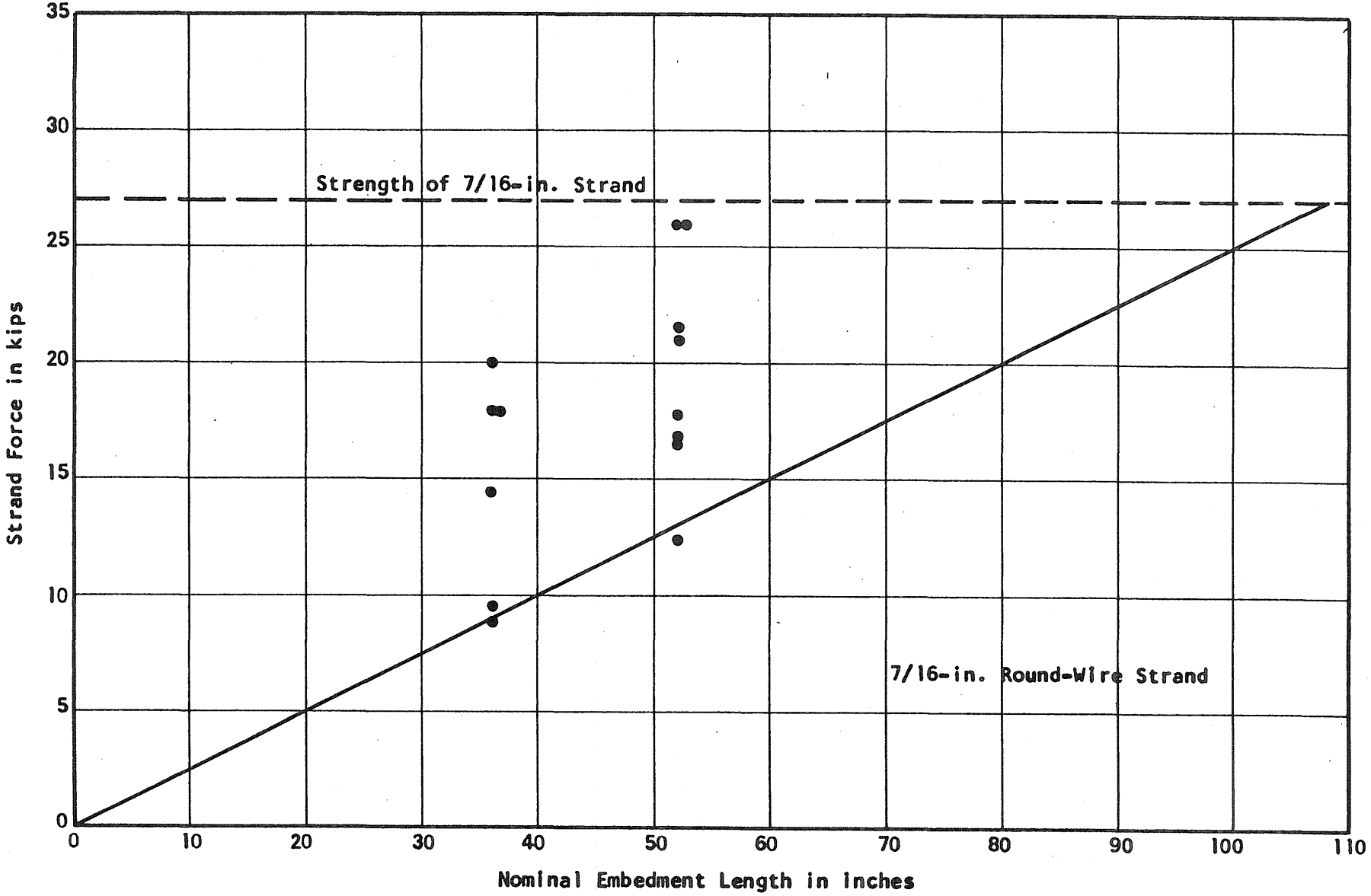

FIG. 6.1 CALCULATED STRAND FORCE VERSUS NOMINAL EMBEDMENT LENGTH. BEAM TESTS

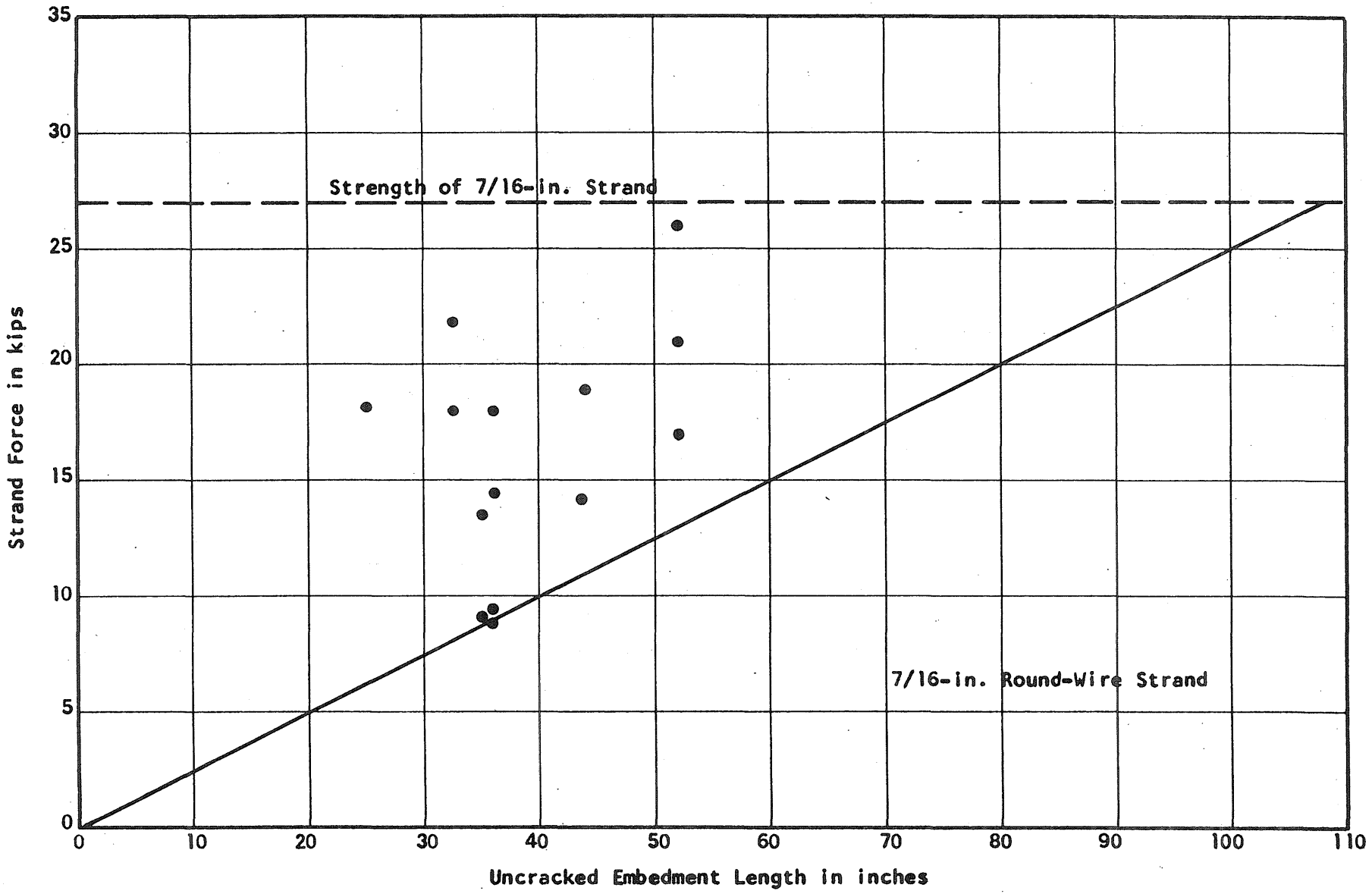

FIG. 6.2 CALCULATED STRAND FORCE VERSUS EMBEDMENT LENGTH IN UNCRACKED CONCRETE. BEAM TESTS

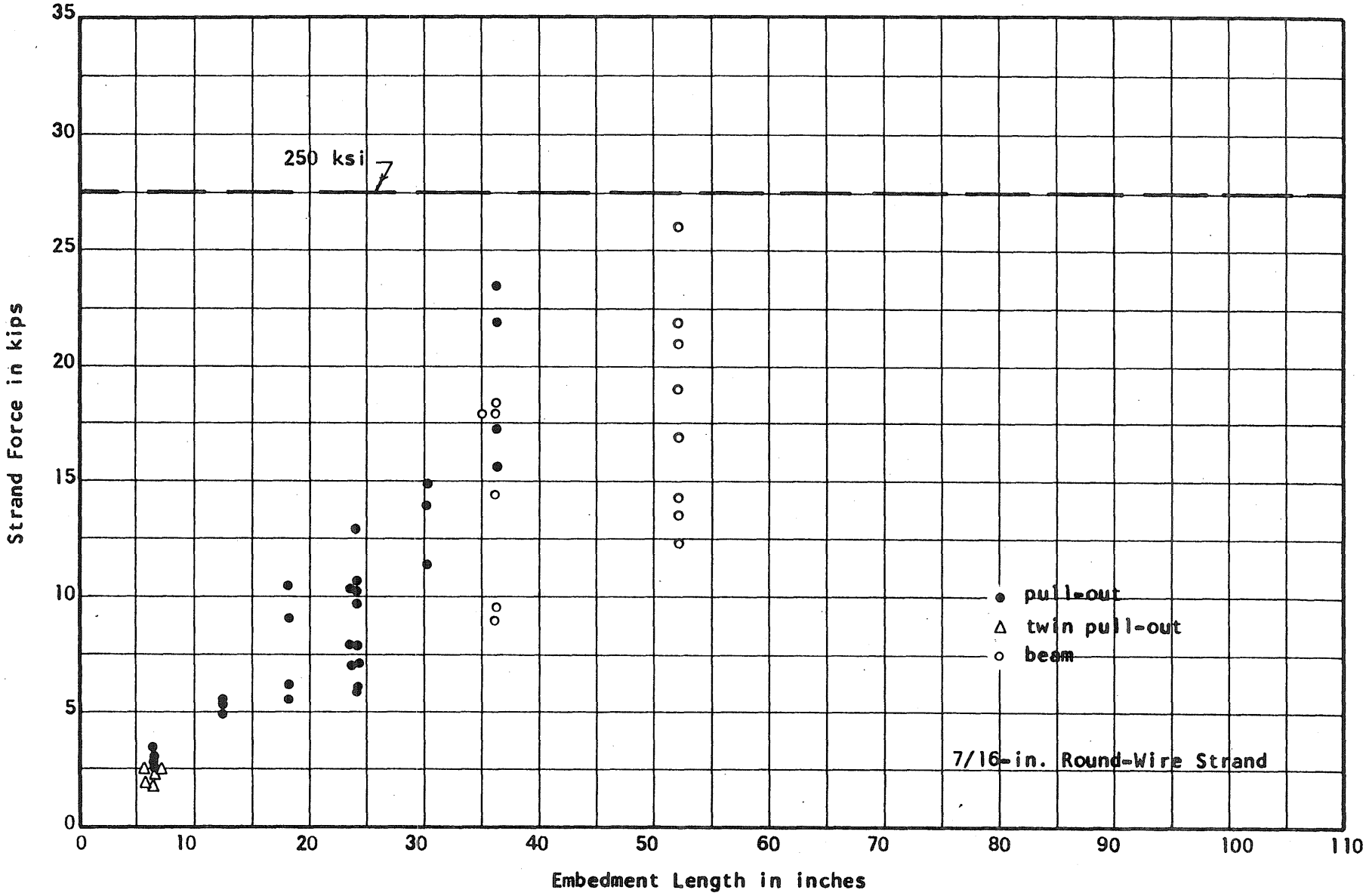

FIG. 7.1 BOND TEST RESULTS, UNIVERSITY OF ILLINOIS

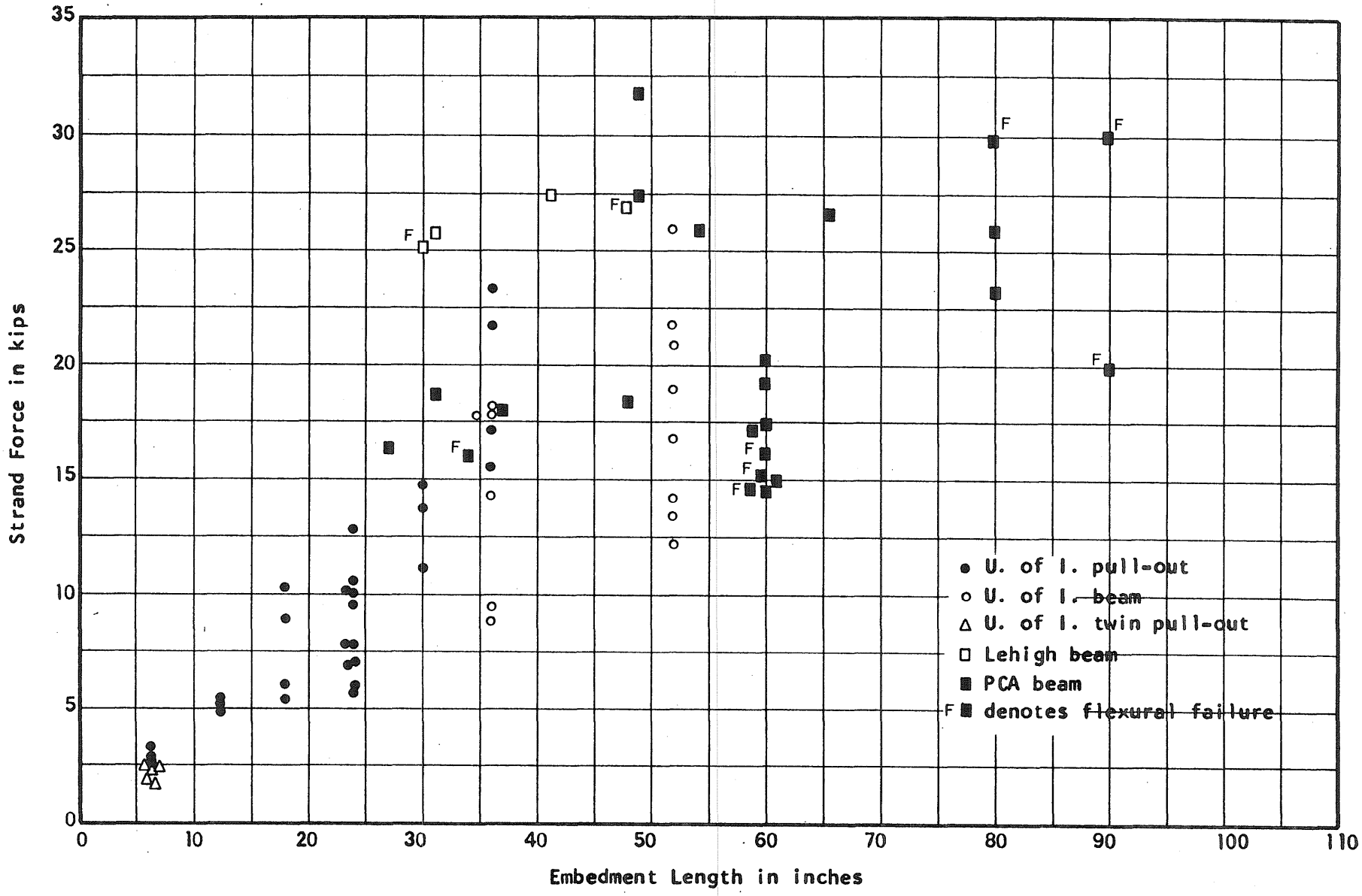

FIG. 7.2 BOND TEST RESULTS, VARIOUS LABORATORIES

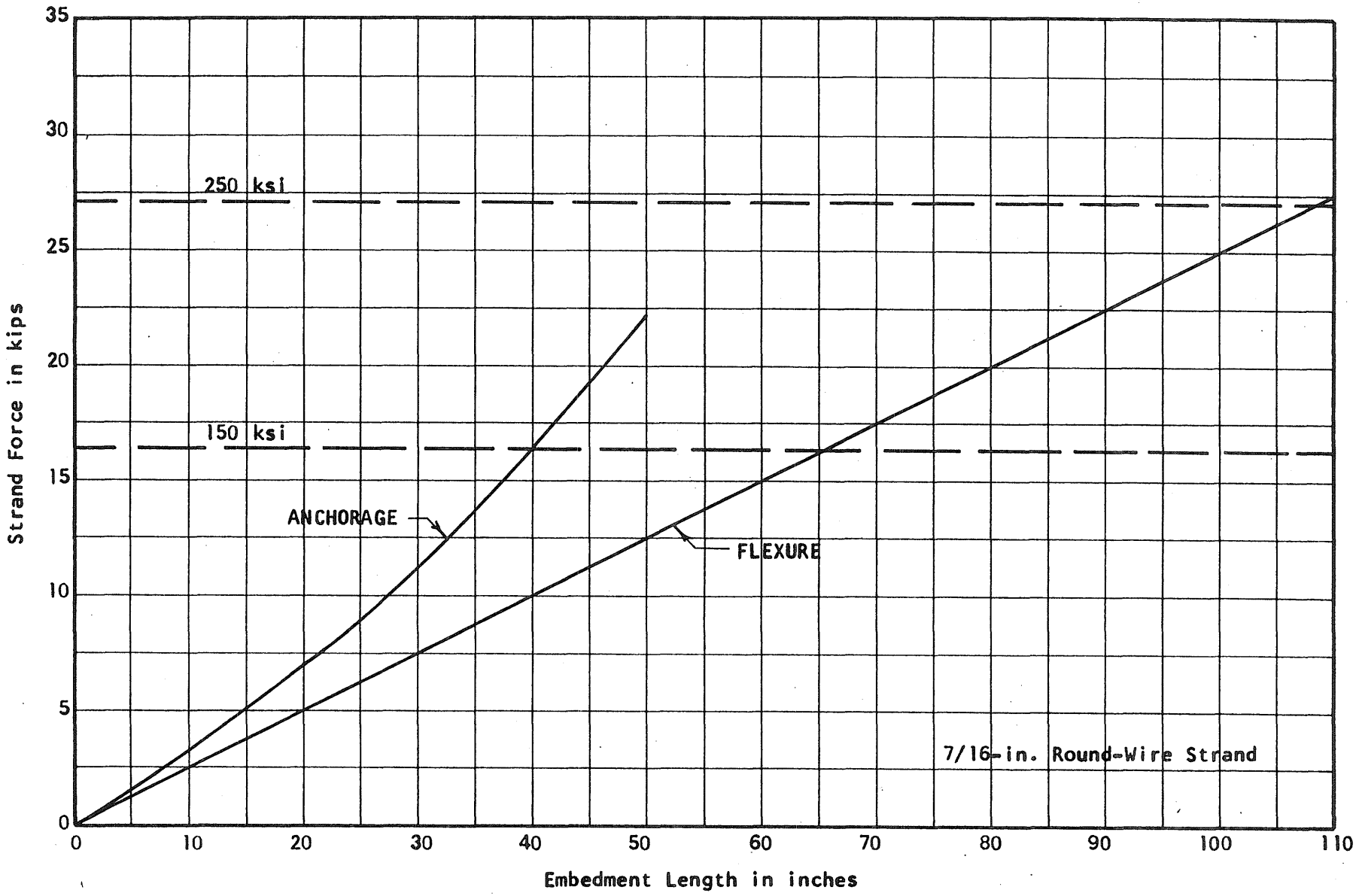

FIG. 7.3 REQUIRED EMBEDMENT LENGTHS IN ANCHORAGE AND FLEXURE

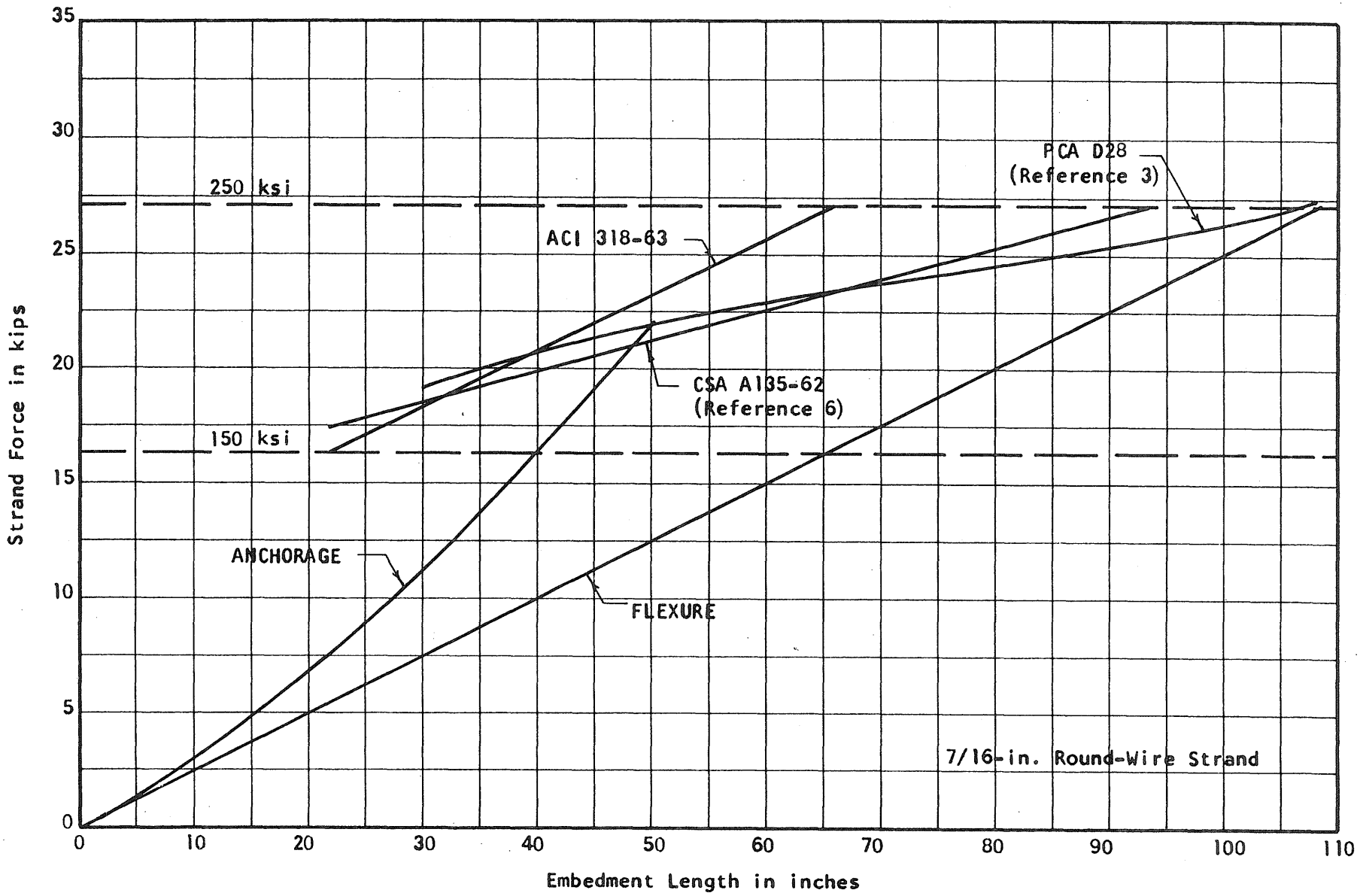

FIG. 7.4 A COMPARISON OF STRAND EMBEDMENT REQUIREMENTS

APPENDIX A.

MATERIALS AND FABRICATION FOR PULL-OUT AND FLEXURE SPECIMENS

A.1 Materials

(a) Cement: Lehigh brand Type III portland cement was used for all specimens.

(b) Aggregates: Wabash River sand and gravel were used in all specimens. The sand had a fineness modulus of approximately three. The maximum size for the gravel was 3/8 in. The absorption capacity was 1.5 percent for the sand and 2.5 percent for the gravel. All sand and gravel was oven-dried and cooled before mixing.

(c) Concrete Mix: The concrete mix proportions were based on previous trial batches and kept the same for all of the pull-out specimens. The water:cement ratio was reduced slightly in the beam specimens to produce less slump. The properties by weight of the mixes and the water:cement ratios are listed in Table 1. A histogram of the individual results of 170 tests on 6 x 12-in. cylinders is given in Fig. A.1. The average strength for all cylinders was 4515 psi, the mean deviation 292 psi, and the standard deviation 373 psi.

(d) Reinforcement: Reinforcing strands used for the specimens were 1/4-in. nominal diameter 3-wire rectangular-wire strand, 7/16-in. nominal diameter 7-wire round-wire strand, and 7/16-in. nominal diameter 7-wire rectangular-wire strand.

The round-wire strand is manufactured from round wire and has been used generally in prestressed concrete construction. The rectangular-wire strand is a relatively new development and is manufactured from flattened or oval wires as shown in Fig. A.2.

Strands used in these tests were cut from rolls designated S4A3-1 (1/4-in. rectangular-wire strand), R7W7-1 (7/16-in. round-wire strand), R7A7-1 (7/16-in. round-wire strand), and S7A7-2 (7/16-in. rectangular-wire strand). Stress-strain curves for

three samples of strand from each roll are given in Figs. A.3 and A.4. An 8-in. extensometer was used to measure the strain in each case.

The physical properties of each type of strand are given in Table 2.

A.2 Casting and Curing of Pull-Out Specimens

All forms were made of 3/4-in. Plypreg (plastic coated plywood) and consisted of removable ends and various lengths of inserts in order to cast specimens of different lengths. Forms were oiled lightly before casting.

The reinforcing strand was stored in a dry room to deter rusting and was cleaned with acetone just prior to casting to insure a clean surface. Care was taken not to allow form oil to come in contact with the strand after cleaning and before casting.

The concrete was cast in 200 to 300-lb. batches in a pan type mixer of 2 cu. ft. capacity. The mixing time for each batch was about three minutes. All sand and gravel was oven dried and cooled before casting. Three or four 6 x 12 and three or four 6 x 6-in. cylinders were cast with each set of specimens. The 6 x 6-in. cylinders were used in tensile splitting tests to obtain a measure of the tensile strength of the concrete. The 6 x 12-in. specimens were tested in compression.

In Series 7, companion pull-out specimens of various lengths were cast with each 3-in. prestressed specimen. The pull-out specimens were cast without the use of the testing frame while each prestressed specimen was cast in the frame. The strand was prestressed in the frame to 70 percent of its strength one day prior to the casting of the specimen.

The twin pull-out specimens of Series 10 each contained two strands placed at mid-height, 9 in. on center as shown in Fig. B.5. The tension steel contained in each of these specimens consisted of two number 4 deformed reinforcing bars hooked

on both ends. The bars were placed 4-in. apart, 1 in. from the trail end of the specimen with 1-in. cover at top and bottom.

All pull-out specimens were cast with the strand in the horizontal plane and at mid-depth of the specimen. A small load was applied to each strand just prior to casting. This was done to minimize the sagging in the strand. The concrete in the specimens and cylinders was vibrated with an internal vibrator. After casting, the specimens were struck off. The 6 x 12-in. compression cylinders were capped with neat cement about two hours after casting.

One day after casting the forms were removed and all specimens and cylinders were wrapped in wet burlap and covered with polyethylene. The burlap was removed on the day of testing.

A.3 Casting and Curing of Flexure Specimens

The forms in which all of the 72-in. and 104-in. beams were cast was made out of 3/4-in. Plypreg (plastic coated plywood). A movable plywood insert was used as one end so that the same form could be used to cast the two different lengths of beams. All of the beams except 72-1 had a preformed crack at the center line. This crack was preformed by inserting a piece of 18-gage aluminum, 8 in. wide and 4 in. high in the bottom of the form at mid-span. The form was oiled lightly before casting.

The reinforcing strand was stored in a dry room and was cleaned with acetone immediately before casting to insure a clean surface. Care was taken not to allow form oil to come in contact with the strand after cleaning and before casting. A pretensioning load of 1000 lb was applied to the strand with a hydraulic jack just prior to casting. This was done to minimize the sagging of the strand. This load was released about ten minutes after completion of casting. All beams were cast in a horizontal position with the strand located 1 1/2-in. from the bottom of the form.

A non-tilting drum type mixer of 6 cu. ft. capacity was used for mixing the concrete. The mixing time for each batch was about three minutes.

Only one batch of 625 lbs. was required to cast each 72-in. beam. Three 6 x 12 and three 6 x 6-in. cylinders were cast with each of these beams.

Two batches of 480 lbs. were required to cast each 104-in. beam. Three 6 x 12 and three 6 x 6-in. control cylinders were cast from each batch. The first batch was placed in a layer of uniform height along the entire length of the form. The second batch was placed on top of the first.

The concrete in the test specimen and in the control cylinders was vibrated with an internal vibrator. About an hour after casting, the specimen and cylinders were struck off. The 6 x 12-in. compression cylinders were capped with neat cement about two hours after casting.

One day after the specimens were cast, the plywood form was removed and the specimen and all cylinders were wrapped in wet burlap and covered with polyethylene plastic to hold in the moisture. The burlap was removed on the day of testing.

APPENDIX B.

INSTRUMENTATION AND TEST PROCEDURE FOR PULL-OUT SPECIMENS

B.1 Test Apparatus

(a) Series 7

The test frame shown in Fig. B.1 was used for testing both the prestressed and the non-prestressed pull-out specimens of Series 7. The frame consists basically of two 1 1/4-in. diameter threaded rods (D in Fig. B.1) and three 2 x 4 x 14-in. plates (C, E, and F), with ten nuts (G) to keep the plates in the desired position.

The two end plates (E and F) have two 1 5/16-in. holes drilled at mid-height on 10-in. centers through which the two rods pass, and one 5/16-in. hole drilled at the center through which the 1/4-in. diameter strand passes. The middle plate (C) is identical to the end plates except that the diameter of the middle hole is 1 5/16 in. rather than 5/16 in. to afford easier access for instrumentation to measure slip.

(b) Series 8 and 9

The test frame shown in Fig. B.3 was used to test the specimens of Series 8 and 9. It is identical in construction to the frame described above, but the rods and plates are larger. In this frame the two threaded rods (D) are 1 3/4 in. in diameter and the three plates (C, E, and F) are 2 x 8 x 18 in. The two end plates have two 1 7/8-in. holes drilled on 14-in. centers through which the rods pass and one 1/2-in. hole drilled at the center through which the 7/16-in. diameter strand passes. The center plate (C) is identical to the end plates except that the center hole diameter is 1 1/4 in. rather than 1/2 in. Ten nuts (G) are used to hold the plates in the desired positions.

(c) Series 10

No test frame such as that used in Series 7, 8, and 9 was used in testing the twin pull-out specimens of Series 10. The test apparatus used for these specimens

is shown in Fig. B.5. The load was applied at the mid-span of the specimen through a 1 x 1 x 6-in. steel loading block. The jack reacted against a 2 x 6 x 15-in. steel plate. This plate had two 1/2-in. holes drilled at mid-height on 9-in. centers through which the 7/16-in. diameter strands passed. A 1 x 6 x 15-in. wood block with 1/2-in. holes drilled at mid-height on 9-in. centers was used to support the two strands on the trail end.

B.2 Load Measurement

(a) Series 7

Two aluminum dynamometers (K and L) shown in Fig. B.1 were used to measure the loads in the case of the prestressed specimens in Series 7. In the case of the pull-out specimens of this series, only one dynamometer (L) was used. These dynamometers were made of 2-in. long hollow aluminum tubes with 5/8-in. outside diameter and a wall thickness of 0.175 in. Each was instrumented with four strain gages to form a four-arm bridge. These dynamometers had a calibration factor of approximately 10 lb per dial division on the strain indicator which could be read consistently to half a dial division.

(b) Series 8 and 9

The ring dynamometer (L) shown in Fig. B.3 was used to measure the loads in the pull-out specimens of Series 8 and 9. The dynamometer ring, made of T-1 steel, was 4/5-in. thick and had an outside diameter of 4 3/5 in. and an inside diameter of 3 1/5 in. The ring was supported between the cover plates by six 3/4-in. balls with the location of the balls alternating from one side of the ring to the other every 60 degrees. The ring was instrumented with twelve strain gages wired in series of three, thus forming a four-arm bridge measuring circuit. This dynamometer had a calibration factor of 41.4 lb per dial division on the strain indicator. Two socket head screws were used to fasten the dynamometer to the end plate (E).

(c) Series 10

The ring dynamometer shown in Fig. B.5 was used to measure the load in the twin pull-out specimens of Series 10. This dynamometer was identical in size and construction to that used in Series 8 and 9. It had a calibration factor of 42.3 lb per dial division on the strain indicator.

B.3 Slip Measurement

(a) Series 7

For the specimens of Series 7, the slip of the strand relative to the concrete was measured with the use of two traveling microscopes, one which could be read to 0.0001 in. placed at the attack end and the other which could be read to 1/6400 in. placed at the trail end of the specimen as shown in Fig. B.2. The attack end is defined as the end first to experience a relative movement between the concrete and reinforcement. Thus, in the case of a pull-out specimen it is the end at which load is applied. In the prestressed specimens it is the end at which load is released into the specimen. The trail end is the end opposite the attack end.

The slip was measured by determining the relative movement of scribe marks on 32 gage sheet metal strips glued on the specimens with Eastman 910 adhesive. The scribe marks were put on these strips with an ordinary flat head pin. At the end of the specimen where the strand slipped out of the concrete, one strip of metal was glued to the strand over a very small area of contact immediate to the face of the concrete. The other strip of metal was glued to the face of the middle steel plate (C) immediately above the strand. Thus, it was possible to eliminate the deformation of the strand outside the concrete section from being recorded.

At the end of the specimen where the strand slipped into the concrete, it was not possible to glue the strip of sheet metal on the steel as close to the face of the concrete. In this case, the strip was glued to the strand about 0.15 in. away

-om the face of the concrete. This limited the extent of measurement to a slip of
)out 0.15 in. The other strip was glued to the concrete about 3/4 in. above the
:rand.

(b) Series 8 and 9

For the specimens of Series 8 and 9, which were all standard pull-out speci-
ens, the slip of the strand with respect to the concrete on the trail end was measured
/ the use of a traveling microscope which could be read to 0.0001 in. and two sheet
etal strips as described above with one small exception. For these specimens the strip
as glued to the strand about 0.4 in. from the face of the concrete rather than 0.15 in.
ence, the slip measurement was limited to a maximum of 0.4 in.

The attack-end slip was measured with the use of a dial gage which could be read
) 0.0001 in. and which had a 0.3-in. travel. A collar made of mild steel was used to
-ansmit the movement of the strand near the face of the concrete out to the dial gage
Fig. B.4). This collar had a barrel length of 4 in., and outside diameter of 1 in.,
id an inside diameter of 1/2 in. The collar lip had a diameter of 1 3/4 in. The bar-
el of the collar was set up against the face of the concrete specimen and secured radially
) the strand by three socket-head screws located at the 1/3-points of the barrel circum-
erence, 3/16 in. from the end of the barrel. The dial gage was supported by a bracket
)unted on the middle plate (C) of the testing frame in a position such that the gage
lunger was in contact with the collar as shown in Fig. B.4. The bracket supporting
ne dial gage was slotted so that when the 0.3 in. travel had been expended during a
est, the gage could be reset, thus allowing attack end slips greater than 0.3 in. to be
easured.

It should be noted here that in the pull-out specimens the strand is not
nitially stressed. Hence, before the load is applied, the strand may not be perfectly
ligned with the line of action of the applied force. This misalignment may be caused
y either the crookedness of the strand resulting from residual stresses or the incor-
ect positioning of the specimen in the frame. When the load is applied the strand

(c) Series 10

The ring dynamometer shown in Fig. B.5 was used to measure the load in the twin pull-out specimens of Series 10. This dynamometer was identical in size and construction to that used in Series 8 and 9. It had a calibration factor of 42.3 lb per dial division on the strain indicator.

B.3 Slip Measurement

(a) Series 7

For the specimens of Series 7, the slip of the strand relative to the concrete was measured with the use of two traveling microscopes, one which could be read to 0.0001 in. placed at the attack end and the other which could be read to 1/6400 in. placed at the trail end of the specimen as shown in Fig. B.2. The attack end is defined as the end first to experience a relative movement between the concrete and reinforcement. Thus, in the case of a pull-out specimen it is the end at which load is applied. In the prestressed specimens it is the end at which load is released into the specimen. The trail end is the end opposite the attack end.

The slip was measured by determining the relative movement of scribe marks on 32 gage sheet metal strips glued on the specimens with Eastman 910 adhesive. The scribe marks were put on these strips with an ordinary flat head pin. At the end of the specimen where the strand slipped out of the concrete, one strip of metal was glued to the strand over a very small area of contact immediate to the face of the concrete. The other strip of metal was glued to the face of the middle steel plate (C) immediately above the strand. Thus, it was possible to eliminate the deformation of the strand outside the concrete section from being recorded.

At the end of the specimen where the strand slipped into the concrete, it was not possible to glue the strip of sheet metal on the steel as close to the face of the concrete. In this case, the strip was glued to the strand about 0.15 in. away

·om the face of the concrete. This limited the extent of measurement to a slip of ›out 0.15 in. The other strip was glued to the concrete about 3/4 in. above the :rand.

(b) Series 8 and 9

For the specimens of Series 8 and 9, which were all standard pull-out speci-ɜns, the slip of the strand with respect to the concrete on the trail end was measured ʻ the use of a traveling microscope which could be read to 0.0001 in. and two sheet ɜtal strips as described above with one small exception. For these specimens the strip ɜs glued to the strand about 0.4 in. from the face of the concrete rather than 0.15 in. ɜnce, the slip measurement was limited to a maximum of 0.4 in.

The attack-end slip was measured with the use of a dial gage which could be read › 0.0001 in. and which had a 0.3-in. travel. A collar made of mild steel was used to ·ansmit the movement of the strand near the face of the concrete out to the dial gage ·ig. B.4). This collar had a barrel length of 4 in., and outside diameter of 1 in., ɜd an inside diameter of 1/2 in. The collar lip had a diameter of 1 3/4 in. The bar-ɜl of the collar was set up against the face of the concrete specimen and secured radially › the strand by three socket-head screws located at the 1/3-points of the barrel circum-ɜrence, 3/16 in. from the end of the barrel. The dial gage was supported by a bracket ›unted on the middle plate (C) of the testing frame in a position such that the gage lunger was in contact with the collar as shown in Fig. B.4. The bracket supporting ɜe dial gage was slotted so that when the 0.3 in. travel had been expended during a ɜst, the gage could be reset, thus allowing attack end slips greater than 0.3 in. to be ɜasured.

It should be noted here that in the pull-out specimens the strand is not ɜitially stressed. Hence, before the load is applied, the strand may not be perfectly ligned with the line of action of the applied force. This misalignment may be caused ʻ either the crookedness of the strand resulting from residual stresses or the incor-ɜct positioning of the specimen in the frame. When the load is applied the strand

will straighten out. Any vertical movement of the strand due to this straightening action will cause a slight change in the readings indicated by the slip instrumentation on the attack end of the specimen. In some specimens tested, the first few attack-end readings recorded indicated a negative slip on the order of 0.001 in. In cases where this happened the initial slip of the strand was considered to have occurred when the readings first indicated positive slip.

The trail-end slip readings were not affected by any misalignment of the specimen since the strand outside the specimen on the trail end was never subjected to load.

(c) Series 10

For the twin pull-out tests of Series 10, the slip of each strand with respect to the concrete on the trail end was measured with sheet metal strips and a traveling microscope which could be read to 0.0001 in. as shown in Fig. B.6. Each set of strips was installed in the same manner as was done in Series 8 and 9. The microscope was placed between the two strands on the trail end and adjusted so that the readings to determine the relative movement of the metal strips on each strand could be taken by rotating the microscope 180 degrees around a vertical axis.

Figure B.6 also shows the instrumentation used to measure the attack-end slip of each strand. This instrumentation consisted of two dial gages mounted on opposite sides of a collar with Eastman 910 adhesive. The dial gages could be read to 0.001 in. and had a 0.5-in. travel. The two collars were made of mild steel and had a barrel length of 4 in., an outside diameter of 1 in., and a hole diameter of 15/32 in. Two sides of each barrel were machined down to flat surfaces 2 1/2-in. long on which the dial gages were mounted. The distance between these two flat surfaces was 3/4 in. The collar was secured radially to the strand by three socket-head screws located at the 1/3 points of the barrel circumference, 1/4 in. from the end of the barrel, in such a position that the plungers of both gages were depressed

just about all the way. To insure a good contact surface between each plunger and the face of the specimen, small pieces of 18-gage aluminum were glued to the specimen at the points of contact.

The magnitude of any relative movement between the strand and the specimen was indicated by a change in the reading of each dial gage. The average of the two readings was taken as the true value of relative movement. The use of two dial gages instead of only one eliminates the errors in the attack-end slip readings discussed in the last paragraph of Section B.3b.

B.4 Test Setup and Procedure

(a) Prestressed Specimens of Series 7

The test frame shown in Fig. B.1 was used to prestress the strand in these specimens before casting. The strand was first threaded through the middle holes of all three plates (C, E, and F). Dynamometers (K and L) were placed on each end of the strand outside the end plates and washers (J) were placed between the dynamometers and the end plate. Strand grips (H) were then placed on the ends of the strands outside the dynamometers.

The prestressing was effected by the use of the nuts bearing on the two end plates. First one set of nuts was brought to a desired location on the rod, making sure that the end plate, when bearing on the nuts, would be perpendicular to the rods. Then the prestressing was completed by tightening the nuts bearing on the other end plate, making sure that this tightening procedure was uniform for the two nuts. The strand was tensioned to 70 percent of its strength one day before casting.

Before casting, the forms were oiled and placed around the strand on the side of the middle plate (C) opposite the nuts. The forms were placed in a position such that there would be ample room between the ends of the specimen and the end plates of the frame for installation of the slip measurement instrumentation.

When the specimen was ready for testing, a strip of the sheet metal used for measuring slip was glued on the strand on the end of the specimen next to the middle plate of the frame. Then a thin layer of hydrocal was put between the specimen and the middle plate to insure a good bearing surface. Before the hydrocal hardened, the middle plate was made to bear on the specimen by turning the two nuts behind the plate. The rest of the slip measurement instrumentation was then installed.

The prestressing force was released by loosening the nuts supporting the end plate (F in Fig. B.1) at the attack end of the specimen. The following procedure was used in releasing the load and recording slip measurements: (1) An increment of load resulting from loosening each nut 1/6 turn was released into the specimen. (2) A time interval of about 2 1/2 minutes was allowed to elapse. (3) Slip measurements were taken with the traveling microscopes situated at the attack and trail ends. (4) Both of the dynamometer readings were taken, the difference in the loads indicated by the dynamometers being the amount of force released into the specimen. The entire cycle required about three minutes. This procedure was repeated until the entire prestress force was released. If a trail end slip of 0.15 in. had not been recorded at this point, additional load was applied at the trail end by turning the nuts behind plate (E) 1/6 turn until a slip of 0.15 in. was recorded.

(b) Pull-Out Specimens of Series 7

The non-prestressed or standard pull-out specimens were not cast in the test frame. To prepare these specimens for testing, the strand was threaded through the center holes of all three plates with the specimen occupying the position shown in Fig. B.1. The dynamometer and the grip were then put on the strand outside plate (E). In the pull-out tests, the dynamometer and the grip on the other end were not used. The sheet metal strip for measuring slip was glued on the strand on the side of

the specimen next to the plate (C), a thin layer of hydrocal was applied between the specimen and the middle plate, and the middle plate was then made to bear on the specimen by the nuts behind the plate. The remainder of the slip measurement instrumentation was then installed.

The same procedure was used for testing these specimens as was used for testing the prestressed specimens, except that the incremental load was applied to the specimen by turning each of the two nuts behind plate (E) 1/6 turn about every three minutes. This procedure was followed until the desired amount of trail-end slip was measured.

(c) Series 8 and 9

To prepare these specimens for testing, the strand was threaded through the center holes of all three plates with the specimen occupying the position shown in Fig. B.3. The collar used in the measurement of the attack-end slip was then butted up against the face of the specimen as shown in Fig. B.4, and the socket screws tightened. Next a thin layer of hydrocal was put between the specimen and the plate (C) to insure a good bearing surface. Before the hydrocal hardened the plate (C) was made to bear on the specimen by turning the two nuts behind this plate. The rest of the slip measurement instrumentation was then installed. Finally, the dynamometer, hydraulic jack, and grip were put on the strand outside plate (E).

The following procedure was used to test these specimens: (1) The load in the specimen was increased by about 600 lb by means of the hydraulic jack. (2) A time interval of about 1 1/2 minutes was allowed to elapse. (3) The strain indicator reading was taken. (4) The attack and trail-end slip readings were taken. The entire cycle required approximately two minutes. This procedure was repeated until 0.30 in. of trail-end slip was measured.

(d) Series 10

To prepare a twin pull-out specimen for testing the specimen was first placed on a level surface between two parallel strips of wood fastened 15 in. apart. These strips were used to maintain the proper alignment of the various components. The attack-end slip instrumentation, as shown in Fig. B.6, was then installed on each strand as described in Section B.3c. Next the two strands were threaded through the holes in the 2 x 6 x 15-in. jack reaction plate and the strand grips put in place. Then the 1 x 1 x 6-in. loading block was placed at the center line of the specimen, the dynamometer centered on the loading block, and the jack put in position with its base centered on the reaction plate and its head centered on the dynamometer. A rounded loading head was used to insure that the applied load would be equally divided between the two strands. A rounded section was milled out of the dynamometer cover plate to insure a good bearing surface for the jack head. The two strands on the trail end were threaded through the holes in the 1 x 6 x 15-in. wood block. The trail-end slip measurement instrumentation was then installed.

The following procedure was used in performing the test: (1) The load on each strand was increased by about 600 lb by means of the hydraulic jack. (2) A time interval of about 1 1/2 minutes was allowed to elapse. (3) The strain indicator reading was taken. (4) The dial indicators on the attack end were read and readings were taken with the traveling microscope on the trail end. The entire cycle required about three minutes. This procedure was repeated until about 0.25 in. trail-end slip had been measured.

APPENDIX C.

INSTRUMENTATION AND TEST PROCEDURE FOR FLEXURE SPECIMENS

C.1 Instrumentation

(a) Load Measurement

As seen in Fig. C.1 the load was applied at the mid-span of the beam by a hydraulic jack through a 1/2 x 2 x 8-in. steel loading plate. Between the jack and the loading plate a ring dynamometer was placed to measure the magnitude of the applied load.

The dynamometer ring, made of T-1 steel, was 5/8 in. thick and had an outside diameter of 4 21/32 in. and an inside diameter of 3 13/32 in. The construction of this ring dynamometer was identical to that used in Series 8 and 9 (Section B.2b) and had a calibration factor of 27.7 lb per dial division on the strain indicator.

(b) Mid-Span Deflection

The mid-span deflection of each beam was measured with a 0.001-in. dial gage having a 2-in. travel. This gage was held in position by an adjustable stand sitting on a channel (5 [6.7) supported at the end bearing blocks which gave a nondeflecting reference for deflections. The position of the dial gage could be readjusted during a test, thus allowing center deflections greater than 2.0 in. to be measured. The movement of the beam was transmitted to the dial gage by a short piece of aluminum angle glued 2 in. from the top of the beam with Eastman 910 adhesive

(c) Slip Measurement

The instrumentation used to measure the relative movement between the strand and the concrete at each end of the beam was identical in construction to that used to measure the attack-end slips of the specimens of Series 10 (Fig. B.6).

For the beam specimens, however, the dial gages used could be read to 0.0001 in. All of the gages had at least 0.1-in. travel. The collars on which the gages were mounted were the same ones used in Series 10. To insure a good contact surface between each plunger and the end face of the specimen, small pieces of 18-gage aluminum were glued to the specimen at the points of contact. Each collar was secured to the strand with the socket screws in a position such that the plungers of both dial gages were just making contact with the bearing plates.

Any relative movement between the strand and the concrete was indicated by a change in the reading of both gages. The average of these two readings was taken as the true magnitude of slip. This procedure insured that only the movement of the strand perpendicular to the face of the concrete was recorded as slip.

C.2 Loading Apparatus

The setup used for all of the beam tests is shown in Fig. C.1. The transverse load was applied by a hydraulic jack through a 1/2 x 2 x 8-in. steel loading plate at the center of the beam. A thin layer of hydrocal was placed between the top of the beam and the loading plate to assure a good bearing surface. The ring dynamometer was carefully centered on the loading plate. The load was transmitted from the jack to the dynamometer through a 3/4-in. steel ball. The jack reacted against the cross-beam of a test frame anchored to the floor of the laboratory.

The beams were simply supported at both ends. Each support consisted of a 2-in. diameter roller, a 3/4 x 6 x 8-in. steel plate, and two 18-gage 2-in. square aluminum bearing plates. The reaction was transmitted to the bottom of the beam through the 2-in. square plates placed in the corners, each having one edge in line with the end of the beam and one edge in line with the side of the beam. Since the beams were all 8-in. wide, there was a 4-in. clear space between the inside edges of the bearing plates as shown in Fig. C.1. This was done to reduce the pinching effect of the reaction on the strand. A thin layer of hydrocal was applied between the

2-in. square plates and the beam. The 3/4 x 6 x 8-in. steel plate was placed between the roller and the aluminum bearing plates. The center of each roller was 1 in. from the end of the beam. Thus the distance between reactions was 70 in. for the 72-in. beams and 102 in. for the 104-in. beams.

C.3 Test Procedure

The following procedure was used to test all of the beams: (1) A load increment of about 250 lb was applied to the beam by means of the hydraulic jack. (2) The strain indicator was read. (3) The center deflection dial gage was read. (4) The four strand slip dial gages were read. (5) Crack progression was marked. On the average, the entire cycle required about two minutes. This procedure was repeated until failure occurred.

If all the travel of the strand slip dial gages was expended before failure occurred, these gages were removed and the test continued. And in the cases where the center deflection was greater than 2 in., the position of the center deflection dial gage was readjusted during the test. Crack widths at the reinforcement level were measured with a crack ruler at various times.

TABLE 1

PROPERTIES OF CONCRETE MIXES

Mark	Cement: Sand: Gravel by weight	W/C Ratio	Slump in.	Comp. Strength f'_c psi	Tensile Strength* f_t psi	Age days
SERIES 7						
N71a	1:2.7:3.1	0.65	2 1/2	4320	395	10
N71b	1:2.7:3.1	0.65	3 1/2	4470	395	7
N71c	1:2.7:3.1	0.65	2 1/2	4710	375	8
N71d	1:2.7:3.1	0.65	4 1/2	5120	375	9
N73a	1:2.7:3.1	0.65	2 1/2	4320	395	10
N73b	1:2.7:3.1	0.65	3 1/2	4470	395	7
N73c	1:2.7:3.1	0.65	2 1/2	4710	375	8
N73d	1:2.7:3.1	0.65	4 1/2	5120	375	9
N76a	1:2.7:3.1	0.65	2 1/2	4320	395	10
N76b	1:2.7:3.1	0.65	3 1/2	4470	395	7
N76c	1:2.7:3.1	0.65	2 1/2	4710	375	8
N76d	1:2.7:3.1	0.65	4 1/2	5120	375	9
N79c	1:2.7:3.1	0.65	2 1/2	4710	375	8
P73a	1:2.7:3.1	0.65	2 1/2	4320	395	10
P73b	1:2.7:3.1	0.65	3 1/2	4470	395	7
P73c	1:2.7:3.1	0.65	2 1/2	4710	375	8
P73d	1:2.7:3.1	0.65	4 1/2	5120	375	9
SERIES 8						
N86a	1:2.7:3.1	0.65	6 1/2	4410	360	7
N86b	1:2.7:3.1	0.65	7 1/2	4880	385	7
N86c	1:2.7:3.1	0.65	6 1/2	4350	340	7
N86d	1:2.7:3.1	0.65	7	4580	385	7

* Based on split cylinders

TABLE 1 cont.

PROPERTIES OF CONCRETE MIXES

Mark	Cement: Sand: Gravel by weight	W/C Ratio	Slump in.	Comp. Strength f'_c psi	Tensile Strength* f_t psi	Age days
N812a	1:2.7:3.1	0.65	6 1/2	4350	340	7
N812b	1:2.7:3.1	0.65	4 1/2	4800	350	7
N812c	1:2.7:3.1	0.65	4	4960	395	7
N818a	1:2.7:3.1	0.65	6 1/2	4140	360	7
N818b	1:2.7:3.1	0.65	7 1/2	4650	440	7
N818c	1:2.7:3.1	0.65	8	4280	370	7
N818d	1:2.7:3.1	0.65	7	3860	385	7
N818e	1:2.7:3.1	0.65	7 1/2	3440	290	7
N824a	1:2.7:3.1	0.65	6	4020	375	7
N824b	1:2.7:3.1	0.65	6	4160	375	7
N822c	1:2.7:3.1	0.65	6	4720	360	7
N824d	1:2.7:3.1	0.65	7	4580	385	7
N824e	1:2.7:3.1	0.65	3	4610	355	7
N824f	1:2.7:3.1	0.65	3	4610	355	7
N824g	1:2.7:3.1	0.65	3	4440	345	7
N824h	1:2.7:3.1	0.65	3	4440	345	7
N824i	1:2.7:3.1	0.65	6 1/2	4140	360	7
N824j	1:2.7:3.1	0.65	7 1/2	4650	440	7
N824k	1:2.7:3.1	0.65	8	4280	370	7
N830a	1:2.7:3.1	0.65	6 1/2	4140	360	7
N830b	1:2.7:3.1	0.65	7 1/2	4650	440	7
N830c	1:2.7:3.1	0.65	8	4280	370	7
N836a	1:2.7:3.1	0.65	6	4440	370	7
N836b	1:2.7:3.1	0.65	6 1/2	4410	360	7
N836c	1:2.7:3.1	0.65	7 1/2	4880	385	7
N836d	1:2.7:3.1	0.65	4 1/2	4800	350	7

* Based on split cylinders

TABLE 1 cont.

PROPERTIES OF CONCRETE MIXES

Mark	Cement: Sand: Gravel by weight	W/C Ratio	Slump in.	Comp. Strength f'_c psi	Tensile Strength* f_t psi	Age days
SERIES 9						
N93a	1:2.7:3.1	0.65	5 1/2	4560	330	7
N93b	1:2.7:3.1	0.65	5 1/2	4570	350	7
N93c	1:2.7:3.1	0.65	5 1/2	4730	370	7
N96a	1:2.7:3.1	0.65	5 1/2	4680	410	7
N96b	1:2.7:3.1	0.65	4 1/2	4630	370	7
N96c	1:2.7:3.1	0.65	5	4680	390	7
N912a	1:2.7:3.1	0.65	5 1/2	4680	410	7
N912b	1:2.7:3.1	0.65	4 1/2	4630	370	7
N912c	1:2.7:3.1	0.65	5	4680	390	7
N918a	1:2.7:3.1	0.65	5 1/2	4560	330	7
N918b	1:2.7:3.1	0.65	5 1/2	4570	350	7
N918c	1:2.7:3.1	0.65	5 1/2	4730	370	7
N924a	1:2.7:3.1	0.65	5	4320	370	7
N924b	1:2.7:3.1	0.65	6	4740	345	7
N924c	1:2.7:3.1	0.65	6 1/2	4420	385	7
N924d	1:2.7:3.1	0.65	6 1/2	4730	415	7
SERIES 10						
N106a	1:2.7:3.1	0.65	7	3860	385	7
N106b	1:2.7:3.1	0.65	7 1/2	3440	290	7
N106c	1:2.7:3.1	0.65	7	4380	365	7
N107a	1:2.7:3.1	0.65	6	3920	380	7
BEAM TESTS						
72-1	1:2.7:3.1	0.60	2 1/2	4500	365	7
72-2	1:2.7:3.1	0.60	5	4720	410	7
72-3	1:2.7:3.1	0.60	4 1/2	4770	385	7

* Based on split cylinders

TABLE 1 cont.

PROPERTIES OF CONCRETE MIXES

Mark	Cement: Sand: Gravel by weight	W/C Ratio	Slump in.	Comp. Strength f'_c psi	Tensile Strength* f_t psi	Age days
104-1+	1:2.7:3.1	0.61	3	4900	390	7
				4860	390	
104-2	1:2.7:3.1	0.61	3 1/2	4910	385	7
				4850	390	
104-3	1:2.7:3.1	0.61	3 1/2	5150	410	7
				4990	345	
104-4	1:2.7:3.1	0.61	3 1/2	4890	360	7
				4960	390	

* Based on split cylinders

+ Each lot in beam was cast in two batches

TABLE 2 STRAND PROPERTIES

TYPE OF STRAND	CROSS - SECTIONAL AREA $(in)^2$	PITCH (in)	APPARENT MODULUS OF ELASTICITY (ksi)	EFFECTIVE PRESTRESS 150 ksi (kips)	MINIMUM STRENGTH (kips)
1/4-in. Round-Wire Strand 7-wire	0.036	4	28,000	5.4	9.6
1/4-in. Rectangular-Wire Strand 3-wire	0.036	3	28,000	5.4	9.6
7/16-in. Round-Wire Strand 7-wire	0.109	5 3/4	28,000	16.3	27.2
7/16-in. Rectangular-Wire Strand 7-wire	0.109	5 3/4	28,000	16.3	27.2

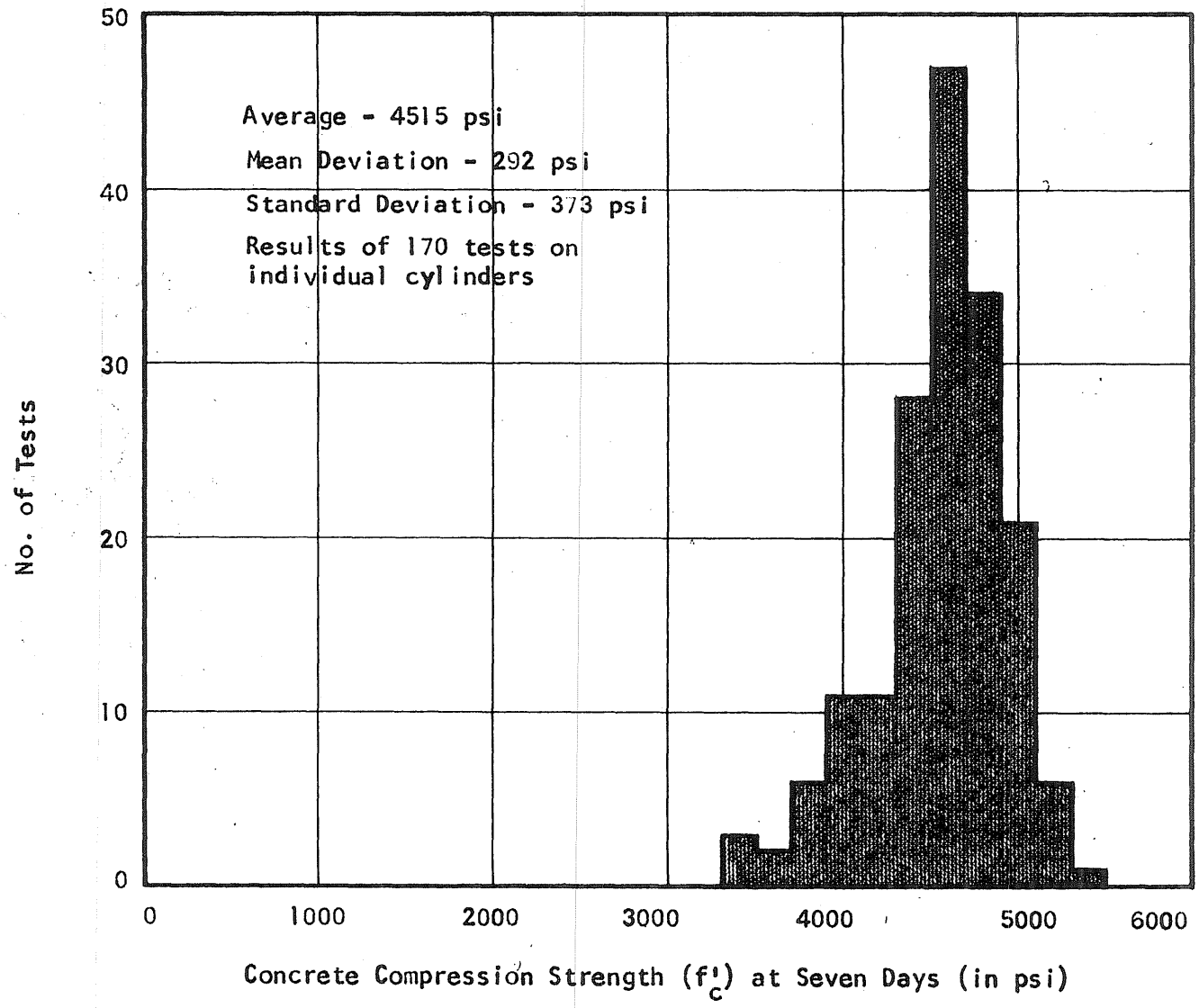

FIG. A.1 HISTOGRAM OF 6 BY 12-IN. CYLINDER STRENGTHS

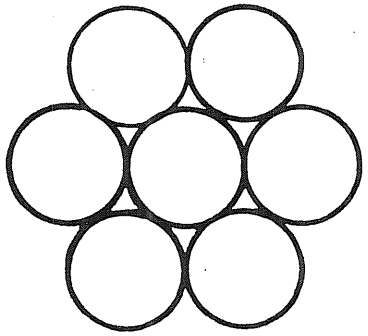

(a) 7/16-in. 7-Wire Round-Wire Strand

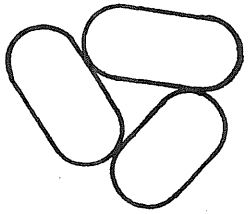

(b) 1/4-in. 3-Wire Rectangular-Wire Strand

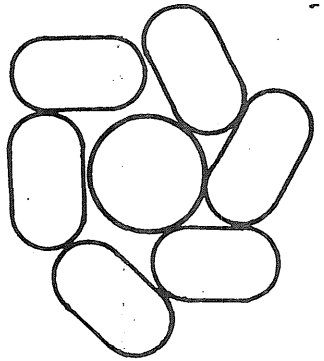

(c) 7/16-in. 7-Wire Rectangular-Wire Strand

FIG. A.2 CROSS SECTIONS OF ROUND-WIRE AND RECTANGULAR-WIRE STRANDS

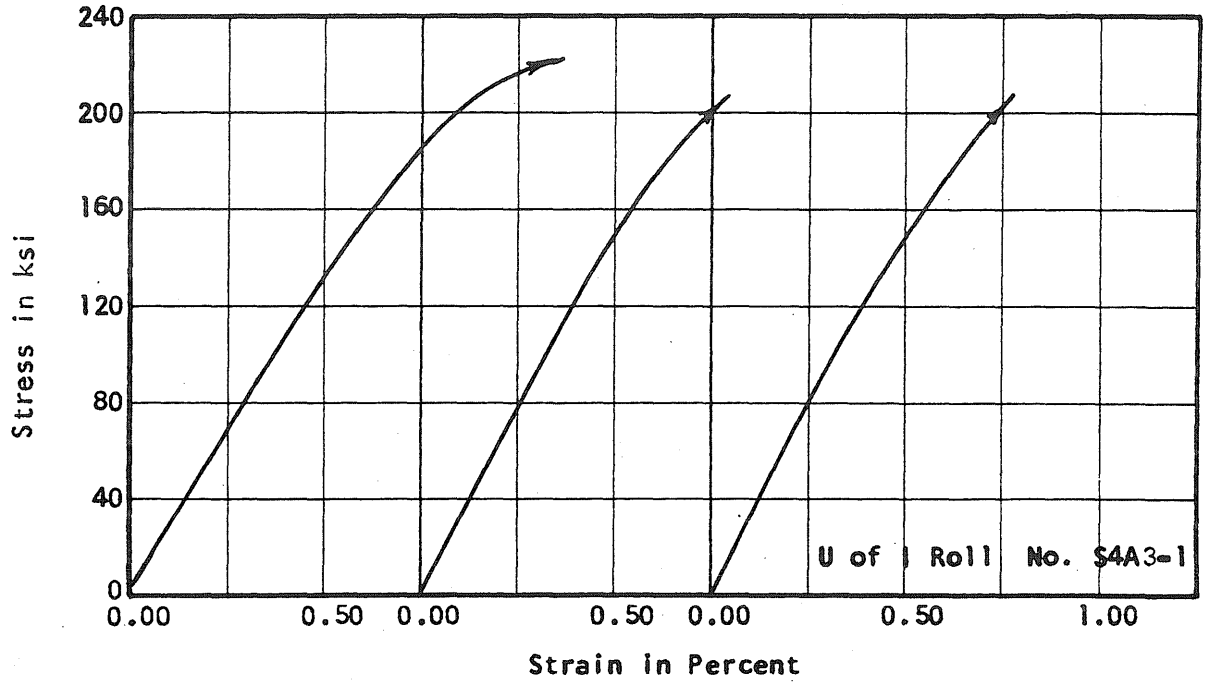

(a) 1/4-in. 3-Wire Rectangular-Wire Strand

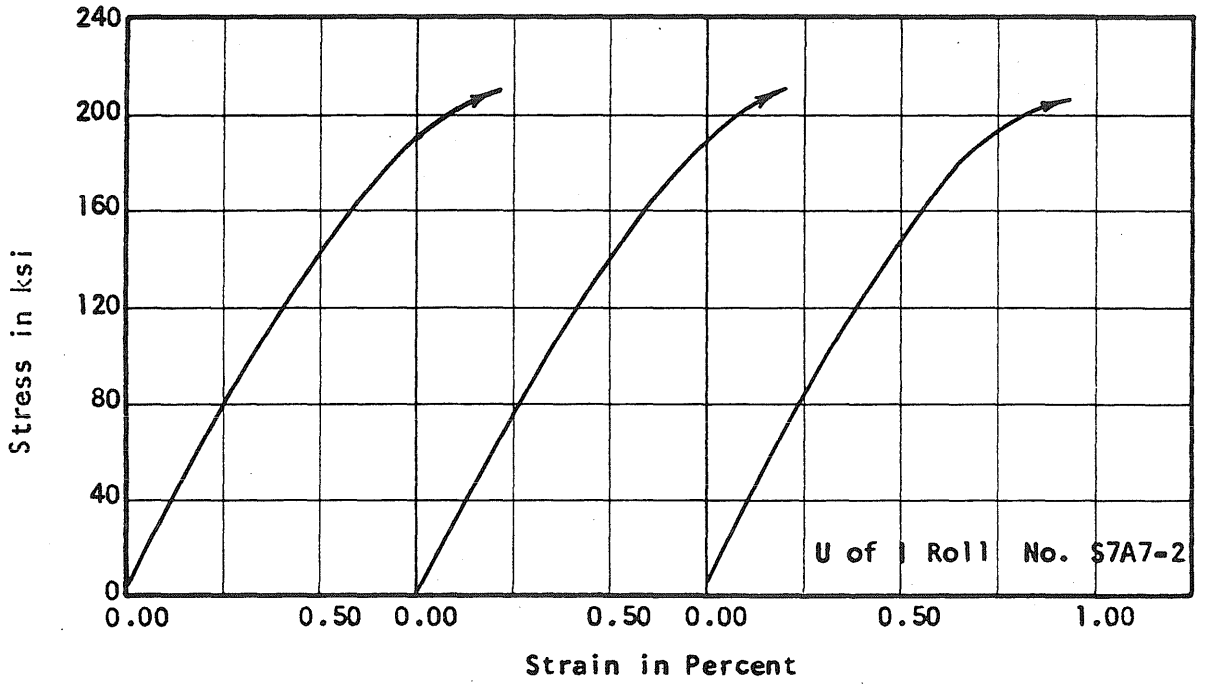

(b) 7/16-in. 7-Wire Rectangular-Wire Strand

FIG. A.3 STRAND STRESS-STRAIN CURVES

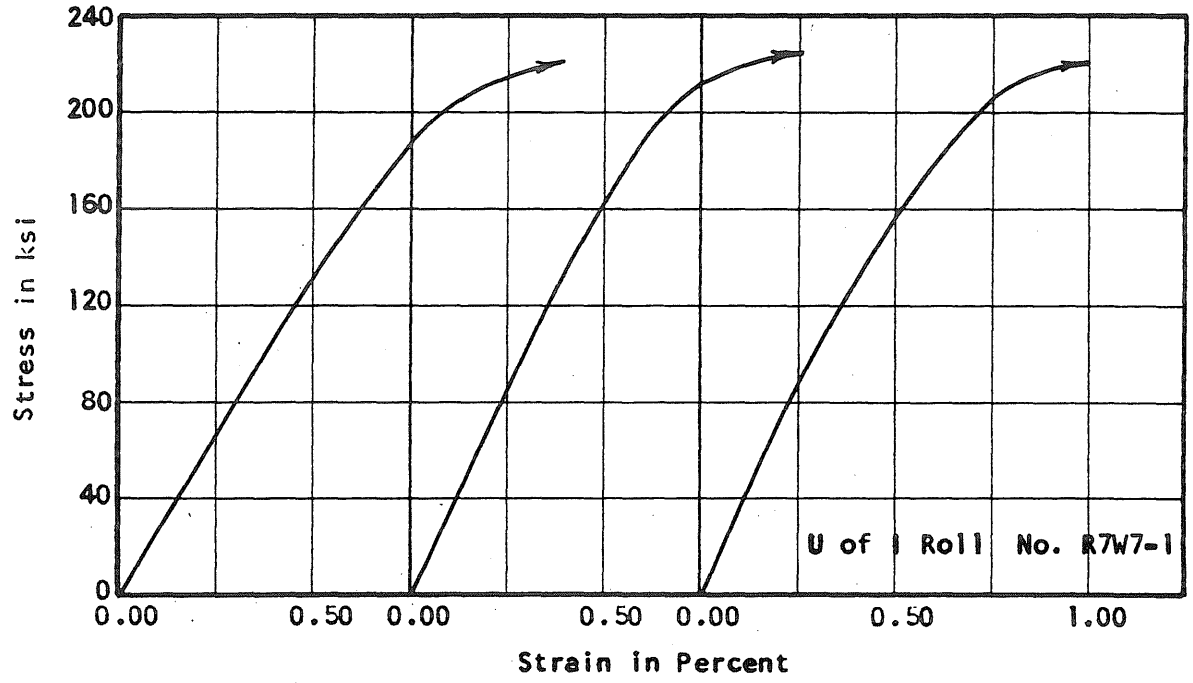

(a) 7/16-in. 7-Wire Round-Wire Strand

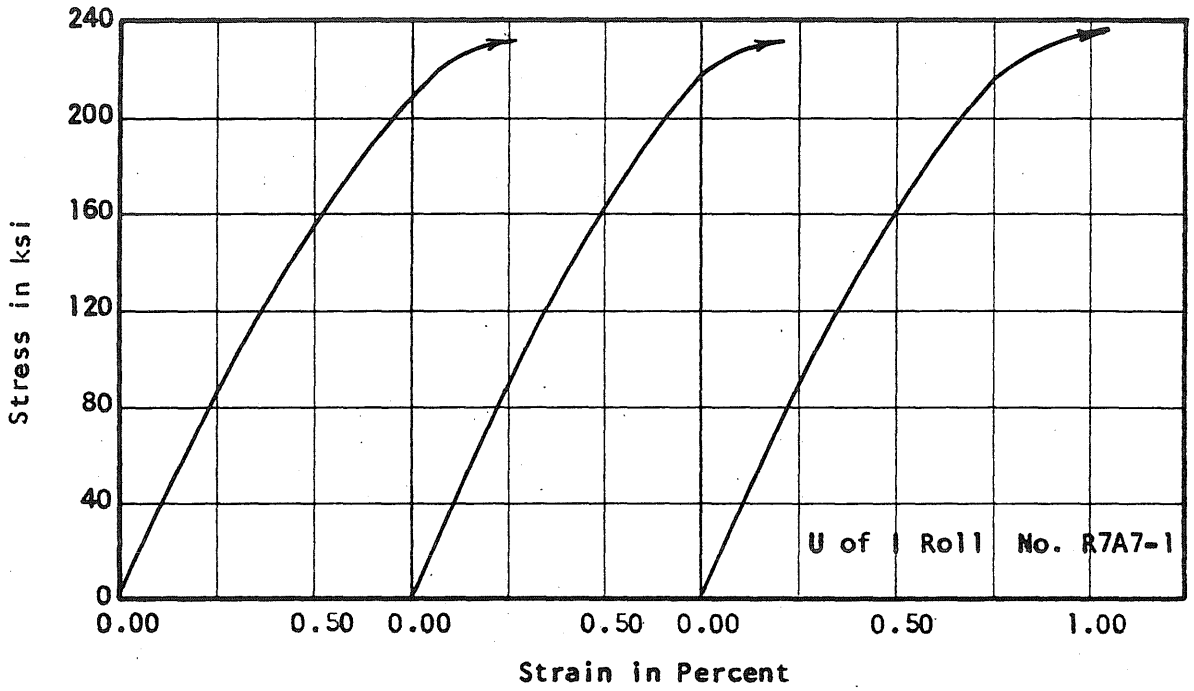

(b) 7/16-in. 7-Wire Round-Wire Strain

FIG. A.4 STRAND STRESS-STRAIN CURVES

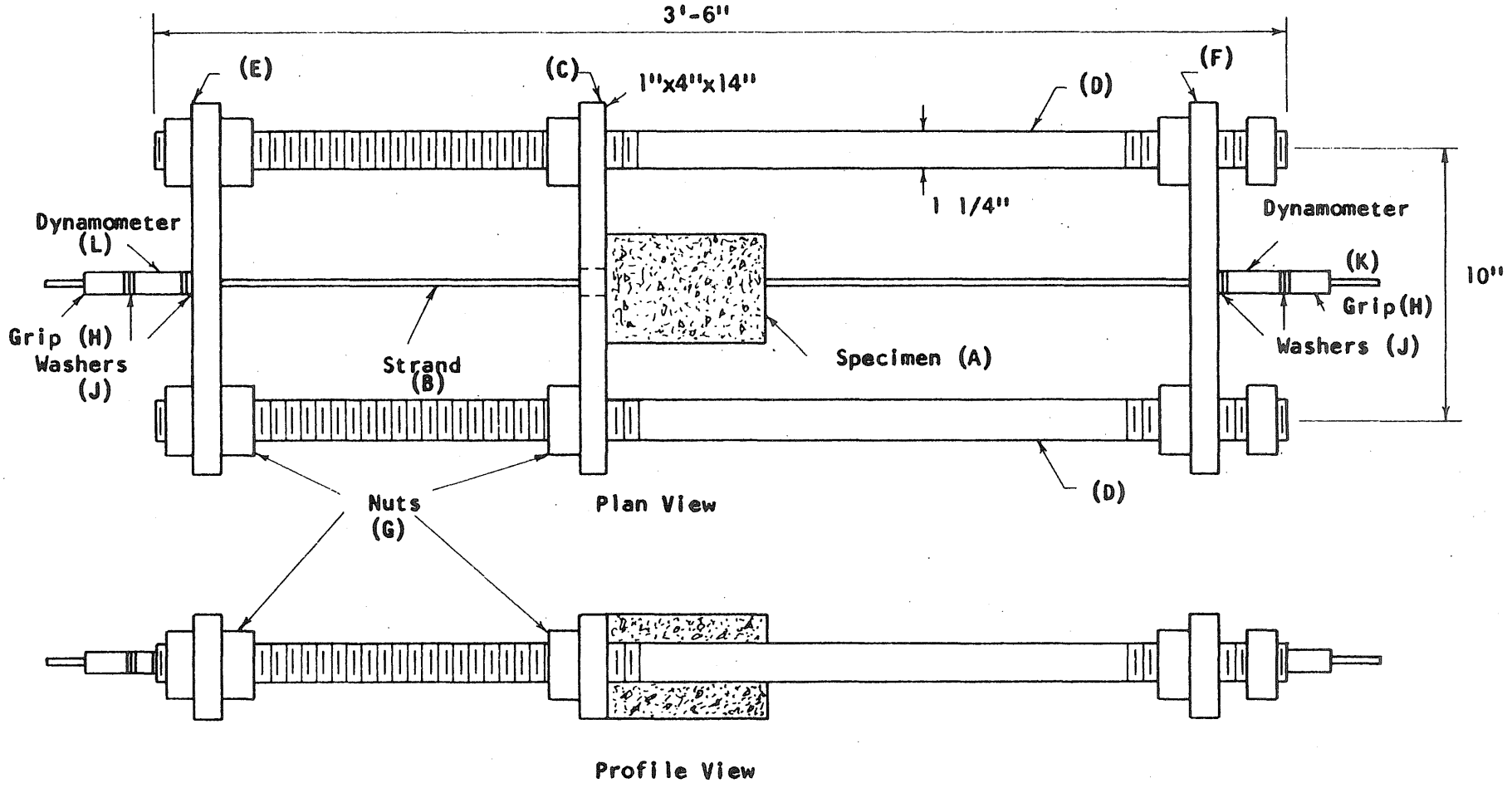

FIG. B.1 TEST FRAME FOR SERIES 7

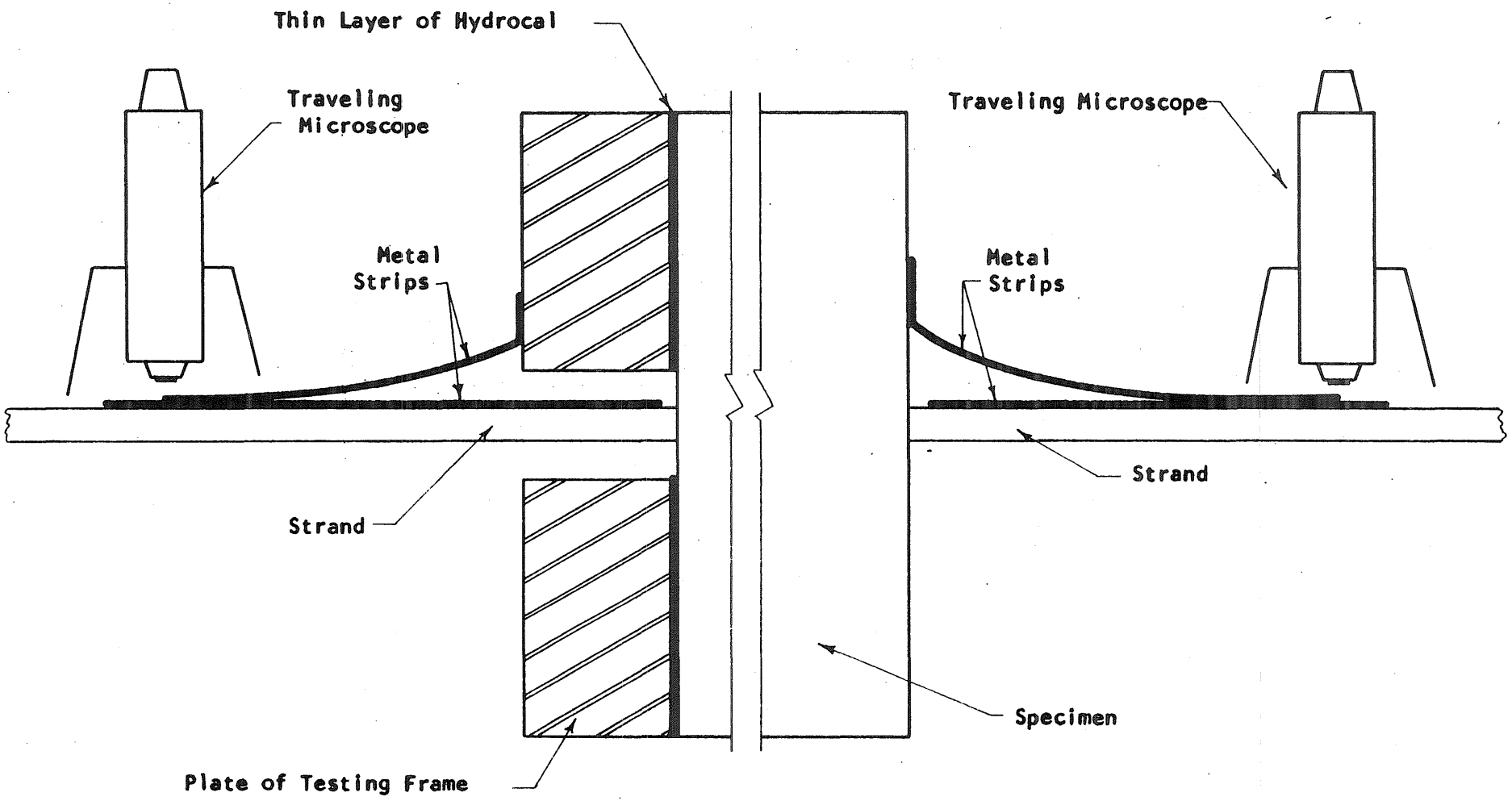

FIG. B.2 INSTRUMENTATION FOR TEST SPECIMENS OF SERIES 7

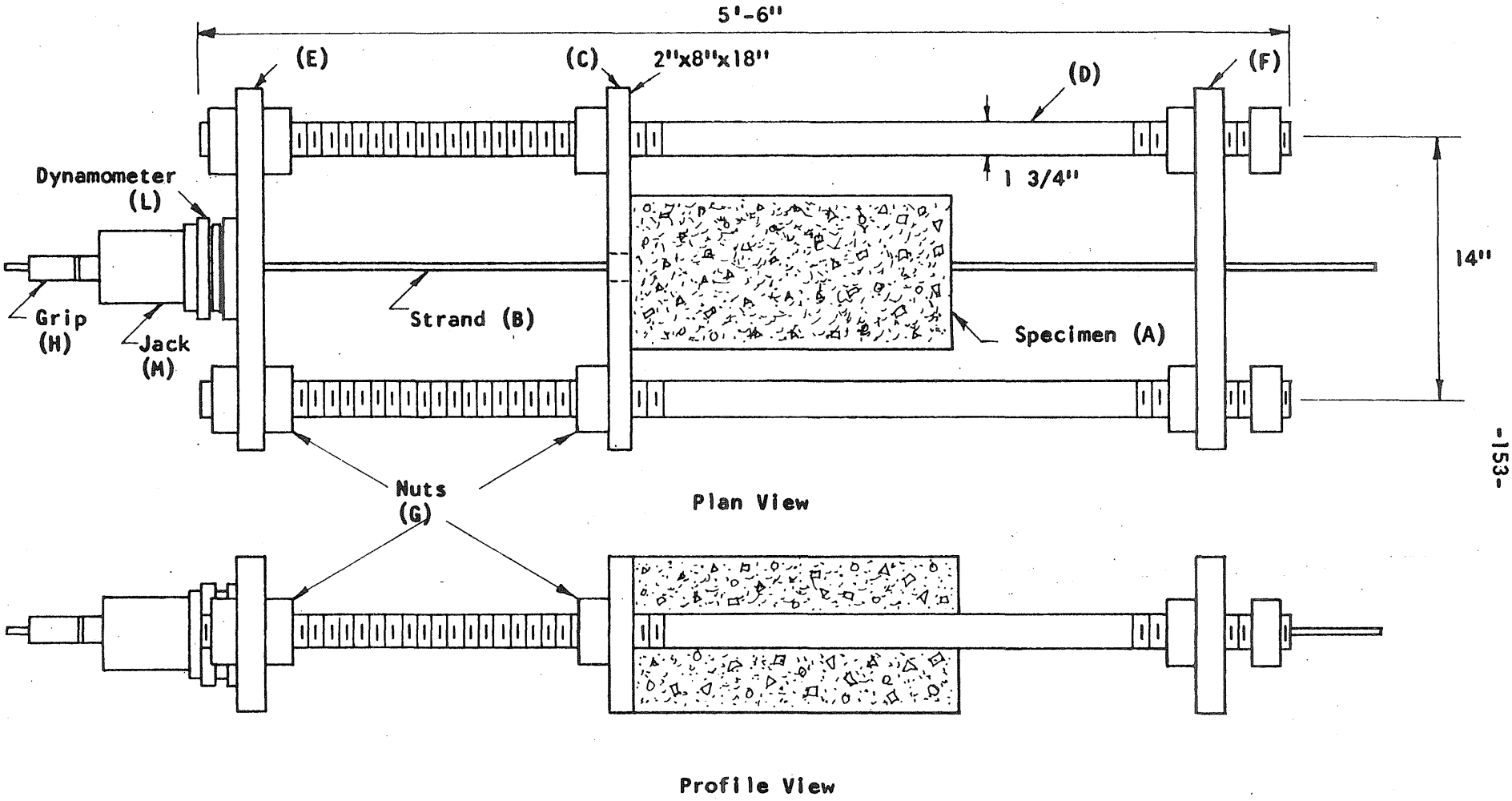

FIG. B.3 TEST FRAME FOR SERIES 8 AND 9

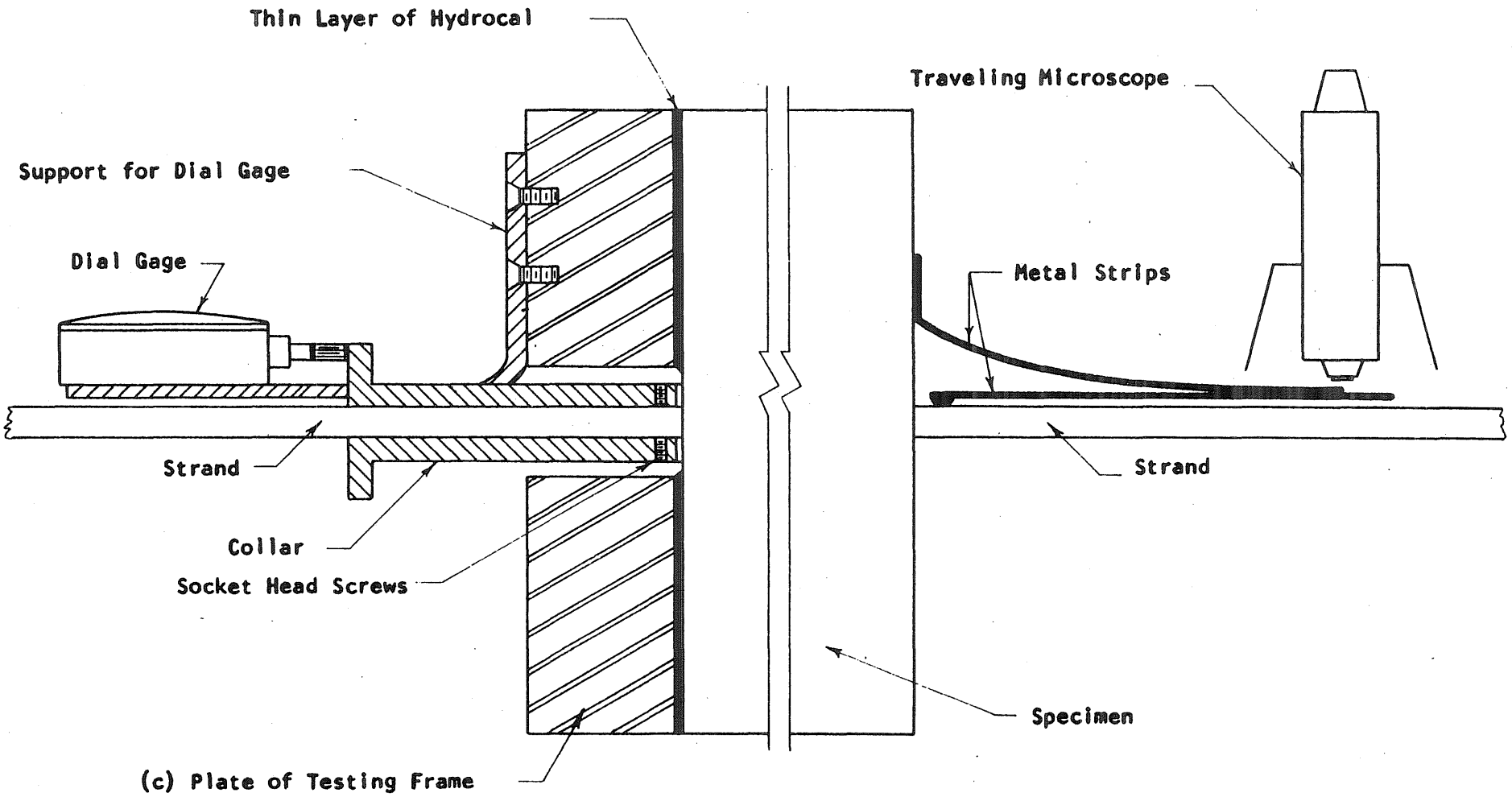

FIG. B.4 INSTRUMENTATION FOR TEST SPECIMENS OF SERIES 8 AND 9

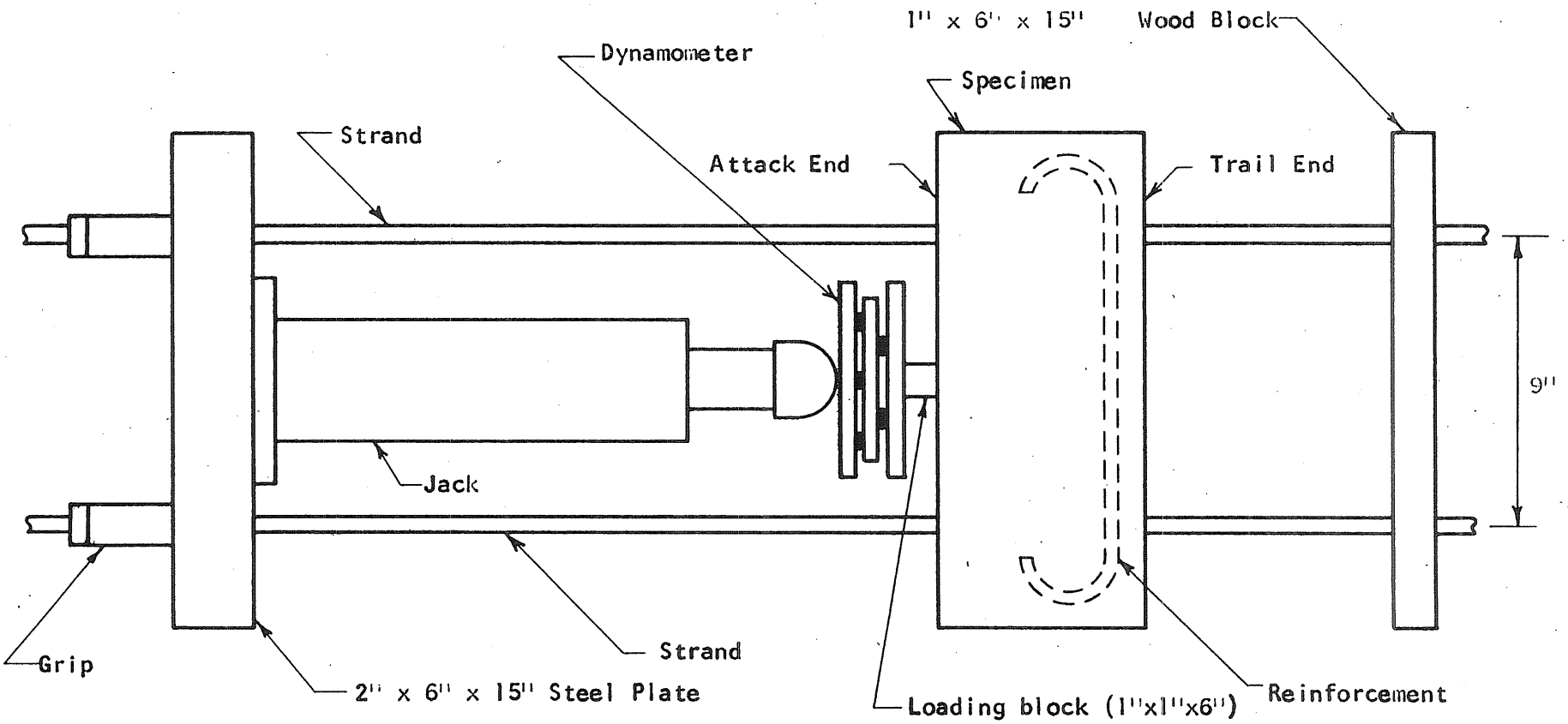

FIG. B.5 TEST APPARATUS FOR SERIES 10

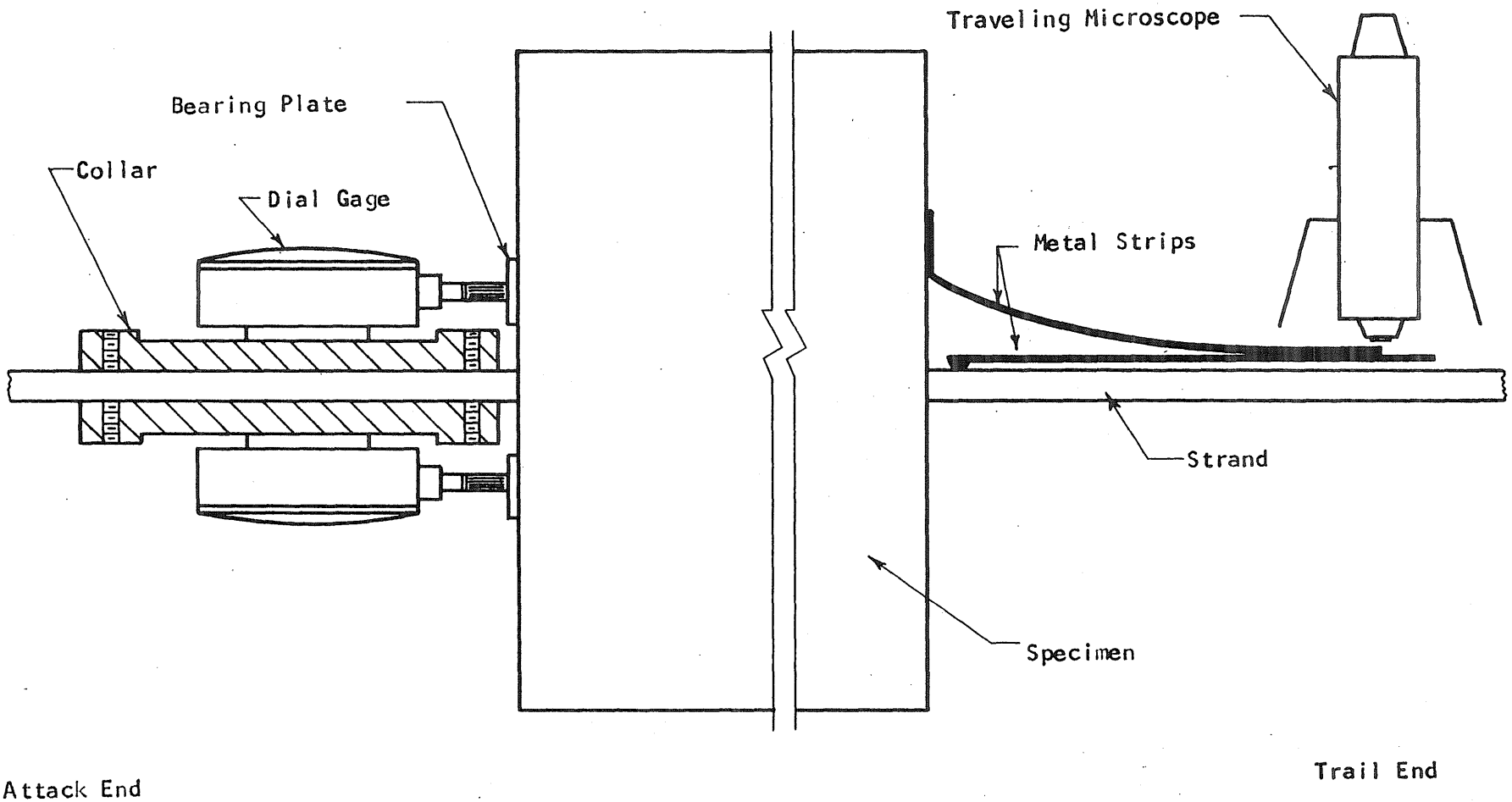

FIG. B.6 INSTRUMENTATION FOR TEST SPECIMENS OF SERIES 10

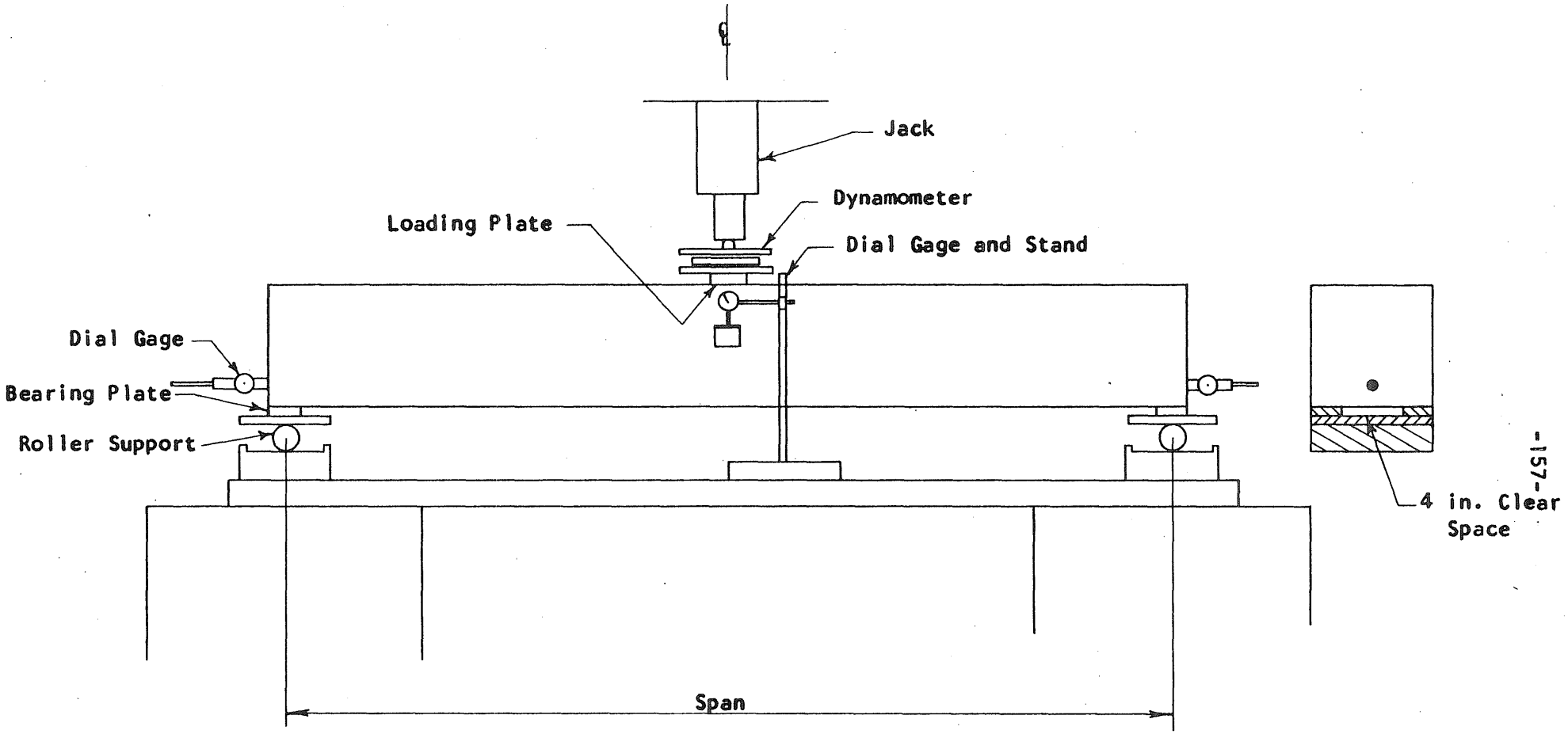

FIG. C.1 BEAM TEST SETUP